PREPARED FOR:

FLOOD CONTROL DISTRICT OF MARICOPA COUNTY

DYNAMICS OF ALLLUVIAL-CHANNEL RESPONSE:

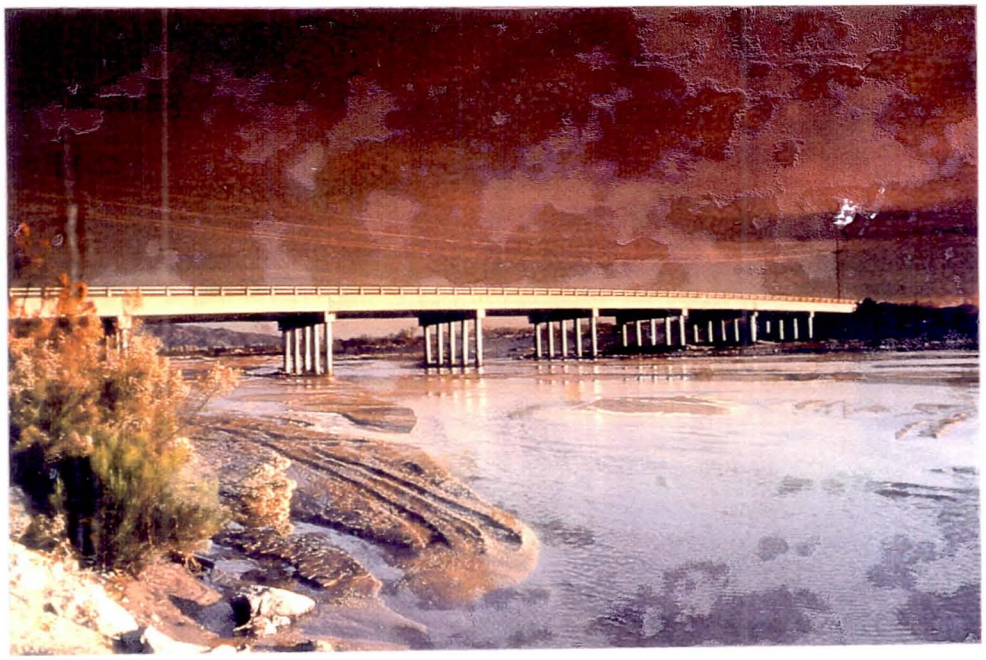

CASE STUDIES WITH THE COMPUTATIONAL MODEL

I A L L U V I A L

PREPARED BY:

JERRY R. JONES & ASSOCIATES, INC.

ENGINEERS PLANNERS SURVEYORS

DECEMBER 10, 1990

PREPARED FOR:

FLOOD CONTROL DISTRICT OF MARICOPA COUNTY

Property of
Flood Control District of MC Library
Please Return to
2801 W. Durango
Phoenix, AZ 85009

DYNAMICS OF ALLUVIAL-CHANNEL RESPONSE: CASE STUDIES WITH THE COMPUTATIONAL MODEL I A L L U V I A L

JERRY R. JONES & ASSOC. INC.
ENGINEERS*PLANNERS*SURVEYORS

PREFACE

The computer program IALLUVIAL, a state-of-the-art model for simulating water and sediment movements in alluvial channels, was developed by Dr. Fazle Karim under the overall guidance of Dr. John F. Kennedy, Professor and Director of the Institute of Hydraulic Research, University of Iowa. Some of the later developments of the model, including improvement in computational efficiency and streamlining of code, was contributed by Dr. Forrest M. Holly of the University of Iowa. Dooley-Jones & Associates (DJA) takes great pleasure in introducing IALLUVIAL for simulating dynamic response of the rivers in Arizona and the Southwestern region of the United States to man-made or natural changes in their water, sediment, or geometric characteristics.

In addition to IALLUVIAL, DJA maintains a competent staff of professionals capable of operating various other computer models, including HEC-1 (flood hydrograph), HEC-2 (water-surface profiles), HEC-5 (reservoir regulation), HEC-6 (water and sediment routing), FLUVIAL-11 (water and sediment routing), WQRRS (water quality), DAMBRK (dam break analysis), DWOPER (channel network), and Kentucky Pipe Network model. Several computer models have been developed in-house at DJA, e.g., SESCAL, HGRAPH, RRAP, PCHYD, HYDRO and COTHYD for hydrologic and hydraulic computations and plotting of results. DJA has performed numerous studies in the past by utilizing these models for the design and implementation of many water resources projects in the states of Arizona and California.

We are confident that the addition of IALLUVIAL to our growing list of computer models will enhance DJA's capability to analyze and simulate morphological characteristics of rivers and the impacts of various improvement works. We are proud of our past association, and look forward to working more closely with the various local, state, and federal agencies in Arizona and the Southwestern region of the United States in planning, design, and implementation of various water resources projects in the future.

Jerry R. Jones, P.E.
Executive Vice President

Roger E. Baele, P.E.
Vice President - Water Resources

DYNAMICS OF ALLUVIAL-CHANNEL RESPONSE: CASE STUDIES WITH THE COMPUTATIONAL MODEL IALLUVIAL

M. F. KARIM

DOOLEY-JONES & ASSOCIATES, INC.
35 E. TOOLE AVE., P.O. BOX 1830
TUCSON, ARIZONA 85702

SEPTEMBER, 1986
DJA JOB NO. 85-215

Rpt. A5

EXECUTIVE SUMMARY

Dynamics of alluvial-channel responses to natural or man-made changes in flow, sediment or geometric regimes are simulated by a computational model, IALLUVIAL, in three case studies. IALLUVIAL incorporates several state-of-the-art formulations of the underlying physical processes, e.g., ability to simulate flow resistances, without the need to specify Manning's "n" a priori; a sediment-transport relation verified for wide ranges of flow and sediment characteristics; consideration of subsurface sediment layers with different compositions; contributions of tributary sediment inflows and bank erosion; and bed armoring and sorting formulations based on the most recent understanding of the phenomena. The formulations incorporated in the model eliminate most of the deficiencies of existing erodible-bed models, which were pointed out in a comprehensive evaluation study by the National Research Council in 1983. Changes in bed and water-surface elevations and bed-sediment characteristics simulated by IALLUVIAL for the Salt and Missouri Rivers have been found to be in good agreement with the corresponding observed values. In particular, IALLUVIAL prediction of the Salt River bed evolution during 1977-83 was in much better agreement with the observed values than that of HEC-6. These applications validate the model as a reliable and useful tool for engineers in predicting dynamic responses (to natural or man-induced changes) of the sand-bed rivers, as well as of the gravel and cobble-bed, relatively steep-slope streams of the Southwestern region of the United States.

TABLE OF CONTENTS

		PAGE NO.
I.	INTRODUCTION	1
II.	THE COMPUTATIONAL MODEL: IALLUVIAL	4
III.	PREDICTION OF SEDIMENT TRANSPORT	7
IV.	PREDICTION OF FRICTION FACTOR	13
V.	CASE STUDY I: SALT RIVER 100-YEAR FLOOD	14
VI.	CASE STUDY II: SALT RIVER BED EVOLUTION, 1977-83	19
VII.	CASE STUDY III: MISSOURI RIVER DEGRADATION DOWNSTREAM OF GAVINS POINT DAM	26
VIII.	CONCLUSIONS	33
IX.	REFERENCES	34

I. INTRODUCTION

Dynamics of alluvial-channel response to natural phenomena or man's activities is complex and is only understood qualitatively. Satisfactory quantification of a river's self-adjustment process in response to man-induced perturbation of its sediment-transport equilibrium (e.g., sand and gravel mining, bridge and highway construction, channelization and realignment, river flow regulation by dams and reservoirs, etc.) or to natural variations in climatic, hydrologic, or sediment inputs during major floods or from year to year, remains a goal of river engineers throughout the world. Availability of fast computers during the last two decades has led to the development of mathematical models as additional tools to aid the engineers to evaluate and implement various river development projects, and to assess the impacts of such projects on the environment and the future evolution of rivers. In spite of their limitations, such models have proved to be invaluable tools in the hands of experienced engineers. This report describes salient features and applications of IALLUVIAL, a mathematical model developed at the Institute of Hydraulic Research, the University of Iowa, under the sponsorship of the U.S. Army Corps of Engineers (Omaha District), and the National Science Foundation. Computer code of IALLUVIAL has been updated by engineers at Dooley-Jones & Associates for application to the rivers of the semi-arid, southwestern region of the United States. The option to use geometric data in HEC-2 (or HEC-6) format has been added in this updated version.

Several erodible-bed numerical models, similar to IALLUVIAL, were evaluated by the National Research Council (1983) on behalf of the Federal Emergency Management Agency. In their recommendations, National Research

Council (1983) pointed out the following deficiencies of the models examined in their study (e.g., HEC2SR, KUWASER, UUSWR, HEC-6, FLUVIAL-11, and SEDIMENT-4H):

"a. Unreliable formulation of the sediment-discharge capacity of flows.

b. Inadequate formulation of the variable friction factor of erodible-bed flows, and, in particular, the dependency of friction factor on depth and velocity of flow, sediment concentration, and temperature.

c. Inadequate understanding and formulation of the mechanics of bed coarsening and armoring, and their effects on sediment-discharge capacity, friction factor, and degradation suppression of flows.

d. Inadequate understanding and formulation of the mechanics of bank erosion, and therefore, limited capability to incorporate this contribution into the sediment input to the flows from bank erosion and the effects of channel widening."

Development of IALLUVIAL was directed towards overcoming these dificiencies (specifically items a, b, and c) by incorporating state-of-the-art knowledge of the constituent physical processes. A brief overview and implementation of these features in the model are described in Sections II, III, and IV.

A numerical model is simply a quantification and solution of the mathematical formulas or relationships governing constituent physical processes; a model is as good as the accuracy of these relations in representing the actual physical processes. Two most important constituent processes in an erodible-bed model are simulations of sediment discharges and friction factors in alluvial-channel flows (as stated by items a and b of NRC's conclusions). In particular, computation of sediment discharges (which, in turn, strongly depend on friction factors), is the single-most important ingredient, because simulation of bed degradation/aggradation results essentially from a book-keeping process involving sediment-transport capacities at the two ends of a computational subreach. Accordingly, the capability of IALLUVIAL to simulate the sediment discharges and friction factors in alluvial channels is described in Sections III and IV. Three case studies are then presented in Sections V, VI, and VII, followed by conclusions in Section VIII.

II. THE COMPUTATIONAL MODEL: IALLUVIAL

Natural streams respond dynamically to natural or man-induced changes in hydrological, sediment and geometrical regimes. A river's self-adjustment process in response to such imposed or natural changes, in the process of restoring to a new quasi-equilibrium state, takes place in a variety of interrelated ways, e.g., changes in depth, velocity, width, slope, friction factor, sediment discharge, bed-sediment composition (coarsening or bed armoring), and channel-bed geometry. The program IALLUVIAL has been developed to simulate these river responses, both short-term and long-term.

IALLUVIAL is a quasi-steady, one-dimensional water-and sediment-routing model. It utilizes finite-difference numerical techniques to solve the governing equations of alluvial-channel flows, e.g., equations of water and sediment continuity (by size fraction), energy equation, and relations for sediment discharge and friction factor. The numerical technique used in the model for backwater (and sediment-discharge) computation includes two options: the standard-step method; and a more efficient and accurate Newton-Raphson scheme which solves simultaneously the equations of energy, water continuity, sediment discharge, and friction factor. A unique feature of IALLUVIAL is the employment of a coupled set of sediment-discharge and friction-factor relations, which incorporates the dependence of alluvial-bed friction factor on sediment discharge. The salient features of the model are summarized below:

* Incorporates a sediment-discharge relation developed from wide ranges of flume and field data; tested and verified for both sandy and gravel-bed streams.

* Dependence of friction factor on sediment discharge is incorporated through a coupled set of sediment-discharge and friction-factor relations. Specification of roughness coefficient, Manning's "n", is thus <u>not needed</u> in input data.

* Simulates sediment sorting and bed armoring. The model incorporates armoring procedures appropriate for both sand-bed and gravel-and cobble-bed streams.

* Effects of bed armoring on sediment discharge and friction factor are included.

* Computationally efficient for simulating long time periods.

* Option to use geometric data in HEC-6 format is included in updated version.

* Capable of utilizing contributions from tributaries and bank erosion.

* Vertical nonhomogeneity in size distribution of different sub-surface layers of bed sediments are accounted for in sediment-sorting procedure.

* Options for river-bed dredging/mining and externally imposed bed-width changes with time are included.

* Tested and verified for simulating observed degradation/aggradation/friction factor/armoring for rivers of Arizona.

Further study is underway at Dooley-Jones & Associates, Inc. to improve the model and incorporate additional features.

III. PREDICTION OF SEDIMENT TRANSPORT

The single most important ingredient in any numerical model for erodible-bed channels is satisfactory simulation of sediment-transport capacities at various channel sections representing a river reach. IALLUVIAL utilizes a coupled set of sediment-discharge and friction-factor relations, known as Total-Load Transport Model (TLTM). The formulation of TLTM takes into account the well-known fact that the friction factors of alluvial streams are heavily dependent on their sediment discharges, and avoids the need to specify a fixed hydraulic roughness, such as Manning's coefficient, a priori. In keeping with this concept, the friction-factor relation includes sediment discharge as one of the independent variables, and an iteration scheme is used to compute sediment discharge and friction factor from the following pair of equations:

<u>Sediment-discharge predictor</u>

$$\text{Log}\left(\frac{q_s}{\sqrt{g(s-1)D^3_{50}}}\right) = -2.278 + 2.972 \log V_1 + 1.006 \log V_1 \log V_3 + 0.299 \log V_2 \log V_3 \qquad (1)$$

<u>Friction-factor predictor</u>

$$\text{Log}\left(\frac{U}{\sqrt{g(s-1)D_{50}}}\right) = 0.102 + 0.269 \text{ Log } V_2 + 0.207 \text{ Log } V_4 - 0.178 \log V_3 + 0.173 \log V_5 \qquad (2)$$

where

$$V_1 = \frac{U}{\sqrt{g(s-1)D_{50}}} \; ; \; V_2 = \frac{d}{D_{50}}; \quad V_3 = \frac{u_* - u_{*c}}{\sqrt{g(s-1)D_{50}}} \; ;$$

$$V_4 = S \cdot 10^3; \quad V_5 = \frac{q_s}{\sqrt{g(s-1)D^3_{50}}} \; ;$$

q_s = volumetric bed-material discharge/unit width (includes both bed load and suspended load, but not wash load), U = mean flow velocity; d = mean flow depth; D_{50} = median bed-material size, S = energy slope; u_* = bed shear velocity; u_{*c} = critical shear velocity obtained from Shields' diagram; g = gravitational constant; and s = specific gravity of sediment particles.

Equations (1) and (2) were developed on the basis of physical and dimensional considerations, and the coefficients obtained from multiple-regression analysis of a large number (615 flows) of flume and river data. For given water discharge, energy slope, and sediment size, TLTM solves equations (1) and (2) simultaneously to obtain depth, velocity, friction factor, and sediment discharge. Application of TLTM to a large body (947 flows) of laboratory and field data yield satisfactory prediction of sediment discharges, as shown in Table 1. The ranges of relevant variables for the data base from which TLTM is developed are as follows:

	Minimum	**Maximum**
Depth (ft.)	0.10	17.35
Velocity (ft./sec.)	1.04	9.45
Slope	0.00015	0.024
D_{50} (mm)	0.13	28.65
Concentration (ppm)	20	49,300
Gradation Coeff.	1.00	1.96
Temperature (^oC)	0.6	38.0
Froude No.	0.09	2.08

TABLE 1
SUMMARY OF SEDIMENT-DISCHARGE AND
FRICTION-FACTOR RESULTS BY TLTM

Data Set	No. of Pts	Sediment Discharge Mean Ratio	Sediment Discharge Mean Norm.* Error (%)	Friction Factor Mean Ratio	Friction Factor Mean Norm.* Error (%)
Guy et al (.19mm)	29	1.45	69.3	1.00	40.6
Guy et al (.27mm)	17	1.51	52.4	0.80	41.1
Guy et al (.28mm)	32	1.36	52.1	0.97	35.9
Guy et al (.32mm)	29	1.97	102.9	0.74	33.0
Guy et al (.45mm)	27	0.95	37.0	1.18	48.0
Guy et al (.93mm)	23	1.07	24.5	0.80	25.1
Williams	24	2.12	112.5	0.85	18.4
Vanoni-Brooks	21	0.92	47.6	1.18	56.9
Missouri R.(Cat. A)	60	1.02	36.9	1.04	32.2
Missouri R.(Cat. B, C)	26	1.20	47.0	0.90	20.0
Missouri R. (RS)	17	1.07	48.9	1.28	33.7
Sato, et al (#1)	136	1.01	32.1	0.92	16.7
Meyer-Peter & Muller	41	0.90	39.7	0.96	15.9
Gilbert	43	0.70	35.0	0.81	35.4
Waterways Expt. Sta. (#1)	90	0.98	29.5	0.93	10.4
Willis-Kennedy	31	0.76	39.2	0.72	28.8
Missouri R. (Sioux City)	51	1.09	41.3	0.46	54.6
Middle Loup R.	45	0.80	31.9	0.80	35.4
Niobrara R.	25	1.72	72.6	0.56	43.7
ACOP Canals	34	0.63	44.6	0.84	29.2
Rio Grande	58	0.80	46.7	0.79	31.5
Elkhorn R.	23	0.35	67.2	0.92	25.4
Sato, et al (#2)	45	0.87	38.4	0.84	21.8
Waterways Expt. Sta. (#2)	20	1.18	45.9	0.93	13.6
All data	947		44.8		28.50

*Mean Normalized Error (%) = $\frac{100}{N} \sum_{i=1}^{N} \frac{|X_{mi} - X_{ci}|}{X_{mi}}$

Where: X_{mi} = measured value of ith flow

X_{ci} = computed value of ith flow

N = total number of flows

The validity of TLTM to predict sediment discharges of the ephemeral streams of Arizona was investigated. A difficulty in this task was the lack of availability of a complete set of sediment discharge and related hydraulic and geometric data for many rivers of Arizona. Even though a relatively large number of sedient-discharge measurements were made for some rivers, the associated data on sediment size distributions were not available, so that estimates of median bed-sediment size (D_{50}) or the portions of measured suspended discharges that are wash load cannot be made. After careful scrutiny, 21 data points from four rivers - San Pedro, Little Colorado, Virgin, and Gila - were found suitable for comparison of measured and computed sediment discharges. Graphical comparison of the measured and computed sediment discharges for these 21 flows are shown in Figure 1. Measured sediment discharges used in Figure 1 include measured suspended-sediment discharges (as reported by USGS), with adjustment made to exclude wash loads estimated from the measured size distributions of bed materials and suspended discharges. Bed load contribution, assumed as 10% of suspended loads, was added to obtain the "measured" total sediment discharges shown in Figure 1.

It is seen from Figure 1 that the computed sediment discharges agree reasonably well with the measured values. Considering the uncertainty and practical difficulties involved in field measurements and the assumptions that have to be made for estimating some quantities, prediction accuracy of TLTM for sediment-discharge capacities of these four rivers may be considered to be satisfactory. Notwithstanding the limited availability of data, this comparison demonstrates the validity of IALLUVIAL simulation of sediment

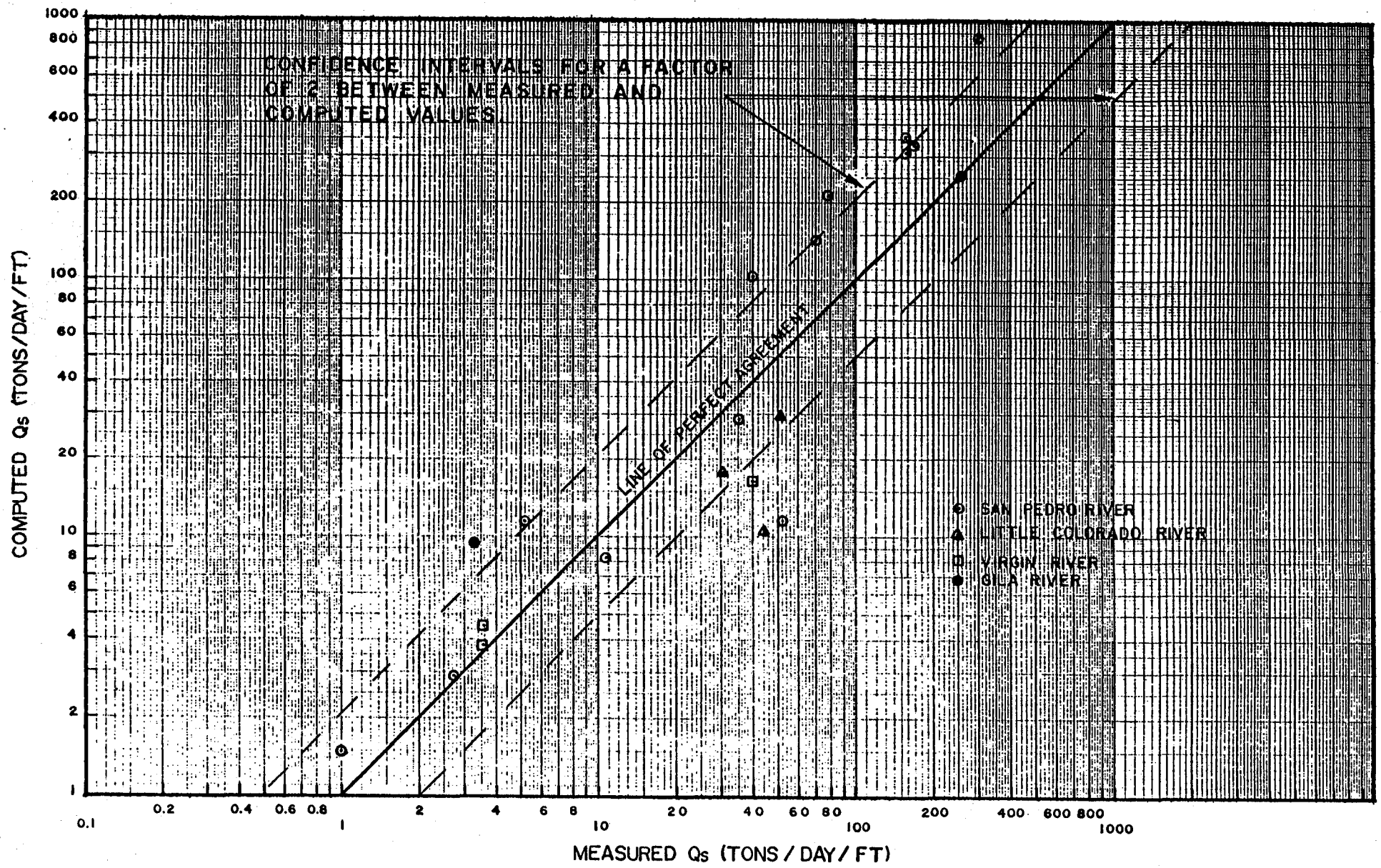

FIGURE I

COMPARISON OF MEASURED AND COMPUTED SEDIMENT DISCHARGES BY IALLUVIAL

CALC. BY F.K., DWN. BY R.H.F. (8-25-86)

discharges for Arizona rivers. It may be noted that, to the best of the author's knowledge, Figure 1 represents the first attempt to compare measured sediment discharges with the values computed by any sediment-transport model for these rivers.

In a recent study at the University of British Columbia, Vancouver, Canada, the sediment discharges predicted by TLTM for the Fraser River were found to be in better agreement with the measured values than those computed by other sediment discharge relations.

IV. PREDICTION OF FRICTION FACTOR

Accurate prediction of the variable friction factor in a movable-bed model is an important factor for valid simulation of sediment discharges and bed evolution over long periods. As discussed before, IALLUVIAL incorporates a friction-factor relation, eqn. (2), which accounts for the dependency of friction factor on sedment discharge. Thus, friction factor or roughness coefficient is continuously updated automatically in each time increment during entire simulation period, and the dynamic interdependence between flow and sediment characteristics, changing channel geometry, bed-form configuration, and roughness coefficient is properly accounted for. This is a significant improvement over the existing models, in which constant roughness coefficients, Manning's "n", are specified and treated as invariant with time.

The friction-factor relation included in IALLUVIAL was found to yield satisfactory prediction for a large number (947 flows) of flume and river data, as shown in Table 1. Relevant measured data are not available to check its validity for rivers in Arizona. However, an indirect validation of the friction-factor relation is presented in the next section in a case study for the Salt River, as demonstrated by the satisfactory prediction of the water-surface profile in Figure 4.

V. CASE STUDY I: SALT RIVER 100-YEAR FLOOD

The Salt River is located in Maricopa County, Arizona and is a tributary to the Gila River. The selected reach for this case study is the same as that used in the comparative analysis of six erodible-bed models by the National Research Council (1983). The study reach, shown in Figure 2, extends from just downstream of I-10 highway bridge to the Hohokam Expressway. Salt River experienced major floods in three years between 1978 and 1980. The 100-year design flood hydrograph, as shown in Figure 3, is used as the input hydrograph. This design hydrograph resembles closely the flood of February 1980, which had a peak flow of 185,000 cfs and a duration of 15 days. Bed-material sizes ranged from 0.22 mm to 185.0 mm, with the median size D_{50} approximately 60 mm. All input data utilized in this case study are the same as those used in NRC (1983) study.

Computed thalweg and water surface profiles simulated by IALLUVIAL are shown in Figure 4. Computed profiles by four other models (HEC2SR, HEC-6, FLUVIAL-11, and SEDIMENT-4H), also shown in Figure 4, are taken from NRC (1983) report. As observed data for this river reach are not available, Figure 4 compares the results simulated by IALLUVIAL with those obtained from four other models. It is seen from Figure 4 that water-surface profiles computed by all five models closely parallel each other, with the exception of HEC2SR which gives consistently lowest elevations. Computed thalweg profiles by different models, however, differ significantly from each other, with FLUVIAL-11 yielding considerably higher bed elevations than other models. Deviations at or near upstream boundary are likely due to somewhat different boundary conditions applied by different models.

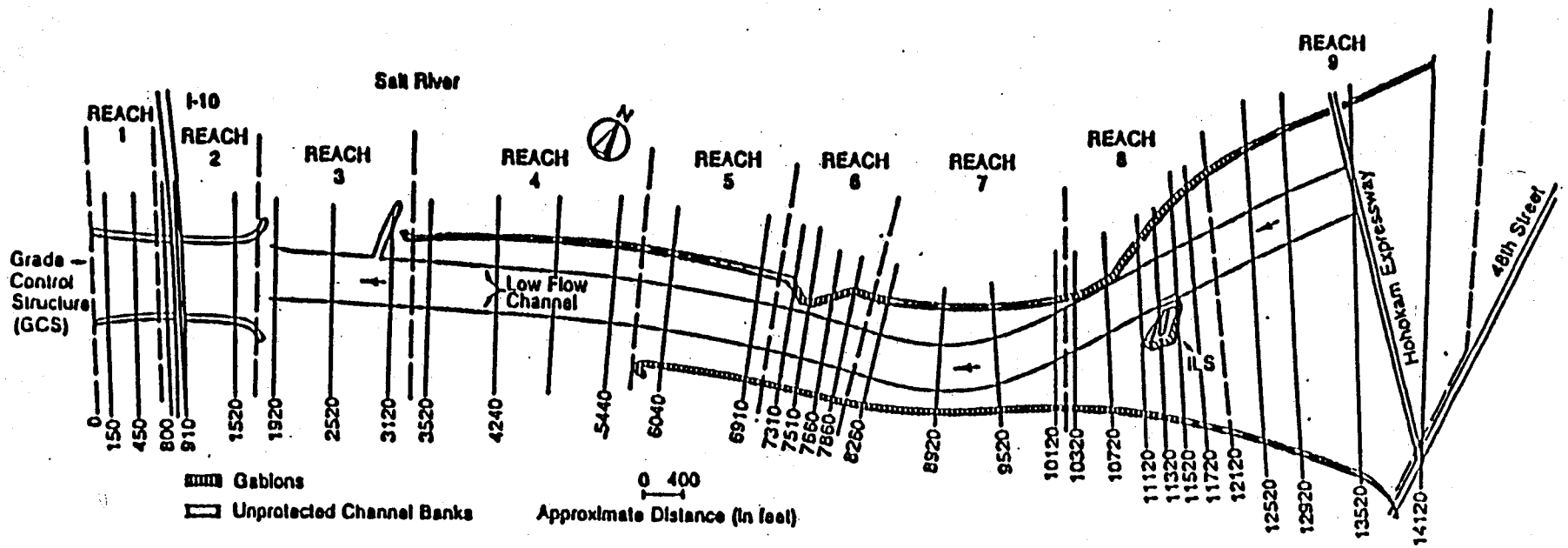

FIGURE 2 SALT RIVER REACH FOR CASE STUDY I (TAKEN FROM THE NATIONAL RESEARCH COUNCIL (1983)).

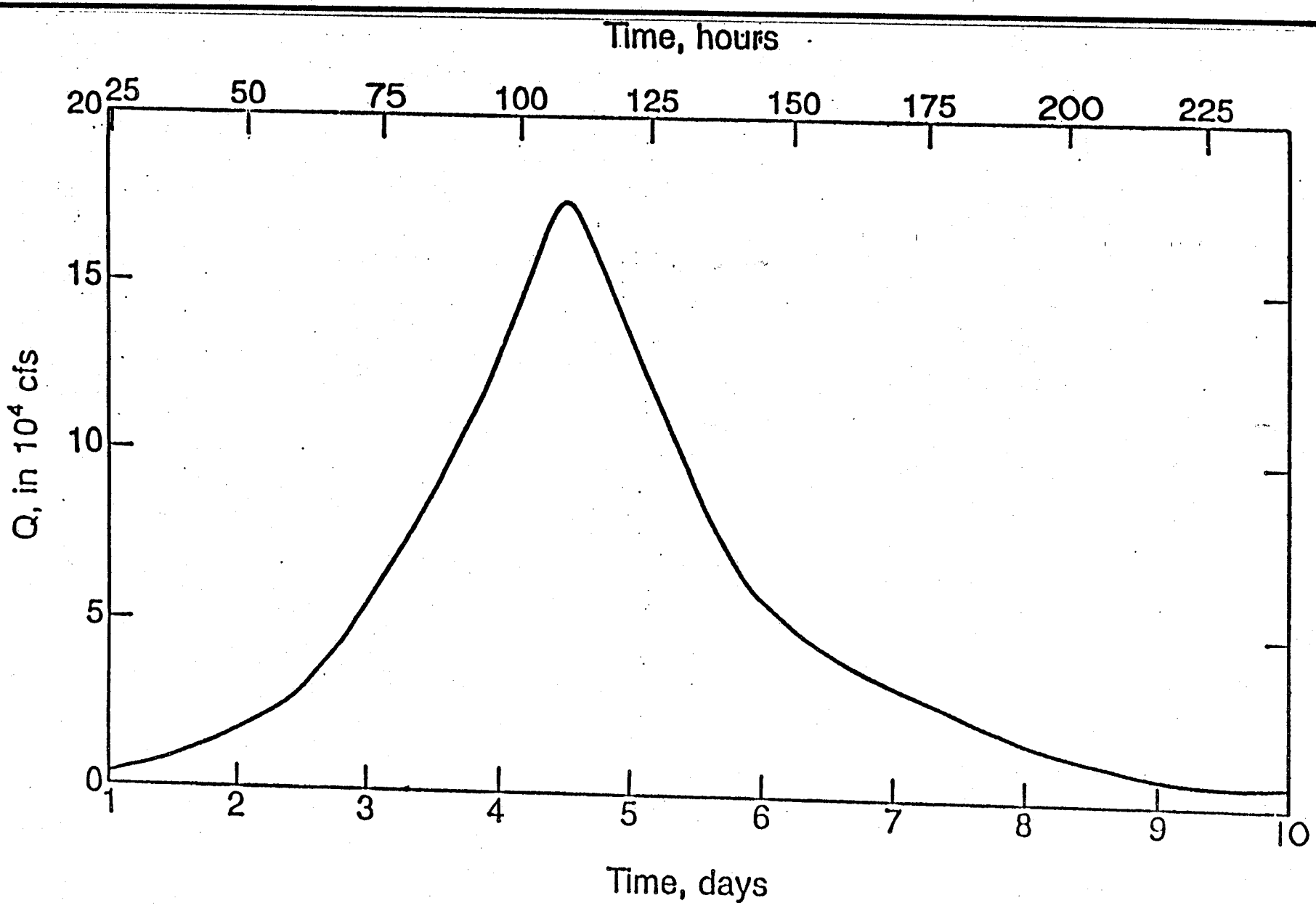

FIGURE 3
SALT RIVER 100-YEAR-FLOOD HYDROGRAPH

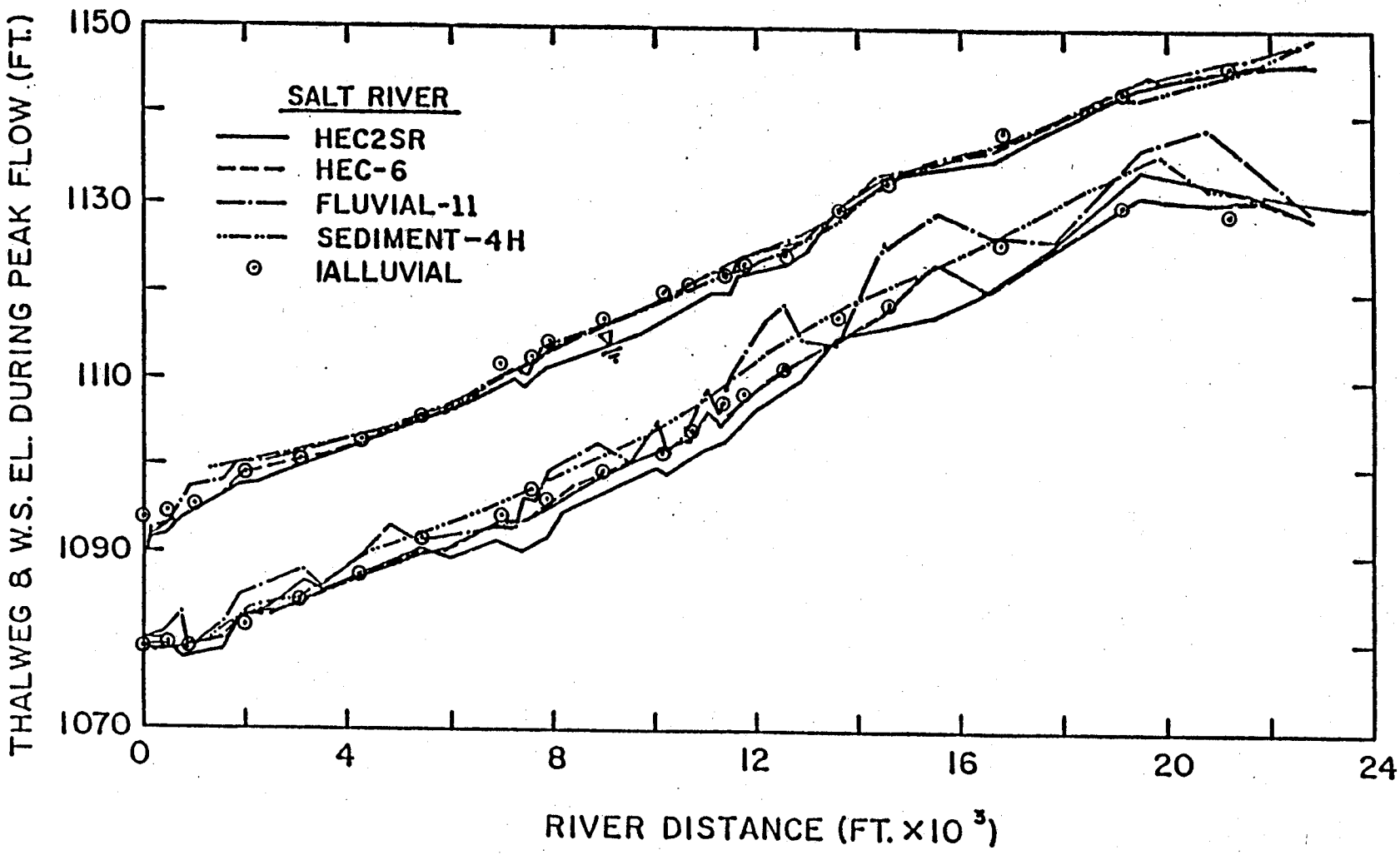

FIGURE 4 COMPARISON OF THALWEG AND WATER-SURFACE PROFILES AT PEAK FLOW COMPUTED USING IALLUVIAL AND FOUR OTHER MOVABLE-BED MODELS.

CALC. BY F.K., DWN. BY R.H.F (8-25-86)

The important point indicated by Figure 4 is that IALLUVIAL simulated water-surface elevations that are close to those computed by other models, even though pre-determined roughness coefficient (Manning's "n") as used by other models are not utilized (or necessary) in IALLUVIAL simulation. Two significant drawbacks of using fixed roughness (Manning's "n") are: (1) even though trial-and-error procedure of selecting Manning's "n" may reproduce closely measured water-surface elevations for a given flow condition, it is likely that the same "n" values are not applicable at other flow conditions during a long simulation period; and (2) computed depths, velocities, and energy slopes resulting from a backwater computation are fairly sensitive to Manning's "n" values while water-surface elevations are less sensitive to "n"; thus, "n" values calibrated on the basis of water-surface elevations may lead to significant errors in calculated depths, velocities, and energy slopes, and even larger errors in sediment discharges which strongly depend on these parameters. For example, "n" values calculated from friction factors given by IALLUVIAL simulation vary from approximately 0.02 to 0.04 at different sections, while a fixed value of 0.03 was used in HEC2SR simulation at all sections (Figure 4). It is likely that such differences in calculated depths and velocities, even though water-surface elevations are nearly the same, resulted in wide variations in computed sediment discharges and therefore in thalweg elevations, as shown in Figure 4 (of course, different sediment-discharge formulas utilized contributed partly to such variations). IALLUVIAL eliminates these shortcomings by incorporating dynamic dependence between flow resistence, hydraulic parameters, and changing bed elevations and sediment characteristics.

VI CASE STUDY II: SALT RIVER BED EVOLUTION, 1977-83

The Salt River reach for this case study, approximately 2 miles long, is located between 35th Avenue and 51st Avenue of the City of Phoenix, Arizona (Figure 5). This reach of the Salt River is the same as that analyzed by Dust, Bowers, and Ruff (1986) for application of HEC-6 model.

Portions of the study reach are braided as shown in Figure 6. The upper layer (1.5 to 2.0 ft.) of the river bed is composed primarily of sandy gravel and well-grounded cobbles (Figure 7), with localized pockets of fine to medium sand. Flow in the study reach of the Salt River is controlled by the Granite Reef Dam located approximately 20 miles upstream.

The simulation period covered in this case study is 1977-83. Geometric data, bed-sediment distribution and flow hydrograph are the same as utilized by Dust, Bowers, and Ruff (1986). Bed-material size distribution with D_{50} approximately 23 mm, measured from samples taken in the summers of 1983-84, was assumed to represent the initial (1977) conditions (since 1977 data were not available). As discussed in Sections IV and V, Manning's "n" values are not required as inputs to IALLUVIAL as a friction-factor predictor is included in its formulation. The 1977-83 study period of the Salt River reach had a total of approximately 180 days of flow, with four major flood events in February 1978, December 1978, January 1979, and February 1980. The input hydrograph representing the study period is shown in Figure 8.

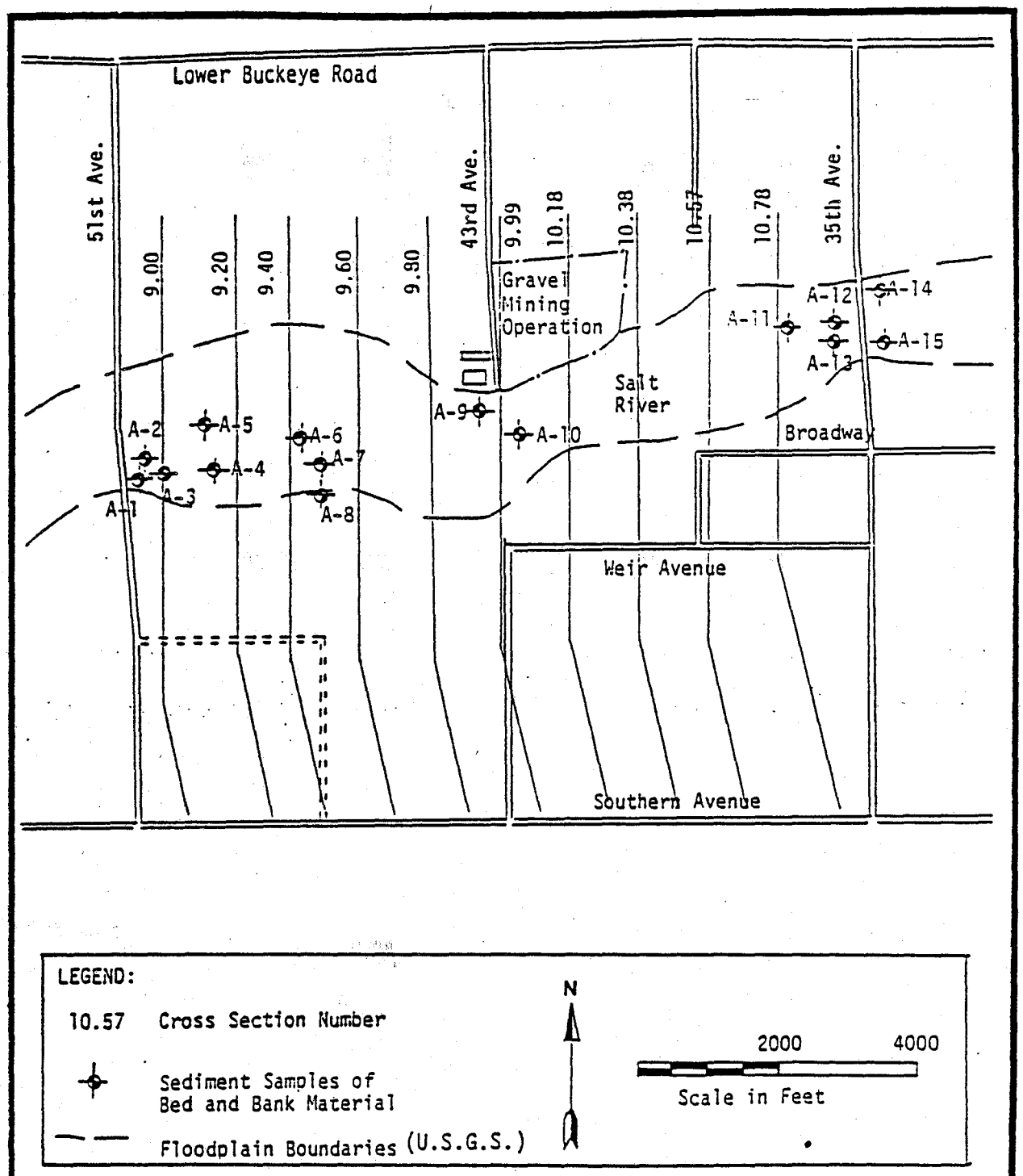

FIGURE 5 SALT RIVER STUDY REACH FOR CASE STUDY II (TAKEN FROM DUST, BOWERS, AND RUFF (1986)).

Figure 6. The Salt River at 35th Avenue; flow direction is from right to left (photograph by Larry Foppe, April 1983), (taken from Dust, Bowers, and Ruff (1986)).

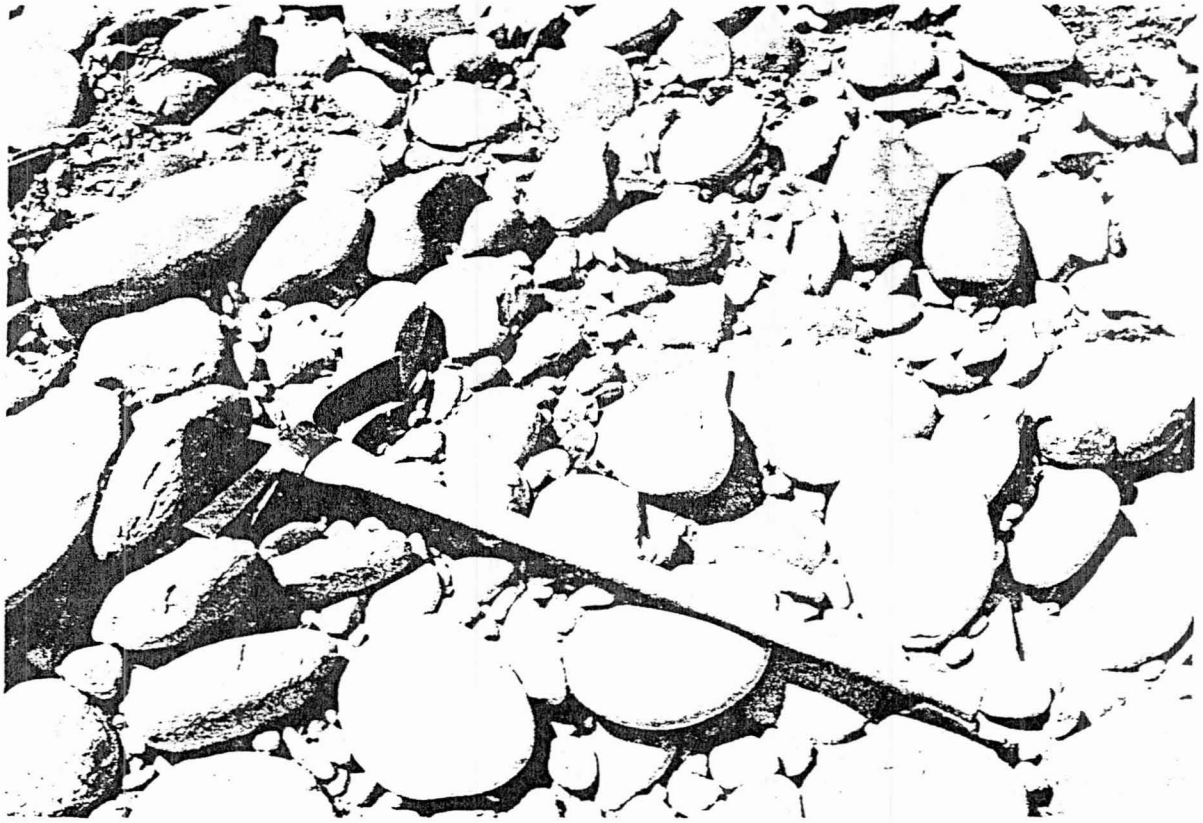

Figure 7. Close-up of Armored bed surface of the Salt River near cross section 9.20; flow direction is from left to right (photograph by David Dust, May 1984), (taken from Dust, Bowers, and Ruff (1986)).

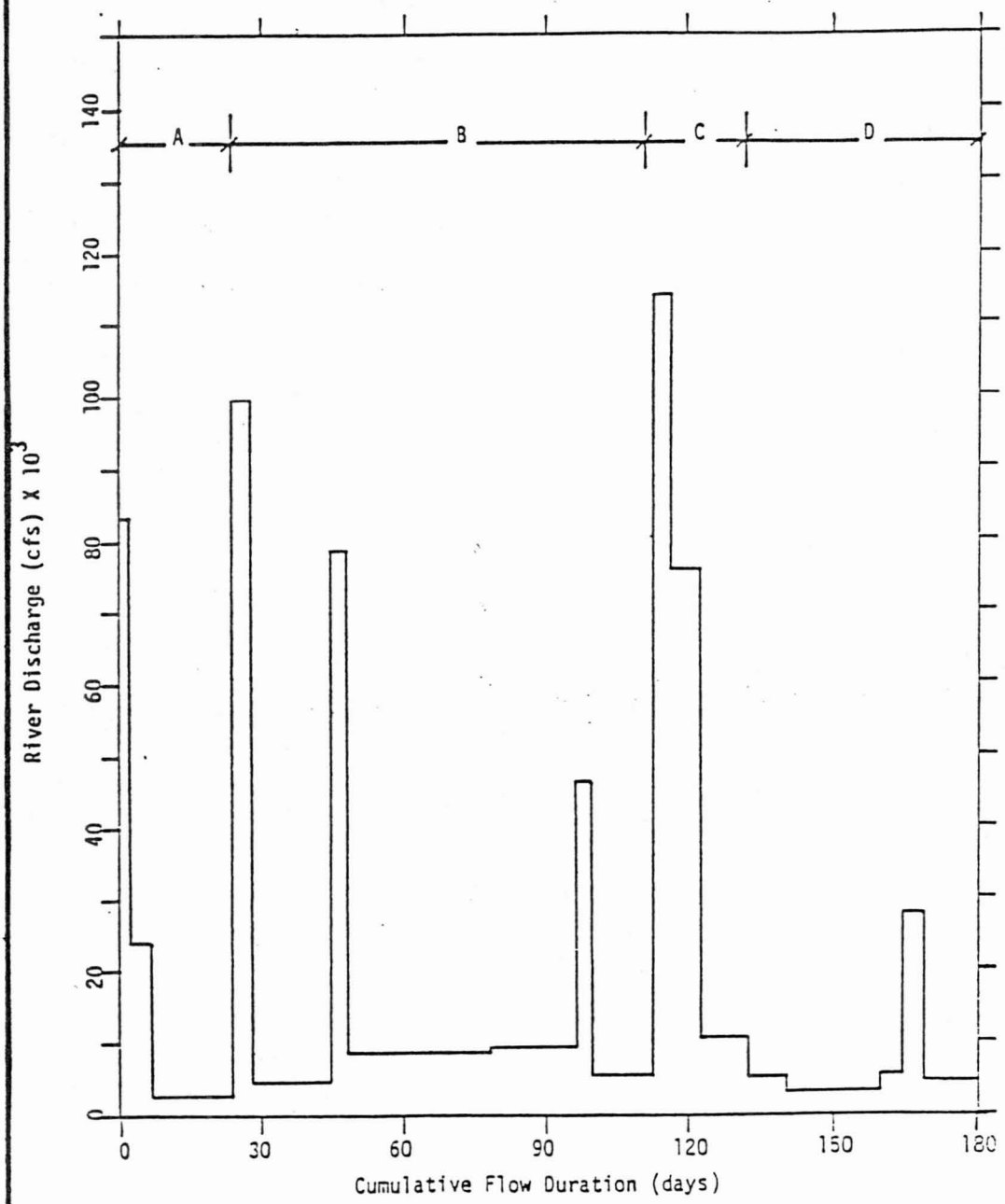

FIGURE 8: FLOW HYSTOGRAM FOR THE SALT RIVER INDICATING MAJOR FLOOD EVENTS, 1977-83 (TAKEN FROM DUST, BOWERS, AND RUFF (1986)).	A: Flood of Feb 28-Apr 11, 1978
	B: Flood of Dec 16, 1978-May 31, 1979
	C: Flood of Jan 29- June 3, 1980
	D: Flood of Dec 9, 1982-Feb 29,1983

The changes in bed elevation in the study reach of the Salt River computed by IALLUVIAL are shown in Figure 9. Also shown in this figure are the measured bed-elevation changes and those computed by HEC-6, which are taken from Dust, Bowers, and Ruff (1986). It is seen from Figure 9 that IALLUVIAL simulation is in good agreement with the measured bed-elevation changes, except at Sections 9.99 and 10.57. The discrepancy between measured and computed bed-elevation changes at these sections is likely due to the location of gravel mining operation in the vicinity and upstream of Section 9.99. In particular, a new main channel developed during the study period near Section 9.99 due to the diversion of flow through the gravel pit; this change of channel geometry is not included in input data set and, therefore, some discrepancy is expected at and in the vicinity of this section. In view of the uncertainties involved in the input data representing the study reach, the IALLUVIAL-simulated bed elevation changes of the Salt River reach, shown in Figure 9, appear to be in excellent agreement with the field measurements.

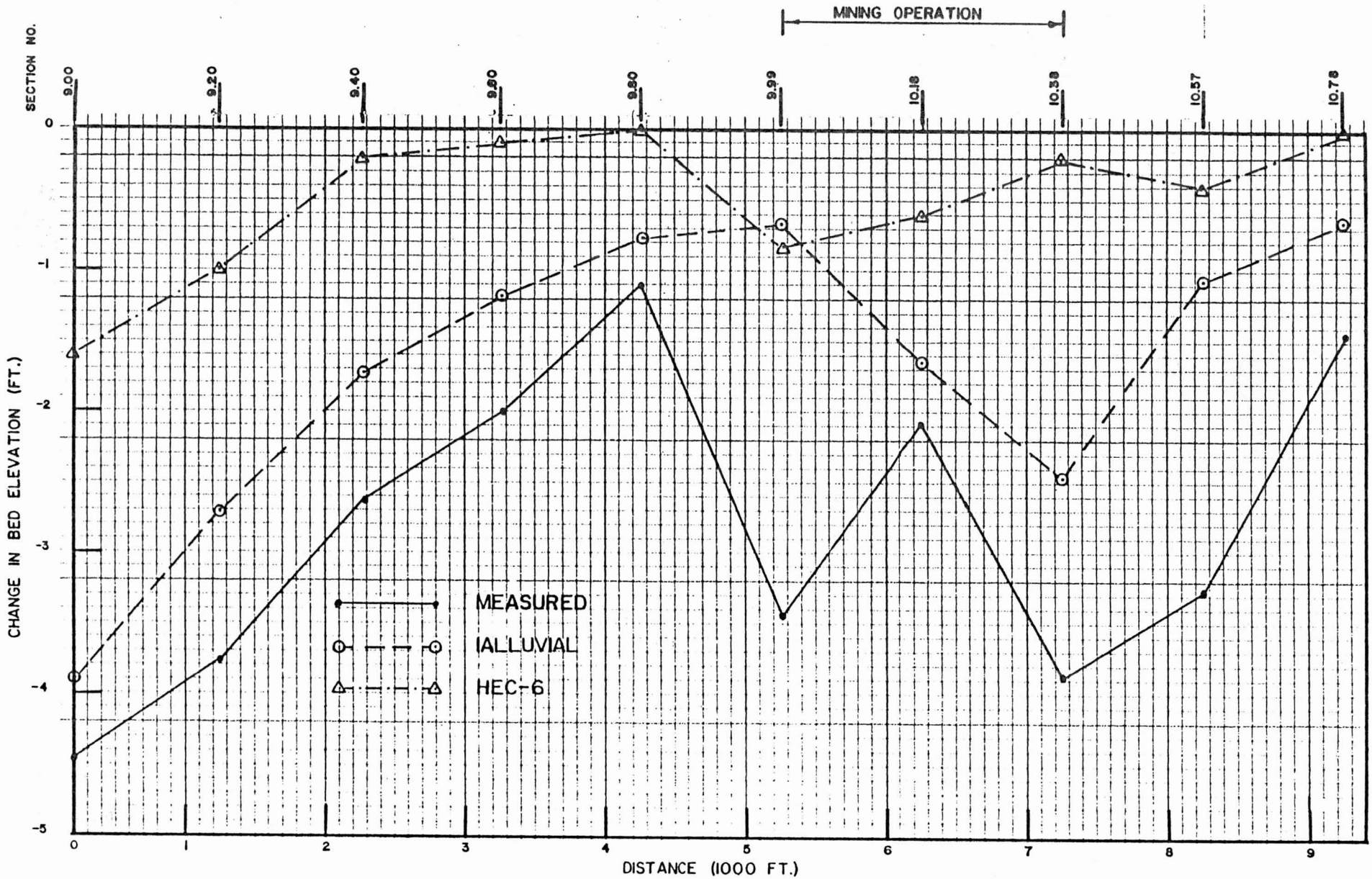

FIGURE 9 COMPARISON OF MEASURED AND COMPUTED BED-ELEVATION CHANGES OF THE SALT RIVER.

DSN. BY F. K., DWN. BY R. H. F. (8-23-86)

VII. CASE STUDY III: MISSOURI RIVER DEGRADATION DOWNSTREAM OF GAVINS POINT DAM

The Missouri River reach included in this case study is about 195 miles long, extending from Gavins Point Dam (RM 810.9) to Omaha (RM 615.9), Nebraska (Figure 10). Since the closure of the dam, in 1956, extensive channelization and bank-stabilization projects have been undertaken along this reach for the purpose of maintaining a navigation channel and other purposes. These activities have transformed a major part of this Missouri River reach from a wide sinuous channel containing numerous islands and bars (Figure 11), to a narrow, straightened channel of relatively uniform width, varying between 600 and 700 feet. The purpose of this case study is to simulate the impacts of the Gavins Point Dam and channelization works during the 20-year period (1956-76) since the closure of the dam in 1956.

Flow in the Missouri River reach is controlled by the Gavins Point Dam. Discharge is approximated by a two-step hydrograph: 36,000 cfs during the navigation season (April to November), and 15,000 cfs during the non-navigation season (December to March). Sediment inflows from eight tributaries joining this river reach and bank erosion from a 50-mile reach downstream of the dam are considered in simulation. The initial bed-material distribution utilized is the same throughout the reach, with D_{50} = 0.30 mm. Sediment concentration at the upstream boundary is zero, assuming complete entrapment of sediments by the dam.

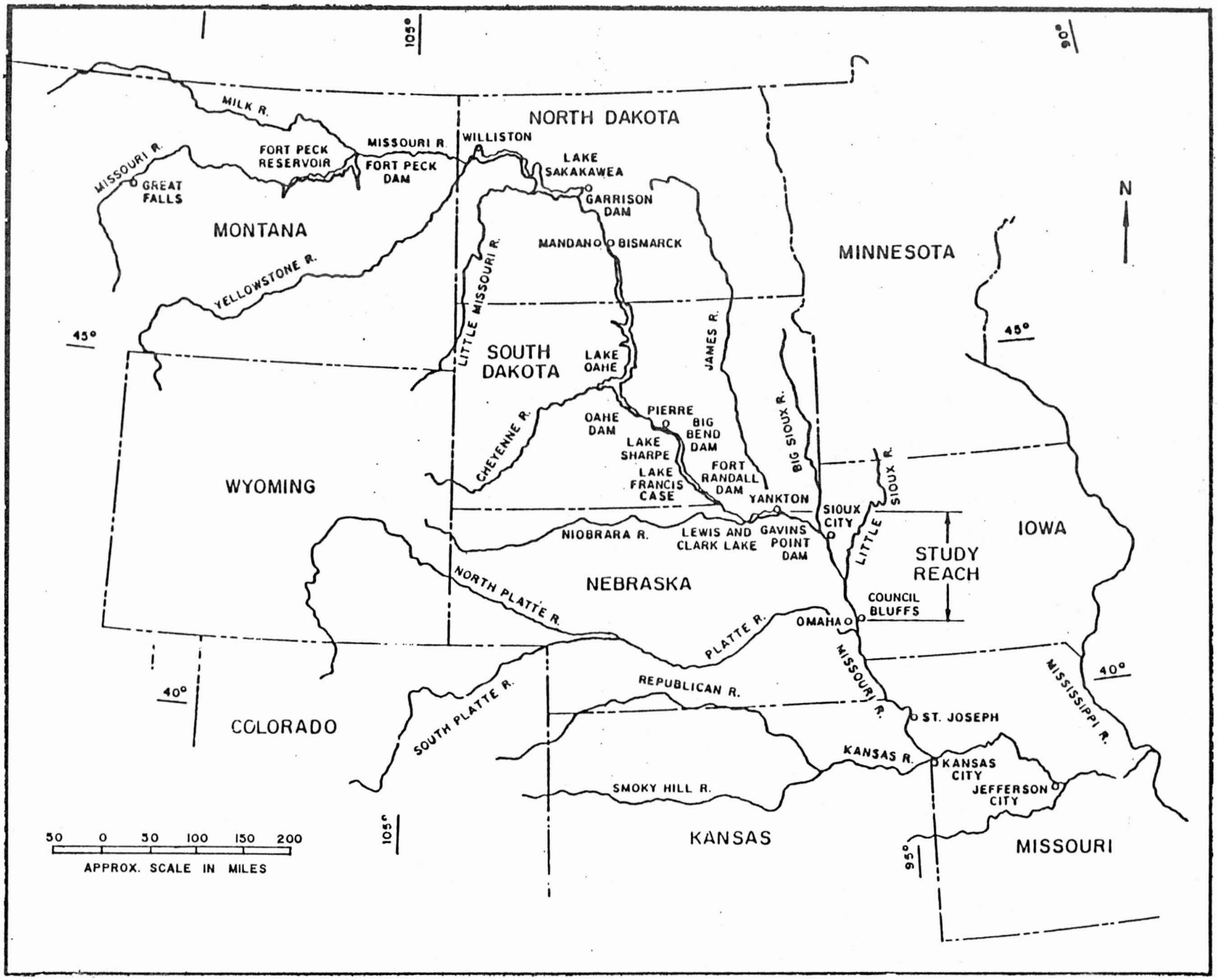

FIGURE 10 MISSOURI RIVER BASIN.

Figure 11. A view of the Missouri River about 4 miles downstream of the Gavins Point Dam, March 1980 (flow was nearly stopped by closing all gates of the dam).

Figure 12 shows excellent agreement between the measured and the computed changes in water-surface elevations after 20 years (1956-76) of simulation by IALLUVIAL (water-surface elevation changes were used in comparison, since data on bed-elevation changes were not available). Measured and computed median grain sizes (D_{50}) are plotted in Figure 13. Measured and computed D_{50}'s are in good agreement (Figure 13), except in a short reach near the dam; this discrepancy is believed to be due to field samples taken in this reach being mixtures of sediments from surface armor layers and the subsurface layers. Bed armoring of the Missouri River near the Gavins Point Dam, shown in Figure 14, was simulated satisfactorily by IALLUVIAL, as depicted in Figure 15.

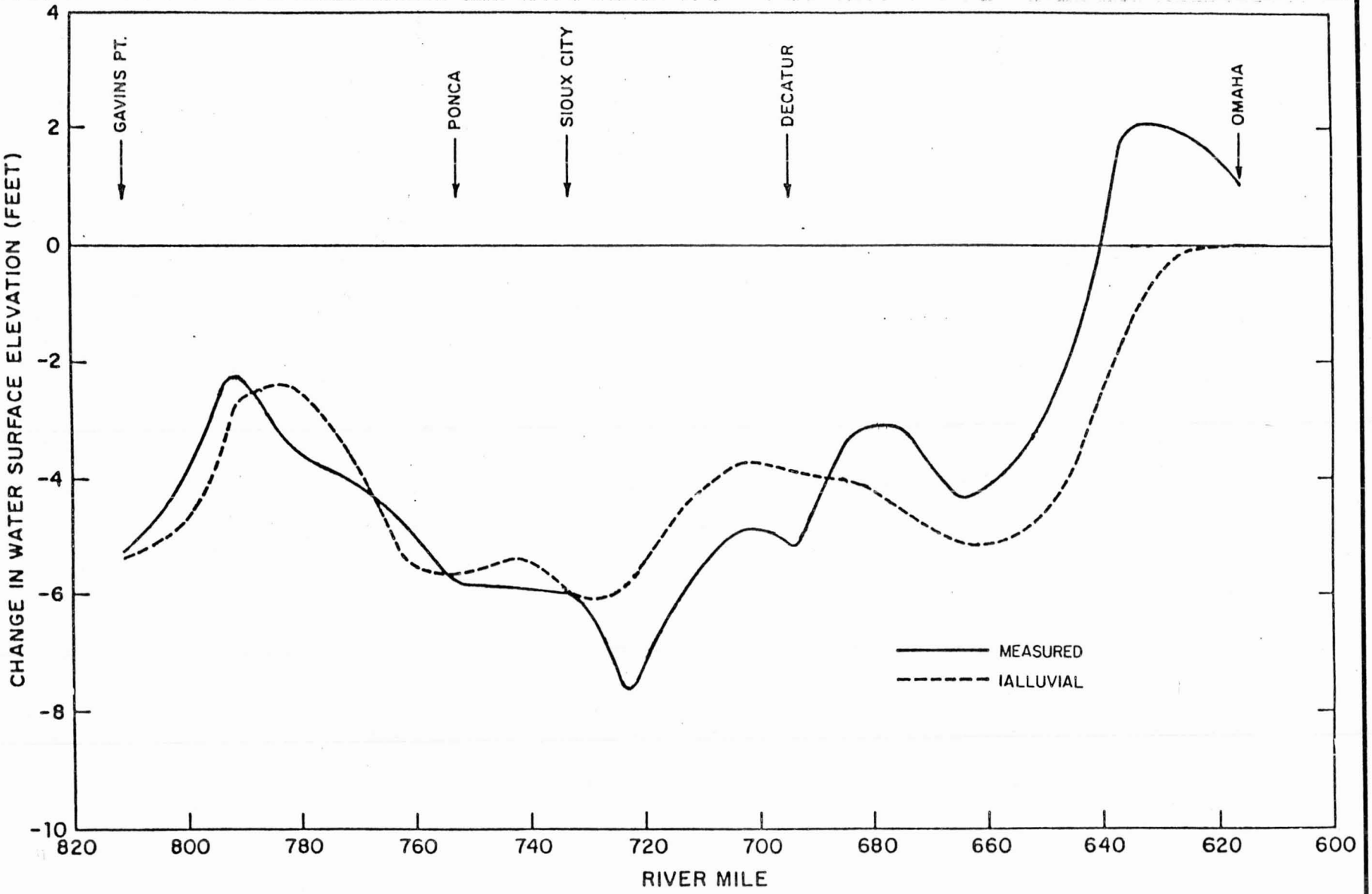

FIGURE 12 COMPARISON OF MEASURED AND COMPUTED CHANGES IN WATER-SURFACE ELEVATION AFTER 20 YEARS FOR THE MISSOURI RIVER.

CALC. BY F. K. , DWN. BY R. H. F. (8-25-86)

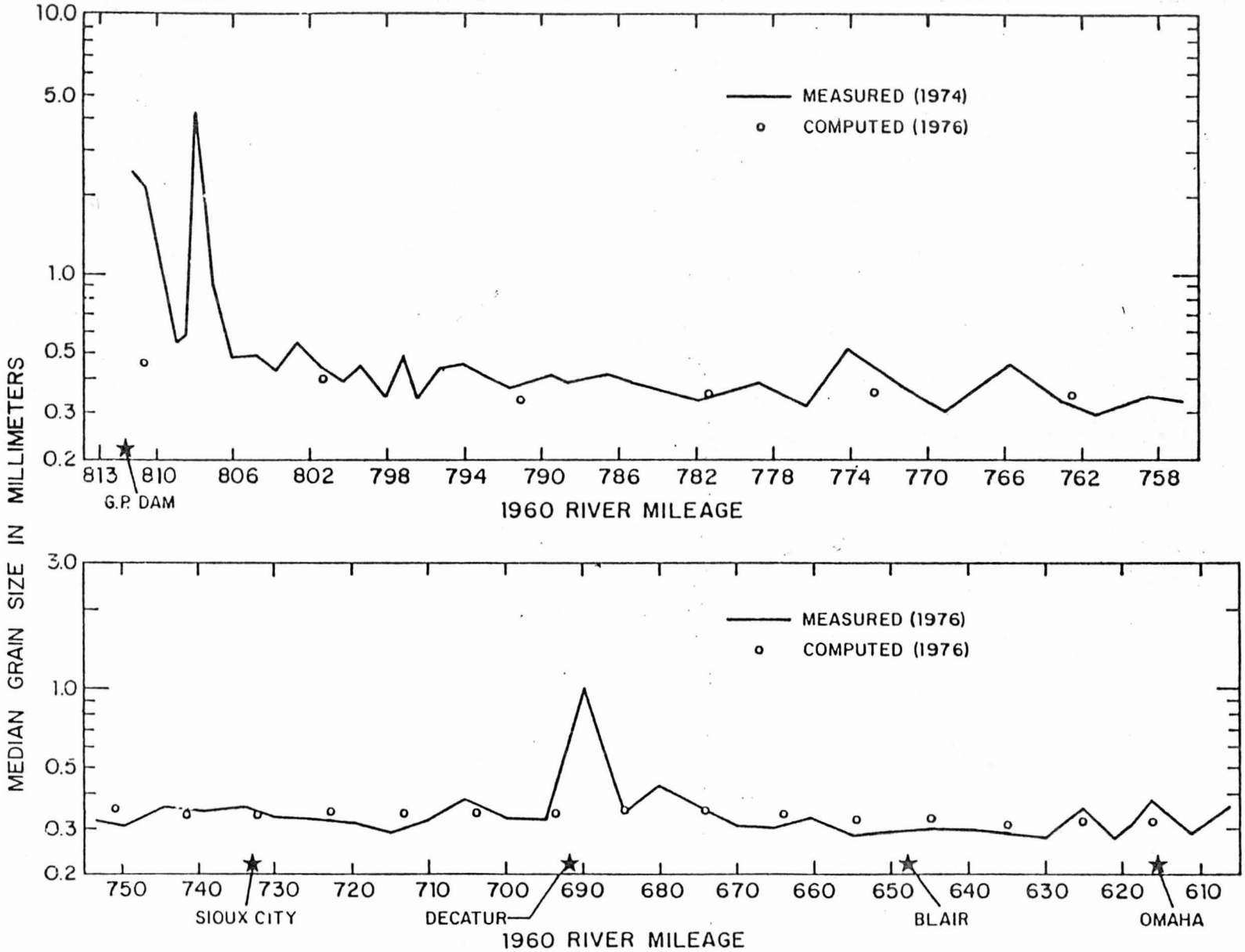

FIGURE 13 COMPARISON OF MEASURED AND COMPUTED MEAN BED-MATERIAL SIZES (D_{50}) OF THE MISSOURI R.

Figure 14. Photograph of the Missouri River bed armoring (March 1980).

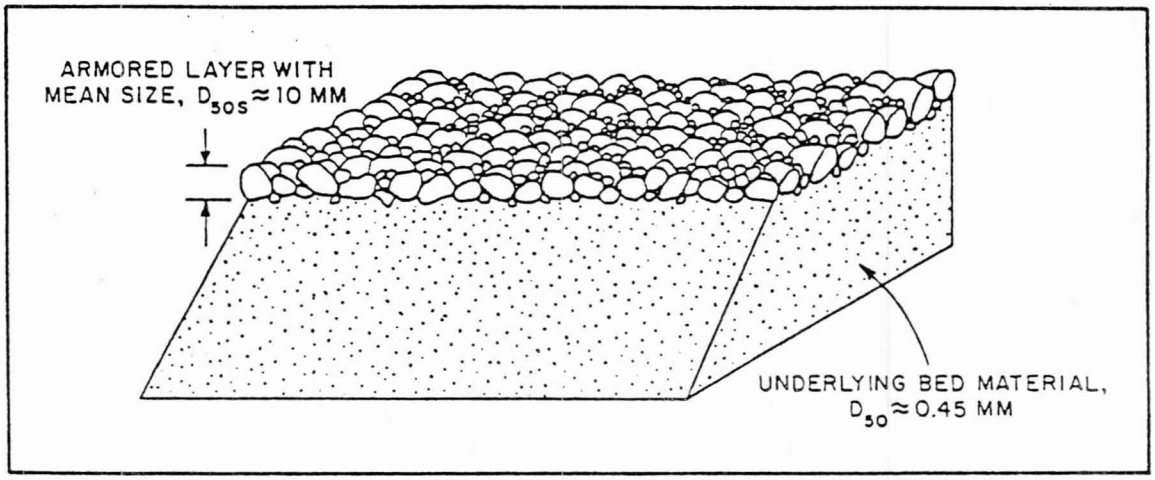

Figure 15. Schematic representation of armored bed near Gavins Point Dam, as simulated by IALLUVIAL.

VIII. CONCLUSIONS

Evolution of bed and water-surface elevations and bed-sediment characteristics in alluvial streams are simulated by IALLUVIAL in three case studies. IALLUVIAL incorporates several state-of-the-art features of alluvial-channel processes, e.g., ability to simulate flow resistance without the need to specify Manning's "n" a priori; a sediment-transport relation verified for a wide range of flow and sediment characteristics; nonhomogeneity of bed-sediment composition in the vertical direction (or subsurface layers with different compositions) are taken into consideration; contributions from tributary sediment inflows and bank erosion are included; formulation of bed armoring and sorting are based on knowledge gained from the most recent research investigations; and computationally efficient for both short and long-term simulations. These features are among the improvements which were recommended by the National Research Council (1983) for improving the existing erodible-bed models.

Changes in bed and water-surface elevations and bed-sediment characteristics simulated by IALLUVIAL for the Salt and Missouri Rivers have been found to be in good agreement with the corresponding observed values. These applications validate the model as a reliable and useful tool for engineers in predicting alluvial-channel responses to natural or man-made changes (e.g., sand and gravel mining, highway and bridge construction, channelization and realignment, river flow regulation by dams and reservoirs, etc.), for the sand-bed rivers, as well as for the gravel and cobble-bed, relatively steep-slope streams of the southwestern region of the United States.

IX. REFERENCES

Bowers, M.T., and Ruff, P.F., 1983, "An Evaluation of Computer Models to Predict the Erosion and Deposition of Sediment for Selected Streams in Arizona", Arizona State University, Tempe, Arizona, August 1983.

Dust, D. W., Bowers, M. T., and Ruff, P. F., 1986, "Application of HEC-6 to Ephemeral Rivers of Arizona", Arizona Department of Transportation, Phoenix, Arizona, January 1986.

Holly, F. M., and Karim, M. F., 1983, "Computer Simulation Prognosis for the Degradation of the Missouri River Between Gavins Point Dam and Iowa's Southern Border", Iowa Institute of Hydraulic Research, University of Iowa, Iowa City, Iowa, August 1983.

Karim, M. F., and Kennedy, J. F., 1982, "IALLUVIAL: A Computer-Based Flow- and Sediment-Routing Model for Alluvial Streams and Its Application to the Missouri River", Iowa Institute of Hydraulic Research, Report No. 250, University of Iowa, Iowa City, Iowa, August 1982.

Karim, M. F., and Kennedy, J. F., 1983, "Computer-Based Predictors for Sediment Discharges and Friction Factors of Alluvial Streams", U.S. Army Corps of Engineers, Missouri River Division, MRD Series No. 29, July 1983.

Karim, M. F., 1985, "IALLUVIAL: Analysis of Sediment Continuity and Application to the Missouri River", Iowa Institute of Hydraulic Research, Report No. 292, University of Iowa, Iowa City, Iowa, December 1985.

National Research Council, 1983, "An Evaluation of Flood-Level Prediction Using Alluvial-River Models", Committee on Hydrodynamic Computer Models for Flood Insurance Studies, National Academy Press, Washington, D.C.

United States Geological Survey, 1965, "Water Resources Data for Arizona", Part 2, Water Quality Records, U.S. Department of the Interior.

United States Geological Survey, 1966, "Water Resources Data for Arizona", Part 2, Water Quality Records, U.S. Department of the Interior.

United States Geological Survey, 1967, "Water Resources Data for Arizona", Part 2, Water Quality Records, U.S. Department of the Interior.

United States Geological Survey, 1969, "Water Resources Data for Arizona", Part 2, Water Quality Records, U.S. Department of the Interior.

United States Geological Survey, 1972, "Quality of Surface Waters of the United States, 1967", Parts 9-11, Water Supply Paper No. 2015.

SIMULATION OF MISSOURI RIVER BED DEGRADATION

by

Forrest M. Holly Jr.,[1], M. ASCE

and

M. Fazle Karim[2], A.M. ASCE

(submitted to

JOURNAL OF HYDRAULIC ENGINEERING, ASCE,

January 1985)

---

[1]Associate Professor, Department of Civil and Environmental Engineering; and Research Engineer, Iowa Institute of Hydraulic Research, The University of Iowa, Iowa City, Iowa 52242.

[2]Assistant Research Scientist, Iowa Institute of Hydraulic Research, The University of Iowa, Iowa City, Iowa 52242.

Key words: Missouri River; sedimentation; computational hydraulics; degradation; simulation.

Abstract: The future course of bed degradation in the middle Missouri River has been predicted using numerical simulation techniques. The simulation required development of the new Total Load Transport Model (TLTM) which incorporates the interdependence of friction factor and sediment transport through data-based empirical relations. TLTM was implemented in a mathematical simulation model called IALLUVIAL, which computes quasi-steady water and sediment flow in natural rivers having nonuniform bed sediments. IALLUVIAL also incorporates bed-sediment sorting and armoring, these being processes of fundamental importance to the future course of Missouri River degradation.

IALLUVIAL was first validated through simulation of the 1960-1980 severe degradation in the Missouri River between Sioux City, Iowa and Omaha, Nebraska. Subsequently IALLUVIAL was used to predict 1980-2000 degradation for several river-management scenarios. The simulations suggest that the worst of the degradation is now over, and that it is the channelization, rather than upstream regulation, which is primarily responsible for the degradation.

A companion paper describes the details of IALLUVIAL's armoring qand sorting simulation procedures.

Summary: Past and future bed evolution in the middle Missouri River between Sioux City, Iowa and Omaha, Nebraska has been simulated using a numerical model. Simulation methodologies and Missouri River predictions are presented.

Table of Contents

Page

I. INTRODUCTION.....1

II. SEDIMENT TRANSPORT AND FRICTION FACTOR RELATIONS.....2

A. Background.....2

B. Sediment Discharge Predictor.....4

C. Friction Factor Predictor.....7

D. Predicted Results with TLTM.....8

III. MATHEMATICAL REPRESENTATION OF BED EVOLUTION PROCESSES...9

A. Sediment Continuity Equation.....9

B. Flow Energy Equation.....11

C. Roles of Sediment Sorting and Bed Armoring.....12

IV. NUMERICAL SOLUTION PROCEDURE.....15

A. Backwater (Upstream) Sweep.....15

B. Bed Evolution (Downstream) Sweep.....16

C. Hydraulic Sorting Sweep.....18

D. Bed Armoring Sweep.....19

E. Iterative Coupling.....20

V. APPLICATION TO THE MISSOURI RIVER.....20

A. Problem Description.....20

B. Model Construction.....21

C. Model Verification.....22

D. Simulation Results and Discussion.....22

VI. SUMMARY AND CONCLUSIONS.....27

ACKNOWLEDGEMENTS.....27

APPENDIX A: References.....28

APPENDIX B: Notation.....32

LIST OF TABLES.....34

LIST OF FIGURES.....34

I. INTRODUCTION

The past three decades have seen the transformation of the middle Missouri River from its natural state of an unstable, heavily sediment-laden, shallow, unregulated stream into a stable, narrow, deep navigation channel with upstream control of water and sediment inflow. This transformation has admirably met its design objectives of providing for continuous navigation from Sioux City, Iowa to the mouth at St. Louis and of allowing reclamation of tens of thousands of acres of productive riparian farmland through bank stabilization and flood control. These benefits have, however, been accompanied by the inevitable environmental and morphological costs associated with the river's response to such major man-imposed changes to its natural equilibrium. The response of particular interest to the river engineer has been a severe scouring, or degradation, of the bed from about 20 miles upstream of Sioux City down to near Omaha, Nebraska. The structural and environmental consequences of this degradation, which has reached as much as eight feet (2.4 m) near Sioux City, are explored in (20).

The purpose of this paper is to describe the development of a numerical model for simulation of long-term bed evolution in a river having nonuniform bed sediment, and its application for guidance in anticipating, accommodating, and possibly arresting Missouri-River bed degradation in the affected reach. The model's development is focussed on several phenomena which are of particular importance to sediment-transport processes in the Missouri River:

* interdependence of sediment-transport capacity and bed roughness;

* gradual coarsening of near-bed sediments as fine particles are selectively removed;

* accumulation of non-transportable large particles on the bed surface to form an armor layer.

One must be circumspect about the completeness of several of the schematic conceptual models employed to represent these complex physical processes; nonetheless, the overall procedure produces surprisingly accurate reproductions of observed historical trends. The model has become not only a useful tool for river-engineering studies on the Missouri River, but also a valuable vehicle for continuing investigation and conceptualization of the relevant constituent processes.

A companion paper (13) presents the details of the armoring and sorting algorithms, for which only summary descriptions are provided herein.

II. SEDIMENT TRANSPORT AND FRICTION FACTOR RELATIONS

A. Background

The principal, and surely the most important, component of a numerical model for alluvial rivers is the mathematical representation of the sediment transport, friction factor, and their interactions with changes in both river-bed elevation and bed-

material size distribution. The dependence of the friction factor on sediment discharge has been well documented, yet no existing relation adequately describes this dependence. The first stage of the present study, therefore, involved the development of new sediment transport and friction factor relationships for application in the computer-based modelling of alluvial rivers.

All existing friction-factor relations, including those arising from the analyses reported in references (1, 2, 5, 6, 7, 16, 19, 22, 24), treat the friction factor or hydraulic roughness as being independent of sediment discharge. It is well known, however, that alluvial-channel friction factors are heavily dependent on sediment discharge. Indeed, it is this dependence that permits a river's variable water discharge to transport the even more variable sediment discharge delivered to the stream from its watershed. This dependence of friction factor on sediment discharge is illustrated in the results of the constant-discharge experiments reported by Kennedy (14). His data show that for a given slope, some flows can occur at up to three different combinations of depth and velocity, each with a different friction factor and sediment discharge. A similar interdependence between friction factor and sediment discharge is demonstrated by the constant-depth experiments of Vanoni and Brooks (21), and by the depth-discharge relation of the Rio Grande in New Mexico reported by Nordin (17). These examples, as well as a careful analysis of the underlying mechanisms which govern the interaction among the flow, the bed with its continuously changing geometry, and sediments transported by the flow, suggest that friction factors for sand-bed alluvial streams cannot be uniquely determined by water

discharge and energy slope; sediment discharge (or its intensity per unit width) must also be specified for unique determination of the friction factor.

Recent research at the Iowa Institute of Hydraulic Research has led to the development of two models which take into account the interdependence between friction factor and sediment discharge described in the preceeding paragraph (11). The Suspended- and Bed-Load Transport Model (SBTM) is based on detailed analysis of vertical distributions of velocity and concentration and includes predictors for friction factor, bed-layer concentration and velocity, bed-load discharge, and suspended-load discharge. The Total-Load Transport Model (TLTM) includes predictors for total sediment discharge and friction factor. Because of its simplicity and adaptability for computer applications, the TLTM was adopted for the present study; it is described in the following sections.

B. Sediment Discharge Predictor

The sediment-discharge predictor of TLTM was developed from regression analysis of an extensive data base comprising both laboratory experiments and field observations. The dimensionless total sediment discharge per unit width was expressed as a function of relevant independent variables through computer-based multiple regression analysis. Fifteen data sets, which included a total of 615 flows (of which 103 were field data) were used in the analysis.

Twenty independent variables, suitably non-dimensionalized, were formed from different combinations of seven basic quantities: flow depth (d), velocity (U), energy slope (S_m), median bed-material size

(D_{50}), bed-material gradation (σ_g), specific gravity of sediment particles (s), and kinematic viscosity of water (ν). Due consideration was given to the non-independence of several of the dimensionless groups in the course of analysis. To facilitate efficient nonlinear regression analysis, all variables were transformed into logarithmic forms, and to further investigate the non-linearity of functional relationships among the dependent and independent variables, additional variables were formed from double and triple products of these transformed variables. Thus, a large number of regression equations, with the dimensionless sediment discharge, $q_s/\sqrt{g(s-1)D_{50}^3}$ expressed as functions of various groups of independent variables, were formed (q_s = volumetric sediment discharge per unit width). These equations were evaluated using the following statistical criteria of multiple-regression analysis: multiple correlation coefficient, standard error of estimate, overall F-statistic, F-statistic for each independent variable, and standard error of the regression coefficient for each independent variable. The interested reader is referred to reference 11 for detailed descriptions of the statistical analyses. The following relation was found to have the best statistical characteristics among those examined, and was adopted as the sediment-discharge predictor:

$$\text{Log}\left(\frac{q_s}{\sqrt{g(s-1)D_{50}^3}}\right) = -2.2786 + 2.9719\ V_1 + 0.2989\ V_2 \cdot V_3 + 1.06\ V_1 \cdot V_3 \qquad (1)$$

in which

$$V_1 = \text{Log}\left(\frac{U}{\sqrt{g(s-1)D_{50}}}\right);\ V_2 = \text{Log}\left(\frac{d}{D_{50}}\right);\ V_3 = \text{Log}\left(\frac{u_* - u_{*c}}{\sqrt{g(s-1)D_{50}}}\right)$$

where u_* = bed shear velocity = $\sqrt{gdS_m}$; u_{*c} = critical bed shear velocity; and g = gravitational constant.

The data base from which Eq. (1) is derived has the following ranges for different measured quantities: depth between 0.10 ft and 17.35 ft (0.03 m and 5.29 m); velocity from 1.04 ft/sec to 9.45 ft/sec (0.32 m/sec to 2.88 m/sec); energy slope from 0.0015 to 0.024; D_{50} from 0.137 mm to 28.65 mm; σ_g from 1.00 to 1.96; water temperature from 0.6°C to 38.0°C; and Froude number from 0.09 to 2.08. Application of Eq. (1) beyond these ranges is subject to uncertainty.

The sediment discharge per unit width for the kth size fraction, q_{sk}, is obtained from q_s calculated by Eq. (1) and the following allocation relation:

$$q_{sk} = q_s \cdot P_k \frac{\left(\frac{D_{50}}{D_k}\right)^x}{\sum_{k=1}^{m} P_k \left(\frac{D_{50}}{D_k}\right)^x} \qquad (2)$$

in which

$$x = 0.0316 \sqrt{\frac{d}{D_{50}}} \qquad (2a)$$

where P_k = the quantity of bed material in the kth size interval, expressed as a fraction of the total; D_k = mean sediment size of the kth fraction; and m = total number of size fractions. The development of Eq. (2) is based on data analysis of the measured

suspended-sediment size distributions of the Missouri, the Niobrara, and the Middle Loup Rivers. D_{50} for these rivers varied from 0.18 mm to 0.40 mm, and σ_g ranged from 1.17 to 2.00. The validity of Eq. (2) beyond these ranges has yet to be established. It may be noted here that the total sediment discharge per unit width, q_s, can be obtained from Eq. (1) alone, while sediment discharge for each size fraction can be calculated from Eq. (2) and the estimate of q_s obtained from Eq. (1) or any other sediment discharge relation. Eq. (2) has been found to yield reasonably accurate predictions of the distribution of transported materials by size (q_{sk}/q_s) for flows transporting sediments predominantly in suspension (11).

C. Friction Factor Predictor

The dependence of the friction factor on sediment discharge in sand-bed alluvial channels has been demonstrated by laboratory experiments as well as field data. For a given water discharge and slope, the specification of sediment discharge is necessary to determine which of the various possible combinations of depth and velocity occurs. In keeping with this concept, the formulation of the friction factor relation of TLTM considers sediment discharge as one of the independent variables. The particle Froude Number, $U/\sqrt{g(s-1)D_{50}}$, is expressed as a function of various groups of dimensionless independent variables, using the same procedure described previously for the development of Eq. (1). The same procedure for evaluating the accuracy of different regression equations developed using the 615 flows led to adoption of the following relation as the friction factor predictor:

$$\log\left(\frac{U}{\sqrt{g(s-1)D_{50}}}\right) = 0.9045 + 0.1665\ V_4 + 0.2166\ V_5 \cdot V_6$$

$$+ 0.0831\ V_4 \cdot V_5 \cdot V_6 - 0.0411\ V_2 \cdot V_5 \cdot V_7 \qquad (3)$$

in which

$$V_4 = \log\left(\frac{q_s}{\sqrt{g(s-1)D_{50}^3}}\right);\ V_5 = \log\left(\frac{u_*}{w}\right);\ V_6 = \log\left(\frac{wD_{50}}{\nu}\right);$$

$$V_7 = \log\left(S_m \cdot 10^3\right)$$

where w = particle fall velocity of median bed-material size (as determined using Ruby's equation); and ν = kinematic viscosity of water. The range of applicability of Eq. (3) is the same as that described previously for Eq. (1). Although the friction factor does not appear explicitly in Eq. (3), it implicitly relates S_m to U and d through the Darcy-Weisbach equation.

D. Predicted Results with TLTM

Because of the dependence of the friction factor relation, Eq. (3), on sediment discharge, and the dependence of Eq. (1) on friction factor through S_m and U, simultaneous solution of Eqs. (1) and (3) is necessary to solve for q_s and friction factor (f). Any convergent iterative scheme, such as the Newton-Raphson method, can be employed for this purpose.

A comparison of predicted and measured values of sediment discharges and friction factors of 24 data sets (total of 947 flows)

is summarized in Table 1. In Table 1, Mean Ratio is the ratio of the computed to measured value; and Mean Normalized Error (%) is the average of the absolute deviations between the measured and computed values expressed as percent of the measured values. It may be noted that the last nine data sets (332 flows) in Table 1 were not used for the development of either Eq. (1) or Eq. (3). D_{50} for these 332 flows varied from 0.083 mm to 3.76 mm, σ_g ranged from 1.0 to 2.0, mean concentration varied from 9 ppm to 21,000 ppm, and Froude number ranged from 0.13 to 1.15. It is seen from Table 1 that the mean normalized error for all 947 flows for the sediment-discharge prediction is 44.8% and for the friction-factor prediction is 28.5%. The prediction accuracy of TLTM as illustrated by Table 1 has been found to compare favorably with several existing sediment discharge and friction factor relations. A more detailed analysis of TLTM's accuracy can be found in (11).

III. MATHEMATICAL REPRESENTATION OF BED EVOLUTION PROCESS

The TLTM sediment transport/friction factor predictor has been implemented in IALLUVIAL, a numerical model for the simulation of bed evolution in non-equilibrium alluvial rivers. The computational procedures are outlined in this section.

A. Sediment Continuity Equation

The central operation of IALLUVIAL is approximate solution of the sediment continuity equation (Exner's equation) to yield changes in bed elevation. This basic equation,

$$(1-p)\frac{\partial z}{\partial t} + \frac{\partial q_s}{\partial x} = 0 \qquad (4)$$

expresses the fact that in a control volume of unit width, any imbalance between sediment inflow and outflow must result in a change in bed elevation, z. In Eq. (4), p = porosity of sediment on the bed, x = streamwise coordinate, and t = time. In IALLUVIAL, Eq. (4) is somewhat modified for application to an entire cross section, and written in the following finite-difference form using Preissmann's (18) four-point discretization:

$$\overline{B}\,\frac{(1-p)}{2\Delta t}\,(z_{i+1}^{n+1} - z_{i+1}^{n} + z_i^{n+1} - z_i^{n}) + \frac{\theta}{\Delta x_i}\,(Q_{si+1}^{n+1} - Q_{si}^{n+1})$$

$$+ \frac{(1-\theta)}{\Delta x_i}\,(Q_{si+1}^{n} - Q_{si}^{n}) = 0 \qquad (5)$$

where the subscript i denotes computational points (the downstream boundary being the first point) on a one-dimensional, streamwise grid; superscript n denotes discrete time levels separated by Δt; B = channel width at the water surface; $Q_s = Bq_s$; $\overline{B} = \theta(B_i^{n+1} + B_{i+1}^{n+1})/2 + (1-\theta)(B_i^n + B_{i+1}^n)/2$; $\Delta x_i = x_{i+1} - x_i$; and θ is a weighting factor normally taken as 1/2. Equation (5) corresponds to a control volume which occupies the entire width of the channel, and for which z represents some representative bed elevation at each end. Solution of Eq. (5) yields z_i^{n+1} (the bed elevations at time $(n+1)\,\Delta t$) at all computational points i = 1,...,N. However Q_s and B are also unknown quantities at time $(n+1)\Delta t$. The water-surface width B depends directly on the water surface elevation y, and Q_s depends indirectly on y through the various hydraulic quantities appearing in TLTM, Eqs.

(1) and (3). Therefore to the simple model represented by Eq. (5) must be added the two-equation TLTM system and an appropriate water-flow equation.

B. Flow Energy Equation

IALLUVIAL is based on the assumption that water wave propagation effects can be ignored insofar as river-bed evolution is concerned. This so-called quasi-steady flow assumption, which has been formally justified for rivers which are not subject to tidal or other strong unsteady influence (4, p. 282; 15; 23), involves representation of mainstem and tributary inflow hydrographs as a series of constant discharges over discrete time intervals. The one-dimensional water flow is then presented by an ordinary water-surface profile (backwater) equation, written in discrete form as follows:

$$y_{i+1}^{n+1} + \frac{(U_{i+1}^{n+1})^2}{2g} = y_i^{n+1} + \frac{(U_i^{n+1})^2}{2g} + \frac{\Delta x_i}{2}(S_{ci}^{n+1} + S_{ci+1}^{n+1}) \quad (6)$$

in which S_c = composite energy slope, see below. Now the velocity U is given by Q/A, and under the steady flow assumption, the water discharge Q is known at any point. The cross-sectional area A, and the top-width B, are unique functions of the water level y and bed level z at any point (at least as long as the cross section shape at a point is assumed to be constant, as is assumed herein). Thus Eqs. (1) and (3) written for each of N computational points, and Eqs. (5) and (6) written for each of N-1 computational reaches, form a system of 4N-2 nonlinear algebraic equations. The unknown dependent variables at each of N points are y_i^{n+1}, z_i^{n+1}, Q_{si}^{n+1}, and S_{ci}^{n+1}, for a

total of 4N, leaving two additional relations needed to close the system. These are a downstream hydrodynamic boundary condition, typically imposition of a known water surface elevation y_1^{n+1}, and an upstream sediment boundary condition, typically imposition of a known volumetric sediment inflow rate, Q_{sN}^{n+1}. Solution of the complete nonlinear system for each time step is described in Section IV below.

C. Roles of Sediment Sorting and Bed Armoring

The above outline of a possible simulation procedure assumes that the median bed material particle size, appearing in Eqs. (1) and (3) as D_{50}, is known. But in fact D_{50}, which changes through hydraulic sorting as bed evolution proceeds, must also be considered to be a dependent variable. Moreover, hydraulic sorting may also lead to formation of an armor layer of coarse material on the bed surface, and this armor layer affects the hydraulic roughness and sediment transport capacity. Consequently the straightforward four-equation model outlined above is incomplete insofar as nonuniform sediment is concerned.

The details of the sorting and armoring procedures used in IALLUVIAL are described in a companion article (13). For the present discussion, it is sufficient to note that these procedures can be represented symbolically as

$$(D_{50})_i^n \rightarrow (D_{50})_i^{n+1} \tag{7}$$

and

$$\xi_i^n \rightarrow \xi_i^{n+1} \tag{8}$$

in which the arrows represent a volume accounting procedure, and ξ is the armoring factor, interpreted as the fraction of the bed surface covered by immobile particles, $0 \leq \xi \leq 1$. The evolution of D_{50} intervenes directly in the TLTM Eqs. (1) and (3); D_{50} is in fact the most important independent variable appearing in TLTM.

When the equilibrium sediment discharge entering a reach is reduced, the flow seeks to augment its diminished sediment supply by entraining sediment from the channel bed. The finer material is removed first, and the mean diameter of the affected bed layer is increased; this is the process known as hydraulic sorting or coarsening. The process continues until the bed becomes partially or wholly armored. Coarsening and armoring both tend to reduce the sediment-transport capacity of a flow, and thereby act to restore equilibrium between the sediment-transport capacity and the reduced sediment-supply rate into the reach. Both also reduce the height and steepness of the bed forms on rippled and duned beds, and thus also reduce the bed-form roughness of the channel. However, coarsening increases the grain roughness. All sediment-transport relations, including TLTM, have been developed from data sets for streams with little or no bed armoring. Moreover, the most reliable of the data--those from laboratory flumes--are from flows in bed-material-size equilibrium (i.e., not undergoing coarsening). It is, therefore, difficult to quantify how bed-surface armoring affects the sediment discharge and bed roughness. It is assumed in IALLUVIAL that sediment discharge is reduced in direct proportion to the fraction of the bed-surface area that is armored (i.e., covered with material which cannot be transported by the flow). Thus, the transport capacity Q_s appearing in Eq. (5) is actually obtained from

$$Q_{si}^{n+1} = B_i^{n+1}(1 - C_1\xi_i^{n+1})q_{si}^{n+1} \qquad (9)$$

with the parameter C_1 normally taken to be 1.0.

The effect of armoring on the friction factor arises from the fact that the hydraulic roughness of the armored portion of the bed is essentially different from the rest of the bed, which is characterized by an active state of sediment transport and often deformed through the presence of ripples and dunes. The interaction between the armor particles and the moving-bed roughness is complex and not yet fully understood or mathematically formulated. Of particular significance is the effect armoring has on the bed-form geometry; specifically, armoring generally diminishes the height and steepness of ripples and dunes. It is assumed in the present study that the resistance of the armored portion of the bed may be approximated by a fixed-bed friction-factor relation (the Colebrook-White relation, for example), and that the composite friction factor, f_c, of the flow may be expressed as

$$f_c = f_a\xi + f_m(1-\xi) \qquad (10)$$

in which f_a is the friction factor corresponding to the mean size of the non-moving armor material (determined using the Colebrook-White relation) and f_m is the moving-bed roughness contribution appearing in TLTM. The Darcy-Weisbach equivalence of energy slope and friction factor is, for Eqs. (1) and (3),

$$S_m = \frac{f_m U^2}{8gd} \tag{11}$$

and for Eq. (6),

$$S_c = \frac{f_c U^2}{8gd} \tag{12}$$

IV. NUMERICAL SOLUTION PROCEDURE

In formal mathematical terms, the armoring and sorting processes add two new dependent variables - ξ_i^{n+1} and D_{50i}^{n+1} - to the nonlinear algebraic system of equations comprising the model. However the two associated additional relations, Eqs. (7) and (8), are not algebraic equations, but complex accounting processes as described below. Therefore it is no longer possible to consider, even in principle, a formal algebraic solution of the complete model in one time step. Instead, an iterative procedure based on a fractional step approach must be employed.

The fractional step algorithm involves successive, independent execution of the following four operations in each iteration of each time step: 1) backwater sweep, Eqs. (1), (3), and (6); 2) bed evolution sweep, Eq. (5); 3) bed-material sorting, Eq. (7); 4) bed armoring, Eq. (8).

A. Backwater (Upstream) Sweep

Once the flow conditions at any point i are known, Eqs. (1), (3) and (6) form a system of three nonlinear equations in the three unknowns q_{si+1}^{n+1}, y_{i+1}^{n+1}, and S_{mi+1}^{n+1}, using values for D_{50i+1}^{n+1}, ξ_{i+1}^{n+1}, and z_{i+1}^{n+1} which are the most recently available, either from the previous

iteration or the previous time step. The upstream sweep is initiated using the imposed value of y_1^{n+1}, and values of q_{s1}^{n+1} and S_{m1}^{n+1} resulting from simultaneous solution of Eqs. (1) and (3) by Newton-Raphson iteration. These values are used to calculate y_2^{n+1}, q_{s2}^{n+1}, and S_{m2}^{n+1} through Newton-Raphson solution of Eqs. (1), (3), and (6), and so on up to i = N.

B. Bed Evolution (Downstream) Sweep

Once the bed elevation is known at point i+1, Eq. (5) can be solved directly for z_i^{n+1} using values for B and Q_s (through Eq. (9)) which resulted from the preceding backwater sweep. The bed level at the upstream limit of the model, z_N^{n+1}, is computed through use of the imposed sediment inflow, Q_{sN}^{n+1}. The procedure, a generalization of one described by Cunge (3), implements the physical requirement that the channel bed level must ultimately change in such a way that its sediment transport capacity is equal to the imposed load. For example, if the imposed load is zero, then the channel must deepen until the transport capacity is zero; this becomes the mechanism for computing the bed level change at the upstream point.

This straightforward physical principle must be slightly modified to account for the fact that the channel cannot instantaneously adjust to a change in the imposed load. Instead, it is assumed that some local degradation or aggradation due to imbalance between the imposed and transportable load can occur in a special computational reach $\beta\Delta x$ adjacent to the upstream limit. One seeks the bed elevation change which satisfies a special sediment continuity equation written for the "buffer" reach,

$$\{\theta(\overline{Q}_s^{n+1} - \tilde{Q}_s^{n+1}) + (1-\theta)(\overline{Q}_s^{n})\}\Delta t = \beta\Delta x B_N(1-p)\Delta z_N \qquad (13)$$

in which $\overline{Q}_s$ = imposed sediment load at the upstream boundary, $\tilde{Q}_s$ = TLTM-derived sediment-discharge capacity at the downstream end of the buffer reach, B_N = some appropriate width, and Δz_N = change in bed elevation of reach $\beta\Delta x$ (and point N) in time Δt. The bed level change Δz_N is expressed as

$$\Delta z_N \doteq z_N^{n+1} - z_N^{n} = y_N^{n+1} - d_N^{n+1} - z_N^{n} \qquad (14)$$

Here the water surface elevation y_N^{n+1} is known from the latest backwater sweep, and the previous bed elevation z_N^n is also known, leaving the depth d_N^{n+1} as an unknown in Eq. (14). Since $\overline{Q}_s^{n+1}$ and $\overline{Q}_s^n$ are given, and $\tilde{Q}_s^n$ is known from the previous time step, the only remaining unknown is $\tilde{Q}_s^{n+1}$, which can be thought of as the sediment transport capacity at the downstream end of the reach $\beta\Delta x$ with the armoring factor taken into account, i.e. $\tilde{Q}_s^{n+1} = B_N(1-\xi_N^{n+1})\,\tilde{q}_s^{n+1}$. Again, one can consider $\tilde{q}_s^{n+1}$ as a function only of d_N^{n+1} through the TLTM sediment discharge predictor, Eq. (1), all parameters other than d_N^{n+1} being known from the most recent backwater sweep and sorting/armoring operations. Consequently Eq. (13) reduces to a nonlinear algebraic equation in the single unknown d_N^{n+1}, whose value can be determined through a Newton-Raphson iteration.

It is instructive to note that if one suppresses the buffer reach by setting $\beta = 0$, then the procedure outlined above simply requires that the bed level adjust immediately so that the TLTM sediment

discharge capacity at point N becomes equal to the imposed load. If $\beta > 0$, then the effect is to require the TLTM capacity to approach, but not equal, the imposed load, the difference being absorbed in aggradation or degradation in the buffer reach.

The value of $\beta\Delta x$ is guided by the physical principle that the length of the buffer reach should correspond roughly to the distance travelled by a bed perturbation in time Δt. Denoting the bed perturbation celerity by c, this yields

$$\beta = c\Delta t/\Delta x \tag{15}$$

The value of c is difficult to ascertain exactly, and depends on changing flow conditions and sediment composition. Current research at the Iowa Institute of Hydraulic Research is directed toward developing estimators for c. For the Missouri River, c would appear to be the order of 10 miles per year. However, the procedure does not appear to be particularly sensitive to β, as is shown in (10).

Once the bed level at the upstream point has been determined, a normal sediment continuity equation is applied to $(1-\beta)\Delta x$ for use in ultimately determining z_{N-1}^{n+1}. In its present form, this equation uses the imposed load $\overline{Q}_s^{n+1}$ as inflow to the shortened reach, though an equally plausible argument could be made for using $\tilde{Q}_s^{n+1}$. It is implicitly assumed - and virtually always true - that $0 \leq \beta \leq 1$.

C. Hydraulic Sorting Sweep

Once the overall change in bed elevation has been computed for each point in the bed evolution sweep, an accounting procedure is

applied to each computational reach (i.e. each river segment between adjacent computational points) to compute the change in bed material composition. This rather tedious procedure is described in detail in (13).

At the completion of the sorting computation for each reach, the updated particle size distribution $p_{i,k}^{n+1}$ is used to compute the new median particle size for each reach. Finally, the point values D_{50i}^{n+1} are taken as weighted averages of the two adjacent reach values, with D_{501}^{n+1} and D_{50N}^{n+1} set equal to the median size in the single adjacent reach.

D. Bed Armoring Sweep

Armoring of the bed surface for each computational subreach is updated at the end of each iteration. Following the procedure described in (13), the contribution of each size fraction to the armor layer is calculated. The increase (or decrease) of the areal coverage of the armoring particles for each size fraction, as a result of the incremental degradation in the current time period, is added to the cumulative value computed at the end of the previous time step, ξ_i^n, to obtain the updated armoring factor, ξ_i^{n+1}. These reach values are then averaged to obtain the armoring factor at each computational point, where they are used in the next time step to modify sediment discharge and friction factor characteristics as described earlier.

E. Iterative Coupling

Iterative repetition of the above four processes results in convergence to a solution in which the values of Q_s^{n+1} and B^{n+1} appearing in Eq. (5) reflect the use of D_{50}^{n+1}, d^{n+1}, ξ^{n+1}, S_m^{n+1}, etc. in Eqs. (1), (3) and (6). It is of interest to note that for uniform sediments, i.e. when neither sorting nor armoring occur, the physical coupling between Eqs. (1, 3, 6) and Eq. (5) is only through bed elevation changes, resulting in such weak interdependence that iterations are not needed. It is for nonuniform sediments, when additional coupling occurs through D_{50} and ξ, that iterations are generally necessary.

V. APPLICATION TO THE MISSOURI RIVER

A. Problem Description

Since 1960, bed elevations in the Missouri River between about Sioux City and Omaha (see Fig. 1) have been steadily decreasing. This degradation, which has attained as much as eight feet near Sioux City, Iowa (20) and is accompanied by a concomitant drop in water-surface elevation, has caused, or is threatening to cause, severe environmental and structural problems. These include loss of wildlife habitat, shrinking of oxbow lakes as the flood-plain water table declines, undermining of bridge and bank-protection structures, decrease in water-intake efficiency, etc.

Most of this reach of the Missouri River has been significantly altered from its natural state. The closure of six major multi-purpose dams, the most downstream of which is Gavins Point Dam (Fig. 1), has greatly reduced the frequency of extreme high or low flow

events, and virtually shut off the downstream release of sediment. Concurrent with the period of dam construction (1930-1965), the Missouri River navigation channel was completed from Ponca State Park, Nebraska downstream to the mouth at St. Louis, Missouri. Stabilization of the channel involved construction of an extensive system of spur dikes designed to provoke accretion of sediment from the natural bankline inwards, effectively creating a navigation channel at least 9-ft (2.7-m) deep and 600 feet (183 m) wide. The river from Gavins Point Dam down to Ponca State Park is still in its natural topographical state, having an average width of some 2,500 feet (762 m).

B. Model Construction

Attempts to simulate the channel degradation using IALLUVIAL have been motivated on the one hand by a desire to ascertain to what extent the reservoir construction and channelization projects might be responsible for the degradation, and on the other hand by a need to forecast the future course of degradation under various river-management scenarios. A preliminary modelling effort, carried out in conjunction with IALLUVIAL development (12), adopted a schematic representation of the channel as rectangular, assumed constant initial bed material properties throughout the reach, and neglected tributary and bank erosion effects. The initial channel and sediment characteristics were taken as those prevailing at the time of dam closure in 1957. The 205-mile (330-kilometer) reach from Gavins Point Dam to Omaha, Nebraska was broken into 22 computational subreaches for application of IALLUVIAL. The upstream boundary

condition consisted of a repeated, two-stage annual hydrograph of 36,000 cfs (1020 cms) for the 8-month navigation season, and 15,000 cfs (425 cms) for the remainder of the year, schematically reproducing the actual regulated releases from Gavins Point Dam, with zero sediment inflow. The downstream boundary condition was an approximate water surface elevation, imposed at a fictitious station far enough downstream not to affect the flow from Omaha on upstream.

C. Model Verification

The schematic model was run for twenty years (1960-1980) with a time step of 30 days, to simulate the simultaneous processes of bed degradation, bed material coarsening, and armoring. Figure 2 is a summary comparison of observed and computed water surface and bed elevation changes after 20 years. The simulation reproduced the overall pattern of bed evolution, including the apparent shift to aggradation near Omaha, quite faithfully, although local differences in water surface elevation of as much as 4 feet (1.2 m) can be seen in the zone where aggradation begins, between Blair and Omaha.

D. Simulation Results and Discussion

The demonstrated success of IALLUVIAL in reproducing the general historical trends of Missouri River bed degradation led the Iowa State Water Resources Research Institute to support modelling efforts focussed on a prognosis of future bed degradation. The schematic model data set of the 1960-1980 simulation was replaced by one incorporating all available data on 1980 channel topography, bed-sediment size distribution, tributary and bank erosion rates (treated

in the model as sediment inputs to the natural channel above Ponca State Park). The model was extended to below the Iowa-Missouri border, and incorporated water and sediment inflow from nine major tributaries as shown on Fig. 3. The tributary water inflows were schematized as repeated annual two-stage hydrographs, four months of spring high flow and eight months of low flow, yielding the correct mean annual flows. The tributary sediment inflows were obtained from power-law total load rating curves, developed from analysis of historical data available from the U.S. Army Corps of Engineers and the U.S. Geological Survey. After removal of the fine (washload) material, these inflow loads were allocated by size fraction based on historical suspended-load size distribution analyses.

The changes in water-surface and thalweg profiles at the end of the base 20-year prognosis run are shown on Figure 4. These results show that apart from an additional two feet (0.6 m) of degradation in the immediate vicinity of Gavins Point Dam, (compared to 4.2 feet (1.3m) computed in the earlier 1960-80 study), very little additional degradation is forecast to occur in the uncontrolled reach from the Dam down to Ponca. However in the controlled reach from Ponca to Omaha, as much as four feet (1.2 m) of additional degradation is expected to occur, being most severe near Sioux City and Decatur Bend. This is to be compared to the 7.2 feet (2.2 m) computed near Sioux City in the 1960-80 simulation. Below Omaha the model predicts continung aggradation; the large inflow of the Platte River (River mile 595) causes a backwater in the Missouri which provokes deposition of transported sediments, and the Platte itself delivers a sediment load which is coarser than that transported by the Missouri,

causing formation of a local delta. A general degradation trend resumes below Plattsmouth.

If one considers the Missouri River bed degradation to be the river's response to an imposed change in its geometry and sediment supply, then one can think of the degradation as a mechanism for transition from a former (undisturbed) equilibrium to a new one. The new state of equilibrium will be reached when, for any given subreach, the sediment transport capacities at its downstream limit is sufficient to carry the mainstem, tributary, and bank-erosion inflow to the reach, both globally and for individual size fractions. Although one thinks naturally of local and overall slope adjustments as one of a river's mechanisms for reaching a new equilibrium, it is clear from Fig. 4 that the overall slope is insignificantly changed by the degradation. Of far more importance for the Missouri's return to equilibrium are bed coarsening and armoring. This is demonstrated on Fig. 5, which shows longitudinal profiles of median bed material size D_{50} and armoring factor at the beginning and end of the simulation. The armoring factor was set to zero throughout the model initially, effectively ignoring the computed (and actual) armoring which had taken place in the 1960-80 period. (Because of this initial condition used in the model, the predicted degradation depths should be considered as upper-bound estimates.) After twenty years the computed armoring factor reaches a maximum of about 0.6 in the vicinity of Sioux City, then decreases gradually toward Omaha. The abrupt increase to about 0.2 near Plattsmouth reflects the deposition of relatively coarse material delivered by the Platte. At Gavins Point Dam, the armoring factor is

a relatively low 0.34; the approach to equilibrium below the dam has been dominated by a coarsening of the mixed layer material rather than by armoring *per se*.

The initial profile of median bed material size distribution shown on Fig. 5 corresponds to the 1980 field data used. The median size is seen to be close to 0.3 mm from Gavins Point Dam down to the vicinity of Plattsmouth, where the Platte's coarser deposited load causes it to increase locally toward 0.5 mm. After the 20-year simulation, the greatest increase in D_{50} is seen below Gavins Point Dam, where the dominant mechanism is apparently hydraulic sorting. In the remainder of the model, sorting has caused a general coarsening of the order of 0.1 mm, though some areas show no significant change at all.

The base simulation described above was complemented by several others designed to test the sensitivity of future degradation to alternative river-management schemes, the more interesting of which are as follows:

Run S2: An out-of-basin diversion was simulated by reducing the Gavins Point Dam water release by 3 million acre feet per year, i.e., 4,100 cfs (116 cms) distributed uniformly over the annual cycle.

Run S4: The effect of the channelization was simulated by widening the navigation channel from 600 ft to 800 ft (183 m to 244 m).

Run S5: The navigation channel was further widened to 1000 ft (305 m).

Run S8: The effect of artificial armoring as a means of locally retarding severe degradation was studied by increasing the amount of bed material between 2.4 mm and 19.1 mm by about 10%, schematically simulating the dumping of fine gravel onto the bed.

Run S9: The potential reduction in degradation which could be obtained by modulating Gavins Point Dam releases was studied by constantly releasing the mean annual discharge of 29,000 cfs (822 cms).

Figure 6 shows the evolution in time of the thalweg elevation at Sioux City for Runs S2, S4, S5, S8 and S9, with the base run S1 shown for comparison. The initial rapid degradation for all runs is caused by the use of an initial armoring factor at zero. It is apparent that all the runs seem to reach a kind of equilibrium from two to six years; then all but Run S5 show the effects of the arrival of the degradation wave from upstream. The asymptotic approach to a new equilibrium appears visible from about 15 years onwards.

Runs S2 and S9 show that reduction and modulation of the mainstem water inflow can reduce the ultimate degradation by 0.3 and 0.6 ft (9 and 18 cm) respectively. Runs S4 and S8 show that a 200-foot widening and local aritifical armoring could reduce the ultimate degradation by about one foot. Run S5 shows that a 400-foot widening, which represents a return to nearly the pre-channelization width, would virtually eliminate further degradation. Analysis of similar results for these and other runs at all computational points of the model can be found in reference (8).

VI. SUMMARY AND CONCLUSIONS

The techniques employed in IALLUVIAL, taken as a whole, have been validated to some extent by the successful Missouri-River simulations. However these modelling results do not signal the end, but rather the beginning, of efforts to achieve a better physical understanding and mathematical formulation of constituent physical processes such as armoring, sorting, mixed-layer dynamics, mixed grain-and-form roughness, etc. There is an urgent need for imaginative comprehensive laboratory experiments on non-equilibrium bed evolution in channels having nonuniform bed sediments. Responsible contributions to the alluvial-river modelling capabilities of computational hydraulics will be those devoted, not to the movement towards user-friendliness and distributed computing systems, but to improved mathematical and numerical formulation of some of the most complex processes to be found in nature (9).

ACKNOWLEDGEMENTS

Support for the development and application of IALLUVIAL has been provided by the Omaha District, U.S. Army Corps of Engineers; the Iowa State Water Resources Research Institute; and the National Science Foundation. J.F. Kennedy of The University of Iowa, A. Harrison, W. Dorough, W. Mellema, and T. Wei of the Corps of Engineers, and J.A. Cunge of SOGREAH Consulting Engineers all provided helpful guidance during the course of the study. J.C. Yang and I. Prasad assisted with data reduction, code development, and program operation. The Graduate College of The University of Iowa underwrote a substantial portion of the required computing effort.

APPENDIX A: REFERENCES

1. Alam, A.M.Z., and Kennedy, J.F., "Friction Factors for Flow in Sand Bed Channels", Journal of the Hydraulics Division, ASCE, Vol. 95, HY6, Nov., 1969.

2. Brownlie, W.R., "Prediction of Flow Depth and Sediment Discharge in Open Channels", Report No. KH-R-43A, W.M. Keck Laboratory of Hydraulics and Water Resources, California Institute of Technology, Pasadena, Nov., 1981.

3. Cunge, J.A., "Programme CHAR 2 - Calcul d'Evolutions Lentes des Fonds en Regimes Non Stationnaires pour les Rivieres Presentant une Resistance du Type Manning-Strickler", Technical Note 36-1328, SOGREAH Consulting Engineers, Grenoble, France, Nov., 1980.

4. Cunge, J.A., Holly, F.M., Jr., and Verwey, A., Practical Aspects of Computational River Hydraulics, Pitman Publishing Ltd., London, England, 1980.

5. Einstein, H.A., and Barbarossa, N., "River Channel Roughness", Transactions, ASCE, Vol. 117, Paper No. 2528, 1952, pp. 1121-1146.

6. Engelund, F., "Hydraulic Resistance of Alluvial Streams", Journal of the Hydraulics Division, ASCE, Vol. 92, HY2, Mar., 1966.

7. Garde, R.J. and Raju, K.G.R., "Resistance Relationships for Alluvial Channel Flow", Journal of the Hydraulics Division, ASCE, Vol. 92, No. HY4, Proceedings Paper 4869, July, 1966.

8. Holly, F.M. and Karim, M.F., "Computer Simulation Prognosis for the Degradation of the Missouri River Between Gavins Point Dam and Iowa's Southern Border", Iowa Institute of Hydraulic Research, The University of Iowa, Report No. 267, Aug., 1983.

9. Holly, F.M. Jr., Nakato, T.N., and Kennedy, J.F., "Computer-Based Prediction of Alluvial River-Bed Changes", Second Bridge Engineering Conference, Highway Research Board, Minneapolis, 24-26 September 1984.

10. Holly, F.M. Jr., Yang, J.C. and Karim, M.F., "Computer-Based Prognosis of Missouri River Bed Degradation - Refinement of Computational Procedures", Iowa Institute of Hydraulic Research, The University of Iowa, Report No. 281, Aug. 1984.

11. Karim, M.F. and Kennedy, J.F., "Computer-Based Predictors for Sediment Discharge and Friction Factor of Alluvial Streams", Iowa Institute of Hydraulic Research, The University of Iowa, Report No. 242, Dec. 1981.

12. Karim, M.F. and Kennedy, J.F., "IALLVUIAL: A Computer-Based Flow- and Sediment Routing Model for Alluvial Streams and its Application to the Missouri River", Iowa Institute of Hydraulic Research, The University of Iowa, Report No. 250, Aug., 1982.

13. Karim, M.F. and Holly, F.M. Jr., "Bed-Armoring and Sorting Simulation in Alluvial Rivers", Technical Paper submitted to Journal of Hydraulic Engineering, ASCE, 1985.

14. Kennedy, J.F., "Laboratory Study of an Alluvial Stream at Constant Discharge", Proceedings of the Federal Inter-Agency Sedimentation Conference, Paper No. 37, 1963, pp. 320-330.

15. Kyozo Suga, "On the Simulation of River-Bed Variations by Characteristics", Proceedings of the 13th Congress of the IAHR, Kyoto, Japan, 1969.

16. Lovera, F., and Kennedy, J.F., "Friction-Factors for Flat-Bed Flows in Sand Channels", Journal of the Hydraulics Division, ASCE, Vol. 95, HY4, July, 1969.

17. Nordin, C.F., "Aspects of Flow Resistance and Sediment Transport, Rio Grande Near Bernalillo, New Mexico", Geological Survey Water Supply Paper, 1498-H, 1964.

18. Preissmann, A.P., "Propagation des Instumescences dans les Canaux et Rivieres", First Congress of the French Association for Computation, Grenoble, September, 1961.

19. Raudkivi, A.J., "Analyses of Resistance in Fluvial Channels", Journal of the Hydraulics Division, ASCE, Vol. 93, HY5, September, 1967.

20. Sayre, W.W. and Kennedy, J.F., "Degradation and Aggradation of the Missouri River", Iowa Institute of Hydraulic Research, University of Iowa, Report No. 215, Jun. 1978.

21. Vanoni, V.A. and Brooks, N.H., "Laboratory Studies of the Roughness and Suspended Load of Alluvial Streams", California Institute of Technology, Pasadena, Ca., 1957.

22. Vanoni, V.A. and Hwang, L.S., "Relation Between Bed Forms and Friction in Streams", Journal of the Hydraulics Division, ASCE, Vol. 93, No. HY3, Proceedings Paper 5242, May, 1967, pp. 121-144.

23. Vreugdenhil, C.B. and de Vries, M., "Computations of Non-steady Bed-Load Transport by a Pseudo-Viscosity Method", Delft Hydraulics Laboratory Publication No. 45, Delft, The Netherlands, 1967.

24. White, W.R., Paris, E., and Bettess, R., "A New General Method for Predicting the Frictional Characteristics of Alluvial Streams", Report No. IT 187, Hydraulics Research Station, Wallingford, England, 1979.

APPENDIX B: NOTATION

B	channel width at water surface
c	celerity of bed disturbance
C_1	weighting parameter for armoring effect on sediment discharge
d	flow depth
D_k	mean sediment size of kth size interval
D_{50}	median bed-material size
f_a	grain-size friction factor
f_c	composite friction factor
f_m	non-armored friction factor
g	gravitational acceleration
i	index of computational points
k	size-fraction index
m	total number of sediment size intervals
n	index of computational time levels
N	total number of computational points
p	bed-sediment porosity
P_k	fraction of material in k^{th} size interval
q_s	volumetric sediment discharge per unit width
Q_s	total volumetric sediment discharge
$\overline{Q_s}$	imposed sediment load at upstream boundary
$\tilde{Q}_s$	TLTM sediment load at end of upstream boundary
s	specific gravity of sediment particles
S_c	composite energy slope on armored beds
S_m	non-armored energy slope
t	time

u_* shear velocity

u_{*c} critical shear velocity (incipient motion)

U cross-sectional average velocity

V_1-V_7 logarithms of dimensionless groups

w particle fall velocity

x exponent in size-fraction allocation equation; longitudinal coordinate

y water surface elevation

z bed elevation

β dimensionless length of buffer reach

Δt length of computational time step

Δx length of computational reach

Δz change in bed elevation

θ weighting factor in time

ν kinematic viscosity of water

ξ armoring factor

σ_g gradation coefficient for nonuniform bed material

List of Tables

Table 1. Summary Comparison of Measured and Computed (TLTM) Sediment Discharges and Friction Factors

List of Figures

Figure 1. Missouri River Basin

Figure 2. Observed and Computed Water-Surface and Bed-Elevation Changes, 1960-1980

Figure 3. Schematic Layout of Study Reach

Figure 4. Computed Water-Surface and Bed Profiles, 1980-2000

Figure 5. Computed Median Bed Material Size (D_{50}) and Armoring Factor (ξ), 1980-2000

Figure 6. Cumulative Computed Degradation at Sioux City, 1980-2000

Table 1

Summary Comparison of Measured and Computed (TLTM)
Sediment Discharges and Friction Factors

Data Set	No of Pts	Sediment Discharge		Friction Factor	
		Mean Ratio	Mean Norm. Error (%)	Mean Ratio	Mean Norm. Error (%)
Guy et al (.19mm)	29	1.45	69.3	1.00	40.6
Guy et al (.27mm)	17	1.51	52.4	0.80	41.1
Guy et al (.28mm)	32	1.36	52.1	0.97	35.9
Guy et al (.32mm)	29	1.97	102.9	0.74	33.0
Guy et al (.45mm)	27	0.95	37.0	1.18	48.0
Guy et al (.93mm)	23	1.07	24.5	0.80	25.1
Williams	24	2.12	112.5	0.85	18.4
Vanoni-Brooks	21	0.92	47.6	1.18	56.9
Missouri R. (Cat. A)	60	1.02	36.9	1.04	32.2
Missouri R. (Cat. B,C)	26	1.20	47.0	0.90	20.0
Missouri R. (RS)	17	1.07	48.9	1.28	33.7
Sato, et al (#1)	136	1.01	32.1	0.92	16.7
Meyer-Peter & Muller	41	0.90	39.7	0.96	15.9
Gilbert	43	0.70	35.0	0.81	35.4
Waterways Expt. Sta. (#1)	90	0.98	29.5	0.93	10.4
Willis-Kennedy	31	0.76	39.2	0.72	28.8
Missouri R. (Sioux City)	51	1.09	41.3	0.46	54.6
Middle Loup R.	45	0.80	31.9	0.80	35.4
Niobrara R.	25	1.72	72.6	0.56	43.7
ACOP Canals	34	0.63	44.6	0.84	29.2
Rio Grande	58	0.80	46.7	0.79	31.5
Elkhorn R.	23	0.35	67.2	0.92	25.4
Sato, et al (#2)	45	0.87	38.4	0.84	21.8
Waterways Expt. Sta. (#2)	20	1.18	45.9	0.93	13.6
All data	947		44.8		28.5

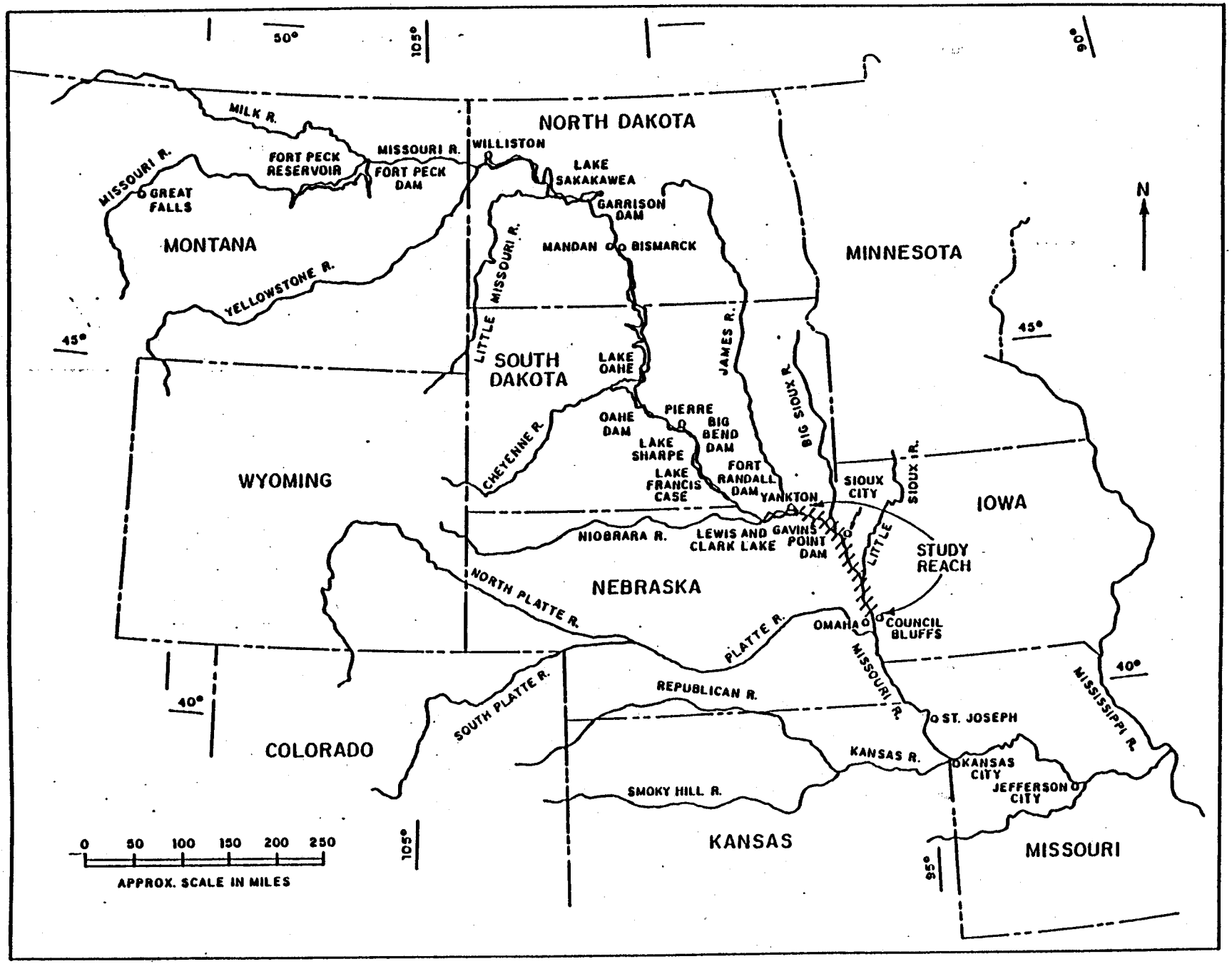

Figure 1. Miss[illegible] River Basin

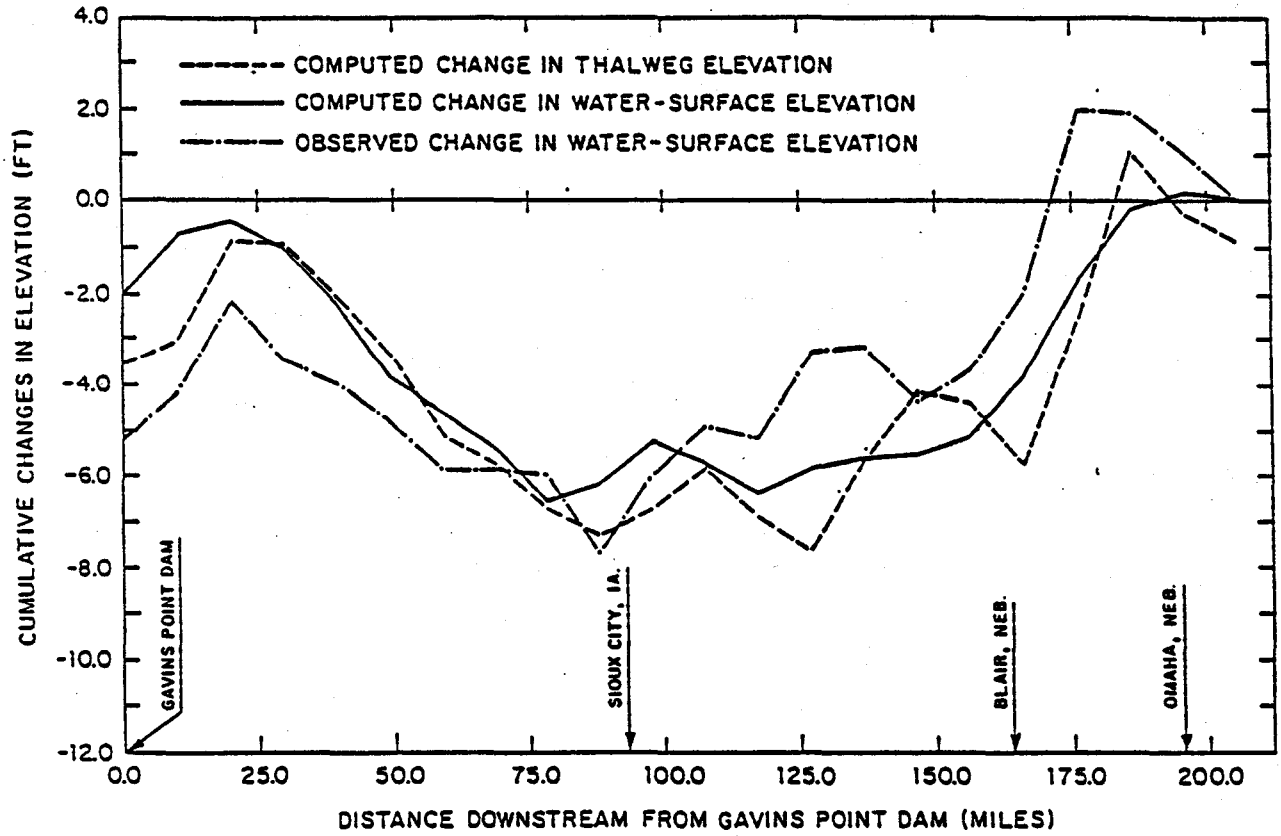

Figure 2. Observed and Computed Water-Surface and Bed Elevation Changes, 1960-1980.

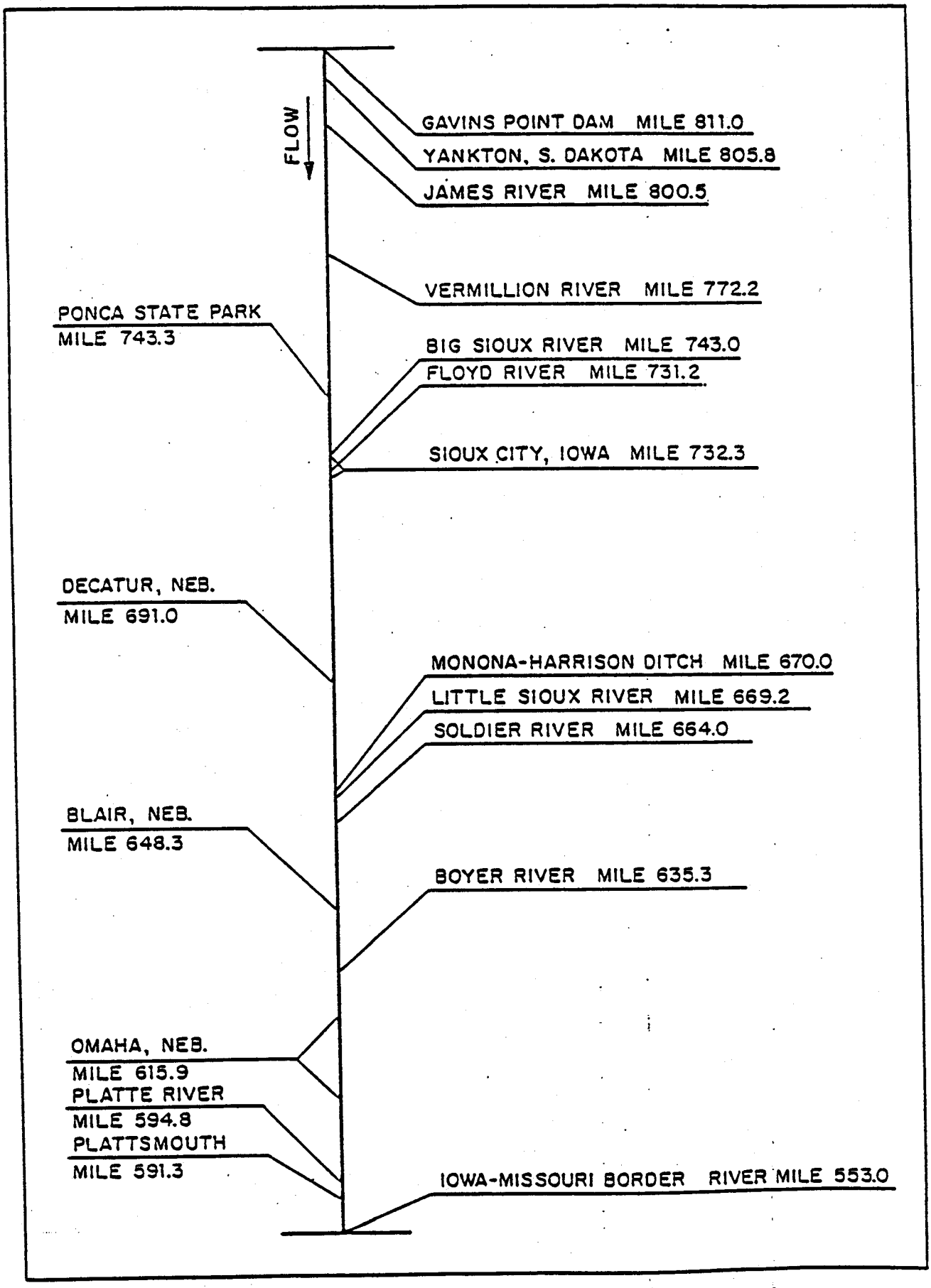

Figure 3. Schematic Layout of Study Reach.

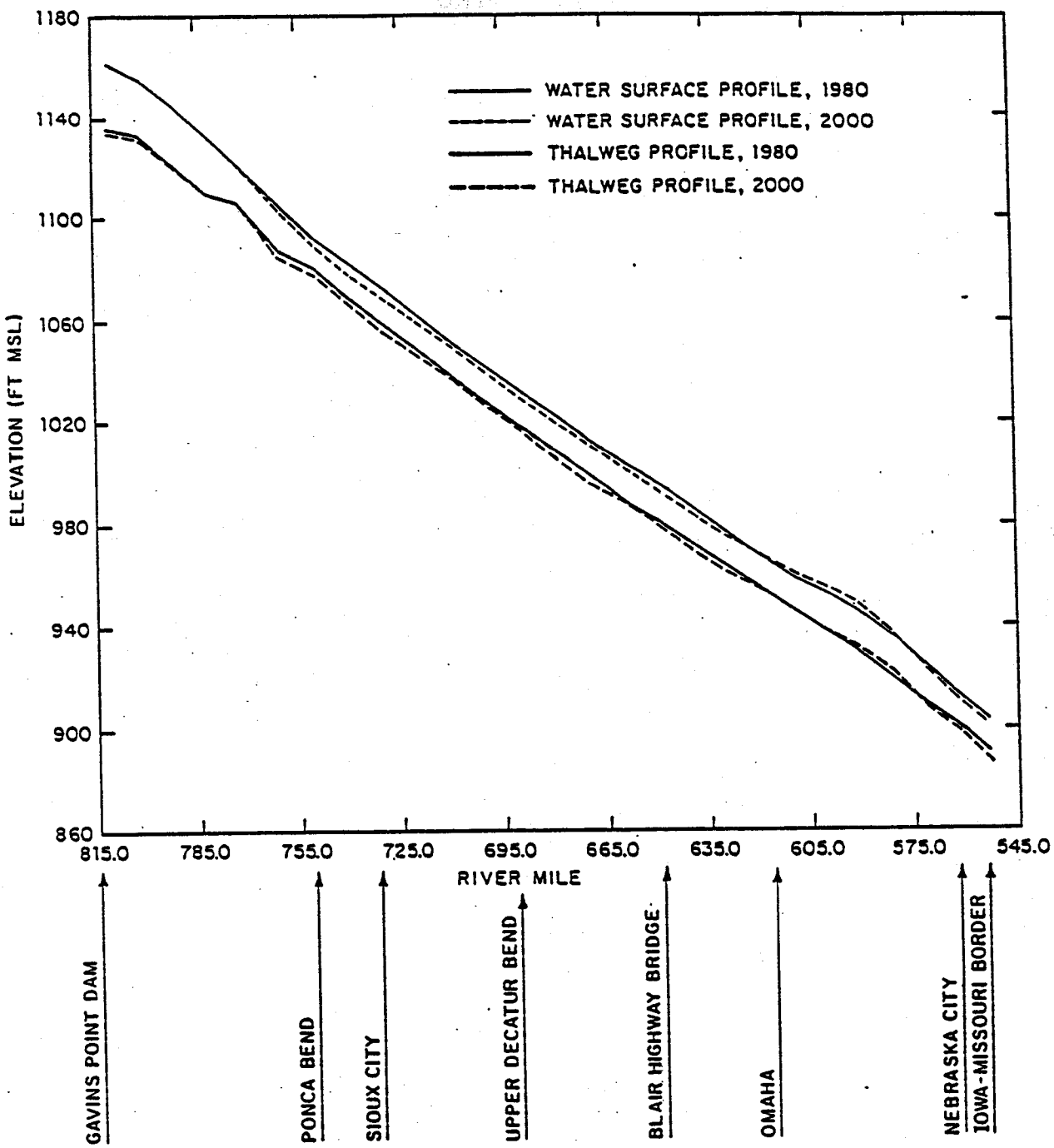

Figure 4. Computed Water Surface and Bed Profiles, 1980-2000.

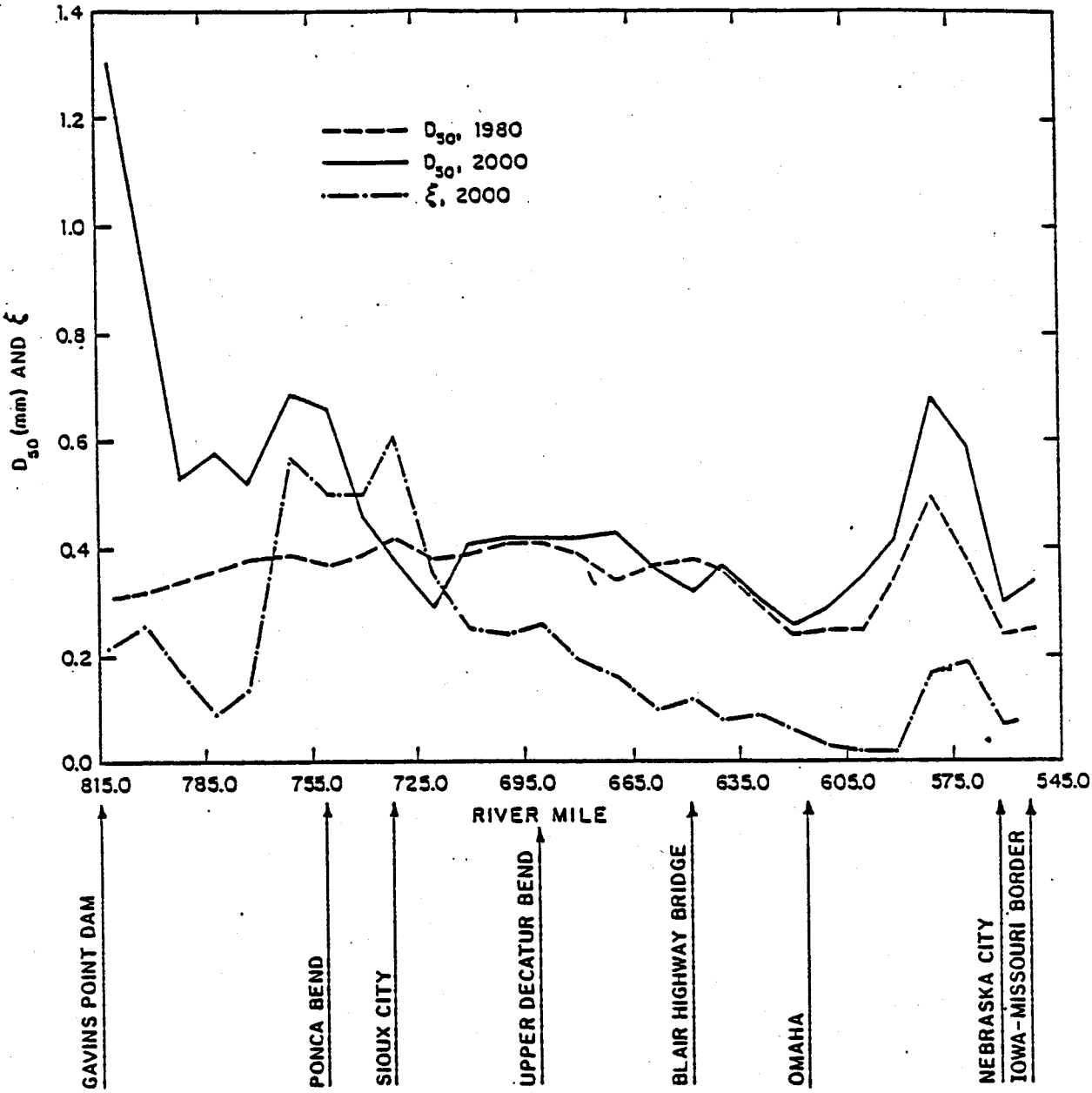

Figure 5. Computed Median Material Size (D_{50}) and Armoring Factor (ξ), 1980-2000.

SIMULATION OF BED ARMORING IN ALLUVIAL CHANNELS

by Hong-Yuan Lee[1] and A. Jacob Odgaard[2], M. ASCE

INTRODUCTION

The stability of a river channel depends to a great extent on sediment characteristics. If the amount of sediment entering a given channel reach for some reason (upstream flow control measures, seasonal changes in sediment yield, etc.) becomes less than the river's sediment-transport capacity in that reach, channel degradation occurs. An example (14) is the Missouri River between Gavins Point Dam and Omaha where, as a result of regulation for navigation, flood control and irrigation, the bed has lowered as much as seven feet in places in the last 25 years (causing problems of bank erosion, undermining of bridge foundations, reduced efficiency of water-intake structures, loss of wildlife habitat, loss of recreational sites, etc.). The rate at which degradation occurs depends very much on the composition of the bed material (9), which can range from well sorted to broadly mixed. Most river beds are made up of grains with a broad spectrum of sizes. If the flow over such a bed is depleted of sediment, and the bed-shear stress is such that coarser fractions of the bed material do not move, only finer fractions will

[1]Senior Water Resources Engineer, Dooley-Jones and Associates, Inc., Tucson, Arizona; formerly Graduate Student, Institute of Hydraulic Research, College of Engineering, The University of Iowa, Iowa City, Iowa.

[2]Associate Professor and Research Engineer, Institute of Hydraulic Research, College of Engineering, The University of Iowa, Iowa City, Iowa 52242.

be entrained into the flow and the bed surface will become progressively coarser. Ultimately, an armor coat of large particles may form that stops further degradation (15). It follows that the degree to which a river bed is armored, and its cumulative frequency, must play an important role in the prediction of rates of river-bed degradation.

Gessler (7) and Little and Mayer (11) were among the first to systematically study the process of bed armoring. In series of laboratory experiments they generated armor layers by running (over an extended period of time) sediment-free water through straight flumes with broadly mixed (nonuniform) sediment. Based on their data, they established relationships between the initial and final bed-material composition. Data obtained by Garde, Al-Shaikh Ali, and Diette (6) in a similar type of experiment supported Gessler's bed-armoring theory, which is a probabilistic approach. Garde et al. also measured the time variation of the median-grain diameter of the bed-surface material. Support for Gessler's approach was provided also by Lane and Carlson's [see Gessler (7)] studies of armoring in the San Luis Valley Canals in Southern Colorado. A method consisting of combining Gessler's theory and Einstein's (3, 4) bed-load theory was used recently by Shen and Lu (12) to predict the composition of the armor-layer in both Little and Mayer's (11) and Gessler's (7) experiments. Shen and Lu's method included modifications of Gessler's theory; Einstein's "hiding function"; and of Shields' curve (13).

None of the aforementioned studies focussed on the relationship between the time scale of the armoring process and the flow and sediment characteristics. Usually, river beds are only partially armored; and the degree of armoring often varies with seasonal changes in the rates of flow and sediment

transport. In order to fully evaluate a channel bed's long term stability it is necessary to be able to relate the degree of armoring to characteristics of the flow and sediment in the channel. In an effort to obtain such a relationship, this study developed a numerical procedure for correlating the temporal change of the composition of the bed-surface layer with changes in the rate of sediment transport near the channel bed. The procedure was based on: (1) Bayazit's (1) scheme for the exchange of grain sizes between a surface and a subsurface layer of bed sediment; (2) Einstein's (3,4) bed-load function with a modified hiding-factor curve; and (3) Karim's (8) mixing-layer concept. The procedure is an alternative to that proposed recently by Borah et al. (2) in their sediment-routing model. Borah et al. also used a mixing-layer concept; however, to control the erosion/deposition process they introduced an additional active-layer concept and a somewhat arbitrary ordering procedure for the removal of the various grain-size fractions. Their procedure is complex. The rate at which they let sediment be entrained into the fluid is dependent on the time step chosen for the numerical computation, and it must be calibrated with measured data. The model presented herein is simpler and it contains a minimum of floating variables.

MODEL

A channel reach of length L and of unit width is considered (Fig. 1). If the flow approaching this reach is sediment depleted, sediment will be picked up from the reach at a rate which may be described, for each grain-size class fraction i, by the equation (1)

$$t_i q \, \Delta t = L \Delta Q_i \tag{1}$$

in which q = bed-load transport capacity of the flow per unit width; t_i = fraction of grains in class interval i; Δt = time interval; and ΔQ_i = weight of the grains in class interval i that are removed from the bed-surface mixing layer during the time interval Δt, per unit area of the mixing layer. The time interval Δt is assumed to be small enough that q and t_i can be taken to be constant within this period of time. The thickness, T, of the mixing layer is taken to be given by

$$T = \frac{1}{2} H \, (1-c) \tag{2}$$

in which c = coefficient with value between 0 and 1; H = dune height as given by Yalin's (16) relation, $H = (d/6)\,(1-\tau_{cr}/\tau)$; d = flow depth; τ bed-shear stress; and τ_{cr} = critical bed shear stress (13). Eq. 2 is a simplified version of the expression suggested by Karim and Kennedy (8). The total weight of bed material that leaves the mixing layer (per unit area) during the time interval Δt is obtained by summing up the contributions from all class intervals:

$$\Delta Q = \sum_i (\Delta Q_i) = \frac{q \Delta t}{L} \sum_i (t_i) = \frac{q \Delta t}{L} \tag{3}$$

It is assumed that the material eroded from the mixing layer (ΔQ) is replaced by bed material of the same weight from the layer below the mixing layer. At the end of the time interval Δt, the weight of the grains in class interval i in the mixing layer is then (per unit area)

$$m_i'Q = m_iQ - t_i\Delta Q + p_i\Delta Q \tag{4}$$

in which $Q = \rho gT$ = weight per unit width of the mixing-layer bed material; ρ = density of sediment; g = acceleration due to gravity; m_i = fractions of grains in class interval i in the mixing layer at the beginning of the time interval Δt; and p_i = the fraction of grains in class interval i in the parent bed. Hence, the fraction of grains in class interval i at the end of time interval Δt is

$$m_i' = m_i + \frac{\Delta Q}{Q}(p_i - t_i) \tag{5}$$

As the numerical process proceeds, the amount (per unit time) of sediment leaving the mixing layer (ΔQ) decreases; and a gradual coarsening of the material in the mixing layer occurs. Eventually, the rate of sediment transport becomes zero, at which point the armor layer is fully developed. The procedure is summarized in Fig. 2.

MODEL RESULTS

Einstein's (3,4) bed-load function was used to determine the rate of bed-load transport (by size fraction). His hiding-factor curve, which has been modified on several occasions since it was first developed [see Shen and Lu (12)], was modified again in this study. Using the hiding-factor curve shown in Fig. 3, and c = 0.3, the model simulated very well both the temporal variation of the sediment-transport rate and the final armor-layer conposition

in all of Little and Mayer's (11) experiments. Figs. 4 and 5 show a comparison between measured and simulated sediment-transport rates for Runs 6-1 and 3-4; measured and simulated armor-layer grain size distributions for the same runs are shown in Figs. 6 and 7. The experimental conditions for these runs are summarized in Table 1. As the flow chart in Fig. 2 indicates the bed is defined herein to be fully armored when the sediment load is less than or equal to one percent of the initial sediment load. The agreement between measured and simulated armor-layer grain size distribution was, in general, closest at the larger size fractions. The discrepancy at the smaller fractions may not reflect any model deficiency. It could be explained by a systematic error in Little and Mayer's (11) bed-sampling technique, which was pointed out by Kellerhals and Church (10) and Ettema (5). Figs. 6 and 7 also show simulated bed-material grain size distribution at an arbitrarily chosen intermediate time, t = 500 min. (No data are available to verify intermediate bed-material compositions).

APPLICATION

Problem. - Assume that the initial conditions for a given reach are known; i.e., a certain composition of bed material corresponding with certain rates of flow and sediment transport. At time zero, the sediment supply upstream from the reach is reduced (or the discharge is increased without the sediment supply being increased correspondingly). Determine the composition of the bed-surface material at time t and the corresponding sediment discharge.

Solution. - Input into the model the initial flow and sediment conditions for the reach; calculate the sediment transport for each size fraction corresponding to the initial flow and sediment conditions (at t = 0) and determine the difference between the total sediment load for the reach, q (sum over all size fractions) and the incoming (reduced) sediment load, q_o. This difference determines the initial amount of bed material leaving the mixing layer, ΔQ. Proceed then as described earlier and prepare graphs similar to Figs. 4, 5, 6, and 7 (with the ordinate in Figs. 4 and 5 being $q - q_o$). The composition of the bed-surface material and the corresponding sediment discharge can then be read from these graphs. For example, in Little and Mayer's Run 3-4, the sediment-transport rate corresponding with the grain size distribution at t = 500 min (Fig. 6) is read by entering Fig. 4 at t = 500 min to be q = 0.001 lb/s (q_o = 0).

DISCUSSION AND CONCLUSIONS

Although the research is still in its early stages of development, important conclusions can be made already. The bed-material exchange model used herein is adequate for a simulation of the temporal variation of sediment-transport rate and corresponding variation of bed-material composition. Only two calibration factors are employed. The hiding-factor, which controls primarily the initial removal rate of the smaller sediment particles; and coefficient c, which, by controlling the thickness of the mixing layer, essentially tunes the overall time variation of the process (and the time to reach "full" armoring).

The model has the advantage of being simple and flexible. Modifications and adjustments can be easily made as more data become available. Modifications are foreseen. For example, in its present form the model takes the hiding factor, ξ, to be a function of x/D, only; x = large particle size that will be subjected to the shielding effect by protruding coarser particles or laminar sublayer; D = local particle diameter. The program calculates x/D at each time step and uses the value of ξ given by the curve in Fig. 3. However, the rationale behind the hiding-factor concept suggests that ξ should also be a function of the geometric standard deviation of the material in the mixing layer. Such a modification is easily incorporated. Also, the simulation procedure in its present form is based on the assumption that the water depth, energy slope, and friction factor remain constant during the development of the armor layer. This is not the case in reality. The model is flexible enough that continuous adjustments of these parameters can be made. Finally, a minor modification is foreseen on account of the fact that Little and Mayer's experiments were conducted with inflow of sediment-free water (q_o = 0); in reality, the inflowing water would be sediment laden with only a certain sediment deficit.

In closing it seems justified to state that the proposed armoring model can be a useful design tool for estimates of the effect of alternative flow regulation measures on a channel bed's long term stability. The simplicity of the model also makes it an attractive framework for further theoretical and experimental studies of armor-layer behavior; in particular, when the flow pattern becomes more complex such as in curved channels.

APPENDIX I - REFERENCES

1. Bayazit, M., "Simulation of Armor Coat Formation and Destruction", Proceedings of the 16th Congress of the International Association for Hydraulic Research, Sao Paulo, Brazil, Paper B10, 1975, pp. 73-78.

2. Borak, D.K., Alonso, C.V., and Prasad, S.N., "Routing Graded Sediments in Streams: Formulations", Journal of the Hydraulics Division, ASCE, Vol. 108, No. HY12, December 1982, pp. 1486-1503.

3. Einstein, H.A., "The Bed-Load Function for Sediment Transportation in Open Channel Flows", Technical Bulletin No. 1026, U.S. Department of Agriculture, Soil Conservation Service, Washington, D.C., September, 1950.

4. Einstein, H.A. and Chien, N., "Transport of Sediment Mixtures with Large Ranges of Grain Sizes," MRD Sediment Series No. 2, U.S. Army Engineering Division, Missouri River, Corps of Engineers, Omaha, Nebraska, 1953.

5. Ettema, R., "Sampling Armor-Layer Sediments", Journal of Hydraulic Engineering, ASCE, Vol. 110, No. 7, July 1984, pp. 922-996.

6. Garde, R.J., Al-Shaikh-Ali, K., and Diette, S., "Armoring Process in Degrading Streams", Journal of the Hydraulics Division, ASCE, Vol. 103, No. HY9, September 1977, pp. 1091-1095.

7. Gessler, J., "The Beginning of Bedload Movement of Mixtures Investigated as Natural Armoring in Channels", Translation T-5, W.M. Keck Laboratory of Hydraulics and Water Resources, California Institute of Technology, Pasadena, California, October 1968.

8. Karim, M.F. and Kennedy, J.F., "IALLUVIAL: A Computer-Based Flow- and Sediment-Routing Model for Alluvial Streams and its Application to the Missouri River", IIHR Report No. 250, Iowa Institute of Hydraulic Research, The University of Iowa, Iowa City, Iowa 1982.

9. Karim, M.F., Holly, F.M., and J.F. Kennedy, "Bed Armoring Procedures in IALLUVIAL and Application to the Missouri River", IIHR Report No. 269, Iowa Institute of Hydraulic Research, The University of Iowa, Iowa City, Iowa, 1983.

10. Kellerhals, R. and Church, M., discussion of "Stability of Channel Beds by Armoring", by William C. Little and Paul G. Mayer, Journal of the Hydraulics Division, ASCE, Vol. 103, No. HY7, July 1977, pp. 826-827.

11. Little, W.C. and Mayer, P.G., "The Role of Sediment Gradation on Channel Armoring", School of Civil Engineering, Georgia Institute of Technology, Atlanta, Georgia, May 1972.

12. Shen, H.W., and Lu, J.Y., "Development and Prediction of Bed Armoring", Journal of Hydraulic Engineering, ASCE, Vol. 109, No. 4, April, 1983, pp. 611-629.

13. Shields, A., "Anvendung der aenlichkeitsmechanik und der Turbulenzforshung auf die Geshiebebewegung", Mitteilungen der Preussischen Versuchsanstalt fur Wasserbau and Schiffbau, Berlin, Germany, Translated to English by W.P. Ott and J.C. van Uchelen, California Institute of Technology, Pasadena, California, 1936.

14. U.S. Army Corps of Engineers, Review Report for Water and Related Land Resources Management Study, Metropolitan Sioux City and Missouri river, Iowa, Nebraska and South Dakota, Vol. 4: Supporting Technical Report - Missouri River Degradation, Omaha District, Corps of Engineers, August 1981.

15. Vanoni, V.A., ed, Sedimentation Engineering, Manual and Report on Engineering Practice No. 4, ASCE, 1976.

16. Yalin, M.S., "Geometrical Properties of Sand Waves", Journal of the Hydraulics Division, ASCE, Vol. 90, No. HY5, 1964, pp. 105-119.

APPENDIX II - NOTATION

The following symbols are used in this paper:

c = coefficient;

d = depth of flow;

g = acceleration due to gravity;

H = dune height;

i = grain-size class interval;

L = length of channel reach;

m = fraction;

p = fraction;

Q = weight of mixing-layer bed material;

q = bed-load transport capacity;

T = mixing-layer thickness;

t = fraction;

Δt = time interval;

ρ = sediment density;

τ = bed-shear stress; and

τ_{cr} = critical bed shear stress.

FIGURE CAPTIONS

Figure

1. Bed-Material Exchange Model

2. Flow Chart for Numerical Computation

3. Hiding-Factor Curve

4. Measured and Simulated Sediment-Transport Rates as a Function of Time for Little and Mayer's (11) Run 6-1.

5. Measured and Simulated Sediment-Transport Rates as a Function of Time for Little and Mayer's (11) Run 3-4.

6. Measured and Simulated Armor-Layer Grain Size Distributions for Little and Mayer's (11) Run 6-1.

7. Measured and Simulated Armor-Layer Grain Size Distributions for Little and Mayer's (11) Run 3-4.

Table 1. Experimental Conditions (11)

Run No.	Flow				Original Bed Material	
	Rate, in cubic feet per second	Velocity, in feet per second	Depth, in feet	Slope of water surface	Median grain diameter, in millimeters	Geometric standard deviation
(1)	(2)	(3)	(4)	(5)	(6)	(7)
3-4	0.572	1.338	0.217	0.0019	1.00	2.50
6-1	0.448	1.236	0.184	0.0020	1.00	3.05

Note: 1 ft = 0.305 m; 1 cfs = 0.0283 m^3/s.

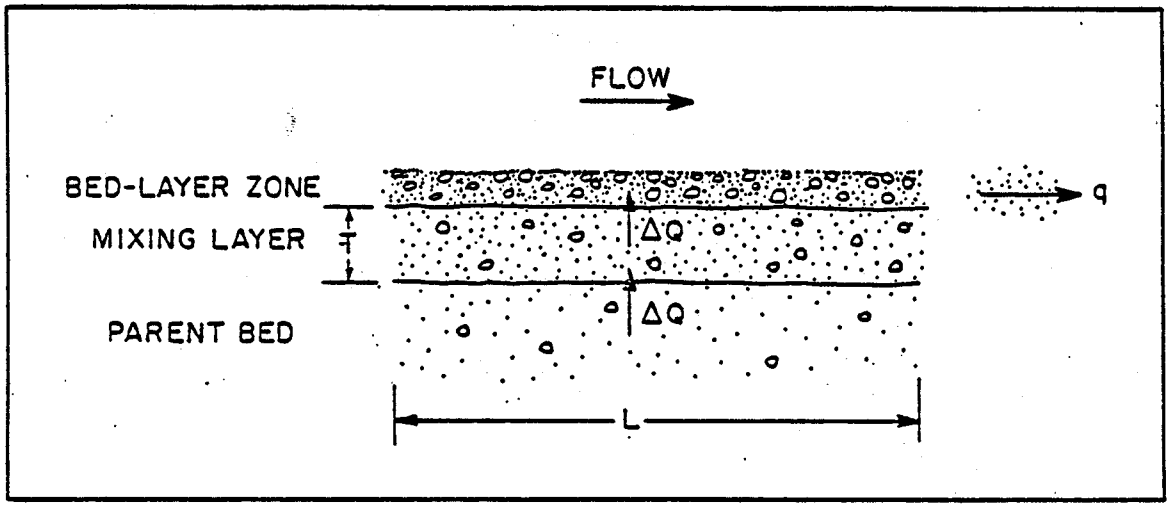

1RD

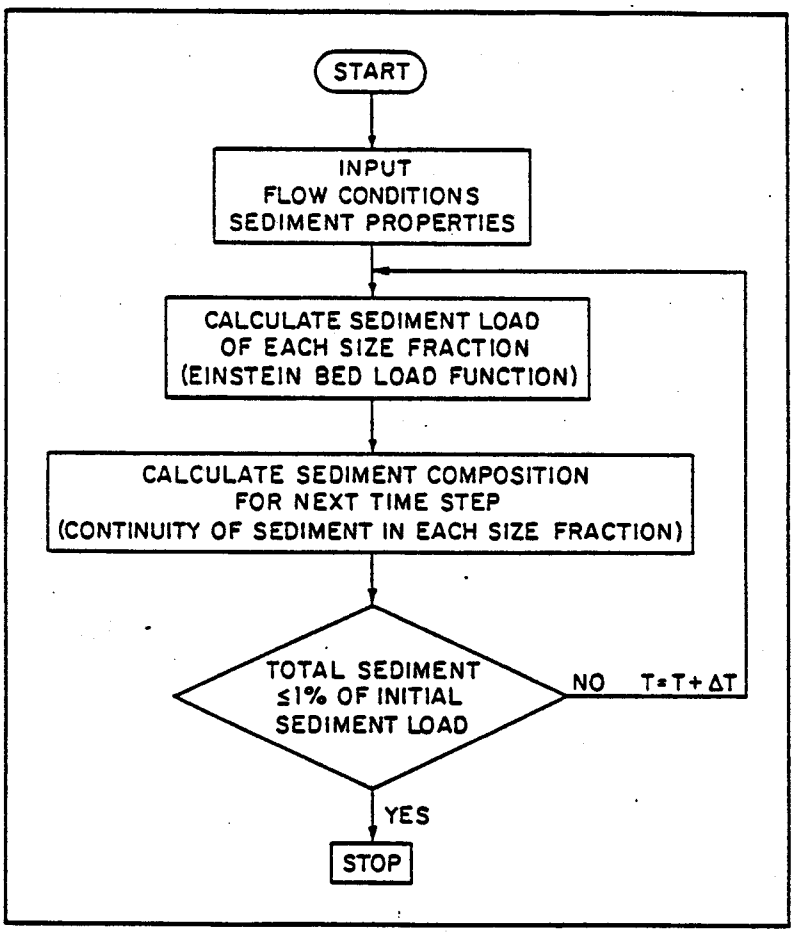

FIG. 2
ODGAARD

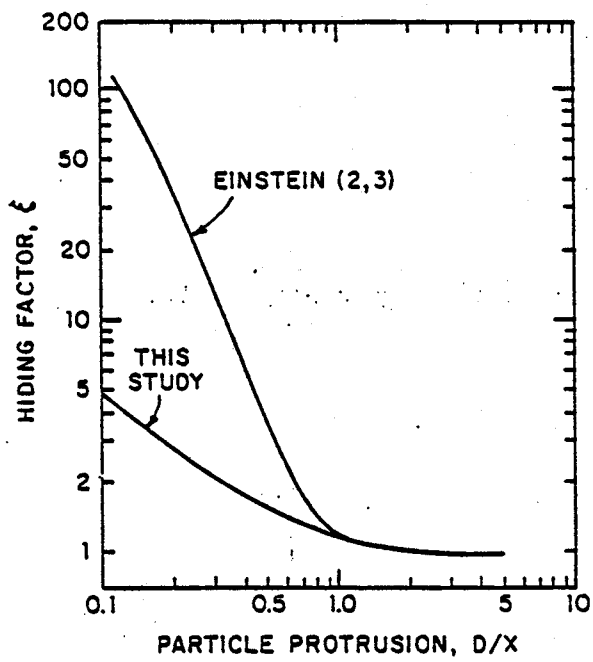
200
100
50
20
10
5
2
1
HIDING FACTOR, ξ
EINSTEIN (2,3)
THIS STUDY
0.1
0.5
1.0
5
10
PARTICLE PROTRUSION, D/X

FIG. 3
DGAARD

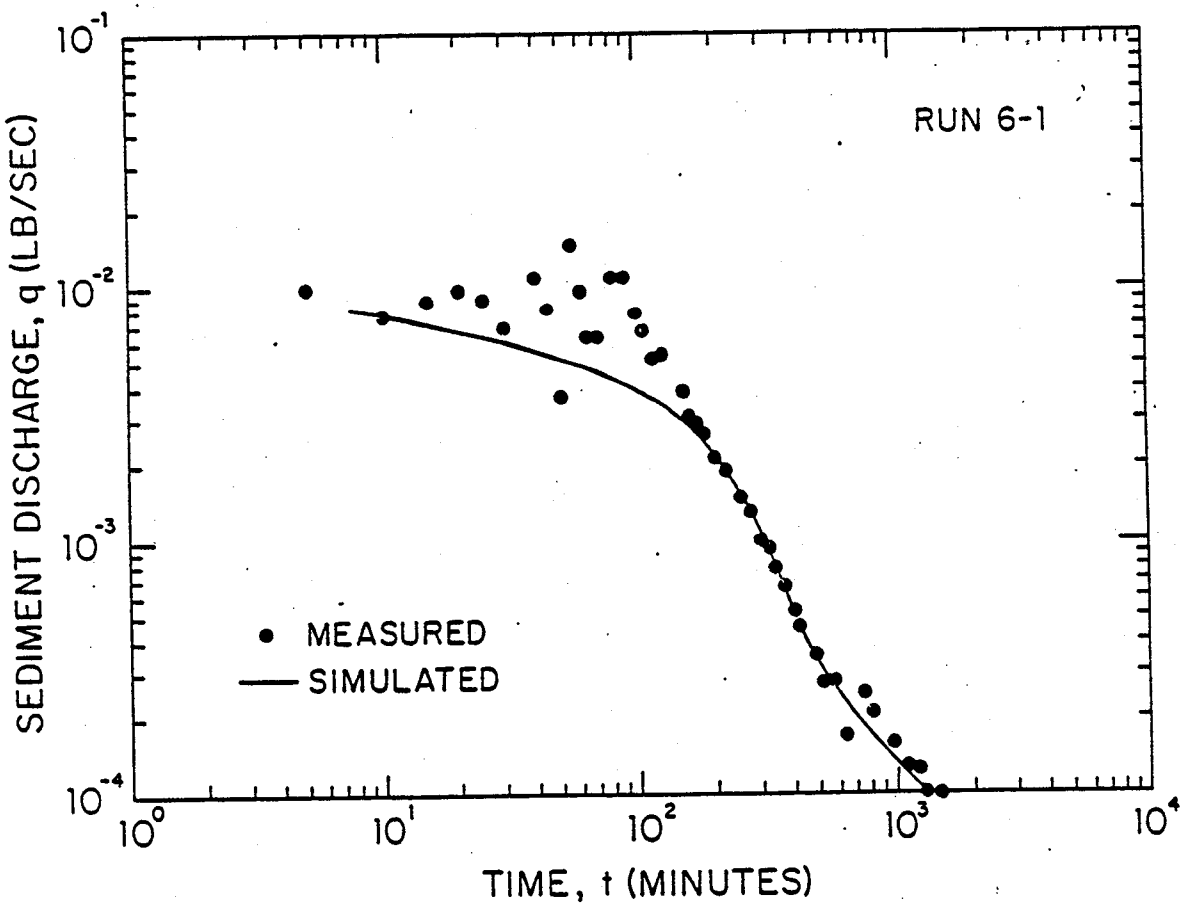

FIG. 4
ODGAARD

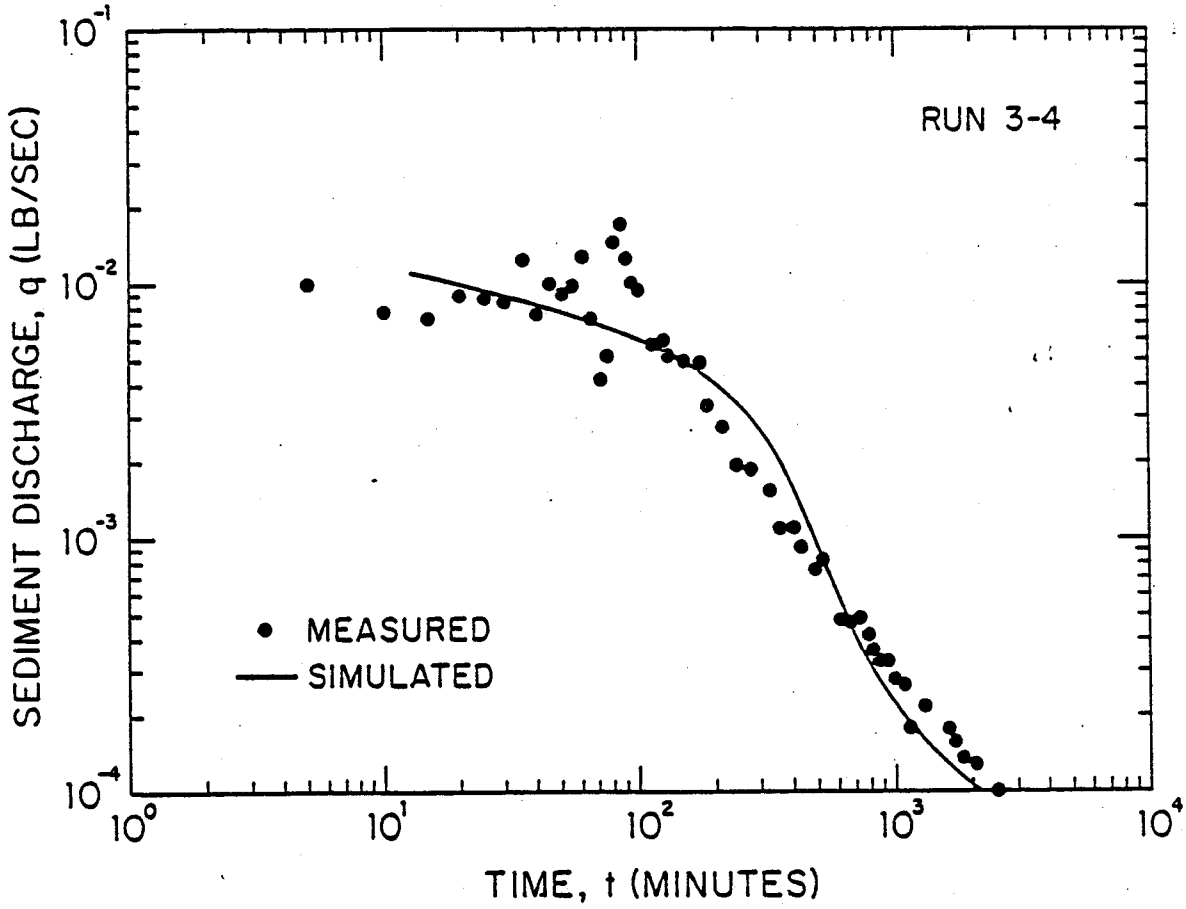

FIG. 5
ODGAARD

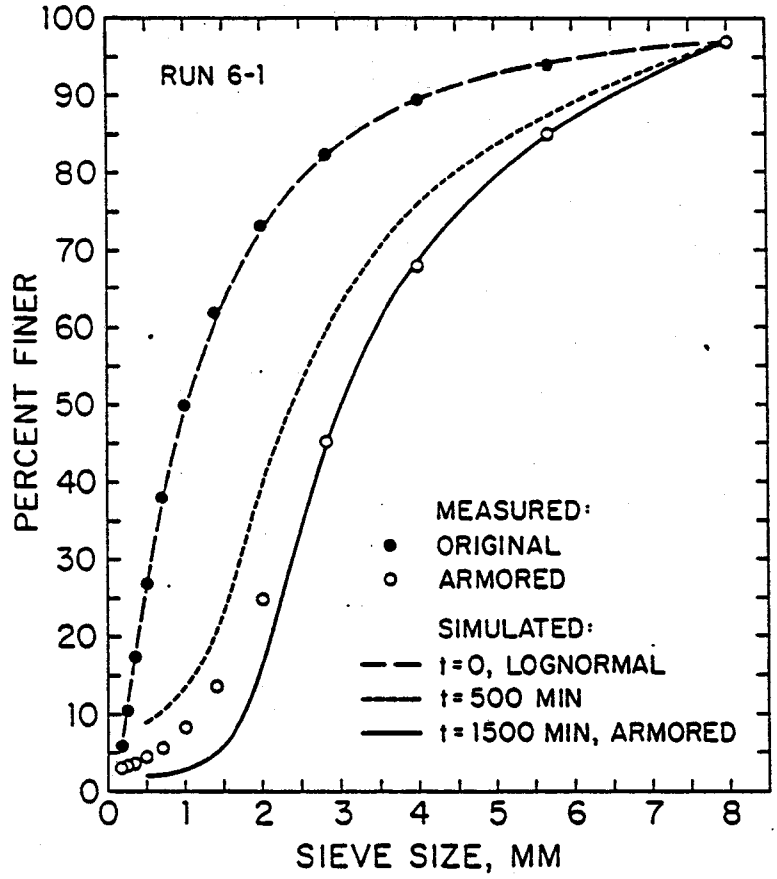

FIG. 6
ODGAARD

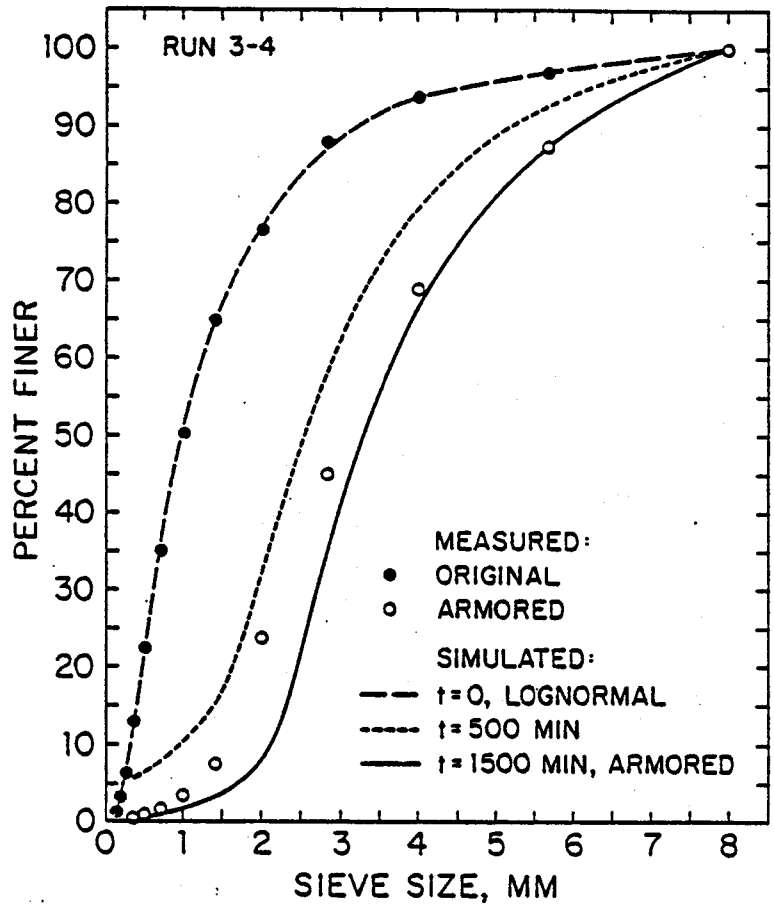

FIG. 7
ODGAARD

ABSTRACT

A numerical procedure for simulating the temporal variation of sediment-transport rate and corresponding variation of bed-material composition in a straight alluvial channel has been developed. The procedure is based on a simple model for the exchange of grain sizes between a surface and a subsurface layer of bed sediment together with a standard bed-load function. Verification was made with laboratory data. The procedure should be a useful tool for estimates of the effect of alternative flow regulation measures on a channel bed's long term stability.

JOHN LIOU, Ph.D., P.E., L.S.
Hydrologist/Hydraulic Engineer

Federal Emergency Management Agency
Region VIII
Denver Federal Center, Bldg. 710
Denver, Colorado 80225

An Evaluation of Flood-Level Prediction Using Alluvial-River Models

Committee on Hydrodynamic Computer Models
for Flood Insurance Studies
Advisory Board on the Built Environment
Commission on Engineering and Technical Systems
National Research Council

NATIONAL ACADEMY PRESS
Washington, DC 1983

NOTICE: The project that is the subject of this report was approved by the Governing Board of the National Research Council, whose members are drawn from the councils of the National Academy of Sciences, the National Academy of Engineering, and the Institute of Medicine. The members of the committee responsibile for the report were chosen for their special competences and with regard for appropriate balance.

This report has been reviewed by a group other than the authors according to procedures approved by a Report Review Committee consisting of members of the National Academy of Sciences, the National Academy of Engineering, and the Institute of Medicine.

The National Research Council was established by the National Academy of Sciences in 1916 to associate the broad community of science and technology with the Academy's purpose of furthering knowledge and of advising the federal government. The Council operates in accordance with general policies determined by the Academy under the authority of its congressional charter of 1863, which establishes the Academy as a private, nonprofit, self-governing membership corporation. The Council has become the principal operating agency of both the National Academy of Sciences and the National Academy of Engineering in the conduct of their services to the government, the public, and the scientific and engineering communities. It is administered jointly by both Academies and the Institute of Medicine. The National Academy of Engineering and the Institute of Medicine were established in 1964 and 1970, respectively, under the charter of the National Academy of Sciences.

This report was prepared under Contract Number EMW-C-0167 between the National Academy of Sciences and the Federal Emergency Management Agency.

For information contact:

Advisory Board on the Built Environment
Committee on Engineering and Technical Systems
National Research Council
2101 Constitution Avenue, N.W.
Washington, D.C. 20418

ADVISORY BOARD ON THE BUILT ENVIRONMENT

Chairman

PHILIP G. HAMMER, Consultant to Industry and Governments, Edgewater, Maryland, and Tampa, Florida.

Members

WERNER, A. BAUM, Dean, College of Arts and Sciences, Florida State University, Tallahassee

RICHARD BENDER, Dean, College of Environmental Design, University of California, Berkeley

WILLIAM S. BIRNEY, Marketing Manager--Washington, United States Steel Corporation, Washington, D.C.

JAMES M. BROWN, Professor, School of Law, George Washington University, Washington, D.C.

G. DAY DING, Research Professor of Architecture, University of Illinois, Champaign

PAUL C. GREINER, Vice President, Edison Electric Institute, Washington, D.C.

ROBERT C. HOLLAND, President, Committee for Economic Development, Washington, D.C.

JOHN C. HORNING, Manager--Engineering and Construction, General Electric Company, Schenectady, New York

GEORGE S. JENKINS, President, Consultation Networks, Inc., Washington, D.C.

JOHN T. JOYCE, President, International Union of Bricklayers and Allied Craftsmen, Washington, D.C.

STANISLAV V. KASL, Professor of Epidemiology and Public Health, Yale University, New Haven, Connecticut

MORTIMER M. MARSHALL, Jr., Department of Defense (Retired), Washington, D.C.

ROBERT P. MARSHALL, Jr., Vice Chairman of the Board, Turner Construction Company, New York, New York

GLORIA S. McGREGOR, Chief, Community Facilities Department, International Energy Company, San Francisco, California

MELVIN A. MISTER, Deputy Executive Director, U.S. Conference of Mayors, Washington, D.C.

C.E. (TED) PECK, Co-Chairman, The Ryland Group, Inc., Columbia, Maryland

L.R. SHAFFER, Deputy Director, U.S. Army Construction Engineering Research Laboratory, Champaign, Illinois

ARTHUR C. STERN, Professor of Air Hygiene, The University of North Carolina, Chapel Hill

WARREN H. TURNER, Director, Central Office of Maintenance Engineering, American Telephone & Telegraph Company, Basking Ridge, New Jersey

SHIRLEY F. WEISS, Professor, Department of City and Regional Planning, The University of North Carolina, Chapel Hill

JOHN H. WIGGINS, Jr., President, J.H. Wiggins, Company, Redondo Beach, California

Liaision Representatives
LEE S. GARRETT, Department of the Army (Retired)
MAXINE SAVITZ, Department of Energy
RICHARD N. WRIGHT, National Bureau of Standards

Ex-Officio
JOSEPH H. ZETTEL, Chairman of the Board, Western Solar Utilization Network, Littleton, Colorado

COMMITTEE ON HYDRODYNAMIC COMPUTER MODELS FOR FLOOD INSURANCE STUDIES

Chairman
JOHN F. KENNEDY, Institute of Hydraulic Research, The University of Iowa, Iowa City, Iowa

Members
DAVID R. DAWDY, Consulting Hydrologist, San Francisco, California
CARL F. NORDIN, Jr., U.S. Geological Survey, Lakewood, Colorado
JOHN SCHAAKE, Hydrologic Services Division, National Weather Service, Silver Springs, Maryland
STANLEY A. SCHUMM, Department of Geology, Colorado State University, Fort Collins, Colorado
VITO A. VANONI, W.M. Keck Laboratory, California Institute of Technology, Pasadena, California

Liaison Representatives
FRANK TSAI, Federal Emergency Management Agency, Washington, D.C.

Consultant
TATSUAKI NAKATO, Institute of Hydraulic Research, The University of Iowa, Iowa City, Iowa

ABBE Staff
JOHN EBERHARD, Executive Director and Program Manager from 1981
JAMES R. SMITH, Program Manager until 1981
DELPHINE D. GLAZE, Administrative Secretary

CONTENTS

Page

Preface.....vii

Summary.....xi

Chapter

I Introduction.....1

II Description of Models Evaluated.....3
A. HEC2SR.....3
B. KUWASER.....7
C. UUWSR.....11
D. HEC-6.....14
E. FLUVIAL-11.....19
F. SEDIMENT-4H.....24

III Description of Study Rivers.....31
A. Study Rivers.....31
B. Summaries of Input Data.....37

IV Presentation and Discussion of Results.....47

V Limitations of Alluvial-River-Flow Models.....113

VI Summary, Conclusions, and Recommendations.....117

APPENDIX: Biographical Sketches of Committee Members and Consultant.....121

List of References.....125

PREFACE

This report presents the results of one of four studies related to the National Flood Insurance Program (NFIP) conducted by the Advisory Board on the Built Environment (ABBE) during 1981-1982. The client for these studies has been the Federal Emergency Management Agency (FEMA), which administers the NFIP. This report addresses the evaluation of flood-level prediction using computer-based models of alluvial-river flows. The other three studies are: (1) an assessment of the conduct of flood insurance studies; (2) the problem of how to map areas of mudslide hazards (including recommendations on how to delineate areas prone to mudslides); and (3) an evaluation of a computer model for coastal flooding from hurricanes (and its specific application to Lee County, Florida).

The study committee was selected after consultation with experts in government, industry and academia, as well as within the National Academy of Sciences/National Academy of Engineering. The committee was chosen to include experts in river engineering, classical and numerical hydraulics, hydrology, and river morphology--the technical disciplines related to the study area under consideration. The Chairman of the Committee was Dr. John F. Kennedy, a specialist in river hydraulics and sedimentary processes. The other members of the Committee were Dr. Vito A. Vanoni and Dr. Carl F. Nordin, Jr., both specialists in sediment-transport mechanics and river hydraulics; Dr. John A. Schaake, an expert in the field of hydrology who specializes in runoff prediction and flood forecasting; Dr. David R. Dawdy, whose specialty is numerical modeling of river-flow and other hydrologic processes; and Dr. Stanley A. Schumm, a specialist in riverine geomorphology. See Appendix for biographical sketches.

The study was initiated by FEMA Regions 8, 9, and 10, primarily the western states, because they had experienced problems with modeling channel erosion and sedimentation using fixed-bed models (e.g., HEC-2) to compute flood-water elevations. The focus of these problems was flood-insurance studies in communities impacted by rivers with movable beds or alluvial channels. It was suggested to FEMA that one or more existing numerical, alluvial-river models might better serve the requirements of flood-stage prediction for the National Flood Insurance Program. This study was organized to address the question of flood-stage prediction and capabilities of computer-based flow- and sediment-routing models for alluvial streams.

The Committee decided early in their deliberations that a subcontract should be awarded to the Institute of Hydraulic Research of The University of Iowa to engage Dr. Tatsuaki Nakato to manage the technical aspects of the study. Specifically, the subcontractor was to:

1. Prepare an inventory of available computer-based flood- and sediment-routing models; a detailed description of each model's capabilities, limitations, required input and input format, and output and output format; and a general evaluation of each model's strengths, weakness and applicability for use in flood insurance studies.
2. Propose, for committee consideration, at least two U.S. river channels and corresponding flood events to be used as test cases in the evaluation and comparison of models deemed appropriate by the Committee.
3. Compile the data required by each model, in the format required, for the test cases selected and transmit these data packages to the appropriate agencies or individuals for use in performing the test-case calculations.
4. Make the arrangements required for the various agencies or individuals responsible for the selected models to perform test-case calculations using their models.
5. Perform, using the test cases selected by the Committee, a set of test-case calculations using one of the selected models in order to provide some indication of the accuracy, resolution, reproducibility, etc., that can be expected from the other models and to ensure that the test cases chosen are appropriate.
6. Prepare a report describing the test cases selected and the test-case calculations.
7. Prepare, in a form suitable for evaluation by the Committee, a compilation of the results of the test-case calculations that includes written narratives describing the technical advantages and disadvantages of the models considered.

In October of 1981 it was further determined that subcontracts should be negotiated with four computer modelers for the performance of test-case calculations, utilizing models selected from the inventory compiled by Dr. Nakato, for at least two U.S. river channels and corresponding flood events. Each modeler selected was to:

1. Supply background information consisting of:

   a. The characteristics and limitations of his model, including background documentation.

   b. A copy of the program or a functional block diagram for each computer-based flow-routing and sediment-routing model.

2. Run his computer model(s) using given input data for given test-river reaches in two phases:

   Phase I: Rigid-bed model calculation
   Phase II: Erodible-bed model calculation

   Provide rationale for selecting the various parameters utilized in his model(s) and final computational outputs tabulated in the format requested by the Committee.

3. Upon request, perform additional computation and clarify any Committee member's questions on the test results.

The four modelers selected for this purpose were:

1. Dr. Ranjan Ariathurai
   Resource Management Associates
   3738 Mt. Diablo Boulevard, Suite 200
   Lafayette, California 94549

2. Dr. Howard H. Chang
   Department of Civil Engineering
   San Diego State University
   San Diego, California 92182

3. U.S. Army Corps of Engineers
   Hydrologic Engineering Center
   609 2nd Street
   Davis, California 95616

4. Simons, Li & Associates, Inc.
   3555 Stanford Road
   Post Office Box 1816
   Fort Collins, Colorado 80552

The report is intended for the use of technical staff members of FEMA. While the report may also be of interest to other professionals in government, universities, and private consulting firms, it is not designed as a document to be used by the general public or those without previous technical background in the subject.

SUMMARY

The primary objective of this investigation was to determine whether river-bed degradation during flood passage has an effect on flood stage that should be incorporated into the calculation of flood-zone limits. The ancilliary question is whether flood-zoning studies should make use of flood-stage prediction models which incorporate river-bed mobility and degradation/aggradation, instead of utilizing fixed-bed models, which have been employed heretofore. The study involved application of six flow- and sediment-routing models for alluvial streams to study reaches of the San Lorenzo, San Dieguito, and Salt Rivers, for which relatively complete input data were available. The developers of the individual models were commissioned to perform the numerical simulations using their models.

From the results of the studies, it was concluded that the effect of river-bed degradation and aggradation on water-surface elevation during flood passage is much smaller than the effects of the uncertainties of channel roughness or flow friction factor, sediment input, and initial channel geometry. Moreover, the available input data on channel geometry, bed-material characteristics, etc., generally are inadequate to permit full utilization of the capabilities of erodible-bed models. Therefore, except in cases of severely disturbed rivers which have experienced extreme local degradation or aggradation through man's intervention, utilization of erodible-bed models instead of fixed-bed models cannot be justified in flood-insurance studies. The principal deficiencies of the erodible-bed models are:

a. Unreliable formulation of the sediment-discharge capacity of flows.

b. Inadequate formulation of the variable friction factor of erodible-bed flows, and, in particular, the dependency of friction factor on depth and velocity of flow, sediment concentration, and temperature.

c. Inadequate understanding and formulation of the mechanics of bed coarsening and armoring, and their effects on sediment-discharge capacity, friction factor, and degradation suppression of flows.

d. Inadequate understanding and formulation of the mechanics of bank erosion, and, therefore, limited capability to incorporate this contribution into the sediment input to the flows from bank erosion and the effects of channel widening.

Numerical modelling of riverine processes will become a steadily more reliable and increasingly powerful tool. The principal limitation on the methodology likely will continue to be inadequate formulation of the constituent processes enumerated above. Until these improvements are made, rigid-boundary models should be utilized for flood-insurance studies, and attention should be directed toward examining the sensitivity of these models to uncertainties and variations in channel roughness, channel geometry, and channel slope.

I. INTRODUCTION

The principal objective of the investigation reported herein was to provide advice and guidance to the Federal Emergency Management Agency (FEMA) concerning the capabilities, limitations, and applicability of available computer models for erodible-bed rivers to flood events, with the goal of improving flood-insurance studies conducted under the National Flood Insurance Program (NFIP). Descriptions of the Committee that was convened and the organizational aspects of the project are presented in the PREFACE. the early stages of the study, a nationwide canvass of river experts was made by the Committee to identify modelers who had developed usable, alluvial-river-flow models. Although the Committee was aware of the several alluvial-river-flow models, developed in Europe and elsewhere, such as those of the Danish Hydraulic Institute in Denmark; Delft Hydraulics Laboratory in the Netherlands, Sogreah in France; and Hydraulics Research Station of Wallingford, England, a decision was made to limit the study to models that had been developed in the USA. This decision was dictated primarily by the time and budgetary constraints of this study. From among the several modelers identified, four agreed to participate in the project: Hydrologic Engineering Center, Corps of Engineers (HEC); Resource Management Associates (RMA); San Diego State University (SDSU); and Simons, Li & Associates, Inc. (SLA). A total of six numerical models was selected by the Committee members: three from SLA, and one from each of the other organizations. The characteristics of the models are summarized in Chapter II. Chapter III presents background on the selection of the three study rivers (the San Lorenzo River (SLR); the San Dieguito River (SDR); and the Salt River (SR)), and describes the characteristics of the rivers and the input data utilized for each. The principal numerical results obtained by each modeler are summarized in Chapter IV. Chapter V describes the limitations of the alluvial-river-flow models, and the principal conclusions and recommendations arrived at by the Committee are summarized in Chapter VI.

II. DESCRIPTION OF MODELS EVALUATED

The characteristics of the six numerical models of flow and sediment transport in movable-bed channels evaluated in the present study are summarized in this chapter. The models are HEC2SR, KUWASER, UUWSR, HEC-6, FLUVIAL-11, and SEDIMENT-4H. Summaries of the models' characteristics were first prepared on the basis of the individual modelers' final reports submitted to the Committee, and the references cited therein. Each modeler then was requested to review the Committee's description of his model. The modelers' suggestions and corrections have been incorporated into the following descriptions.

A. HEC2SR (HEC-2 with Sediment Routing):

1. Developer: Simons, Li & Associates, Inc. (SLA), 1980
2. Previous Applications:
   (1) Boulder Creek, Larimer County, Colorado (SLA, 1980)
   (2) Salt River, Phoenix, Arizona (SLA, 1980)
   (3) Santa Cruz River, Tucson, Arizona (SLA, 1981)
   (4) Cañada del Oro Wash, Pima County, Arizona (SLA, 1981)
   (5) Rillito Creek, Pima County, Arizona (SLA, 1981)

3. Basic Concepts:

The model was developed for simulating watershed sediment yield and the attendant aggradation and degradation in a river system. HEC2SR uses the HEC-2 backwater-computation program developed by Eichert (1976), at the Corps of Engineers (COE), Hydrologic Engineering Center (HEC), for calculation of backwater profiles. The following assumptions are incorporated into the HEC-2 program (Eichert, 1981):

(1) Flow is steady and gradually varied.
(2) Flow is one dimensional and hydrostatic pressure prevails at any point in the channel.
(3) The total energy head is the same for all points in a cross section (one-dimensional assumption).

(4) Channel slope is small.

The following basic equations are employed:

(1) Flow-continuity equation:

$$\frac{dQ}{dx} = q \qquad \text{....(2-1)}$$

(2) Sediment-continuity equation:

$$\frac{\partial Q_s}{\partial x} + (1 - \lambda)\frac{\partial A_b}{\partial t} = q_{s\ell} \qquad \text{....(2-2)}$$

(3) Flow-energy equation:

$$y_2 + \frac{\alpha_2 V_2^2}{2g} = y_1 + \frac{\alpha_1 V_1^2}{2g} + h_e \qquad \text{....(2-3)}$$

(4) Energy head-loss equation:

$$h_e = L\overline{S}_f + C\left|\frac{\alpha_2 V_2^2}{2g} - \frac{\alpha_1 V_1^2}{2g}\right| \qquad \text{....(2-4)}$$

where Q & Q_s = water and sediment discharges in volume units

q = lateral water inflow per unit width

A_b = bed cross-section area

$q_{s\ell}$ = lateral sediment inflow in volume per unit time and length

λ = porosity of bed sediment

y_1 & y_2 = water-surface elevations at ends of reach

V_1 & V_2 = mean velocities at ends of reach

α_1 & α_2 = velocity-head correction factors for flow at ends of reach

h_e = energy head loss

L = discharge-weighted reach length

$\overline{S}_f$ = representative friction slope for reach

C = expansion or contraction loss coefficient

4. Sediment-Transport Function:

The bed-load transport rate, q_b in volume per unit width, is computed from the Meyer-Peter and Müller formula (Meyer-Peter and Müller, 1948):

$$q_b = \frac{12.85}{\sqrt{\rho}\,\gamma_s}(\tau_o - \tau_c)^{1.5} \qquad \text{....(2-5)}$$

where τ_o = bed shear stress
τ_c = critical shear stress = $0.047\,(\gamma_s - \gamma)d_s$
ρ = density of water
γ_s = specific weight of sediment
γ = specific weight of water
d_s = median sediment particle size

The suspended-load transport rate, q_s in volume per unit width, is given by the Einstein formula (Einstein, 1950):

$$q_s = \frac{q_b}{11.6}\,\frac{G^{w-1}}{(1-G)^w}\left((V/u_*) + 2.5\right) I_1 + 2.5\, I_2) \qquad \text{....(2-6)}$$

where G = depth of bed layer divided by sediment diameter
u_* = shear velocity
V = mean flow velocity
I_1 & I_2 = Einstein's integrals
w = Rouse Number = particle fall velocity/$(0.4u_*)$

The combined bed-material transport rates are further corrected for the fine-sediment concentration using Colby's empirical relationships (Colby, 1957). During the sediment-routing phase, armoring effect and bed-material composition changes are considered. In determining the armored layer, a functional relationship between mean flow velocity and median sediment size, which determines the size of sediment that will not move, was first derived using Shields' criterion. The channel is assumed to be armored when a layer of nonmoving sediment that is twice as thick as the smallest size of moving sediment particles is established.

5. Numerical Scheme:

HEC2SR first runs the HEC-2 program to solve (2-3) and (2-4) by the standard, iterative-step method. The computational procedure is as follows:

(1) Assume a water-surface elevation, y_2, at section 2.
(2) Based on the assumed value of y_2, determine the corresponding total conveyance and velocity head.
(3) Compute $\overline{S}_f$ and compute h_e from (2-4).
(4) Check the equality of (2-3) with the computed value using the assumed y_2.
(5) Adjust y_2 if the error in step (4) is significant, repeat steps 1 through 5 until the values agree to within 0.01 ft.

After the HEC-2 computation, the bed-material discharge, which considers both sediment availability and transport capacity, is estimated for each computational reach. The channel aggradation/degradation corresponding to the difference between the sediment inflow and outflow is also determined for each reach. This sediment-volume change is distributed uniformly along the reach. The change in elevation at each cross-section vertical is determined by a weighting factor based on flow conveyances in adjacent lateral subsections. This technique is also used in KUWASER (see Section II-B)

6. Data Requirement:

HEC2SR requires the following input data:

(1) Data on channel geometry in HEC-2 format.
(2) Information on subreaches which are divided according to hydraulic and sediment-transport characteristics, including number of cross sections, reach length, number of tributaries, surface and subsurface sediment-size distributions, and potential armor layer.
(3) Watershed data, including channel-geometry representation and sediment-size distribution; this can be neglected if the sediment inflow from the lateral tributaries is neglected and/or the upstream reach does not connect to the upland watershed area.

(4) Inflow hydrographs and downstream boundary condition (stage hydrograph if available) throughout the flood.

7. Model Limitations and Applicability:

The use of HEC2SR is limited to a reach for which the one-dimensional-flow approximation is applicable. The model accounts for neither lateral channel migration nor secondary currents. The model assumes a uniform aggradation or degradation pattern along the reach, so that localized scour or deposition cannot be predicted. The model is not suitable for studying long-term river-bed changes, because of the high cost of backwater computation using HEC-2. However, HEC2SR offers the option to input sediment inflows directly or internally to generate sediment-loading data by considering the sediment-transport capacities in the upstream main-channel and tributary reaches. The backwater results obtained using HEC-2 can be directly compared to stage predictions utilized in the conventional flood-insurance studies. The model also features modular structure, which enables users to modify each functional component.

B. KUWASER (Known discharge, Uncoupled, WAter and SEdiment Routing):

1. Developer: Simons, Li, and Brown (Colorado State University), 1979

2. Previous Applications:

(1) Yazoo River Basin (Simons, Li, and Brown, 1979)

3. Basic Concepts:

The model was developed for simulating one-dimensional, spatially-varied, steady water and sediment flows. The principal assumptions it employs are as follows:

(1) Hydraulic characteristics of flow remain constant for a specified time interval.
(2) Hydrostatic pressure distribution prevails over any channel section.
(3) Secondary flow is negligible.
(4) Friction loss at a section is the same as that for a uniform flow with the same velocity and hydraulic radius.

(5) Channel slope is small.

The following basic equations are employed:

(1) Flow-continuity equation:

$$\frac{dQ}{dx} = q \qquad \text{....(2-7)}$$

(2) Sediment-continuity equation:

$$\frac{\partial Q_s}{\partial x} + (1 - \lambda)\frac{A_b}{\partial t} = q_{s\ell} \qquad \text{....(2-8)}$$

(3) Flow-energy equation:

$$(z + D + \alpha \frac{V^2}{2g})_1 = (z + D + \alpha \frac{V^2}{2g})_2 + H_\ell + H_{\ell v} \qquad \text{....(2-9)}$$

where

Q & Q_s = water and sediment discharges

q = lateral water inflow per unit width

A_b = bed cross-section area

$q_{s\ell}$ = lateral sediment inflow

λ = porosity of bed material

z = channel bed elevation

D = flow depth

H = total head above datum

α = correction factor for velocity head

V = mean flow velocity

H_ℓ = friction loss = $S_f \Delta x$

$H_{\ell v}$ = losses due to all other factors except friction = $S_{\ell v} \Delta x$

4. Sediment-Transport Function:

The sediment discharge per unit width, q_s, is expressed by

$$q_s = a\, V^b\, y^c \qquad \text{....(2-10)}$$

where

V = mean flow velocity

y = flow depth

a, b, and c = coefficients determined by means of regression analysis

The regression coefficients are determined either from field data or by generating data using the Meyer-Peter and Müller formula and Einstein's bed-load function for bed-load and suspended-load discharges, respectively. The model does not take into account changes in bed-material composition.

5. Numerical Scheme:

KUWASER first solves (2-7) and (2-9) for a spatially-varied, steady flow by means of the first order Newton-Raphson method. Equations (2-7) and (2-9) are combined to yield the following expression for the sole unknown, flow depth at section 2, D_2:

$$a_1 \frac{Q_2^2}{2g} D_2^{a_2} + D_2 - \frac{4\Delta x\, Q_2^2}{K_1^2 + 2K_1 a_3 D_2^{a_4} + a_5 D_2^{a_6}} + a_6 \frac{\alpha_1 V_1^2}{2g} + z_2 - H_1 = 0 \qquad \text{....(2-11)}$$

where

Q_2 = water discharge at section 2

K_1 = conveyance at section 1

z_2 = bed elevation at section 2

a_1, a_2, a_3, a_4, a_5, and a_6 = regression coefficients determined from field data

Note that effective depth and width, cross-section area, conveyance, and velocity-head correction factor are all expressed in terms of power functions of the thalweg flow depth, D. Once the backwater calculation is completed, sediment-transport rates at all cross sections are computed from (2-10). The

sediment routing is then made by a two-step finite-difference algorithm. The first step is to compute the change in sediment volume between two cross sections:

$$\Delta V_i = (Q_{s_{i+1}} - Q_{s_i} + q_{s\ell_i})\Delta t \qquad \text{....(2-12)}$$

The second step is determination of the change in cross-section area at each cross section. The model assumes that one-quarter of ΔV_i is deposited or eroded in the upstream half of the segment between sections i and i+1, while three-quarters of ΔV_{i-1} is deposited or eroded in the downstream half of the reach between sections i and i-1. Therefore, when $q_{s\ell}$ is neglected, (2-8) can be expressed as

$$\Delta A_{b_i} = \frac{1}{1-\lambda} \frac{\frac{3}{2} Q_{s_{i+1}} - Q_{s_i} - \frac{1}{2} Q_{s_{i-1}}}{\Delta x_{i-1} + \Delta x_i} \Delta t \qquad \text{....(2-13)}$$

Finally, the model distributes ΔA_{bi} over the cross section to determine the new channel geometry. The method used is to relate the bed-elevation change at a point to the local conveyance. The elevation change at the j-th vertical, Δz_j, is computed as follows:

$$\Delta z_j = \frac{k_\ell + k_{\ell+1}}{K_i} \frac{\Delta A_{b_i}}{y_{j+1} - y_{j-1}} \qquad \text{....(2-14)}$$

where

k_ℓ and $k_{\ell+1}$ = conveyances of the incremental areas to the right and left of the j-th vertical

y_{j+1} and y_{j-1} = lateral coordinates of the (j+1)st and (j-1)st verticals

K_i = total conveyance of the i-th cross section

6. Data Requirements:

KUWASER requires the following input data:

(1) Number of cross sections and individual reach lengths.

(2) Number of subdivided reaches.
(3) Locations of tributaries.
(4) Cross-section geometries of all sections.
(5) Manning's n at each section.
(6) Upstream and tributary inflow hydrographs and stage data for every time step.
(7) Sediment-transport coefficients.
(8) Characteristic parameters for each dam, including its discharge coefficient, width, and height.

7. Model Limitations and Applicability:

The use of KUWASER is limited to subcritical flows. The model does not predict channel armoring or two-dimensional flow effects. KUWASER cannot effectively model a river reach with extremely irregular channel grade and geometry, but has the capability to model the main stem and tributaries in an entire river system. KUWASER can simulate divided flows associated with bars, islands, or channel breaches. The model finds its best application in long-term degradation/aggradation analysis.

C. UUWSR (Uncoupled, Unsteady Water and Sediment Routing):

1. Developer: Tucci, Chen, and Simons (Colorado State Univeristy), 1979

2. Previous Applications:

(1) Upper Mississippi and Lower Illinois Rivers (Simons, et al., 1975)
(2) Upper Mississippi and Lower Chippewa Rivers (Simons & Chen, 1976 & 1977; Simons et al., 1979; Simons & Chen, 1979; Chen & Simons, 1980)
(3) Lower Mississippi River (Simons & Chen, 1978)

3. Basic Concepts:

This model was developed for simulating one-dimensional, gradually-varied, unsteady, water and sediment flows in complicated river networks. The principal assumptions included in this model are as follows:

(1) The river channel is sufficiently straight and uniform that the one dimensional flow approximation can be employed.

(2) Hydrostatic pressure prevails at any point in the channel, and the water-surface slope is small.

(3) The density of sediment-laden water is constant over the cross section.

(4) The resistance coefficient for the unsteady flow is assumed to be the same as that for a steady flow.

The following basic equations are employed:

(1) Flow-continuity equation:

$$\frac{\partial Q}{\partial x} + T\frac{\partial y}{\partial t} - q_\ell = 0 \qquad \text{....(2-15)}$$

(2) Sediment-continuity equation:

$$\frac{\partial Q_s}{\partial x} + (1 - \lambda)\frac{\partial A_d}{\partial t} - q_s = 0 \qquad \text{....(2-16)}$$

(3) Flow-momentum equation:

$$\frac{\partial Q}{\partial t} + \frac{\partial(\beta QV)}{\partial x} + gA\frac{\partial y}{\partial x} = \rho gA(S_o - S_f + D_\ell) \qquad \text{....(2-17)}$$

where

Q & Q_s = water and sediment discharges

$T = \partial A/\partial y$

y = flow depth

A = cross-section area for water

A_d = sediment volume deposited per unit channel length

$q_\ell = q_s + q_w$

q_s = lateral sediment inflow

q_w = lateral water inflow

λ = porosity of bed material

V = mean flow velocity

β = momentum correction factor

ρ = density of water

S_o = bed slope

S_f = friction slope

D_ℓ = dynamic contribution of lateral inflow ($q_\ell V_\ell / Ag$)

To solve these three equations for the three primary unknowns, Q, y, and A_d, other variables are expressed in terms of Q, y, and A_d.

4. Sediment-Transport Function:

The sediment discharge per unit width, q_s, is expressed by

$$q_s = a\ V^b\ y^c \qquad \text{....(2-18)}$$

where

V = mean flow velocity

y = flow depth

a, b, and c = coefficients determined by means of regression analysis

The regression coefficients are determined either from field data or by generating data using the Meyer-Peter and Muller formula and Einstein's bed-load function for bed-load and suspended-load discharges, respectively. Changes in bed-material composition are not taken into account.

5. Numerical Scheme:

UUWSR first solves (2-15) and (2-17) by a four-point, implicit, finite-difference scheme (unconditionally stable) assuming a fixed bed. The resulting flow information is used to compute the sediment-transport capacity by means of (2-18). Computed sediment discharges then are applied to the sediment-continuity equation, (2-16), to estimate the change in the cross-section area. Equation (2-16) is solved using an explicit, finite-difference approximation. Therefore, UUWSR is an uncoupled, unsteady, water- and sediment-routing model.

6. Data Requirements:

UWSR requires the following input data:

(1) Number of cross sections and individual reach lengths.

(2) Number of subreaches.

(3) Locations of tributaries.

(4) Cross-section geometries of all computational sections (arranged from upstream to downstream).

(5) Manning's roughness coefficient at each cross section.

(6) Boundary conditions specified by either a discharge hydrograph, or a stage hydrograph, or a stage-discharge rating curve.

(7) Sediment-transport function.

(8) Characteristic parameters for each dam, including its discharge coefficient, width, and height.

7. Model Limitations and Applicability:

The use of UUWSR is limited to a modeling reach for which the one-dimensional flow approximation and steady-state solutions at confluences and dams are applicable. However, the model can simulate, with minimal computer cost, a complex river-network system in which islands, branches, meander loops, and tributaries are connected to the main channel. The model can also simulate effects of hydraulic structures such as dikes, locks and dams, etc. The capability of unsteady flow routing of this model enables users to simulate the flood-wave movement in a long reach.

D. HEC-6 (Hydrologic Engineering Center):

1. Developer: William A. Thomas (Hydrologic Engineering Center, Corps of Engineers), 1977

2. Previous Applications:

(1) Atchafalaya River Basin, Louisiana (Jennings & Land, 1977)

(2) Clearwater River, Idaho (Williams, 1977)

(3) Boise River, Idaho (Thomas & Prasuhn, 1977)

(4) San Lorenzo River (Jones-Tillson & Associates, 1980)

(5) Mississippi River (Nakato & Vadnal, 1981)

(6) Cottonwood Creek (Prasuhn & Sing, 1981)

3. Basic Concepts:

The model was developed to analyze scour and deposition of movable-bed channels by simulating one-dimensional, steady, gradually-varied water and sediment flows. The principal assumptions employed in the model are as follows:

(1) Flow is one dimensional and hydrostatic pressure prevails at any point in the channel.
(2) Manning's n is applicable to gradually-varied flow and is expressed as a function of either water-surface elevation or water discharge (the model incorporates indirectly the roughness effects of changes in bed forms).
(3) The entire movable-bed portion of a cross section is scoured or deposited at the same rate.
(4) Channel slope is small.

The following basic equations are employed in the model:

(1) Flow-continuity equation:

$$\frac{dQ}{dx} = q_\ell \quad \text{....(2-18)}$$

(2) Sediment-continuity equation:

$$\frac{\partial G}{\partial x} + B\frac{\partial y}{\partial t} = 0 \quad \text{....(2-19)}$$

(3) Flow-energy equation:

$$\left(h + \frac{\alpha Q^2}{2gA^2}\right)_{k-1} = \left(h + \frac{\alpha Q^2}{2gA^2}\right)_k + H_L \quad \text{....(2-20)}$$

where

Q = water discharge

q_ℓ = lateral water inflow per unit width
G = volumetric sediment-transport rate
B = movable-bed width
y = movable-bed elevation
h = water-surface elevation
α = velocity-head correction factor
A = cross-section area
H_L = head loss between sections k-1 and k

4. Sediment-Transport Function:

Five options are available for computing bed-material transport rates: Laursen's relationship, as modified by Madden for large rivers (Laursen, 1958); Toffaleti's formula (Toffaleti, 1968); Yang's stream-power formula (Yang, 1973); DuBoys' formula (Brown, 1950); and a special relationship between unit-width sediment-transport capacity and the product of flow depth and energy slope which is developed for a particular river reach.

Laursen's relationship is expressed by

$$q_s = 283.39\ q \sum_i p_i (d_{si}/D)^{7/6} (\tau_0^i/\tau_{ci} - 1) \qquad \text{....(2-21)}$$

where

q_s = bed-material transport rate per unit width
q = water discharge per unit width
p_i = fraction by weight of the i-th fraction of the bed sediment with mean size, d_{si}
D = flow depth
τ_0' = Laursen's bed-shear stress due to grain roughness $= \rho V^2/(58(d_{50}/D)^{1/3})$
d_{50} = median sediment size
V = mean flow velocity
τ_{ci} = critical shear stress for mean particle size, d_{si}

The second option, the Toffaleti formula, is based on Einstein's bed-load function and various empirical data and is expressed by

$$q_{si} = q_{sbi} + q_{ssLi} + q_{ssMi} + q_{ssUi} \qquad \text{....(2-22)}$$

where

q_{si} = bed-material discharge for the i-th fraction of bed sediment
q_{sbi} = bed-load discharge for the i-th fraction of the bed sediment
q_{ssLi} = suspended-load discharge in lower zone
q_{ssMi} = suspended-load discharge in middle zone
q_{ssUi} = suspended-load discharge in upper zone

Detailed procedures for computation of q_{sbi}, q_{ssLi}, q_{ssMi}, and q_{ssUi} are given by Toffaleti (1966).

5. Numerical Scheme:

HEC-6 first solves the one-dimensional energy and continuity equations, (2-20) and (2-18), using an iterative, standard step-backwater method, to obtain basic hydraulic parameters such as depth, width, and slope at each section which are necessary to compute the sediment-transport capacity. Friction loss is calculated from Manning's equation with specified n values. A functional relationship between Manning's n and water discharge or flow stage can be used if available. Expansion and contraction losses are calculated using loss coefficients. The potential sediment-transport capacities at all cross sections are computed next, using one of the five optional sediment-transport functions. Note that the sediment discharge at the upstream boundary must be related to the water discharge by a rating table for different sediment-size fractions. Computations of sediment-transport capacity begin at the upstream boundary and move reach by reach to the downstream boundary. Equation (2-19) is then solved using an explicit, finite-difference scheme:

$$\frac{-(G_R - G_L)}{0.5(X_L + X_R)} + \frac{B(Y_{p'} - Y_p)}{\Delta t} = 0 \qquad \text{....(2-23)}$$

or

$$Y_{p'} = Y_p + \frac{\Delta t}{0.5B}(G_R - G_L)/(X_L + X_R) \qquad \text{....(2-24)}$$

where

G_R = volumetric sediment-transport rate at the (k+1)st cross section

G_L = volumetric sediment-transport rate at the (k-1)st cross section

$Y_{p'}$ = movable-bed thickness at the kth cross section at the time of $(j+1)\Delta t$

Y_p = movable-bed thickness at the kth cross section at the time of $j\Delta t$

X_L = reach length between (k-1)st and kth cross sections

X_R = reach length between kth and (k+1)st cross sections

Note that the transport capacity is calculated at the beginning of the time interval, and is not recalculated during that interval. However, the gradation of the bed material is recalculated during the time interval in order to account for armoring effects. An equilibrium water depth below which sediment with a particular grain size becomes immobile is introduced using Manning's equation, Strickler's equation, and Einstein's bed-load function:

$$D_{eq} = (q/(10.21d^{1/3}))^{6/7} \qquad \text{....(2-25)}$$

where

q = water discharge per unit width

d = sediment particle size

A zone of bed between the bed surface and the equilibrium depth is designated the active layer. When all material is removed from the layer, the bed is considered to be completely armored for that particular hydraulic condition. When a mixture of grain sizes is present, the equilibrium depth calculations utilize the given gradation curve to relate the quantity of each grain size present in the bed to the depth of scour. The armor layer formed by a previous discharge is tested for stability using Gessler's (1971) stability-analysis procedure. If Gessler's stability number is less than 0.65, the armor layer is treated as unstable and the bed-layer size distribution is computed for the next time step.

6. Data Requirements:

HEC-6 requires the following input data:

(1) Number of cross sections, individual reach lengths, and tributary locations.
(2) Geometric data on movable-bed portion of each cross section, thickness of movable bed, and bridges, and dredging information.
(3) Manning's roughness coefficient at each cross section.
(4) Data on sediment inflow, bed-material gradation, and sediment properties.
(5) Upstream and lateral inflow hydrographs, downstream boundary condition (stage-discharge curve or stage hydrograph), and water temperatures.

HEC-6 is a one-dimensional model with no provision for simulating the development of meanders or specifying a lateral distribution of the sediment-transport rate across the section. The entire movable-bed portions of the cross sections are assumed to aggrade or degrade uniformly. The model is not suitable for rapidly-changing flow conditions. The model can be applied to predict reservoir sedimentation, degradation of the stream bed downstream from a dam, and log-term trends of scour or deposition in a stream channel. The influence of dredging activity can also be simulated. The model can be run in the fixed-bed mode, similar to HEC-2, by removing all sediment-data cards.

E. FLUVIAL-11:

1. Developer: Chang and Hill (San Diego State University), 1976

2. Previous Applications:

(1) San Dieguito River (Chang & Hill, 1976)
(2) San Elijo Lagoon entrance channel (Chang & Hill, 1977)
(3) San Diego River (Chang, 1982)

3. Basic Concepts:

FLUVIAL-11 was developed to simulate one-dimensional, unsteady,

gradually-varied water and sediment flows, as well as width changes, erodible channels. The principal assumptions incorporated into this model ar as follows:

(1) Flow is one dimensional, and hydrostatic pressure prevails at any point in the channel.

(2) Channel slope is small.

(3) The Manning equation and the sediment-transport formula are applicable to gradually-varied flow.

(4) Storage effect due to unsteady flow is negligible in the backwater computation.

The following basic equations are employed:

(1) Flow-continuity equation:

$$\frac{\partial Q}{\partial x} + \frac{\partial A}{\partial t} - q = 0 \qquad \text{....(2-26)}$$

(2) Sediment-continuity equation:

$$(1 - \lambda)\frac{\partial A_c}{\partial t} + \frac{\partial Q_s}{\partial x} - q_s = 0 \qquad \text{....(2-27)}$$

(3) Flow-momentum equation:

$$g\frac{\partial H}{\partial x} + \frac{1}{A}\frac{\partial Q}{\partial t} + \frac{1}{A}\frac{\partial}{\partial x}\left(\frac{Q^2}{A}\right) + gS - \frac{Q}{A^2}q = 0 \qquad \text{....(2-28)}$$

where

Q & Q_s = water and sediment discharges

A = cross-section area of flow

A_c = channel cross-section area within some reference frame

q = lateral water inflow

q_s = lateral sediment inflow

H = water-surface elevation

S = energy slope

λ = porosity of bed material

Equations (2-26) and (2-28) are solved for two unknowns, Q and H, by an iterative method. Note, however, that in this NRC study, a simpler method of computing the water-surface profile, using the energy equation, was utilized instead of solving the unsteady equations, (2-26) and (2-28). A standard step method similar to that incorporated into HEC-2 was utilized in solving the energy equation.

4. Sediment-Transport Equation:

The following formula developed by Graf (1968) was used to compute the bed-material discharge for the San Dieguito River and the Salt River:

$$\overline{C}VR/((s_s - 1)gd^{1/3})^{1/2} = 10.39((s_s-1)d/(SR))^{-2.52} \qquad \text{....(2-29)}$$

where

$\overline{C}$ = mean volumetric concentration of bed-material sediment

s_s = ratio of sediment specific weight to water specific weight

d = median sediment size

S = energy slope

V = mean flow velocity

R = hydraulic radius

The Engelund-Hansen formula (1967) was used for the San Lorenzo River to compute the total-load discharge:

$$q_T = 0.05\gamma_s V^2(d/g(\gamma_s/\gamma - 1))^{1/2}(\rho u_*^2/(\gamma_s - \gamma)d^{3/2} \qquad \text{....(2-30)}$$

where

q_T = total-load discharge per unit width

γ_s = specific weight of sediment

γ = specific weight of water

u_* = shear velocity

ρ = density of water

5. Numerical Scheme:

FLUVIAL-11 first solves the water-continuity equation, (2-26), and momentum equation, (2-28), by an iterative, four-point, implicit, finite-difference scheme developed by Amein and Chu (1975). The flow information is next used to compute the sediment-transport rate from either (2-29) or (2-30). The sediment-continuity equation, (2-27), is then solved to obtain ΔA_c in the following way: from (2-27)

$$\Delta A_c = -\frac{\Delta t}{1-\lambda}\left(\frac{\partial Q_s}{\partial x} - q_s\right) \qquad \text{....(2-31)}$$

$$q_{s_i} = \frac{1}{2}\left(q_{s_i}^{j} + q_{s_i}^{j+1}\right) \qquad \text{....(2-32)}$$

$$\left(\frac{\partial Q_s}{\partial x}\right)_i = \frac{1}{\Delta x_{i-1}}\left[\frac{Q_{s_i}^{j} + Q_{s_i}^{j+1}}{2} - \frac{Q_{s_{i-1}}^{j} + Q_{s_{i-1}}^{j+1}}{2}\right] \qquad \text{....(2-33)}$$

$$(\Delta A_c)_i = \frac{\Delta t}{1-\lambda}\left[\frac{Q_{s_{i-1}}^{j} + Q_{s_{i-1}}^{j+1} - Q_{s_i}^{j} - Q_{s_i}^{j+1}}{2\Delta x_{i-1}} + \frac{q_{s_i}^{j} + q_{s_i}^{j+1}}{2}\right] \qquad \text{....(2-34)}$$

Note that a backward-difference scheme was used in x and a forward-difference scheme was used in t. The quantity ΔA_c obtained from (2-34) is then corrected for the following effects:

(1) Adjustment in channel width:
Width adjustments are made in such a way that the spatial variation in power expenditure per unit channel length (γQS) is reduced along the channel. The width is adjusted until the value which gives minimum total stream power (integration of γQS over the reach length) at each time step is found. To determine the width change at each section, the actual energy gradient at this section S_i is compared with the weighted, average energy gradient $\overline{S}_i$ of its adjacent sections given by

$$\overline{S}_i = (S_{i-1}\Delta X_i + S_{i+1}\Delta X_{i-1})/(2(\Delta X_{i-1} + \Delta X_i))$$

If S_i is greater than $\overline{S}_i$, the channel width is reduced so as to decrease S_i, and vice versa. The new channel width is determined by a trial and error technique. Width changes are subject to the physical constraints of rigid banks or the angle of repose of the bank material.

(2) Adjustment in cross-section profile:
Deposition at an aggrading section is assumed to start from the lowest point and to build up the bed in horizontal layers. At a degrading section, the change in cross-section area is distributed in proportion to the local tractive force. These types of adjustment reduce the spatial variation in power expenditure along the channel.

(3) Lateral channel migration:
The model solves the sediment-continuity equation in the transverse direction:

$$(1 - \lambda)\frac{\partial z}{\partial t} + \frac{\partial q_s'}{\partial y} = 0 \qquad \text{....(2-35)}$$

where

q_s' = $q_s \tan\beta$ = transverse sediment-transport rate per unit width

β = $\tan^{-1}(11D/r)$ = angle deviation of transverse flow from the direction tangent to the centerline of a bend given by Rozovskii(1957)

D = mean flow depth

r = radius of curvature of the bend

z = bed elevation

Using a forward-difference scheme in y, Δz_k is obtained from

$$\Delta z_k = -\frac{\Delta t}{1-\lambda}\frac{q_{s_{k+1}}' - q_{s_k}'}{\Delta y_k} \qquad \text{....(2-36)}$$

where

Δy_k = transverse distance between points k and k+1

6. Data Requirements:

FLUVIAL-11 requires the following input data:

(1) Number of cross sections and individual reach lengths.
(2) Tributary locations.
(3) Flood hydrographs for main and tributary streams.
(4) Downstream boundary conditions.
(5) Cross-section geometries of all computational sections and Manning's n at each cross section.
(6) Initial bed-material sediment compositions for the upstream and downstream ends. Sediment compositions at intermediate cross sections are computed using an exponential decay relationship.
(7) Description of channel bends, if any, by their radii of curvature.

7. Model Limitations and Applicability

The use of FLUVIAL-11 is limited to a modeling reach for which the one-dimensional flow approximation is applicable. However, the model can predict changes in erodible channel width, changes in channel-bed profile, and lateral migration of a channel in bends.

F. SEDIMENT-4H:

1. Developer: Ranjan Ariathurai (Resource Management Associates), 1977

2. Previous Applications:

(1) The Osage River, Missouri (Ariathurai, 1980)

3. Basic Concepts:

The model was developed for simulating two-dimensional, gradually-varied, unsteady, water and sediment flows. The model utilized in the present study, however, is a one-dimensional version of SEDIMENT-4H. The principal assumptions employed in this model are as follows:

(1) Flow is one dimensional and hydrostatic pressure prevails at any point in the channel.

(2) Similarity of both velocity and suspended-sediment concentration profiles in a vertical at all locations in the flow field is assumed.

(3) The resistance coefficient for the unsteady flow is the same as that for a steady flow.

(4) Channel slope is small.

The following basic equations are employed:

(1) Flow-continuity equation:

$$\frac{\partial h}{\partial t} = \frac{1}{b}\frac{\partial q}{\partial x} \pm s \qquad \text{....(2-37)}$$

(2) Sediment-continuity equation:

$$\frac{\partial C}{\partial t} + u_{\alpha s}\frac{\partial C}{\partial x} = \frac{\partial}{\partial x}\left(D_x \frac{\partial C}{\partial x}\right) + S \qquad \text{....(2-38)}$$

(3) Flow-momentum equation:

$$\frac{\partial \bar{u}}{\partial t} + u\frac{\partial \bar{u}}{\partial x} + g\frac{\partial h}{\partial x} + gS_e = 0 \qquad \text{....(2-39)}$$

where

h = water-surface elevation

b = mean channel width

q = inflow rate to a node

s = lateral inflow or outflow rate

C = mass concentration

$u_{\alpha s}$ = longitudinal component of sediment-particle velocity

D_x = turbulent mass diffusivity in the logitudinal direction

S = source/sink term produced by scour or deposition

$\bar{u}$ = mean flow velocity

S_e = friction slope

4. Sediment-Transport Function:

SEDIMENT-4H calculates total-load sediment discharge for an idealized, single, median grain size. The basic concept is similar to Einstein's bed-load function; however, in SEDIMENT-4H the sediment concentration in the bed layer is set to a maximum and is assumed to be transported at the local mass-weighted velocity. The concentration of sediment in the bed layer is assumed to be dependent on the amount of sediment in suspension, but not to exceed 100 lbs/cu ft.

The Rouse (1937) equation for the vertical distribution of suspended-sediment concentration in a fully-developed, turbulent flow is normalized by the depth-averaged sediment concentration, $\langle C \rangle$, and the concentration distribution is expressed in dimensionless terms by

$$\Phi(\lambda) = \Phi_{\Delta}(\Delta(1/\lambda - 1)/(1 - \Delta))^{\xi}; \lambda > \Delta \qquad \text{....(2-40)}$$

and

$$\Phi(\lambda) = \Phi_{\Delta} \quad ; \lambda < \Delta \qquad \text{....(2-41)}$$

where

λ	=	y/d
d	=	flow depth
$\Phi(\lambda)$	=	$C(y)/\langle C \rangle$
Δ	=	a/d (nondimensional sublayer thickness)
a	=	reference level where C is given
ξ	=	$V_s/\kappa U_*$
V_s	=	sediment fall velocity
κ	=	von Karman's constant
U_*	=	shear velocity

The sediment concentration in the sublayer, Φ_{Δ}, is obtained from the following relation:

$$\int_0^1 \Phi(\lambda)\, d\lambda = 1 \qquad \text{....(2-41)}$$

Therefore,

$$\Phi_\Delta = 1/\ (\Delta + \int_0^1 (\Delta(1/\lambda - 1)/(1 - \Delta))^\xi d\lambda \qquad \text{....(2-42)}$$

A logarithmic-type vertical velocity distribution in normalized form is utilized:

$$\Psi = \Psi_*(\frac{1}{\kappa} \ln(\lambda/\gamma) + a_r) \qquad \text{....(2-43)}$$

where

Ψ = $u/\langle U\rangle$

u = local streamwise velocity

$\langle U\rangle$ = depth-averaged streamwise velocity

Ψ_* = $U_*/\langle U\rangle$

γ = k_s/d

k_s = equivalent roughness height

Finally, depth-averaged, sediment-particle velocity, $\langle U_s\rangle$, is expressed as

$$\langle U_s\rangle = \langle U\rangle \int_0^1 \beta\Phi\Psi\ d\lambda \qquad \text{....(2-44)}$$

where

$\beta(\lambda)$ = proportionality coefficient to relate sediment particle velocity, $U_s(y)$, to the mass-weighted fluid velocity, $U(y)$, such that $U_s = \beta U(y)$

Empirical formulas for the rate of scour during stream-bed erosion, E, and the rate of deposition, D, are expressed by

$$E = M(\tau/\tau_{ce} - 1)(C_{max}-C_b)/C_{max}\ ;\ \tau > \tau_{ce} \qquad \text{....(2-45)}$$

and

$$D = -\ V_s C_b(1 - \tau/\tau_{cd})\ ;\ \tau < \tau_{cd} \qquad \text{....(2-46)}$$

where

M = erosion-rate constant

τ = bed shear stress

τ_{ce} = critical shear stress for erosion

τ_{cd} = critical shear stress for deposition

C_b = sediment concentration in bed layer

C_{max} = maximum concentration in bed layer

5. Numerical Scheme:

The Link-Node Hydrodynamic model first solves (2-37) and (2-39), which yield the depth-averaged mass-velocity component, u_α, and flow depth. The depth-averaged sediment-particle velocity, $\langle U_s \rangle$, then is calculated from (2-44). The convective-diffusion equation, (2-38), is next solved using the finite-element method with isoparametric, quadrilateral elements. Time marching is effected by a two-point implicit scheme. At each time step, the model provides the average sediment concentration at every computational node point and the cross-section bed profile. Note that (2-45) and (2-46) are used to determine the source/sink term, S, in (2-38).

6. Data Requirements:

SEDIMENT-4H requires the following input data:

(1) Number of cross sections.

(2) Initial cross-section geometries of all cross sections.

(3) Manning's n at each cross section.

(4) Downstream stage hydrograph.

(5) Bed-material characteristics: median size, fall velocity, critical shear stress, maximum permissible concentration in bed layer, bed-strata data, and initial suspended-sediment concentration.

(6) Diffusion coefficient in the longitudinal direction.

(7) Upstream sediment boundary condition: suspended-sediment concentration specified as a function of time.

7. Model Limitations and Applicability:

SEDIMENT-4H considers only a single sediment-particle size. Suspended sediment particles are assumed to be convected at the local water-flow

velocities except in the vertical direction, in which the particles are allowed to settle due to the gravity effect. This assumption becomes invalid when the sediment is transported primarily in the bed-load mode, in which velocities of sediment particles and flow are significantly different. The two-dimensional version of the model is applicable to highly unsteady flow over a river bed composed of fine sediment in which the transverse velocity and concentration profiles vary significantly.

III. DESCRIPTION OF STUDY RIVERS

A. Study Rivers. The study rivers were selected on the basis of the following three criteria. First, the Federal Emergency Management Agency (FEMA) requested that rivers be selected which historically have experienced flash-flood type events with appreciable river-bed changes and channel migration during floods. Such rivers are found typically in the western United States. Second, the Committee Members wanted to include two different types of rivers: those which are characterized by stable, confined channels; and those which have unstable, disturbed channels. Third, and most importantly, it was necessary that adequate input information on the study rivers be available for testing the different numerical models. The input data generally had to satisfy the requirements of the individual numerical models, as set forth in Chapter II. In the search for appropriate study rivers which satisfy these conditions, various regional FEMA offices were contacted, including Denton, Texas; Bothell, Washington; San Francisco, California; and Denver, Colorado. After reviewing the recommended rivers, the San Lorenzo River (SLR), the San Dieguito River (SDR), and the Salt River (SR) were selected by the Committee. Note that these rivers had been previously investigated using movable-bed numerical models by Corps of Engineers (COE), San Diego State University (SDSU), and Simons, Li & Associates (SLA), respectively. Among these three rivers, SLR is a channelized, stable, sand-bed river; SDR is characterized by an unstable, disturbed, sand-bed channel conditions; and SR is an unstable, gravel-bed river. Other characteristics of these rivers are as follows:

1. San Lorenzo River. The San Lorenzo River is located in Santa Cruz County in northern California, and meets the Pacific Ocean at the northern end of Monterey Bay in the City of Santa Cruz, as shown in figure 1. SLR historically has flooded frequently and caused substantial flood damage to the City of Santa Cruz before the COE's flood-control project, which included a leveed channel, was completed in 1959. Since completion of the project, sediment has accumulated in the channel, resulting in a loss of channel capacity. A photograph of the river supplied by COE, San Francisco District, taken upstream of the Water Street Bridge looking downstream, is shown in

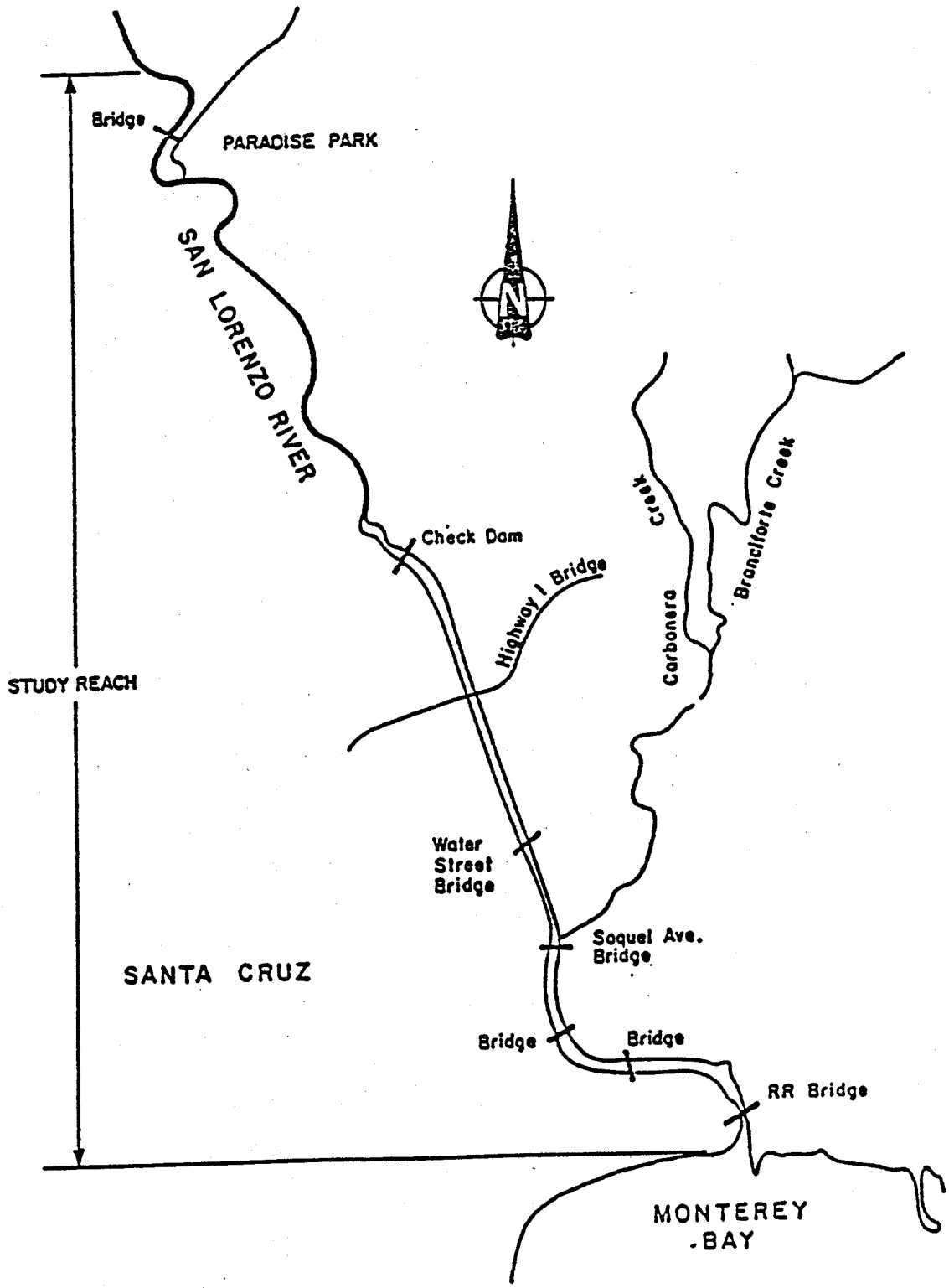

Figure 1 Map showing San Lorenzo River study reach

figure 2. The northern portion of the watershed has steep slopes and unstable rock structures with high landslide susceptibility. The southern portion has relatively low erosion potential, due to dense vegetation cover and stable granitic soils. The southeastern part is covered by loose, sandy soils with high erosion potential.

2. San Dieguito River. The San Dieguito River flows through San Diego County in southern California, and flows through the City of Del Mar into the Pacific Ocean. The approximately 2-mi long study reach, delineated in figure 3, was innundated by recent floods, including those of March 1978 and February 1980. The reach shown in the figure is approximately 4 mi from the Pacific Ocean and 5 mi below Lake Hodges Dam, which was constructed in 1918. The drainage area above Lake Hodges is about 300 sq mi. During the 15 March 1978 flood, a peak flow of 4,400 cfs was recorded downstream from the reservoir. An estimated peak reservoir outflow of 22,000 cfs, corresponding to a 40-yr flood, was recorded during the 21 February 1980 flood. The SDR channel has a wide, flat cross section with highly erodible banks, as can be seen in figure 4, an aerial photograph taken above the Via de Santa Fe Road Bridge during the 21 February 1980 flood. This photograph was supplied by San Diego County Flood Control District through Dr. Howard Chang of SDSU. The river channel had been disturbed prior to the 1978 and 1980 floods by sand-mining activities and construction of the Via de Santa Fe Road and its SDR bridge. Several large borrow pits, with depths up to 25 ft, were produced by sand-mining operations. Although these borrows were partially refilled after the 1978 flood, major borrow-pit aggradation took place during the 1980 flood. The channel bed is composed of primarily sand-range materials.

3. Salt River. The Salt River is located in Maracopa County, Arizona, and flows from Granite Reef Dam to the confluence with the Gila River. A reach of the river through the City of Phoenix has drawn the most attention because recent development within the flood plain has resulted in recurrent damage to structures and facilities. SR experienced four major floods in three years between 1978 and 1980 (March 1978, peak flow = 99,000 cfs; December 1978, peak flow = 112,000 cfs; January 1979, peak flow = 73,500 cfs; and February 1980, peak flow = 185,000 cfs) which produced extensive damage to the Sky Harbor

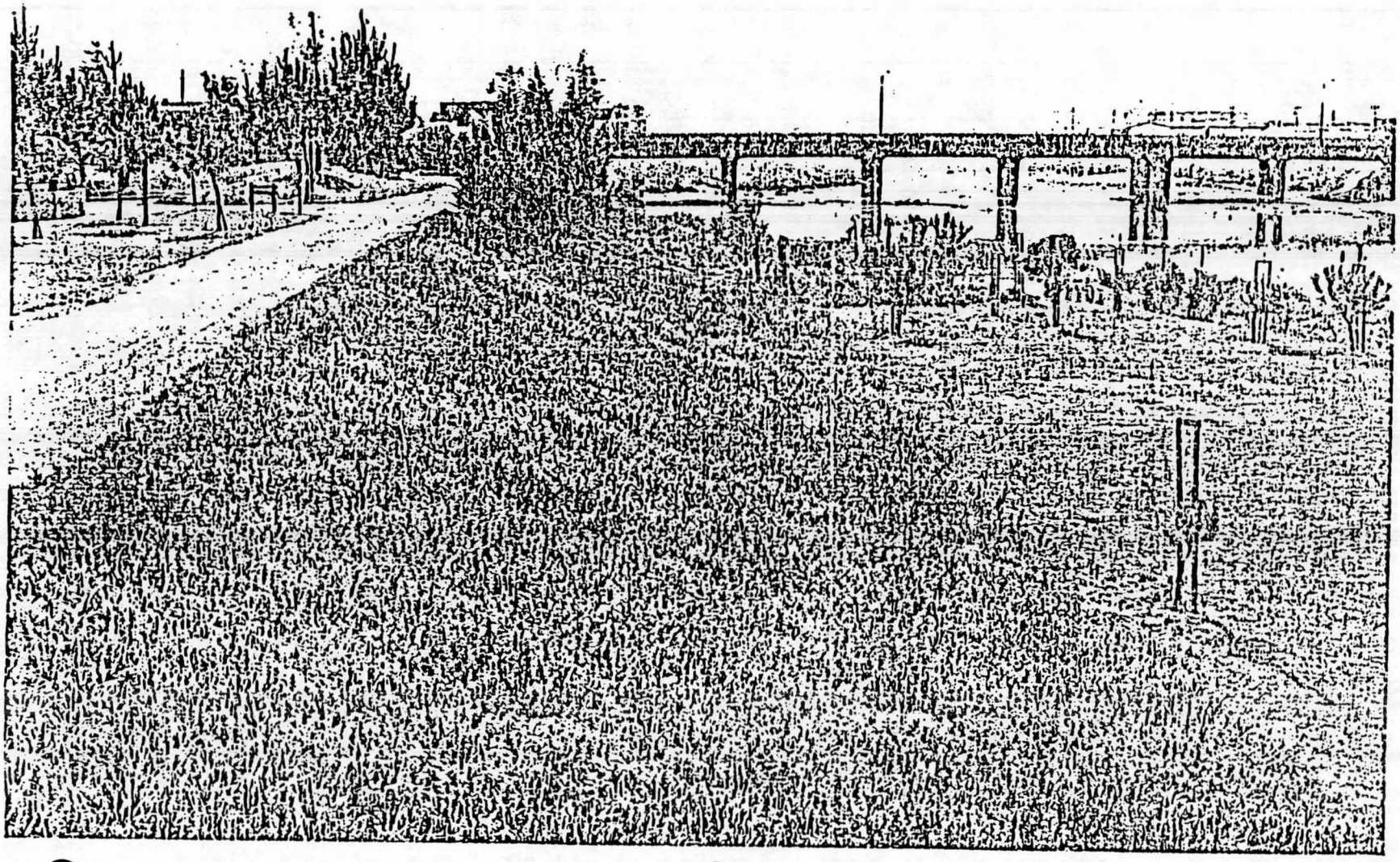

ure 2 Photograph showing the San Lorenzo Ri

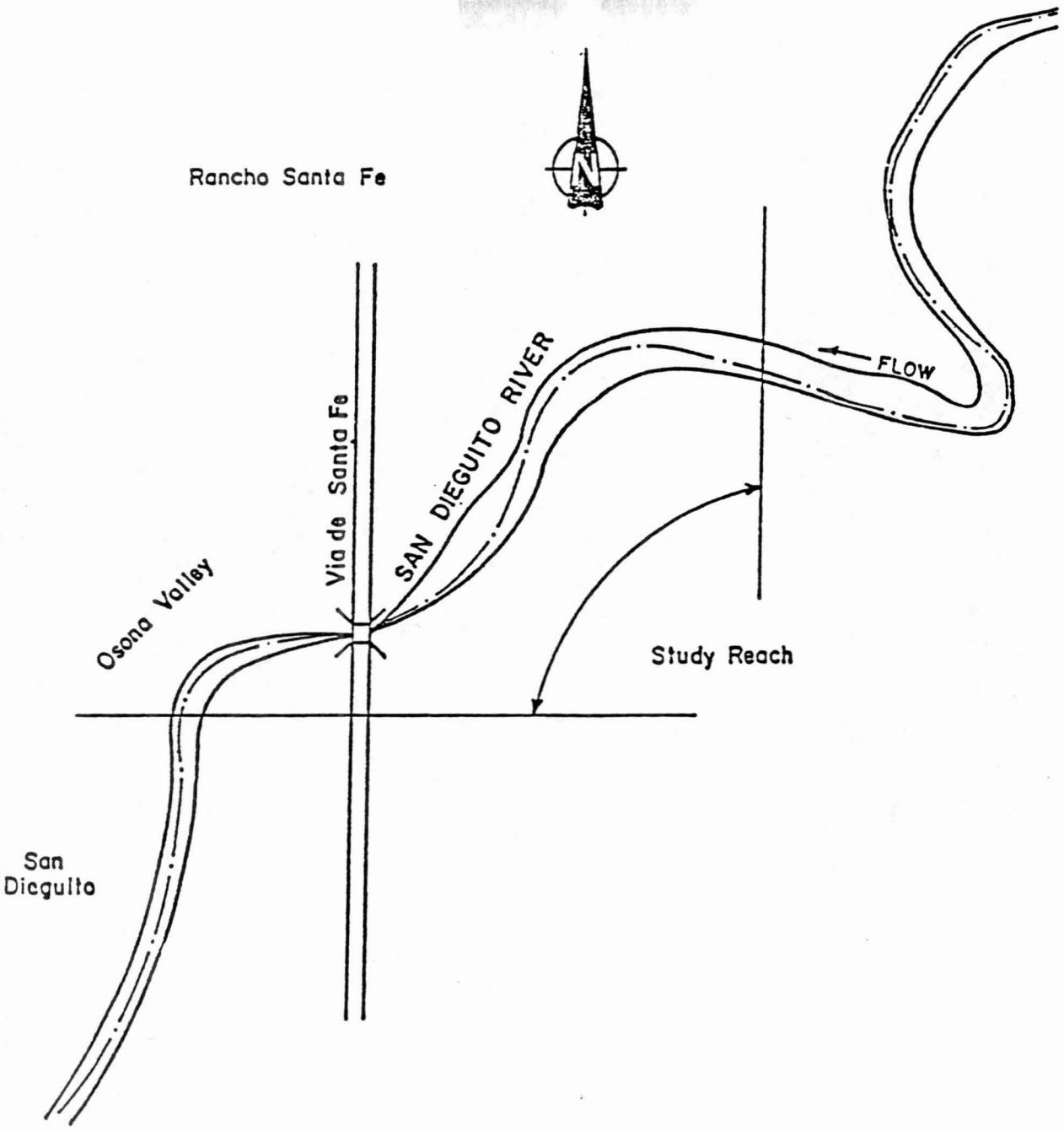

Figure 3 San Dieguito River study reach

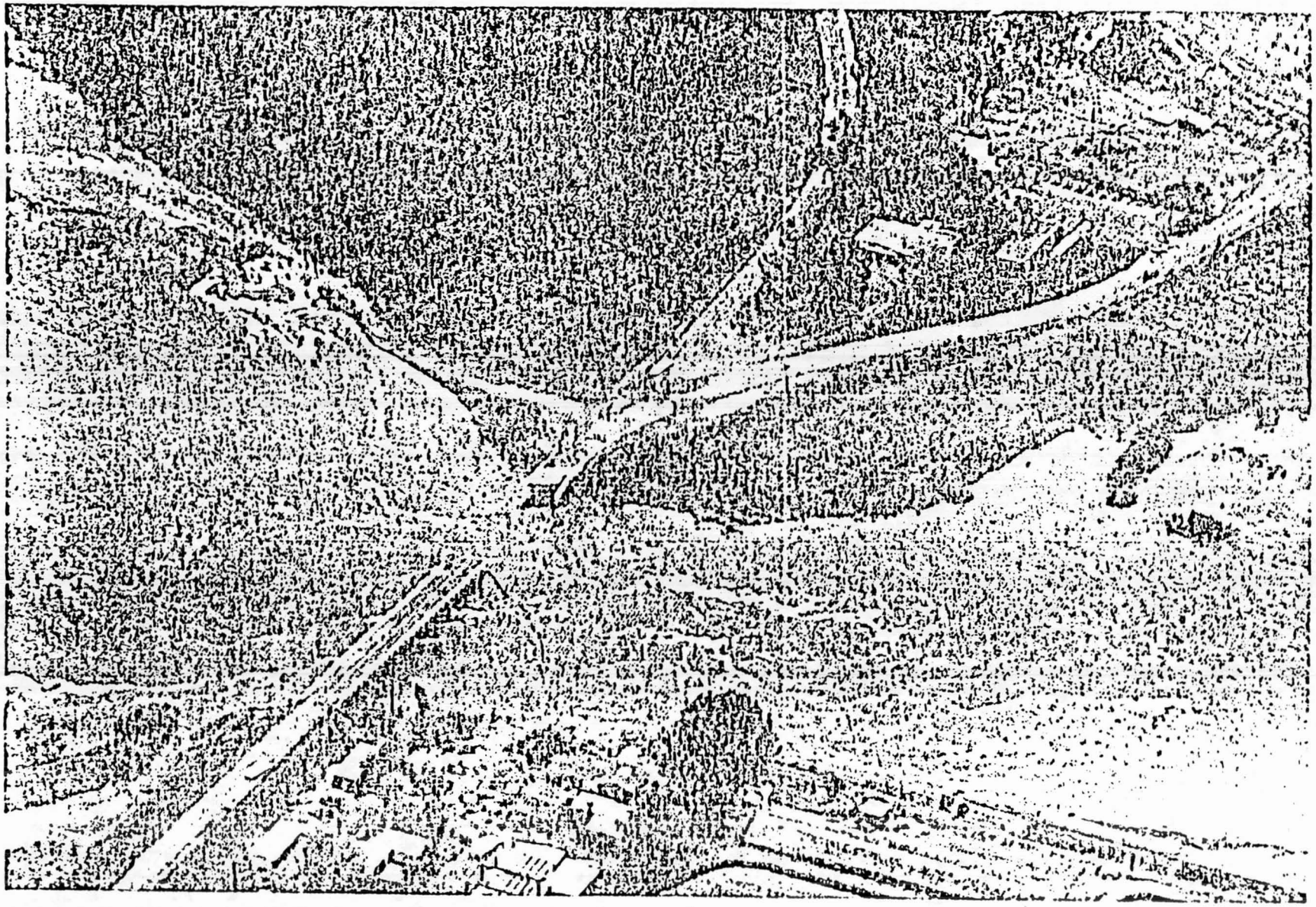

Figure 4 Photograph showing the San Dieguito River

Airport facilities as well as to the streets and bridges in the vicinity. In order to mitigate future flood damage, and to become eligible for federal assistance to compensate for previous flood losses, the City of Phoenix proposed channelization of SR from just downstream of the I-10 Bridge to the Hohokam Expressway, as shown in figure 5. A photograph of SR taken near the Sky Harbor International Airport and supplied by SLA is shown in figure 6. The bed material is composed primarily of gravel with a median diameter of about 64 mm. There are many gravel-mining operations currently (1982) underway within the proposed channelization area.

B. Summaries of Input Data. A brief description of the input data utilized in this study is given in this section. Detailed input data are on file at the Iowa Institute of Hydraulic Research, The University of Iowa, Iowa City, Iowa, and are available through the Institute's library.

1. San Lorenzo River. Input data used previously by Jones-Tillson & Associates, et al. in 1980 were furnished by COE, San Francisco District, in HEC-6 format. The approximately 4.7-mi long study reach consists of two different subreaches: the upper half is approximately 2.3 mi long and is relatively steep; and the lower half, which is approximately 2.4 mi long, has a much smaller slope. Data on 38 cross sections with subreach length varying between 150 ft and 770 ft were supplied. Input hydrographs for the February 16-20, 1980 flood, with a peak flow of 12,800 cfs, are shown in figure 7, and the downstream boundary condition, which reflects tidal effects, is shown in figure 8. Pre-flood channel cross-section profiles were coded in HEC-6 format. Suspended-sediment discharge rating curves by particle sizes constructed from United States Geological Survey (USGS) data collected at Big Trees Gauging Station, which is 7 mi upstream of the study reach, were supplied to the modelers. Bed-material composition data were also coded in HEC-6 format. The median bed-material size in the study reach varied from 0.34 mm at the downstream end to 0.93 mm at the upstream end of the study reach.

2. San Dieguito River. Input data were provided by Dr. Howard Chang of SDSU and San Diego County, California. Twenty-one detailed cross sections based on

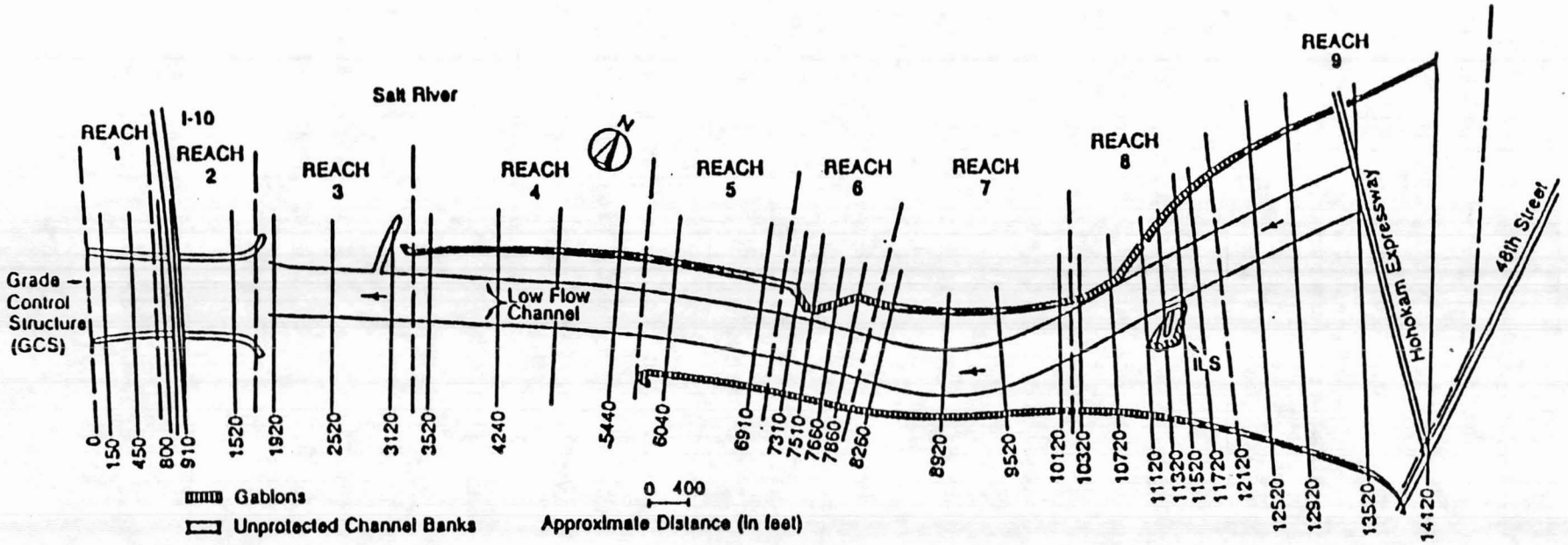

Figure 5 Salt River study reach

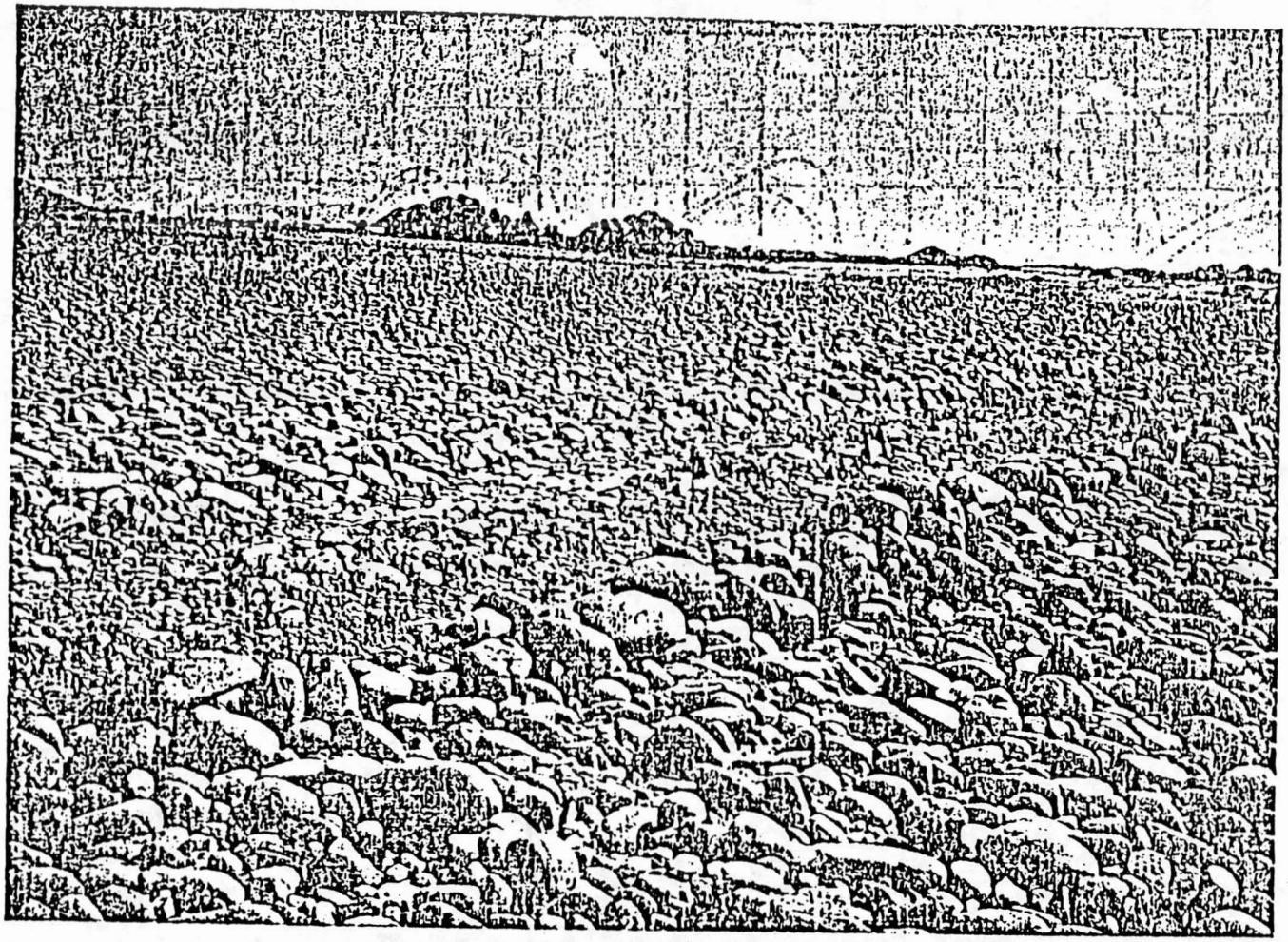

Figure 6 Photograph showing the Salt River

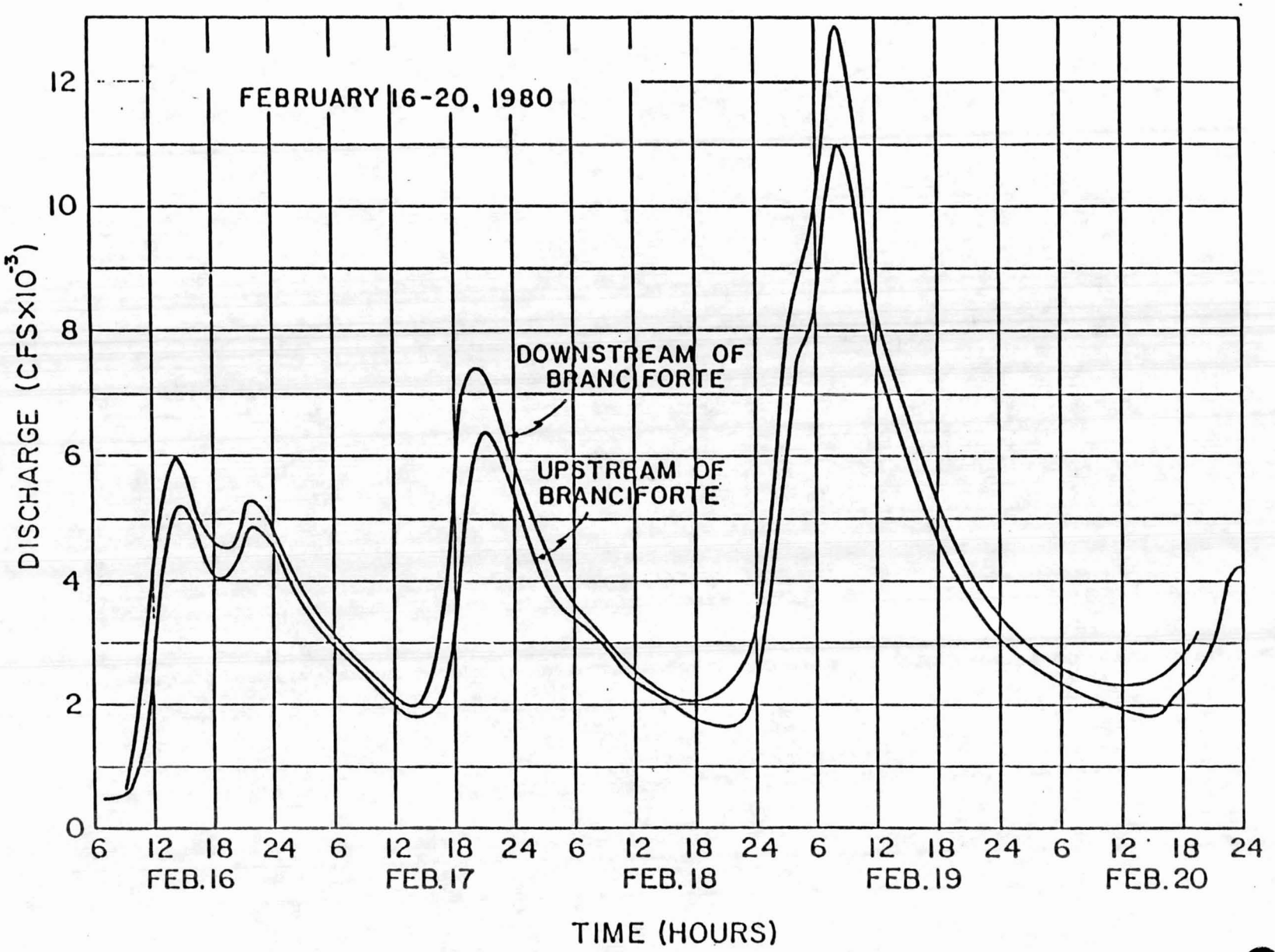

Figure 7 San Lorenzo River hydrographs

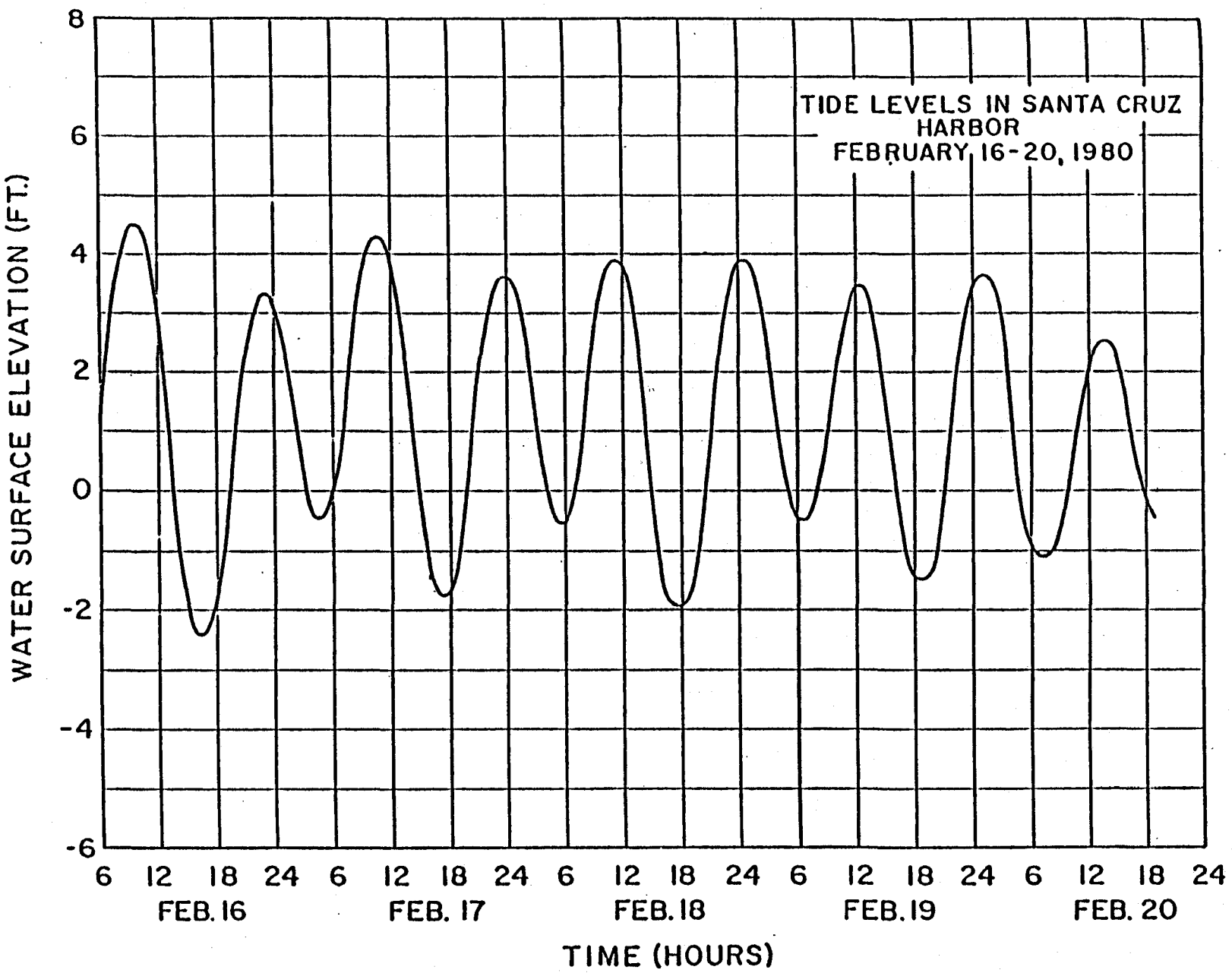

Figure 8 Stage hydrograph at the downstream boundary for the San Lorenzo River

the 1973 survey by San Diego County for the 1.9-mi long study reach were supplied in HEC-2 format. Input hydrographs at the upstream boundary, upstream from the Via de Santa Fe bridge, for the March 1978 and February 1980 floods with peak discharges of 4,400 cfs and 22,000 cfs, respectively, are shown in figure 9. The locations of the cross sections and pre-flood channel topography for the lower two-thirds of the study reach are presented in figure 10. No sediment-transport rating curve was available. Bed-material data were provided for only Sections 44 and 59; the median bed-material sizes for the main channel and south overbank area at Section 44 were 0.46 mm and 0.25 mm, respectively; and those at Section 59 were 0.70 mm and 0.36 mm, respectively.

3. Salt River. All input information was provided by SLA. Channel profiles for 41 designed cross sections were furnished in HEC-2 format. The total reach length was 4.34 mi, and each reach length varied from 150 ft to 1,100 ft. The projected 100-year-flood hydrograph, with a peak discharge of 176,000 cfs and a flood duration of 10 days, is shown in figure 11. The lower and upper limits of the geometric mean size of bed material were 0.22 mm and 185.0 mm, respectively, and the median diameter for all sections was 64.0 mm. Downstream boundary conditions were given in two different modes: one assuming the critical depth at the I-10 drop structure (see figure 5); and another with the assumed stage-discharge relationship at the I-10 bridge. Both conditions are possible, depending on the degradation below the I-10 drop structure. Initially, the area is backfilled and the second boundary condition is valid; however, if degradation removes this material, the first, critical-depth boundary condition is valid. The SR study reach was previously investigated by Colorado State University (CSU), in 1980, using fixed-bed and movable-bed physical models and SLA's HEC2SR numerical model (Anderson-Nichols, 1980).

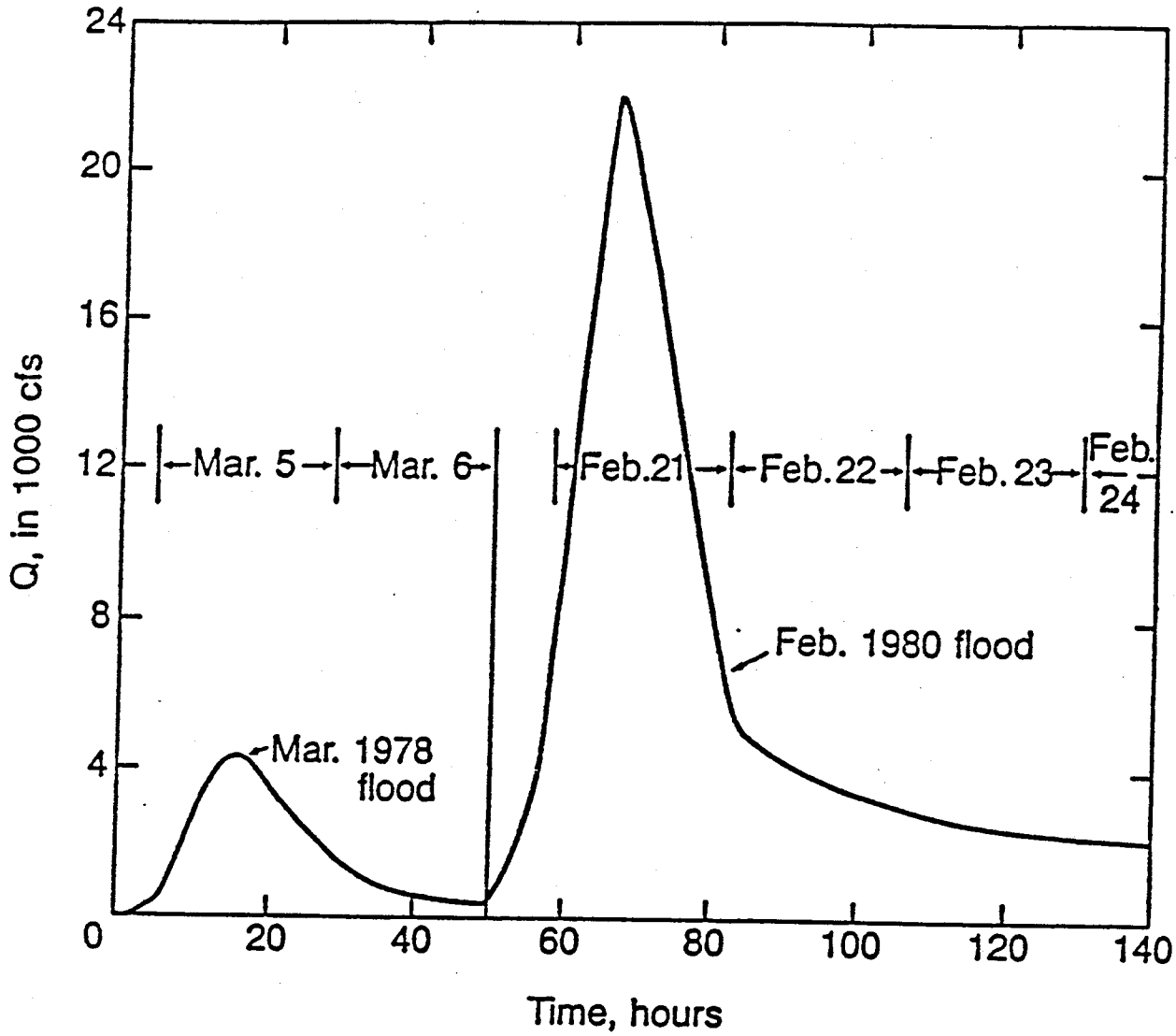

Figure 9 San Dieguito River hydrographs

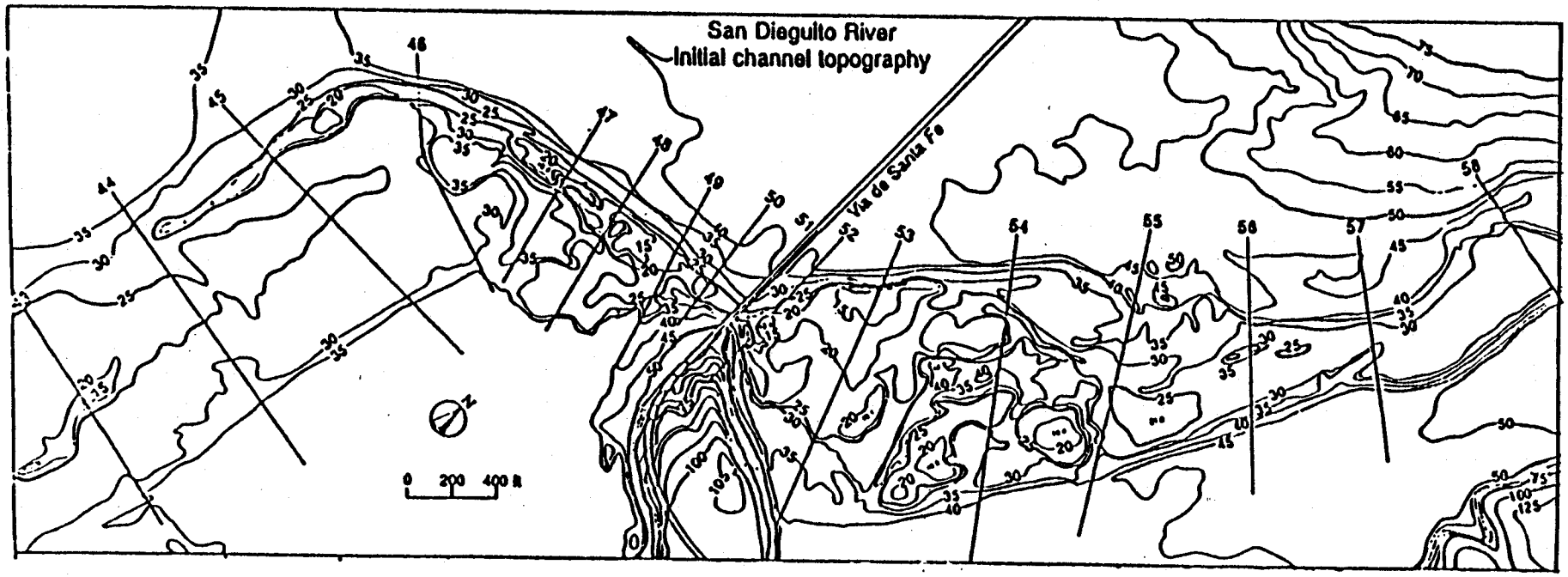

Figure 10 Topographic map of the San Dieguito River study reach

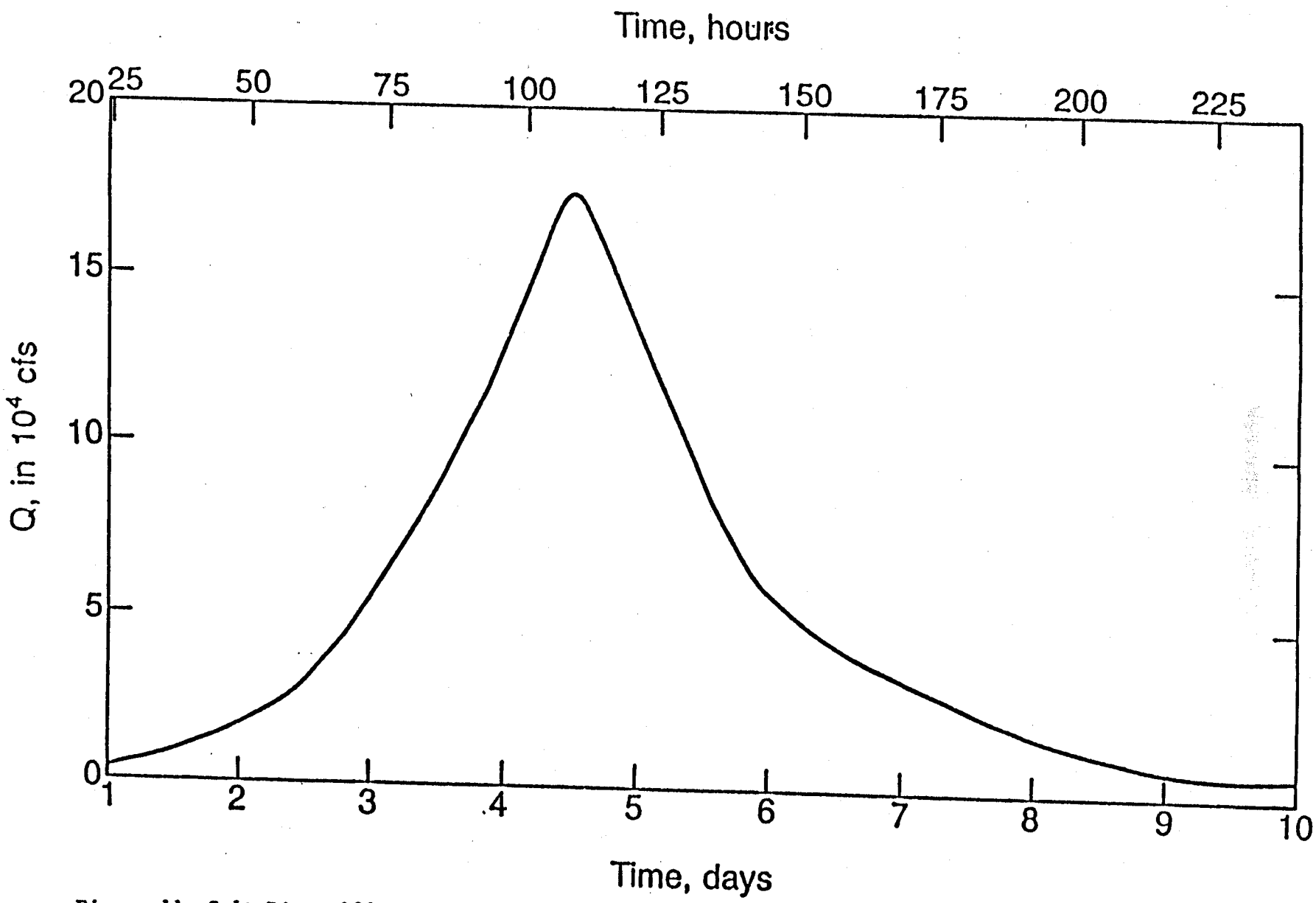

Figure 11 Salt River 100-year-flood hydrograph

IV. PRESENTATION AND DISCUSSION OF RESULTS

The input data summarized in Chapter III were sent to all modelers who participated in this project. A total of six models, the characteristics of which are summarized in Chapter II, was utilized. The models tested and the computational modes utilized for each of the three rivers (SLR, SDR, and SR) are summarized in table 1. It should be noted that the simulation of SR using HEC2SR was already developed in 1980 by SLA; these computational results were furnished to the Committee by SLA (SLA, 1980). All modelers submitted final reports describing their efforts and results (SLA, 1982; HEC, 1982; SDSU, 1982; and RMA, 1982), and also furnished computer outputs; these materials are on file at the Iowa Institute of Hydraulic Research Library. For this study, only the principal results were extracted from the vast computer-output listings, and were compiled in a uniform format to facilitate direct comparison. Each modeler was sent the summary tables based on his results to review for accuracy and correct interpretations. All numerical results presented in this chapter have been reviewed by the respective modelers. The figures included in this chapter were prepared on the basis of the reviewed output summaries. The principal results obtained from each simulation are summarized in the following sections.

1. San Lorenzo River. The principal results for a peak flow of 12,800 cfs computed using HEC2SR (SLA), HEC-6 (HEC), FLUVIAL-11 (SDSU), and SEDIMENT-4H (RMA) are tabulated in tables 2, 3, 4, and 5, respectively. In tables 4 and 5, the predicted water-surface elevations are shown for both movable-bed and fixed-bed simulations of FLUVIAL-11 and SEDIMENT-4H. Definitions of the symbols utilized are given in the individual tables. Thalweg and water-surface elevations at peak flow computed by the four movable-bed models are plotted together in figure 12, which also includes available field data on water-surface elevation between stations 1,150 ft and 10,150 ft (see table 6). The computed water-surface elevations are seen to agree with the measured values fairly well for all models over the lower half (roughly) of the study reach. However, computed elevations are seen to differ among the models over the upper part of the study reach. FLUVIAL-11 predictions are much higher than those of the other models; at a river distance of 18,258 ft, for example,

RIVER	MODEL	TESTED RIVER-BED CONDITIONS
SAN LORENZO (CALIFORNIA)	HEC2SR (SLA)	MOVABLE-BED & FIXED-BED*
	KUWASER (SLA)	MOVABLE-BED ONLY
	UUWSR (SLA)	MOVABLE-BED & FIXED-BED
	HEC-6 (HEC)	MOVABLE-BED & FIXED-BED**
	FLUVIAL-11 (SDSU)	MOVABLE-BED & FIXED-BED*
	SEDIMENT-4H (RMA)	MOVABLE-BED & FIXED-BED
SAN DIEGUITO (CALIFORNIA)	HEC2SR (SLA)	MOVABLE-BED & FIXED-BED*
	UUWSR (SLA)	MOVABLE-BED & FIXED-BED
	FLUVIAL-11 (SDSU)	MOVABLE-BED & FIXED-BED*
	SEDIMENT-4H (RMA)	MOVABLE-BED & FIXED-BED
SALT (ARIZONA)	HEC2SR (SLA)***	MOVABLE-BED & FIXED-BED*
	HEC-6 (HEC)	MOVABLE-BED & FIXED-BED**
	FLUVIAL-11 (SDSU)	MOVABLE-BED & FIXED-BED*
	SEDIMENT-4H (RMA)	MOVABLE-BED & FIXED-BED

* : HEC-2 (Fixed-bed model developed at HEC)
** : HEC-6 (Fixed-bed model) & HEC-2 (Fixed-bed model)
*** : Results were obtained from SLA's previous study in 1980
SLA : Simons, Li & Associates, Inc.
HEC : Hydrologic Engineering Center
SDSU : San Diego State University
RMA : Resource Management Associates

Table 1 List of models and their computational modes

SAN LORENZO RIVER: HEC2SR

ID	X	Y0	YF	Y	H	W	Q	V	QB	QS	QT	DS0
	FT	FT	FT	FT	FT	FT	CFS	FPS	T/D	T/D	T/D	MM
3	0	-4.5	-4.7	-4.7	1.6	246	12000	11.9	23160	221010	244170	0.47
4	558	-4.2	-4.4	-4.3	4.0	281	12000	8.1	23160	221010	244170	0.47
8	1183	-4.0	-4.2	-4.1	4.8	265	12000	7.9	23160	221010	244170	0.47
9	1700	-1.3	-1.4	-1.3	5.4	282	12000	7.3	23160	221010	244170	0.47
10	2200	-1.0	-1.6	-1.6	5.9	284	12000	6.6	17400	187810	205210	0.50
11	2600	-0.6	-1.2	-1.2	6.2	281	12000	6.8	17400	187810	205210	0.50
12	2800	-0.4	-1.1	-1.0	6.0	200	12000	9.2	17400	187810	205210	0.50
14	2950	-0.3	-1.1	-1.0	6.2	209	12000	9.2	17400	187810	205210	0.50
15	3575	0.2	-0.6	-0.5	7.6	235	12000	7.4	17400	187810	205210	0.50
19	4345	0.6	-0.2	-0.1	8.9	240	12000	6.6	17400	187810	205210	0.50
20	4955	1.4	1.9	1.8	9.6	237	12000	7.7	8160	145070	153230	0.58
21	5360	1.8	2.3	2.2	10.4	238	12000	7.3	8160	145070	153230	0.50
22	5610	2.0	2.3	2.3	11.3	340	12000	4.6	8160	145070	153230	0.58
25	6095	2.5	2.9	2.8	11.5	267	11000	5.2	8160	145070	153230	0.58
26	6745	3.0	4.1	3.9	11.9	226	11000	6.8	8160	160720	168880	0.41
27	7325	3.2	4.2	4.0	12.8	263	11000	5.9	8160	160720	168880	0.41
30	7575	3.4	4.4	4.2	13.1	237	11000	5.9	8160	160720	168880	0.41
31	8080	3.7	4.7	4.6	13.4	235	11000	6.0	8160	160720	168880	0.41
32	8585	4.1	6.2	5.9	13.6	229	11000	6.9	12610	195280	207890	0.35
33	9090	4.4	6.5	6.2	14.0	228	11000	6.9	12610	195280	207890	0.35
34	9595	4.8	6.9	6.6	14.4	226	11000	7.0	12610	195280	207890	0.35
35	9935	5.0	7.2	6.9	14.7	223	11000	7.1	12610	195280	207890	0.35
36	10140	5.2	5.5	5.4	14.7	172	11000	7.9	18020	252730	270750	0.64
38	10400	5.6	5.9	5.8	14.9	176	11000	8.1	18020	252730	270750	0.64
39	10780	6.4	6.7	6.6	15.4	175	11000	8.5	18020	252730	270750	0.64
40	11260	7.2	7.5	7.4	16.0	156	11000	9.5	18020	252730	270750	0.64
41	11800	8.2	10.4	10.0	17.0	171	11000	10.7	15910	256140	272050	0.51
42	12305	9.2	11.5	11.0	18.6	178	11000	9.5	15910	256140	272050	0.51
43	12645	9.8	12.3	11.8	19.1	153	11000	11.4	15910	256140	272050	0.51
46	14118	10.0	13.1	12.6	23.1	257	11000	6.7	15910	256140	272050	0.51
47	15308	12.8	12.4	12.5	24.3	221	11000	7.1	20600	314530	335130	1.50
48	16908	16.5	15.9	16.0	26.5	157	11000	13.2	20600	314530	335130	1.50
49	18258	20.6	20.1	20.2	32.2	204	11000	8.6	20600	314530	335130	1.50
50	19238	24.2	23.4	23.6	35.3	123	11000	14.2	20600	314530	335130	1.50
51	20578	29.8	30.8	30.8	41.7	107	11000	14.2	18130	301180	319310	0.64
52	21508	32.8	35.5	35.2	46.1	137	11000	10.8	18130	301180	319310	0.64
53	22968	35.7	35.7	35.7	49.1	145	11000	8.5	18260	306260	324520	1.25
54	24758	41.2	41.2	41.2	53.6	108	11000	15.0	18260	306260	324520	1.25

ID=SECTION I.D.
X =RIVER DISTANCE
Y0=INITIAL THALWEG EL
YF=FINAL THALWEG EL
Y =THALWEG EL AT PEAK FLOW
H =W.S. EL AT PEAK FLOW
W =TOP WIDTH AT PEAK FLOW

Q = WATER DISCHARGE AT PEAK FLOW
V = MEAN VELOCITY AT PEAK ALOW
QB = BED-LOAD DISCHARGE AT PEAK FLOW
QS = SUS-LOAD DISCHARGE AT PEAK FLOW
QT = TOTAL-LOAD DISCHARGE AT PEAK FLOW
DS0= MEDIAN DIAMETER OF BED MATERIAL AT PEAK FLOW

Table 2 Principal results computed by HEC2SR for the San Lorenzo River

SAN LORENZO RIVER: HEC-6

ID	X	Y0	YF	Y	H	W	Q	V	QB	QS	QT	DS0
	FT	FT	FT	FT	FT	FT	CFS	FPS	T/D	T/D	T/D	MM
3	0	-4.5	-4.6	-4.6	1.7	247	12800	12.0	74	46600	46680	0.71
4	558	-4.2	-3.7	-3.7	4.1	284	12800	8.4	203	41020	41230	0.70
8	1183	-4.0	-3.4	-3.4	5.0	258	12800	8.5	326	38630	38960	0.69
9	1700	-1.3	-0.7	-0.6	5.8	282	12800	7.7	489	38620	39110	0.66
10	2200	-1.0	-0.8	-0.7	6.4	284	12800	6.9	625	39730	40360	0.52
11	2600	-0.6	-0.7	-0.6	6.7	282	12800	7.0	197	41170	41370	0.56
12	2800	-0.4	-0.9	-0.8	6.7	202	12800	8.5	149	39390	39540	0.58
14	2950	-0.3	-1.3	-1.1	6.9	212	12800	8.2	115	37580	37700	0.60
15	3575	0.2	-0.9	-0.6	8.4	240	12800	6.7	69	36500	36570	0.61
19	4345	0.6	-0.7	-0.5	9.3	243	12800	6.1	92	30080	30180	0.65
20	4955	1.4	1.3	1.3	9.8	240	12800	7.0	72	17990	18060	1.17
21	5360	1.8	1.7	1.7	10.4	239	12800	6.9	52	16840	16890	1.18
22	5610	2.0	2.0	2.0	11.1	340	12800	4.5	74	16330	16400	1.23
25	6095	2.5	2.6	2.6	11.3	267	11000	5.2	112	13240	13350	1.08
26	6745	3.0	3.0	3.0	11.7	227	11000	6.3	84	12550	12640	1.21
27	7325	3.2	3.2	3.2	12.4	249	11000	5.7	91	11640	11730	1.34
30	7575	3.4	3.4	3.4	12.6	236	11000	5.7	176	10520	10700	1.30
31	8080	3.7	3.9	3.9	12.8	235	11000	5.9	293	9230	9520	1.48
32	8585	4.1	4.3	4.3	13.1	231	11000	6.1	280	9600	9880	1.44
33	9090	4.4	4.6	4.6	13.3	229	11000	6.2	259	9890	10150	1.43
34	9595	4.8	5.2	5.2	13.6	225	11000	6.6	244	10220	10460	1.38
35	9935	5.0	5.4	5.3	13.8	222	11000	6.6	44	9670	9720	1.37
36	10140	5.2	5.5	5.5	13.5	166	11000	9.4	41	10420	10460	1.73
38	10400	5.6	5.7	5.7	14.1	170	11000	9.1	46	9480	9520	1.76
39	10780	6.4	6.5	6.5	14.7	172	11000	9.1	43	9720	9770	1.75
40	11260	7.2	7.1	7.1	15.5	155	11000	9.7	47	9940	9980	1.86
41	11800	8.2	8.5	8.4	16.7	173	11000	8.9	43	9580	9630	1.72
42	12305	9.2	9.3	9.3	17.6	176	11000	8.7	42	10610	10650	1.77
43	12645	9.8	9.7	9.7	18.0	151	11000	10.1	43	11050	11100	1.86
46	14118	10.0	10.3	10.2	21.3	227	11000	7.7	33	10850	10880	1.66
47	15308	12.8	13.0	13.0	23.1	203	11000	8.9	31	14970	15000	1.74
48	16908	16.5	16.8	16.7	27.0	164	11000	12.3	29	17420	17450	1.76
49	18258	20.6	20.9	20.7	32.1	184	11000	9.8	23	20230	20260	1.77
50	19238	24.2	23.8	23.6	34.9	123	11000	14.2	27	20780	20810	2.02
51	20578	29.8	29.5	29.4	40.6	97	11000	13.4	24	18050	18070	1.93
52	21508	32.8	34.6	33.8	44.1	128	11000	11.1	18	18200	18210	1.45
53	22968	35.7	35.9	35.8	47.5	131	11000	10.3	20	34900	34920	1.75
54	24758	41.2	41.8	42.1	54.3	112	11000	14.6	15	51090	51110	1.54

ID=SECTION I.D.
X =RIVER DISTANCE
Y0=INITIAL THALWEG EL (T=0 HR)
YF=FINAL THALWEG EL (T=102 HR)
Y =THALWEG EL AT PEAK FLOW
H =W.S. EL AT PEAK FLOW
W =TOP WIDTH AT PEAK FLOW

Q =WATER DISCHARGE AT PEAK FLOW
V =MEAN VELOCITY AT PEAK FLOW
QB =BED-LOAD DIS. AT PEAK FLOW
QS =SUS-LOAD DIS. AT PEAK FLOW
QT =TOTAL-LOAD DIS. AT PEAK FLOW
DS0=MEDIAN DIAMETER OF BED MATERIAL AT PEAK FLOW

Table 3 Principal results computed by HEC-6 for the San Lorenzo River

SAN LORENZO RIVER: FLUVIAL-11

ID	X	Y0	YF	Y	H	H1	W	Q	V	QB	QS	QT	DS0
	FT	FT	FT	FT	FT	FT	FT	CFS	FPS	T/D	T/D	T/D	MM
3	0	-4.5	-7.5	-9.5	1.3	1.9	239	12870	9.0	-	-	158700	0.89
4	558	-4.2	-6.2	-7.8	2.0	4.1	239	12870	9.3	-	-	168380	0.97
8	1183	-4.0	-4.7	-6.2	3.0	4.8	232	12870	9.6	-	-	170590	0.98
9	1700	-1.3	-1.6	-1.6	4.0	5.6	274	12870	8.9	-	-	165180	1.02
10	2200	-1.0	-0.8	-0.8	4.8	6.0	274	12870	9.0	-	-	160760	1.20
11	2600	-0.6	-0.2	-0.2	5.5	6.3	274	12870	8.8	-	-	153930	1.09
12	2800	-0.4	-0.5	-2.0	5.7	6.1	201	12870	9.1	-	-	147460	0.89
14	2950	-0.3	-0.6	-0.6	5.5	6.4	206	12870	11.0	-	-	215140	1.68
15	3575	0.2	-0.1	-0.1	8.0	8.2	237	12870	7.4	-	-	141620	1.55
19	4345	0.6	0.3	0.3	9.4	9.6	243	12870	6.6	-	-	95720	1.08
20	4955	1.4	0.8	0.5	10.1	10.3	245	12870	6.2	-	-	86250	0.81
21	5360	1.8	1.2	1.0	10.4	10.8	243	12870	6.3	-	-	91380	0.96
22	5610	2.0	2.8	2.5	10.9	11.5	337	12870	5.0	-	-	80490	0.27
25	6095	2.5	2.9	2.9	11.2	11.7	265	10980	5.5	-	-	104050	0.30
26	6745	3.0	2.8	2.7	11.7	12.0	227	10980	6.1	-	-	116360	0.36
27	7325	3.2	3.6	3.2	12.3	12.6	247	10980	5.8	-	-	118490	0.31
30	7575	3.4	4.0	3.5	12.5	12.8	236	10980	5.8	-	-	116500	0.30
31	8080	3.7	5.3	5.2	12.8	13.1	228	10980	7.1	-	-	126680	0.31
32	8585	4.1	5.9	5.8	13.2	13.3	226	10980	7.4	-	-	145960	0.34
33	9090	4.4	6.5	6.5	13.6	13.5	224	10980	7.7	-	-	164040	0.39
34	9595	4.8	7.1	7.3	14.2	13.8	221	10980	8.1	-	-	181050	0.47
35	9935	5.0	7.5	7.8	14.6	13.9	218	10980	8.4	-	-	192720	0.56
36	10140	5.2	6.7	6.6	14.7	13.7	169	10980	9.2	-	-	190620	0.65
38	10400	5.6	6.0	5.7	15.7	14.0	181	10980	7.2	-	-	211080	0.91
39	10780	6.4	6.6	6.1	16.5	14.6	203	10980	6.9	-	-	202400	1.06
40	11260	7.2	7.0	6.4	17.4	15.4	166	10980	7.1	-	-	186100	1.10
41	11800	8.2	8.3	8.0	18.4	16.8	184	10980	6.8	-	-	174570	0.94
42	12305	9.2	9.3	8.6	19.3	17.6	187	10980	6.6	-	-	165460	0.85
43	12645	9.8	9.4	9.2	19.7	17.9	161	10980	7.6	-	-	198410	1.65
46	14118	10.0	13.9	14.1	23.2	21.1	263	10980	6.8	-	-	152940	0.37
47	15308	12.8	18.1	17.8	26.1	24.0	238	10980	7.4	-	-	199120	0.45
48	16908	16.5	20.6	20.1	30.8	28.0	221	10980	7.7	-	-	256410	0.59
49	18258	20.6	25.9	26.0	35.4	33.0	228	10900	8.1	-	-	291070	0.74
50	19238	24.2	25.6	23.6	39.0	37.0	160	10980	8.4	-	-	338320	1.39
51	20578	29.8	29.0	26.6	43.6	42.2	109	10980	8.7	-	-	363590	2.78
52	21508	32.8	33.7	33.6	46.4	44.5	142	10980	8.4	-	-	333840	1.01
53	22968	35.7	39.9	40.2	50.5	47.5	139	10980	9.1	-	-	348360	1.35
54	24758	41.2	41.2	41.2	57.3	53.9	144	10980	9.1	-	-	367860	3.15

ID=SECTION ID
X =RIVER DISTANCE
Y0=INITIAL THALWEG EL
YF=FINAL THALWEG EL
Y =THALWEG EL AT PEAK FLOW
H =W.S. EL AT PEAK FLOW
H1=W.S. EL AT PEAK FLOW (HEC-2)
W =TOP WIDTH AT PEAK FLOW
NOTE: QB & QS WERE NOT COMPUTED WITH FLUVIAL-11

Q =WATER DISCHARGE AT PEAK FLOW
QB =BED-LOAD DIS. AT PEAK FLOW
QS =SUS-LOAD DIS. AT PEAK FLOW
QT =TOTAL-LOAD DIS. AT PEAK FLOW
DS0=MEDIAN SIZE OF BED MATERIAL AT PEAK FLOW

Table 4 Principal results computed by FLUVIAL-11 for the San Lorenzo River

SAN LORENZO RIVER: SEDIMENT-4H

ID	X	Y0	YF	Y	H	H1	W	Q	V	QT	D50
	FT	FT	FT	FT	FT	FT	FT	CFS	FPS	T/D	MM
3	0	-4.8	-5.3	-5.3	1.9	2.2	264	12701	9.3	1580	0.50
4	558	-4.3	-4.5	-4.3	3.3	3.8	260	12704	8.9	1070	0.50
8	1183	-3.8	-4.2	-4.0	4.2	4.6	233	12706	8.4	1170	0.50
9	1700	-2.5	-2.5	-2.5	4.8	5.1	282	12707	6.7	224	0.50
10	2200	-1.3	-1.6	-1.5	5.2	5.5	280	12708	7.3	849	0.50
11	2600	-0.8	-1.2	-1.0	5.6	5.9	277	12709	7.4	863	0.50
14	2750	-0.3	-1.5	-1.1	6.1	6.5	206	12710	9.1	1830	0.50
15	3375	0.2	-0.4	-0.2	7.3	7.8	220	12711	8.2	1610	0.50
19	4145	0.6	0.4	0.5	8.9	9.3	238	12712	7.1	833	0.50
20	4755	1.2	1.1	1.2	9.9	10.1	241	12713	6.8	417	0.50
21	5160	1.7	1.5	1.6	10.4	10.7	242	12713	6.6	190	0.50
22	5410	1.9	1.9	1.9	10.7	10.9	337	12714	4.6	11	0.50
25	5895	2.3	2.3	2.3	11.0	11.2	270	10895	5.1	24	0.50
26	6545	2.8	2.8	2.8	11.6	11.8	226	10895	6.2	93	0.50
27	7125	3.1	3.1	3.1	11.9	12.0	235	10896	5.9	29	0.50
30	7375	3.3	3.3	3.3	11.9	12.1	233	10896	6.1	25	0.50
31	7880	3.6	3.6	3.6	12.2	12.3	231	10897	6.2	30	0.50
32	8385	4.0	4.0	4.0	12.5	12.6	229	10897	6.3	26	0.50
33	8890	4.4	4.4	4.4	12.8	12.9	228	10898	6.4	24	0.50
34	9395	4.8	4.8	4.8	13.1	13.2	224	10898	6.6	20	0.50
35	9735	5.0	5.0	5.0	13.4	13.4	222	10899	6.6	14	0.50
36	9940	5.2	5.1	5.1	13.6	13.7	169	10899	8.6	79	0.50
38	10200	5.6	5.5	5.6	14.2	14.2	176	10899	8.5	99	0.50
39	10580	6.1	6.1	6.1	14.9	14.9	173	10899	8.5	91	0.50
40	11060	7.0	6.9	7.0	15.8	15.8	157	10899	9.2	144	0.50
41	11600	8.1	8.1	8.1	16.8	16.8	168	10899	8.6	96	0.50
42	12105	9.1	8.9	9.0	17.8	17.9	144	10899	10.1	179	0.50
43	12445	9.7	9.7	9.7	19.1	19.2	158	10900	8.6	140	0.50
46	13910	10.7	10.7	10.7	21.2	21.2	222	10900	7.9	113	0.50
47	15100	13.0	13.0	13.0	23.8	23.8	198	10900	8.2	51	0.50
48	16700	16.6	16.6	16.6	27.0	27.0	200	10900	8.7	93	0.50
49	18058	20.6	20.6	20.6	31.5	31.5	182	10900	9.9	135	0.50
50	19038	24.7	24.7	24.7	37.2	37.2	139	10900	11.3	190	0.50
51	20378	29.1	29.1	29.1	41.6	41.6	114	10900	10.4	54	0.50
52	21308	32.7	32.7	32.7	44.0	44.0	130	10900	9.8	26	0.50
53	22768	36.3	36.3	36.3	47.1	47.1	131	10900	10.0	37	0.50
54	24558	40.2	40.1	40.1	54.5	54.6	103	10900	12.9	350	0.50

ID=SECTION ID
X =RIVER DISTANCE
Y0=INITIAL THALWEG EL
YF=FINAL THALWEG EL
Y =THALWEG EL AT PEAK FLOW
H =W.S. EL AT PEAK FLOW
H1=W.S. EL AT PEAK FLOW
COMPUTED USING FIXED-BED FLOOD-ROUTING MODEL

W =TOP WIDTH AT PEAK FLOW
Q =WATER DISCHARGE AT PEAK FLOW
V =MEAN VELOCITY AT PEAK FLOW
QT =TOTAL-LOAD DISCHARGE AT PEAK FLOW
D50=MEDIAN DIAMETER OF BED MATERIAL AT PEAK FLOW

Table 5 Principal results computed by SEDIMENT-4H for the San Lorenzo River

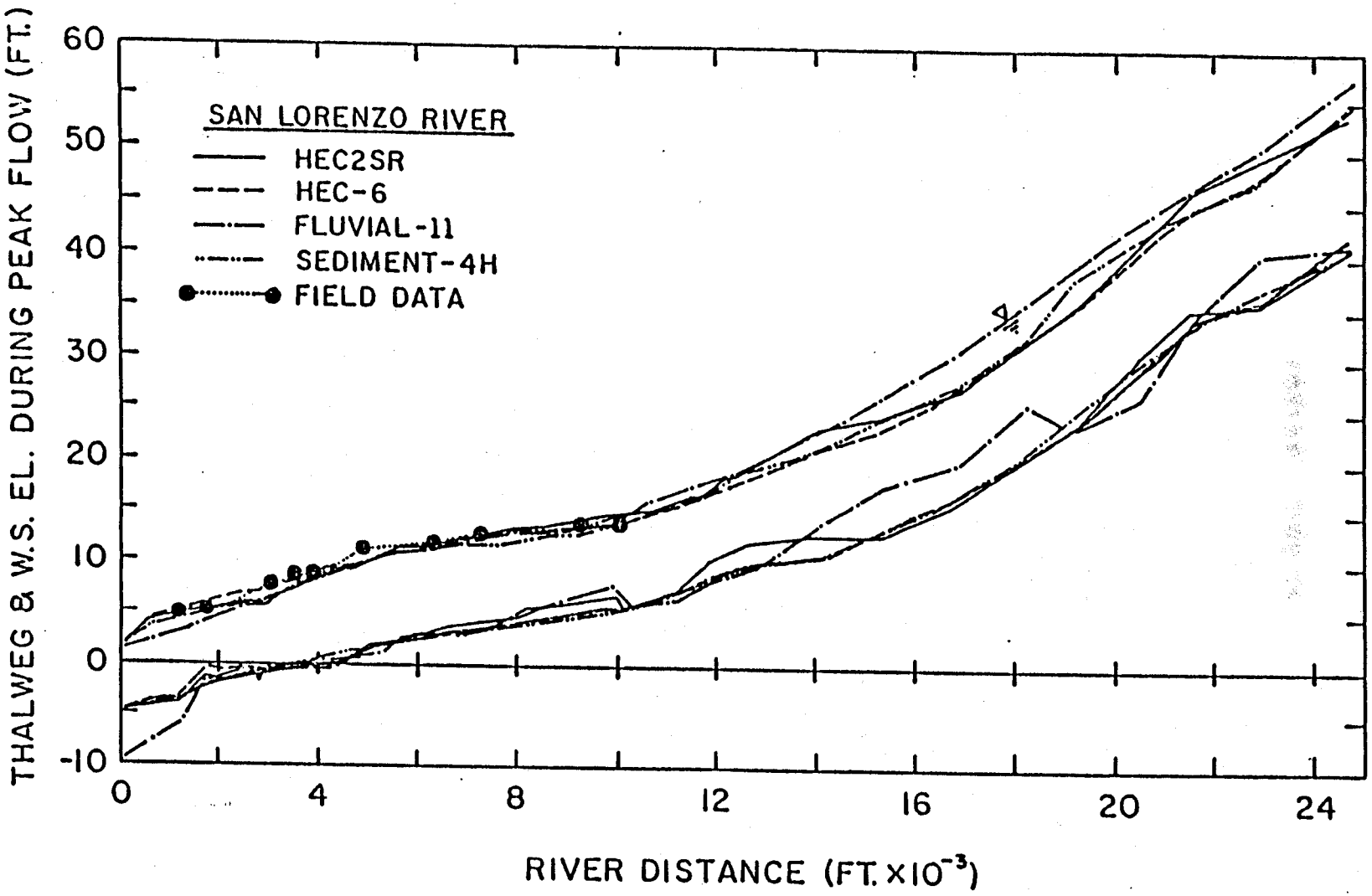

Figure 12 Comparison of thalweg and water-surface profiles at peak flow computed using the HEC2SR, HEC-6, FLUVIAL-11, and SEDIMENT-4H movable-bed models for the San Lorenzo River

SAN LORENZO RIVER

GAGE NO	RIVER DISTANCE	OBSERVED W.S. EL
	FT	FT
2	1150	5.0
3	1950	4.9
4	3070	7.6
5	3650	8.3
6	3950	8.3
7	4950	11.2
8	6400	11.8
9	7250	12.9
10	9300	13.5
11	10150	13.5

NOTE: THESE VALUES WERE RECORDED AT 8 A.M., 19 FEBRUARY 1980 DURING THE FLOOD-PEAK DISCHARGE OF 12,800 CFS

DATA SOURCE: "WATER SURFACE ELEVATION PLOTS"---SAN LORENZO RIVER STUDY, STAGE II, FIELD AND SIMULATION STUDIES, FINAL REPORT PREPARED BY JONES-TILLSON & ASSOCIATES, WATER RESOURCES ENGINEERS, H. ESMAILI & ASSOCIATES, SEPTEMBER 1980.

Table 6 Water-surface elevations observed during 19 February 1980 flood for the San Lorenzo River

the deviation amounts to over 3 ft in the water-surface elevation (see tables 2 through 5). Predictions of thalweg elevations also differ quite widely along the upper portion of the study reach, as seen in figure 12. Table 7 lists the water-surface and thalweg elevations at a peak flow of 12,800 cfs computed by SLA using three different movable-bed models (HEC2SR, KUWASER, and UUWSR). The results are depicted in figure 13. Among these three models, HEC2SR is seen to predict greater water-surface elevations for the lower reach, and smaller values for the upper reach. At a river distance of 19,238 ft, the prediction gap between HEC2SR and UUWSR is 3.6 ft (see table 7).

Table 8 summarizes the water-surface elevations predicted by HEC using the HEC-6 movable-bed model, HEC-6 fixed-bed model, and HEC-2 fixed-bed model. As seen in the table, there are no significant differences among these three models. According to the HEC report, the computed water-surface profiles rarely differed by more than 0.5 ft at any cross section, although thalweg-elevation changes of more than a foot occurred at some cross sections during the simulations. The report also stated that local scour or deposition does not translate directly into water-surface changes at a cross section because sediment movement is often limited to only a portion of the channel by specifying movable-bed limits. Figure 14 shows the water-surface elevations predicted by SDSU using the FLUVIAL-11 movable-bed model (comparison of H and H1 given in table 4). FLUVIAL-11 is seen to predict much smaller water-surface elevations in the upper reach than the HEC-2 fixed-bed model simulation. SEDIMENT-4H movable-bed model predicts a water-surface profile that is almost identical to that yielded by SEDIMENT-4H fixed-bed model, as seen in figure 15 (comparison of H and H1 in table 5).

The final post-flood thalweg profile predicted by HEC2SR is shown in figure 16, together with the initial thalweg profile (YF and YO in table 2). The largest thalweg deposition, 3.1 ft, was predicted to occur at a river distance of 14,118 ft. As stated earlier, HEC-6 did not predict significant changes in thalweg elevation. As can be seen in table 4 (YO and YF), FLUVIAL-11 predicted significant changes in thalweg elevation; as much as 5.3 ft of deposition was computed at river distance of 15,308 ft and 18,258 ft. On the other hand, SEDIMENT-4H predicted practically no change (see YO and YF in table 5). Typical longitudinal mean flow-velocity distributions at peak flow

SAN LORENZO RIVER: HEC2SR, KUWASER, & UUWSR

ID	X	Y0	Y1	H1	Y1F	Y2	H2	Y2F	Y3	H3	Y3F
	FT	FT	FT	FT	FT	FT	FT	FT	FT	FT	FT
3	0	-4.5	-4.7	1.6	-4.7	-4.5	1.2	-4.5	-4.5	1.2	-4.5
4	558	-4.2	-4.3	4.0	-4.4	-6.1	4.6	-6.8	-4.8	2.8	-4.4
8	1183	-4.0	-4.1	4.8	-4.2	-4.4	4.7	-3.7	-4.4	3.7	-4.2
9	1700	-1.3	-1.3	5.4	-1.4	-1.7	5.6	-1.7	-1.3	4.5	-1.8
10	2200	-1.0	-1.6	5.9	-1.6	-0.6	5.8	-1.0	-1.3	5.1	-2.0
11	2600	-0.6	-1.2	6.2	-1.2	0.2	6.3	-1.2	-1.3	5.5	-2.0
12	2800	-0.4	-1.0	6.0	-1.1	-1.0	6.3	-2.5	-2.5	5.7	-3.0
14	2950	-0.3	-1.0	6.2	-1.1	-2.0	6.3	-2.0	-2.9	5.8	-3.3
15	3575	0.2	-0.5	7.6	-0.6	-0.8	7.3	-1.3	-2.1	6.5	-2.7
19	4345	0.6	-0.1	8.9	-0.2	0.2	8.5	-0.5	-1.7	7.5	-2.1
20	4955	1.4	1.0	9.6	1.9	0.0	9.5	-0.3	-0.1	8.3	-0.4
21	5360	1.8	2.2	10.4	2.3	0.0	10.2	0.4	-0.1	8.8	0.6
22	5610	2.0	2.3	11.3	2.3	2.4	10.6	2.9	2.0	9.1	2.1
25	6095	2.5	2.8	11.5	2.9	2.9	10.8	2.7	3.0	9.7	2.5
26	6745	3.0	3.9	11.9	4.1	2.6	11.4	3.9	2.3	10.5	2.7
27	7325	3.2	4.0	12.8	4.2	3.8	11.9	5.0	3.6	11.3	4.0
30	7575	3.4	4.2	13.1	4.4	5.2	12.2	5.4	4.1	11.6	4.6
31	8080	3.7	4.6	13.4	4.7	6.1	12.6	6.6	4.9	12.1	5.4
32	8585	4.1	5.9	13.6	6.2	7.1	13.1	7.6	5.5	12.6	6.1
33	9090	4.4	6.2	14.0	6.5	8.0	13.6	7.7	6.4	13.1	6.7
34	9595	4.8	6.6	14.4	6.9	8.1	14.0	8.5	7.0	13.6	7.1
35	9935	5.0	6.9	14.7	7.2	9.0	15.7	9.2	7.6	14.0	7.5
36	10140	5.2	5.4	14.7	5.5	6.5	15.9	7.4	6.4	14.3	7.1
38	10400	5.6	5.8	14.9	5.9	6.6	16.1	7.5	7.0	14.7	7.4
39	10780	6.4	6.6	15.4	6.7	8.7	16.5	8.2	7.7	15.5	8.1
40	11260	7.2	7.4	16.0	7.5	8.2	17.1	9.1	8.2	16.4	8.8
41	11800	8.2	10.0	17.0	10.4	9.6	18.1	10.1	10.0	17.5	10.0
42	12305	9.2	11.0	18.6	11.5	9.9	18.8	11.1	10.9	18.5	11.0
43	12645	9.8	11.8	19.1	12.3	10.8	19.3	11.5	10.9	19.2	11.4
46	14118	10.0	12.6	23.1	13.1	13.1	21.5	13.3	13.3	22.1	13.9
47	15308	12.8	12.5	24.3	12.4	14.9	23.3	16.2	16.7	24.9	17.6
48	16908	16.5	16.0	26.5	15.9	17.2	28.6	16.6	19.7	29.9	20.9
49	18258	20.6	20.2	32.2	20.1	24.1	34.6	24.0	27.8	35.3	27.5
50	19238	24.2	23.6	35.3	23.4	27.4	37.1	27.6	27.9	38.9	30.3
51	20578	29.8	30.8	41.7	30.8	31.8	42.5	33.0	32.2	42.8	33.8
52	21508	32.8	35.2	46.1	35.5	34.0	44.0	34.4	36.1	45.8	36.1
53	22968	35.7	35.7	49.1	35.7	41.2	51.9	40.5	40.7	50.0	41.1
54	24758	41.2	41.2	53.6	41.2	41.2	53.6	41.2	41.2	54.5	41.2

ID = SECTION I.D.
X = RIVER DISTANCE
Y0 = INITIAL THALWEG EL
Y1 = THALWEG EL AT PEAK FLOW: (HEC2SR)
H1 = W.S. EL AT PEAK FLOW: (HEC2SR)
Y1F= FINAL THALWEG EL: (HEC2SR)
Y2 = THALWEG EL AT PEAK FLOW: (KUWASER)
H2 = W.S. EL AT PEAK FLOW: (KUWASER)
Y2F= FINAL THALWEG EL: (KUWASER)
Y3 = THALWEG EL AT PEAK FLOW: (UUWSR)
H3 = W.S. EL AT PEAK FLOW: (UUWSR)
Y3F= FINAL THALWEG EL: (UUWSR)
NOTE: PEAK-FLOW DISCHARGE = 12,800 CFS

Table 7 Comparison of thalweg and water-surface elevations computed by SLA using HEC2SR, KUWASER, and UUWSR for the San Lorenzo River

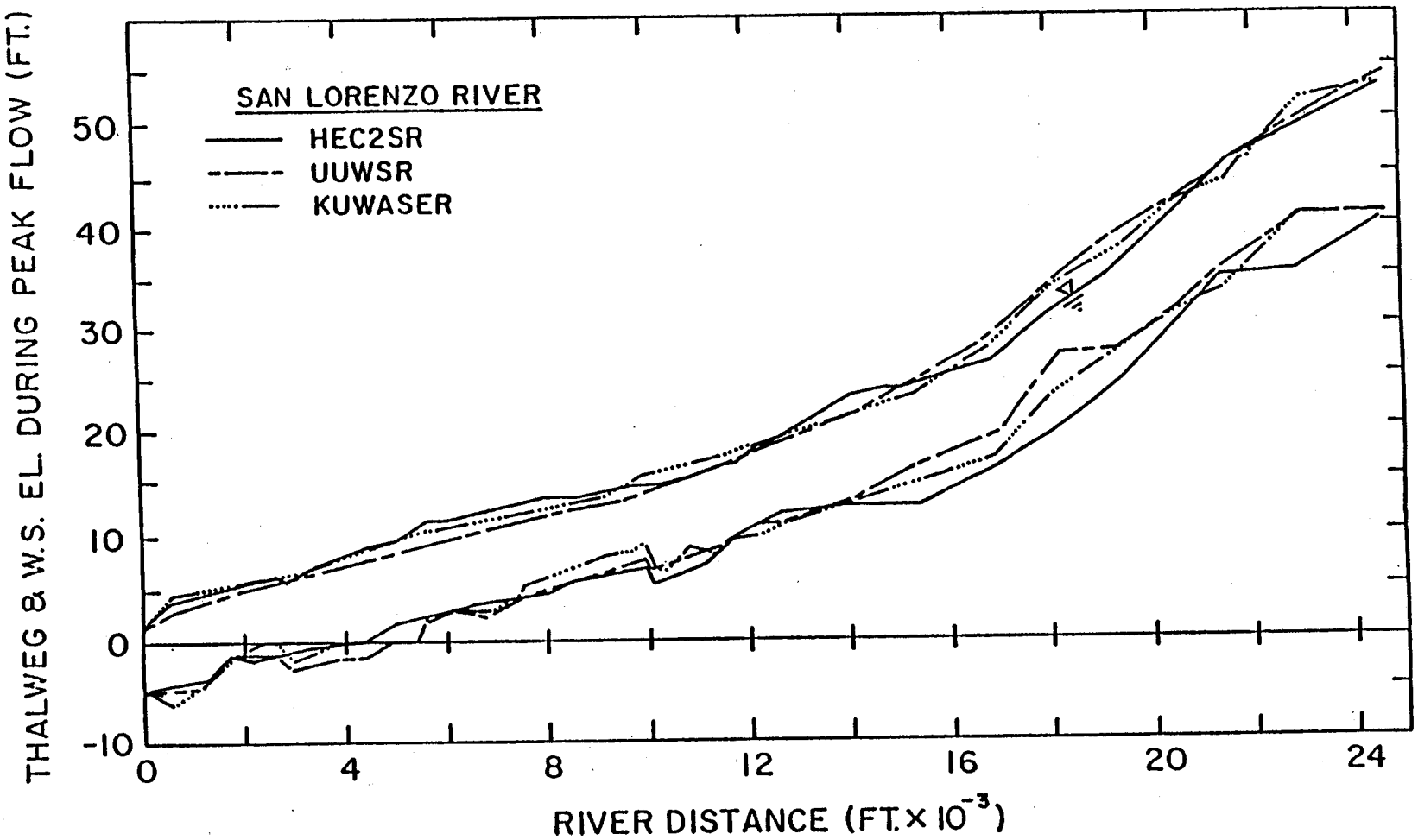

Figure 13 Comparison of thalweg and water-surface profiles at peak flow computed using the three SLA movable-bed models for the San Lorenzo River

SAN LORENZO RIVER: HEC-6

ID	X	H1	H2	H3	Q
	FT	FT	FT	FT	CFS
3	0	1.67	1.67	1.66	12800
4	558	4.14	4.17	4.07	12800
8	1183	4.97	4.88	4.82	12800
9	1700	5.80	5.51	5.47	12800
10	2200	6.41	5.94	5.90	12800
11	2600	6.69	6.20	6.17	12800
12	2800	6.67	6.14	6.11	12800
14	2950	6.92	6.34	6.31	12800
15	3575	8.36	8.71	8.17	12800
19	4345	9.26	9.76	9.52	12800
20	4955	9.80	10.41	10.23	12800
21	5360	10.37	10.87	10.72	12800
22	5610	11.11	11.52	11.41	12800
25	6095	11.31	11.68	11.62	11000
26	6745	11.74	12.04	11.98	11000
27	7325	12.39	12.62	12.58	11000
30	7575	12.60	12.82	12.77	11000
31	8080	12.82	13.02	13.05	11000
32	8585	13.05	13.21	13.25	11000
33	9090	13.32	13.45	13.48	11000
34	9595	13.57	13.69	13.72	11000
35	9935	13.79	13.86	13.89	11000
36	10140	13.51	13.60	13.63	11000
38	10400	14.05	14.00	13.96	11000
39	10780	14.72	14.62	14.60	11000
40	11260	15.49	15.38	15.37	11000
41	11800	16.72	16.79	16.80	11000
42	12305	17.62	17.54	17.54	11000
43	12645	17.95	17.84	17.86	11000
46	14118	21.26	21.29	21.31	11000
47	15308	23.08	22.94	22.94	11000
48	16908	27.02	26.84	26.85	11000
49	18258	32.14	32.00	32.01	11000
50	19238	34.94	35.50	35.36	11000
51	20578	40.64	41.13	41.25	11000
52	21508	44.13	44.44	44.47	11000
53	22968	47.46	46.94	46.93	11000
54	24758	54.26	53.73	53.64	11000

ID=SECTION I.D.
X =RIVER DISTANCE
H1=W.S. EL BY HEC-6 (MOVABLE BED)
H2=W.S. EL BY HEC-6 (FIXED BED)
H3=W.S. EL BY HEC-2 (FIXED BED)
Q =PEAK FLOW WATER DISCHARGE

Table 8 Comparison of water-surface elevations computed by the HEC-6 movable-bed and fixed-bed models and HEC-2 for the San Lorenzo River

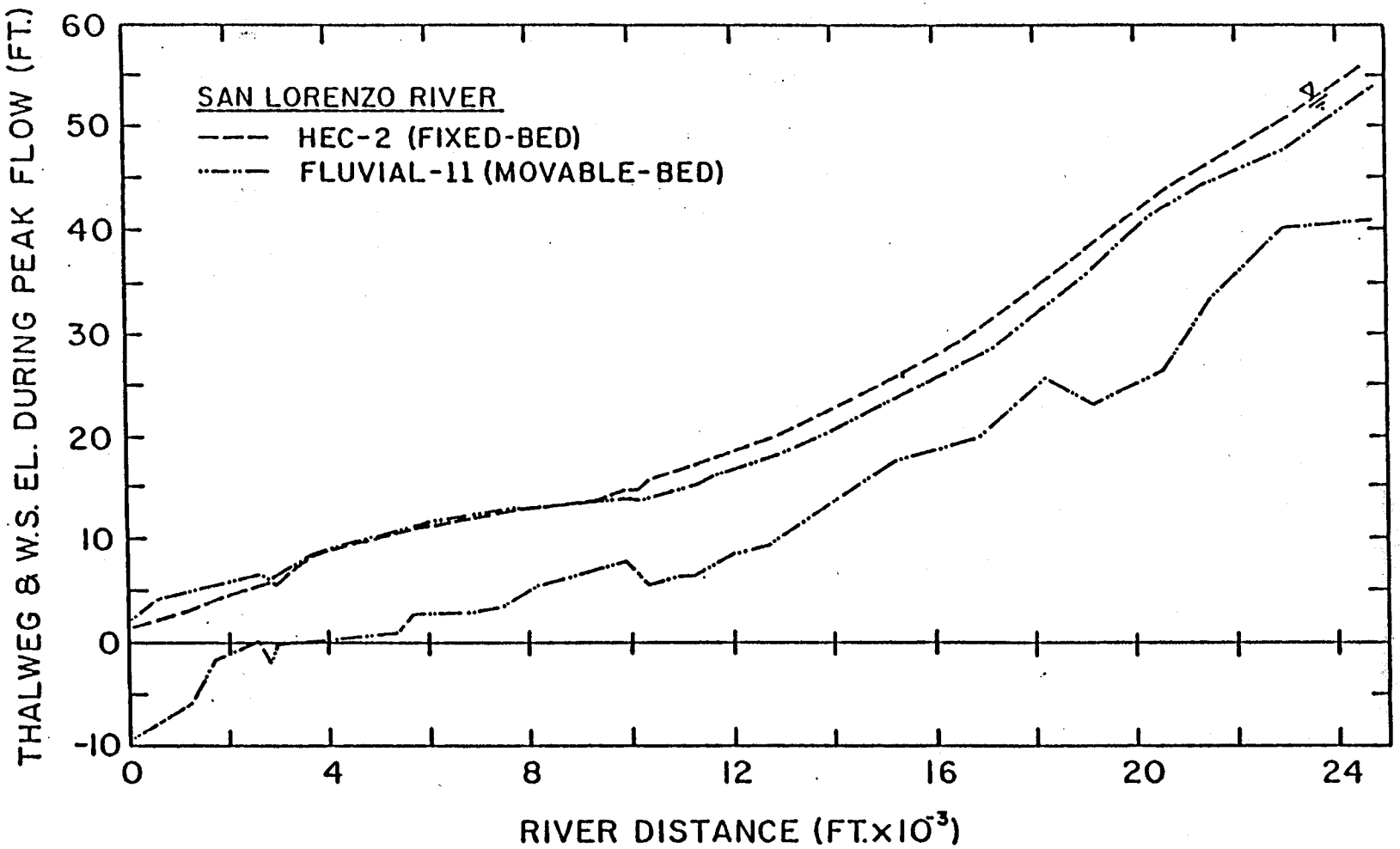

Figure 14 Comparison of thalweg and water-surface profiles computed by SDSU using HEC-2 and FLUVIAL-11 for the San Lorenzo River

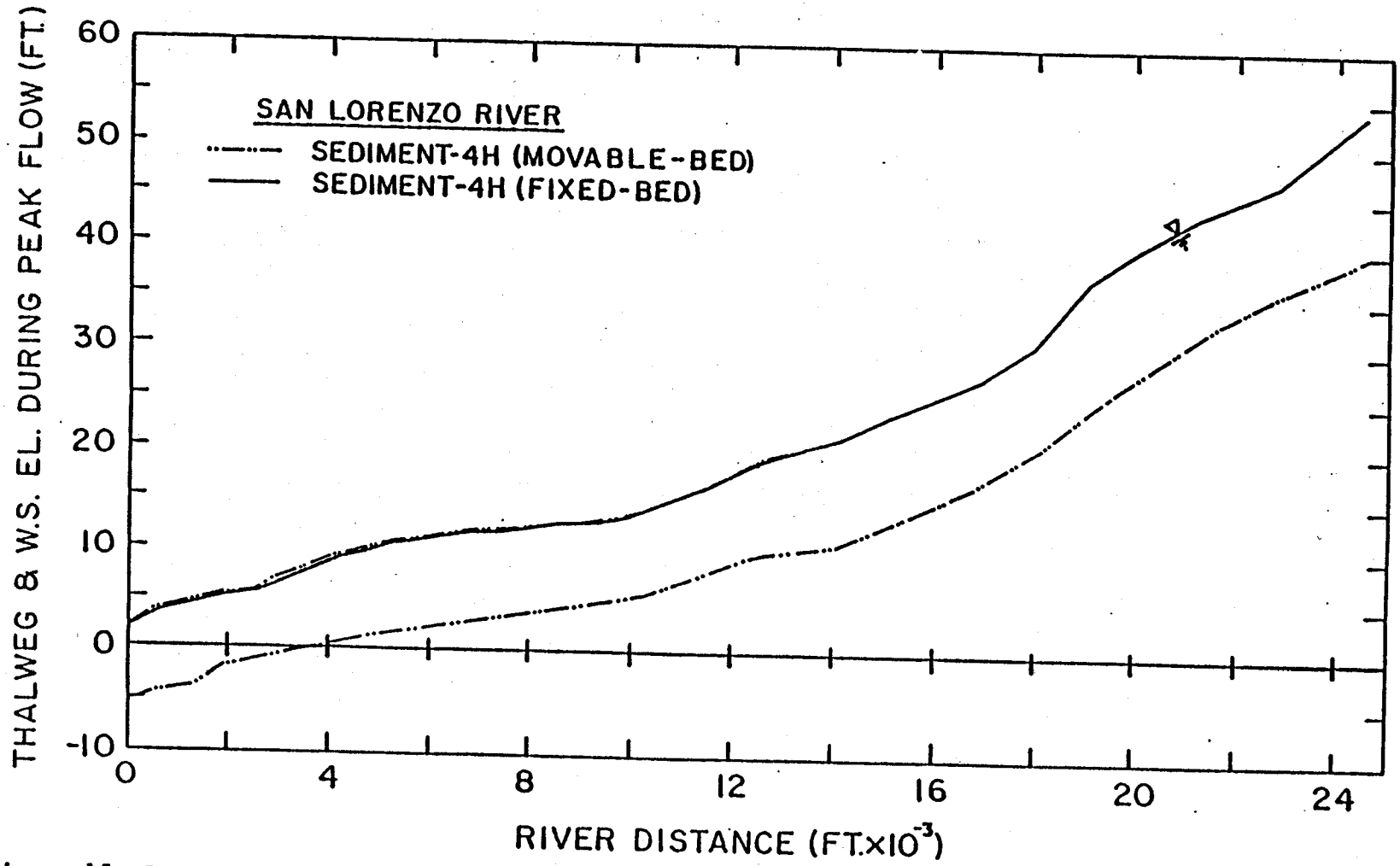

Figure 15 Comparison of thalweg and water-surface profiles at peak flow computed by RMA using the SEDIMENT-4H movable-bed and fixed-bed models for the San Lorenzo River

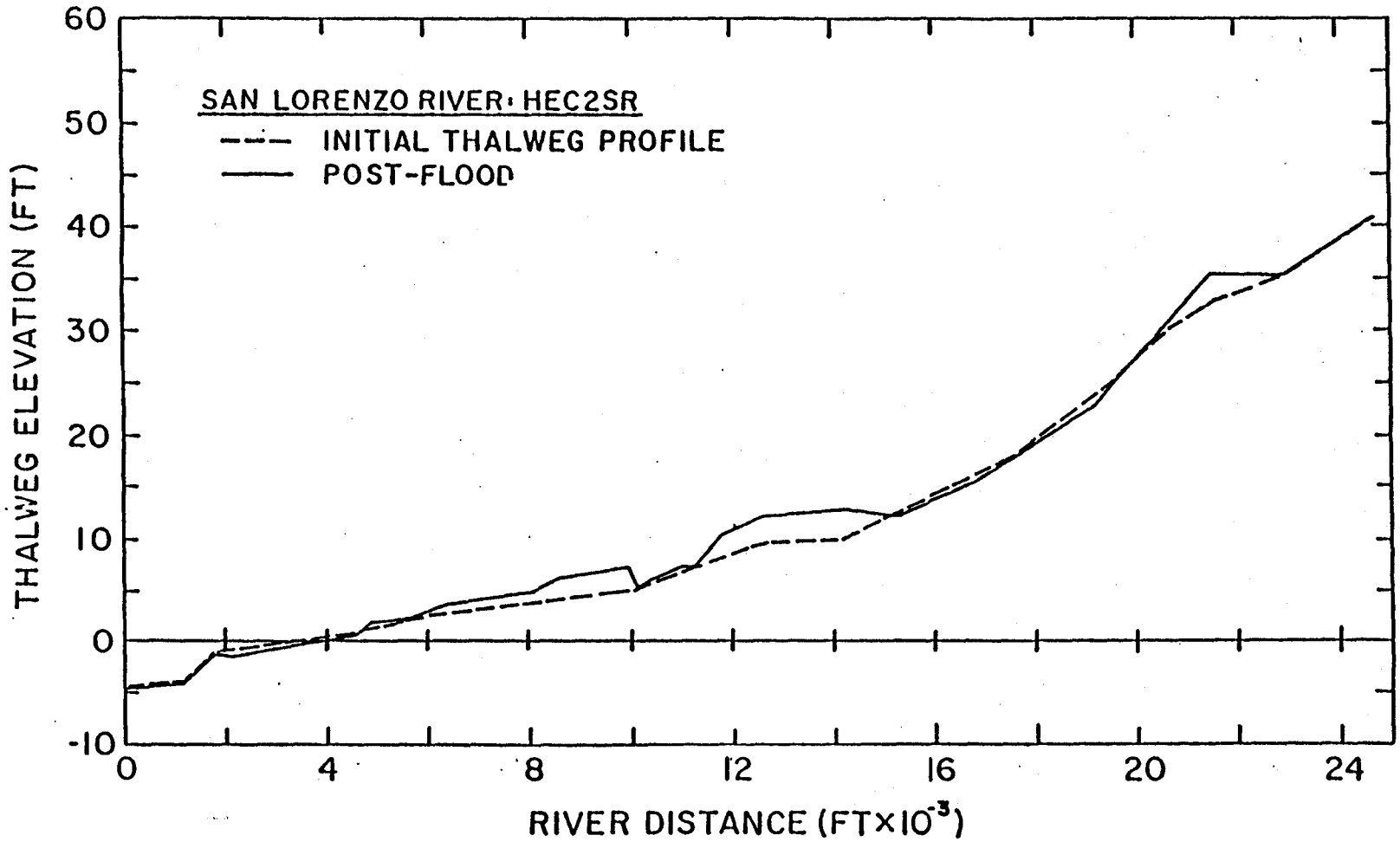

Figure 16 Comparison of initial and post-flood thalweg profiles computed using HEC2SR for the San Lorenzo River

are shown in figure 17 for HEC-6 and FLUVIAL-11; mean velocities predicted by HEC-6 are seen to be much higher than those of FLUVIAL-11 in the upper part of the study reach. Mean velocities predicted by HEC2SR and SEDIMENT-4H are closer to those computed by HEC-6, as can be seen in tables 2,3, and 5.

The total-load discharges at peak flow and the post-flood median bed-material sizes that were predicted by HEC2SR, HEC-6, FLUVIAL-11, and SEDIMENT-4H are summarized in table 9. Longitudinal distributions of the total-load discharge computed by these four models are plotted in figure 18. HEC2SR predictions are seen to be very high compared with those of HEC-6, in spite of the fact that both models predicted very similar mean velocities, as mentioned earlier. SEDIENT-4H predicted extremely low total-load sediment-transport rates, as is shown in table 9 (its predicted total-load discharges are too small to plot visibly in figure 18). Total-load discharges and mean flow velocities computed by the three SLA models (HEC2SR, KUWASER, and UUWSR) are tabulated in table 10 and plotted in figure 19. Although KUWASER and UUWSR used the same sediment-transport function, as mentioned in Chapter II, their predictions are seen to differ substantially because their predicted mean-flow-velocity predictions were quite different. Post-flood median bed-material sizes predicted by HEC2SR, HEC-6, FLUVIAL-11 are plotted in figure 20, together with the pre-flood values (see table 9 also). Note that SEDIMENT-4H does not account for sediment sorting processes. HEC-6 predicted significant coarsening of the river-bed material over the entire study reach.

In order to demonstrate model prediction of thalweg and water-surface elevations during both rising and falling stages of the hydrograph, numerical values predicted by HEC2SR, HEC-6, FLUVIAL-11, and SEDIMENT-4H are summarized in tables 11, 12, 13, and 14, respectively. Direct comparisons of these results are not possible because time-discretization intervals of the hydrograph differed from model to model, resulting in the modelers' computer outputs being prepared for different water discharges. However, approximate comparisons can be made. For example, thalweg and water-surface elevations predicted by FLUVIAL-11 and SEDIMENT-4H during the rising stage can be compared because water discharges of 7,690 cfs and 7,960 cfs used by the two models, respectively, are nearly equal. As seen in tables 13 and 14 (YR and HR), their predictions of the thalweg elevation differed considerably,

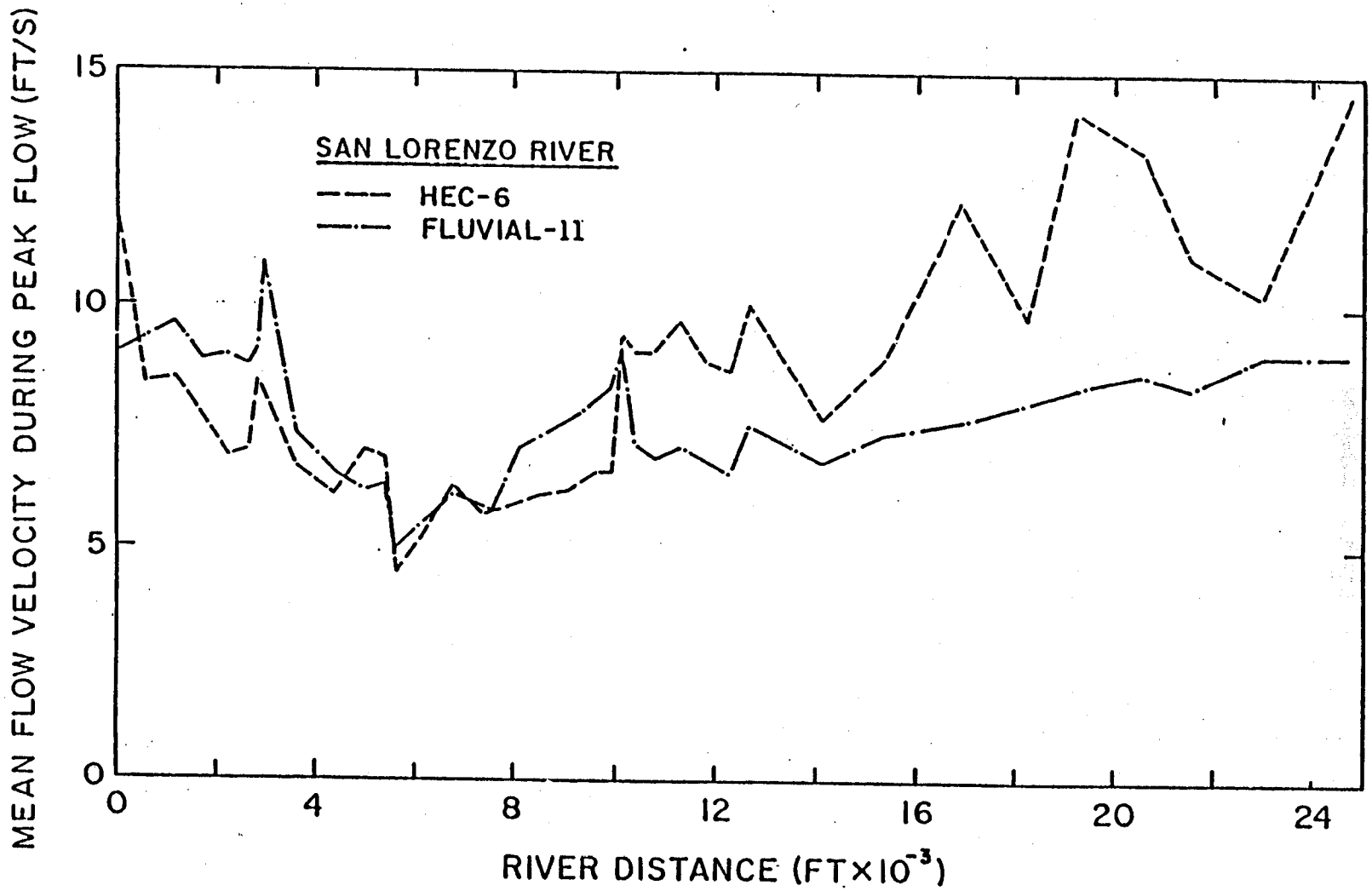

Figure 17 Longitudinal distributions of mean flow velocity at peak flow computed using the HEC-6 and FLUVIAL-11 movable-bed models for the San Lorenzo River

SAN LORENZO RIVER			(HEC-6)		(FLUVIAL-11)		(HEC2SR)		(SEDIMENT-4H)	
ID	X	D50I	QT	D50F	QT	D50F	QT	D50F	QT	D50F
	FT	MM	T/D	MM	T/D	MM	T/D	MM	T/D	MM
3	0	0.34	46670	0.71	158700	0.57	244170	0.47	1580	0.50
4	558	0.34	41230	0.70	168380	0.59	244170	0.47	1070	0.50
8	1183	0.34	38960	0.69	170590	0.65	244170	0.47	1170	0.50
9	1700	0.34	39110	0.68	165180	0.77	244170	0.47	224	0.50
10	2200	0.27	40360	0.54	160760	1.13	205210	0.50	849	0.50
11	2600	0.27	41370	0.58	153930	1.25	205210	0.50	863	0.50
12	2800	0.27	39540	0.59	147460	1.31	205210	0.50	1830	0.50
14	2950	0.27	37700	0.65	215140	1.15	205210	0.50	1830	0.50
15	3575	0.27	36570	0.67	141620	1.28	205210	0.50	1610	0.50
19	4345	0.27	30180	0.72	95720	0.50	205210	0.50	833	0.50
20	4955	0.53	18060	1.14	86250	0.39	153230	0.53	417	0.50
21	5360	0.53	16890	1.37	91380	0.37	153230	0.53	190	0.50
22	5610	0.53	16400	1.05	80490	0.35	153230	0.53	11	0.50
25	6065	0.53	13350	1.10	104050	0.37	153230	0.53	24	0.50
26	6745	0.53	12640	1.16	116360	0.39	168880	0.37	93	0.50
27	7325	0.53	11730	1.21	118490	0.32	168880	0.37	29	0.50
30	7575	0.53	10700	1.06	116500	0.35	168880	0.37	25	0.50
31	8080	0.93	9520	0.93	126680	0.42	168880	0.37	30	0.50
32	8585	0.93	9880	1.06	145960	0.46	207890	0.34	26	0.50
33	9090	0.93	10150	1.24	164040	0.51	207890	0.34	24	0.[illegible]
34	9595	0.93	10460	1.15	181050	0.56	207890	0.34	20	0.50
35	9935	0.93	9720	0.98	192720	0.55	207890	0.34	14	0.50
36	10140	0.93	10460	1.68	198620	0.41	270750	0.58	79	0.50
38	10400	0.93	9520	1.75	211080	0.40	270750	0.58	99	0.50
39	10780	0.93	9770	1.72	202400	0.44	270750	0.58	91	0.50
40	11260	0.93	9980	1.83	186100	0.51	270750	0.58	144	0.50
41	11800	0.93	9620	1.66	174570	0.46	272050	0.50	96	0.50
42	12305	0.93	10650	1.75	165460	0.53	272050	0.50	179	0.50
43	12645	0.93	11090	1.84	198410	0.59	272050	0.50	140	0.50
46	14118	0.93	10880	1.55	152940	0.51	272050	0.50	113	0.50
47	15308	0.93	15000	1.68	199120	0.50	335130	1.62	51	0.50
48	16908	0.93	17450	1.71	256410	0.61	335130	1.62	93	0.50
49	18258	0.93	20260	1.64	291070	1.03	335130	1.62	135	0.50
50	19238	0.93	20810	1.93	338320	0.83	335130	1.62	190	0.50
51	20570	0.93	18070	1.93	363590	1.19	319310	0.64	54	0.50
52	21508	0.93	18210	0.98	333840	1.53	319310	0.64	26	0.50
53	22968	0.93	34920	1.80	348360	2.37	324520	1.25	37	0.50
54	24758	0.93	51110	1.68	367860	3.15	324520	1.25	350	0.50

ID = SECTION I.D.
X = RIVER DISTANCE
D50I = INITIAL MEDIAN SIZE OF BED MATERIAL (PRE-FLOOD)
D50F = FINAL MEDIAN SIZE OF BED MATERIAL (POST-FLOOD)
QT = TOTAL-LOAD DISCHARGE AT PEAK-FLOW DISCHARGE OF 12,800 CFS

Table 9 Comparison of total-load discharges computed by HEC2SR, HEC-6, FLUVIAL-11, and SEDIMENT-4H for the San Lorenzo River

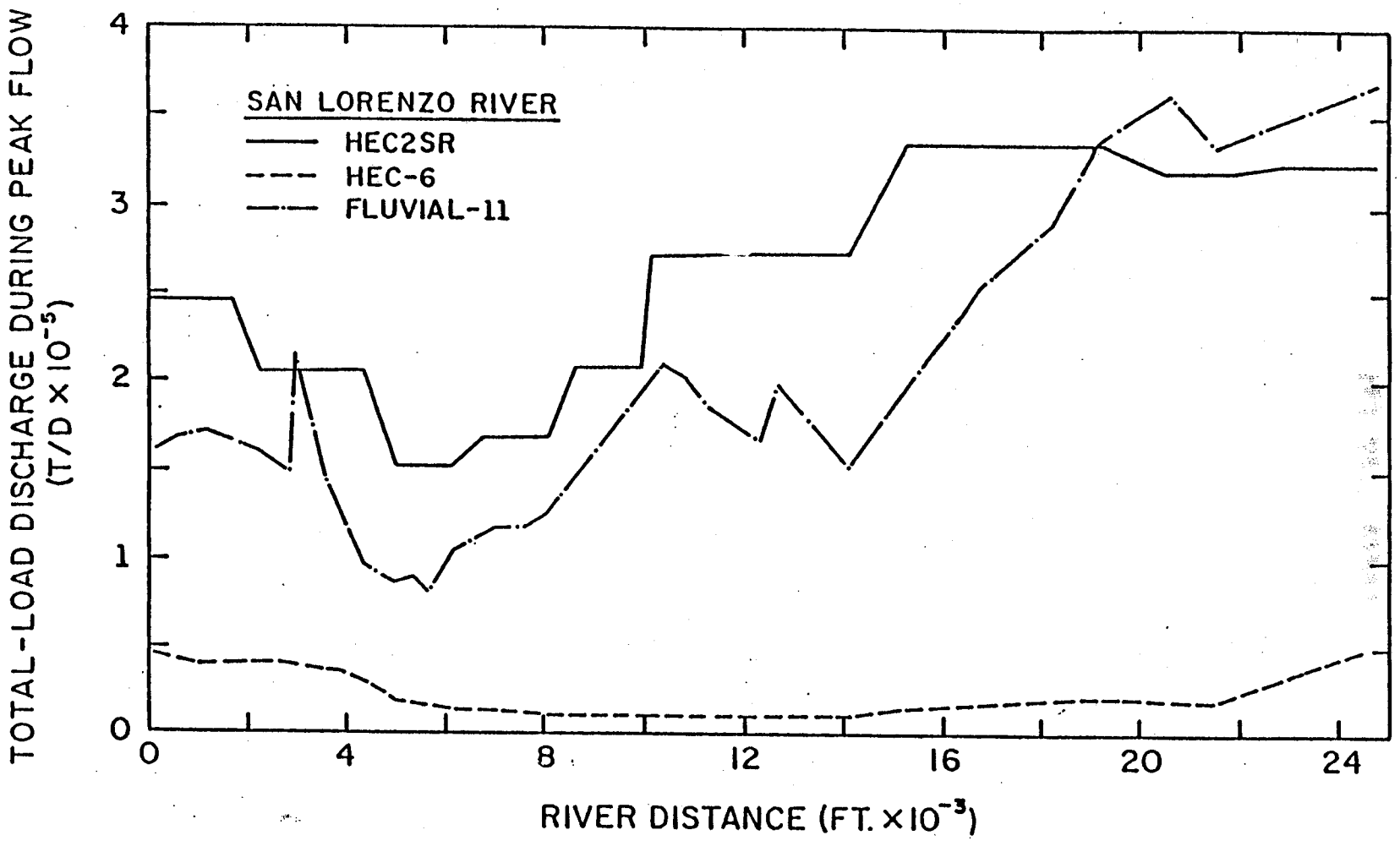

Figure 18 Total-load discharges at peak flow computed using HEC2SR, HEC-6, and FLUVIAL-11 for the San Lorenzo River

SAN LORENZO RIVER		THREE SLA MODELS					
		(HEC2SR)		(KUWASER)		(UUWSR)	
ID	X FT	QT T/D	V FPS	QT T/D	V FPS	QT T/D	V FPS
3	0	244170	11.9	555200	13.5	1287340	13.2
4	558	244170	8.1	60420	6.6	321070	9.2
8	1183	244170	7.9	151730	8.5	304990	9.1
9	1700	244170	7.3	70750	6.7	285810	8.7
10	2200	205210	6.6	114940	7.8	255480	7.5
11	2600	205210	6.8	88220	7.3	243420	7.4
12	2800	205210	9.2	158590	8.9	234260	7.7
14	2950	205210	9.2	134010	8.5	226080	7.5
15	3575	205210	7.4	84720	7.4	184530	7.0
19	4345	205210	6.6	73440	7.2	125610	6.4
20	4955	153230	7.7	58500	6.6	87100	7.1
21	5360	153230	7.3	41210	6.1	69250	6.7
22	5610	153230	4.6	25120	5.1	51840	6.0
25	6095	153230	5.2	31670	5.7	54460	6.4
26	6745	168880	6.8	25400	5.5	59430	6.7
27	7325	168880	5.9	38320	6.0	60410	6.8
30	7575	168880	5.9	66830	6.9	68370	6.9
31	8080	168880	6.0	90650	7.5	76190	7.2
32	8585	207890	6.9	173520	7.7	94430	7.6
33	9090	207890	6.9	300240	9.9	110410	7.9
34	9595	207890	7.0	187300	8.9	134960	8.2
35	9935	207890	7.1	102510	7.7	143090	8.4
36	10140	270750	7.9	159160	7.5	151710	9.3
38	10400	270750	8.1	164450	7.6	159140	9.4
39	10780	270750	8.5	179380	7.8	166600	9.4
40	11260	270750	9.5	279530	8.8	170190	9.6
41	11800	272050	10.7	252600	8.4	174060	9.6
42	12305	272050	9.5	272380	8.6	183110	9.7
43	12645	272050	11.4	222590	8.1	188660	9.9
46	14118	272050	6.7	204450	7.9	186720	9.4
47	15308	335130	7.1	378890	10.9	226690	9.7
48	16908	335130	13.2	268030	10.6	269100	10.2
49	18258	335130	8.6	292460	8.2	259530	10.7
50	19238	335130	14.2	527770	13.1	441080	11.8
51	20578	319310	14.2	566560	10.9	429780	12.7
52	21508	319310	10.8	738640	15.1	420910	12.4
53	22968	324520	8.5	306820	9.0	459860	12.3
54	24758	324520	15.0	683280	14.5	497220	13.1

ID = SECTION I.D.
X = RIVER DISTANCE
QT = TOTAL-LOAD DISCHARGE AT PEAK FLOW
V = MEAN FLOW VELOCITY AT PEAK FLOW
NOTE: PEAK-FLOW DISCHARGE = 12,800 CFS

Table 10 Comparison of total-load discharges and mean flow velocities computed by SLA using HEC2SR, KUWASER, and UUWSR for the San Lorenzo River

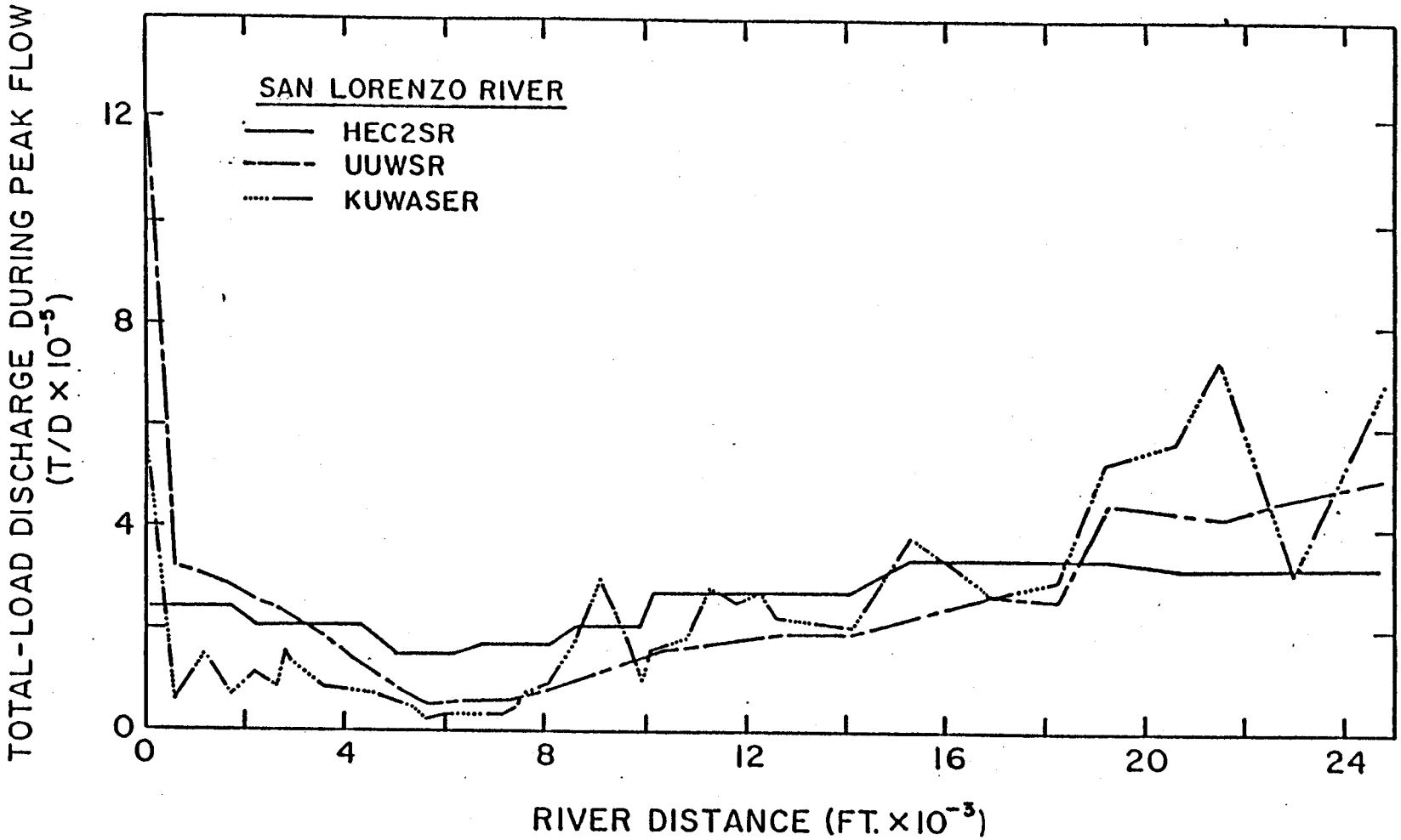

Figure 19 Total-load discharges at peak flow computed by SLA using the three SLA models for the San Lorenzo River

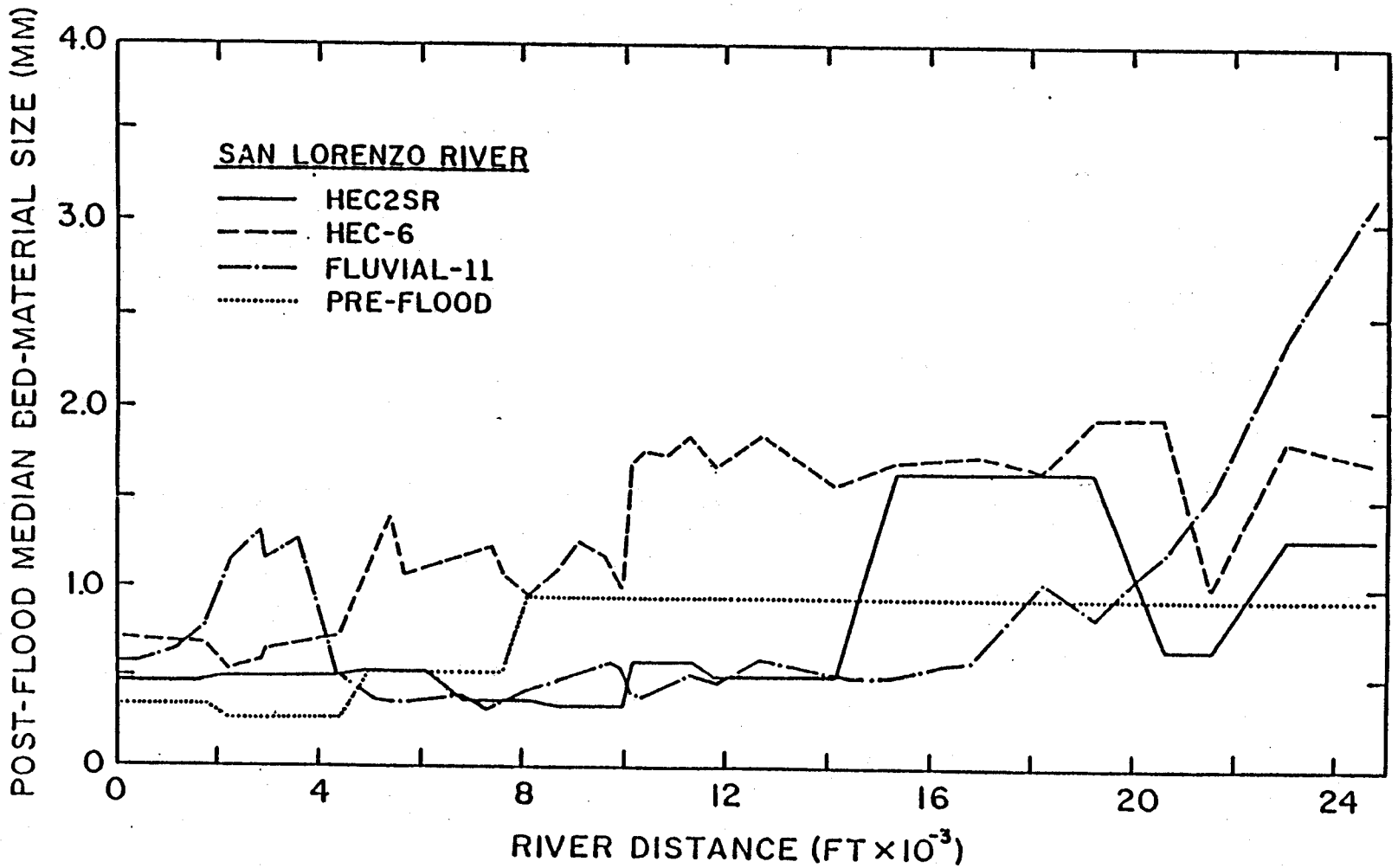

Figure 20 Longitudinal distributions of post-flood median bed-material size computed using HEC2SR HEC-6, FLUVIAL-11, and SEDIMENT-4H for the San Lorenzo River

SAN LORENZO RIVER: HEC2SR

ID	X	YR	HR	YFA	HFA
	FT	FT	FT	FT	FT
3	0	-4.4	2.3	-4.6	3.4
4	558	-4.1	2.8	-4.3	3.7
8	1183	-3.9	3.3	-4.1	4.1
9	1700	-1.2	3.7	-1.3	4.4
10	2200	-1.4	4.2	-1.6	4.8
11	2600	-1.0	4.4	-1.2	5.0
12	2800	-0.9	4.4	-1.1	4.9
14	2950	-0.8	4.5	-1.1	5.1
15	3575	-0.3	5.6	-0.6	6.1
19	4345	0.1	6.8	-0.1	7.2
20	4955	1.7	7.4	1.9	7.9
21	5360	2.1	8.1	2.3	8.7
22	5610	2.2	8.7	2.3	9.4
25	6095	2.8	9.0	2.9	9.7
26	6745	3.7	9.4	4.0	10.2
27	7325	3.9	10.2	4.1	11.1
30	7575	4.0	10.4	4.3	11.4
31	8080	4.4	10.8	4.6	11.7
32	8585	5.5	11.0	6.0	11.9
33	9090	5.8	11.4	6.3	12.5
34	9595	6.3	11.8	6.8	12.9
35	9935	6.5	12.0	7.0	13.2
36	10140	5.4	12.1	5.4	13.3
38	10400	5.8	12.3	5.8	13.5
39	10780	6.6	12.8	6.6	13.9
40	11260	7.4	13.5	7.4	14.5
41	11800	9.8	14.6	10.2	15.4
42	12305	10.8	16.2	11.2	17.4
43	12645	11.5	16.8	12.0	17.9
46	14118	12.4	20.3	12.8	21.6
47	15308	12.5	21.6	12.5	22.8
48	16908	16.1	24.2	16.0	25.0
49	18258	20.2	29.7	20.1	30.6
50	19238	23.7	32.6	23.5	33.5
51	20578	30.8	39.4	30.8	40.3
52	21508	35.2	43.0	35.3	44.1
53	22968	35.7	46.1	35.7	47.2
54	24758	41.2	50.5	41.2	51.7

ID =SECTION I.D.
X =RIVER DISTANCE
YR =THALWEG EL AT Q=7,250 CFS (RISING STAGE)
HR =W.S. EL AT Q=7,250 CFS (RISING STAGE)
YFA=THALWEG EL AT Q=8,570 CFS (FALLING STAGE)
HFA=W.S. EL AT Q=8,570 CFS (FALLING STAGE)

Table 11 Thalweg and water-surface elevations during rising and falling stages computed by HEC2SR for the San Lorenzo River

SAN LORENZO RIVER: HEC-6

ID	X	YR	HR	YFA	HFA
	FT	FT	FT	FT	FT
3	0	-4.2	1.6	-4.6	3.5
4	558	-3.7	2.7	-3.7	3.7
8	1183	-3.4	3.5	-3.4	4.1
9	1700	-0.7	4.2	-0.6	4.6
10	2200	-0.7	4.8	-0.7	5.1
11	2600	-0.5	5.0	-0.7	5.3
12	2800	-0.6	5.1	-0.8	5.3
14	2950	-1.0	5.4	-1.1	5.5
15	3575	-0.5	6.6	-0.8	6.5
19	4345	-0.2	7.4	-0.7	7.2
20	4955	1.4	8.0	1.3	7.7
21	5360	1.7	8.5	1.7	8.3
22	5610	2.0	9.1	2.0	8.9
25	6095	2.6	9.3	2.5	9.1
26	6745	3.0	9.7	3.0	9.7
27	7325	3.2	10.4	3.2	10.4
30	7575	3.5	10.5	3.4	10.6
31	8080	3.9	10.8	3.9	10.8
32	8585	4.3	11.0	4.3	11.0
33	9090	4.5	11.3	4.6	11.3
34	9595	5.2	11.5	5.2	11.6
35	9935	5.3	11.8	5.4	11.9
36	10140	5.6	11.6	5.5	11.7
38	10400	5.7	12.2	5.7	12.2
39	10780	6.5	12.8	6.5	12.9
40	11260	7.1	13.6	7.1	13.8
41	11800	8.4	14.7	8.4	14.9
42	12305	9.2	15.6	9.3	15.8
43	12645	9.7	16.0	9.7	16.3
46	14118	10.2	19.1	10.3	19.4
47	15308	12.9	21.2	13.0	21.4
48	16908	16.7	25.3	16.7	25.6
49	18258	20.7	30.2	20.8	30.5
50	19238	23.7	32.9	23.6	33.0
51	20578	27.5	38.6	29.5	38.8
52	21508	33.4	41.4	34.2	41.7
53	22968	35.5	44.9	36.0	45.9
54	24758	40.8	50.7	42.4	52.7

ID =SECTION I.D.
X =RIVER DISTANCE
YR =THALWEG EL AT Q=8,200 CFS (RISING STAGE)
HR =W.S. EL AT Q=8,200 CFS (RISING STAGE)
YFA=THALWEG EL AT Q=8,100 CFS (FALLING STAGE)
HFA=W.S. EL AT Q=8,100 CFS (FALLING STAGE)

Table 12 Thalweg and water-surface elevations during rising and falling stages computed by HEC-6 for the San Lorenzo River

SAN LORENZO RIVER: FLUVIAL-11

ID	X	YR	HR	YFA	HFA
	FT	FT	FT	FT	FT
3	0	-6.8	2.7	-8.3	3.0
4	558	-5.3	2.9	-6.8	3.2
8	1183	-3.9	3.2	-5.3	3.5
9	1700	-1.5	3.8	-1.5	3.9
10	2200	-0.7	4.1	-0.8	4.4
11	2600	0.1	4.4	-0.3	4.8
12	2800	-0.4	4.5	-1.3	4.9
14	2950	-0.6	4.8	-0.6	4.9
15	3575	-0.1	6.1	-0.1	6.7
19	4345	0.3	7.2	0.3	8.0
20	4955	0.5	7.8	0.5	8.6
21	5360	1.0	8.1	1.0	9.0
22	5610	2.1	8.5	2.7	9.4
25	6095	2.6	8.8	2.9	9.7
26	6745	2.7	9.2	2.7	10.3
27	7325	3.2	9.7	3.4	10.9
30	7575	3.4	9.9	3.7	11.1
31	8080	4.6	10.1	5.3	11.4
32	8585	5.2	10.5	5.9	12.0
33	9090	5.8	10.9	6.6	12.5
34	9595	6.5	11.4	7.3	13.1
35	9935	7.0	11.7	7.7	13.5
36	10140	6.3	11.9	6.7	13.7
38	10400	5.7	12.6	5.7	14.6
39	10780	6.4	13.2	6.2	15.2
40	11260	6.9	13.9	6.3	15.9
41	11800	8.2	14.9	8.0	16.8
42	12305	9.3	15.7	8.8	17.6
43	12645	9.4	16.3	9.2	18.1
46	14118	13.4	19.6	14.3	21.6
47	15308	17.2	22.6	18.1	25.0
48	16908	19.9	27.5	20.3	30.0
49	18258	24.5	31.8	26.2	34.2
50	19238	22.9	34.9	24.5	37.7
51	20578	28.7	39.1	26.6	41.7
52	21508	33.2	41.8	33.6	44.1
53	22968	39.2	46.0	40.2	48.6
54	24758	41.2	52.9	41.2	55.6

ID =SECTION I.D.
X =RIVER DISTANCE
YR =THALWEG EL AT Q=7,690 CFS (RISING STAGE)
HR =W.S. EL AT Q=7,690 CFS (RISING STAGE)
YFA=THALWEG EL AT Q=9,440 CFS (FALLING STAGE)
HFA=W.S. EL AT Q=9,440 CFS (FALLING STAGE)

Table 13 Thalweg and water-surface elevations during rising and falling stages computed by FLUVIAL-11 for the San Lorenzo River

SAN LORENZO RIVER:SEDIMENT-4H

ID	X	YR	HR	YFA	HFA
	FT	FT	FT	FT	FT
3	0	-5.0	1.4	-5.3	3.5
4	558	-4.4	2.1	-4.4	3.7
8	1183	-4.0	2.7	-4.2	3.9
9	1700	-2.5	3.2	-2.5	4.2
10	2200	-1.5	3.6	-1.6	4.4
11	2600	-1.0	4.0	-1.1	4.6
14	2750	-0.9	4.5	-1.3	4.9
15	3375	0.0	5.7	-0.3	5.8
19	4145	0.5	7.1	0.4	7.1
20	4755	1.2	8.0	1.1	8.0
21	5160	1.7	8.5	1.6	8.5
22	5410	1.9	8.8	1.9	8.8
25	5895	2.3	9.0	2.3	9.1
26	6545	2.8	9.6	2.8	9.7
27	7125	3.1	9.9	3.1	10.1
30	7375	3.3	10.0	3.3	10.2
31	7860	3.6	10.3	3.6	10.5
32	8385	4.0	10.6	4.0	10.8
33	8890	4.4	10.9	4.4	11.1
34	9395	4.8	11.2	4.8	11.4
35	9735	5.0	11.4	5.0	11.6
36	9940	5.2	11.7	5.1	11.9
38	10200	5.6	12.2	5.5	12.4
39	10580	6.1	12.9	6.0	13.1
40	11060	7.0	13.7	6.9	14.0
41	11600	8.1	14.7	8.1	14.9
42	12105	9.0	15.8	9.0	16.0
43	12445	9.7	17.0	9.7	17.3
46	13918	10.7	19.1	10.7	19.4
47	15108	13.0	21.7	13.0	22.0
48	16708	16.6	25.0	16.6	25.2
49	18058	20.6	29.5	20.6	29.8
50	19038	24.7	35.0	24.6	35.3
51	20378	29.1	39.0	29.1	39.3
52	21308	32.7	41.4	32.7	41.7
53	22768	36.3	44.6	36.3	45.0
54	24558	40.1	51.3	40.1	51.8

ID =SECTION I.D.
X =RIVER DISTANCE
YR =THALWEG EL AT Q=7,960 CFS (RISING STAGE)
HR =W.S. EL AT Q=7,960 CFS (RISING STAGE)
YFA=THALWEG EL AT Q=8,260 CFS (FALLING STAGE
HFA=W.S. EL AT Q=8,260 CFS (FALLING STAGE)

Table 14 Thalweg and water-surface elevations during rising and falling stages computed by SEDIMENT-4H for the San Lorenzo River

although the predicted water-surface elevations are in relatively good agreement.

2. San Dieguito River. The principal hydraulic and sediment-transport characteristics at a peak flow of 22,000 cfs computed by HEC2SR, FLUVIAL-11, and SEDIMENT-4H are shown in tables 15, 16, and 17, respectively. Water-surface elevations computed using the fixed-bed models (FLUVIAL-11 and SEDIMENT-4H) are also listed in tables 16 and 17 (see H1). Thalweg and water-surface elvations during the peak flow predicted by these three movable-bed models are presented in figure 21, in which the three models are seen to predict widely differing elevations. HEC2SR predicted the backwater profile upstream of the Via de Santa Fe bridge located at a river distance of 3,780 ft; however, both FLUVIAL-11 and SEDIMENT-11 4H predicted smooth water-surface profiles in the vicinity of the bridge. Figure 22 shows two different water-surface profiles obtained by SDSU using the HEC-2 fixed-bed and FLUVIAL-11 movable-bed models. At a river distance of 3,925 ft, immediately upstream of the bridge, the HEC-2 fixed-bed model is seen to predict a water-surface elevation 5.8 ft higher than that of FLUVIAL-11. According to the SDSU report, the river channel in the vicinity of the bridge was predicted by FLUVIAL-11 to be scoured and widened extensively during the peak flow, resulting in much lower water-surface elevations than those predicted by the fixed-bed model. The results obtained by SLA using the UUWSR fixed-bed and movable-bed models are compared with the SLA's HEC-2 simulation in figure 23. The UUWSR fixed-bed model predicted much lower water-surface elevation upstream of the Via de Santa Fe bridge than HEC-2. The SLA report states that as much as 20 ft of scour was predicted by the UUWSR movable-bed model at the bridge section during the peak flow, lowering the water-surface elevation considerably, as seen in figure 23.

Thalweg elevations predicted by HEC2SR are shown in figure 24 together with field data acquired by the County of San Diego, California, in June 1981 (see table 18). The field data indicate that sand-mining pits were completely filled during the 1980 flood. HEC2SR predicted scour along the lower part of the study reach, downstream from the bridge, and stable river-bed patterns for the upper reach. On the other hand, UUWSR predicted a generally aggrading

SAN DIEGUITO RIVER: HEC2SR

ID	X	YO	YF	Y	H	W	Q	V	QB	QS	QT	DSO
	FT	FT	FT	FT	FT	FT	CFS	FPS	T/D	T/D	T/D	MM
43	0	14.5	11.1	12.0	26.1	601	22000	10.6	20070	183930	204000	0.58
44	800	23.6	22.6	22.9	30.0	736	22000	6.5	20070	183930	204000	0.58
45	1610	16.8	13.7	14.5	31.4	1009	22000	4.6	20070	183930	204000	0.58
46	2310	23.6	18.8	20.0	32.2	563	22000	10.3	20070	183930	204000	0.58
47	2790	19.7	15.5	16.7	33.6	326	22000	9.7	20070	183930	204000	0.58
48	3190	13.7	11.9	12.6	35.9	765	22000	2.8	5660	48280	53940	0.86
49	3440	18.2	15.1	16.3	35.9	467	22000	5.4	5660	48280	53940	0.86
50	3600	18.8	12.4	14.7	35.7	170	22000	11.6	5660	48280	53940	0.86
50.1	3780	25.0	15.1	17.5	38.4	317	22000	5.5	2680	21190	23870	0.91
51.1	3805	25.0	14.5	17.2	38.4	307	22000	5.8	2680	21190	23870	0.91
52	3930	10.9	16.5	11.8	39.0	474	22000	3.0	250	3570	3820	0.38
53	4350	13.3	14.8	13.5	39.2	1143	22000	1.2	250	3570	3820	0.38
54	4950	17.5	18.4	18.6	39.2	940	22000	2.2	4200	38700	42900	0.50
55	5460	22.7	24.9	25.0	39.1	616	22000	5.3	4200	38700	42900	0.50
56	6060	25.7	27.2	27.0	39.7	438	22000	5.2	4200	38700	42900	0.50
57	6590	27.2	27.6	27.5	40.0	294	22000	7.7	15560	164950	180510	0.57
58	7260	27.0	27.4	27.3	41.3	551	22000	4.0	15560	164950	180510	0.57
59	7770	27.8	28.5	28.3	41.2	230	22000	10.5	15560	164950	180510	0.57
60	8290	33.4	33.4	33.4	44.5	516	22000	11.3	14480	179730	194210	0.59
61	8870	37.3	37.3	37.3	50.8	493	22000	6.4	14480	179730	194210	0.59
62	9370	40.5	40.5	40.5	52.2	493	22000	5.0	14480	179730	194210	0.59
63	9820	40.9	40.9	40.9	52.9	507	22000	5.1	14480	179730	194210	0.59

ID=SECTION I.D.
X =RIVER DISTANCE
YO=INITIAL THALWEG EL
YF=FINAL THALWEG EL
Y =THALWEG EL AT PEAK FLOW
H =W.S. EL AT PEAK FLOW
W =TOP WIDTH AT PEAK FLOW

Q =WATER DISCHARGE AT PEAK FLOW
V =MEAN VELOCITY AT PEAK FLOW
QB =BED-LOAD DISCHARGE AT PEAK FLOW
QS =SUS-LOAD DISCHARGE AT PEAK FLOW
QT =TOTAL-LOAD DISCHARGE AT PEAK FLOW
DSO=MEDIAN DIAMETER OF BED MATERIAL AT PEAK FLOW

Table 15 Principal results computed by HEC2SR for the San Dieguito River

SAN DIEGUITO RIVER: FLUVIAL-11

ID	X	Y0	YF	Y	H	H1	W	Q	V	QB	QS	QT	D50
	FT	FT	FT	FT	FT	FT	FT	CFS	FPS	T/D	T/D	T/D	MM
43	0	18.0	18.0	18.0	31.1	31.2	963	22000	4.0	-	-	366360	0.25
44	800	23.6	20.6	18.4	31.7	31.6	787	22000	4.3	-	-	373270	0.25
45	1610	16.8	23.5	26.3	32.5	32.4	1166	22000	3.8	-	-	396320	0.24
46	2310	23.6	25.6	22.5	33.1	32.9	857	22000	4.4	-	-	518590	0.25
47	2790	19.7	26.2	20.5	33.5	36.4	491	22000	5.5	-	-	637080	0.28
48	3190	13.7	26.4	24.7	33.9	36.8	482	22000	5.5	-	-	645830	0.25
49	3440	18.2	26.4	23.2	34.0	36.8	359	22000	6.2	-	-	719270	0.27
50	3600	18.0	26.5	21.1	34.1	36.8	266	22000	6.9	-	-	811580	0.27
51	3780	25.0	27.1	23.1	34.5	37.2	345	22000	5.8	-	-	902600	0.27
52	3925	10.9	26.9	24.9	34.7	40.5	439	22000	6.0	-	-	896690	0.27
53	4345	13.3	27.3	29.8	35.4	40.8	829	22000	5.1	-	-	960950	0.28
54	4945	17.5	29.3	30.3	36.5	40.9	758	22000	5.5	-	-	1189820	0.33
55	5455	22.7	30.4	27.7	37.4	41.0	644	22000	6.1	-	-	1377560	0.37
56	6055	25.7	31.6	31.1	38.4	41.2	452	22000	7.0	-	-	1491140	0.43
57	6585	27.2	32.4	30.9	39.4	41.4	346	22000	7.8	-	-	1502880	0.47
58	7255	27.0	33.4	34.4	41.0	42.3	451	22000	7.6	-	-	1828820	0.53
59	7765	27.8	35.5	34.8	42.5	42.4	501	22000	7.5	-	-	1860140	0.58
60	8285	33.4	37.7	37.1	44.1	44.5	536	22000	7.4	-	-	1861060	0.64
61	8865	37.3	39.2	40.4	46.0	49.6	517	22000	7.9	-	-	2251690	0.74
62	9365	40.5	41.2	40.9	47.7	51.0	442	22000	8.3	-	-	2088720	0.79
63	9815	40.9	40.9	40.9	49.4	51.7	444	22000	8.5	-	-	2344990	0.85

ID=SECTION I.D.
X =RIVER DISTANCE
Y0=INITIAL THALWEG EL
YF=FINAL THALWEG EL
Y =THALWEG EL AT PEAK FLOW
H =W.S. EL AT PEAK FLOW
H1=W.S. EL AT PEAK FLOW (HEC-2)
W =TOP WIDTH AT PEAK FLOW
NOTE: QB & QS WERE NOT COMPUTED WITH FLUVIAL-11

Q = WATER DISCHARGE AT PEAK FLOW
V = MEAN VELOCITY AT PEAK FLOW
QB = BED-LOAD DISCHARGE AT PEAK FLOW
QS = SUS-LOAD DISCHARGE AT PEAK FLOW
QT = TOTAL-LOAD DISCHARGE AT PEAK FLOW
D50= MEDIAN DIAMETER OF BED MATERIAL AT PEAK FLOW

Table 16 Principal results computed by FLUVIAL-11 for the San Dieguito River

SAN DIEGUITO RIVER: SEDIMENT-4H

ID	X	Y0	YF	Y	H	H1	W	Q	V	QT	DS0
	FT	FT	FT	FT	FT	FT	FT	CFS	FPS	T/D	MM
43	600	21.9	21.7	21.8	29.9	29.9	846	22100	5.1	2670	0.46
44	1400	24.1	24.0	24.1	30.6	30.6	818	22100	5.5	2760	0.46
45	2210	25.0	24.8	25.0	31.4	31.4	1165	22100	5.1	3100	0.46
46	2910	25.0	23.8	24.6	32.7	32.8	488	22100	8.7	4150	0.46
47	3390	23.0	23.8	23.1	33.7	34.0	693	22100	4.7	3670	0.46
48	3790	21.6	21.2	21.9	33.8	34.1	690	22100	3.2	3130	0.46
49	4040	22.9	22.4	22.8	33.9	34.2	415	22100	7.1	3430	0.46
50	4200	24.4	22.9	24.1	34.2	34.5	237	22100	9.0	3940	0.46
51	4380	24.4	20.2	22.4	34.6	35.3	283	22100	9.6	4290	0.46
52	4530	20.6	21.0	20.9	34.8	35.9	523	22100	3.8	3140	0.46
53	4950	18.2	19.0	18.7	34.8	35.9	944	22099	1.8	1543	0.46
54	5550	21.2	22.7	21.2	34.8	36.0	1066	22099	3.0	2550	0.46
55	6060	24.9	20.3	24.6	35.3	36.3	313	22100	8.6	3920	0.46
56	6600	26.9	28.9	27.0	35.9	36.7	544	22099	5.6	3790	0.46
57	7190	27.2	27.2	27.1	36.8	37.3	325	22100	9.3	3700	0.46
58	7860	27.8	30.5	28.1	37.7	38.1	470	22100	6.1	3980	0.46
59	8370	28.9	31.1	28.3	38.8	39.3	193	22100	12.2	4260	0.70
60	8890	34.1	33.0	34.0	45.9	46.1	495	22100	10.6	4680	0.70
61	9470	39.6	40.6	40.1	52.2	52.0	625	22100	4.9	5130	0.70
62	9920	41.0	41.9	41.6	52.5	52.2	544	22100	5.2	7460	0.70
63	10420	41.1	41.3	41.2	52.7	52.4	542	22100	5.0	9780	0.70

ID=SECTION ID
X =RIVER DISTANCE
Y0=INITIAL THALWEG EL
YF=FINAL THALWEG EL
Y =THALWEG EL AT PEAK FLOW
H =W.S. EL AT PEAK FLOW
H1=W.S. EL AT PEAK FLOW COMPUTED USING FIXED-BED FLOOD-ROUTING MODEL
W = TOP WIDTH AT PEAK FLOW
Q = WATER DISCHARGE AT PEAK FLOW
V = MEAN VELOCITY AT PEAK FLOW
QT = TOTAL-LOAD DISCHARGE AT PEAK FLOW
DS0= MEDIAN SIZE OF BED MATERIAL AT PEAK FLOW
NOTE: RESULTS SHOWN ARE FOR ENTIRE CROSS-SECTION OF MAIN AND OVERBANK CHANNELS

Table 17 Principal results computed by SEDIMENT-4H for the San Dieguito River

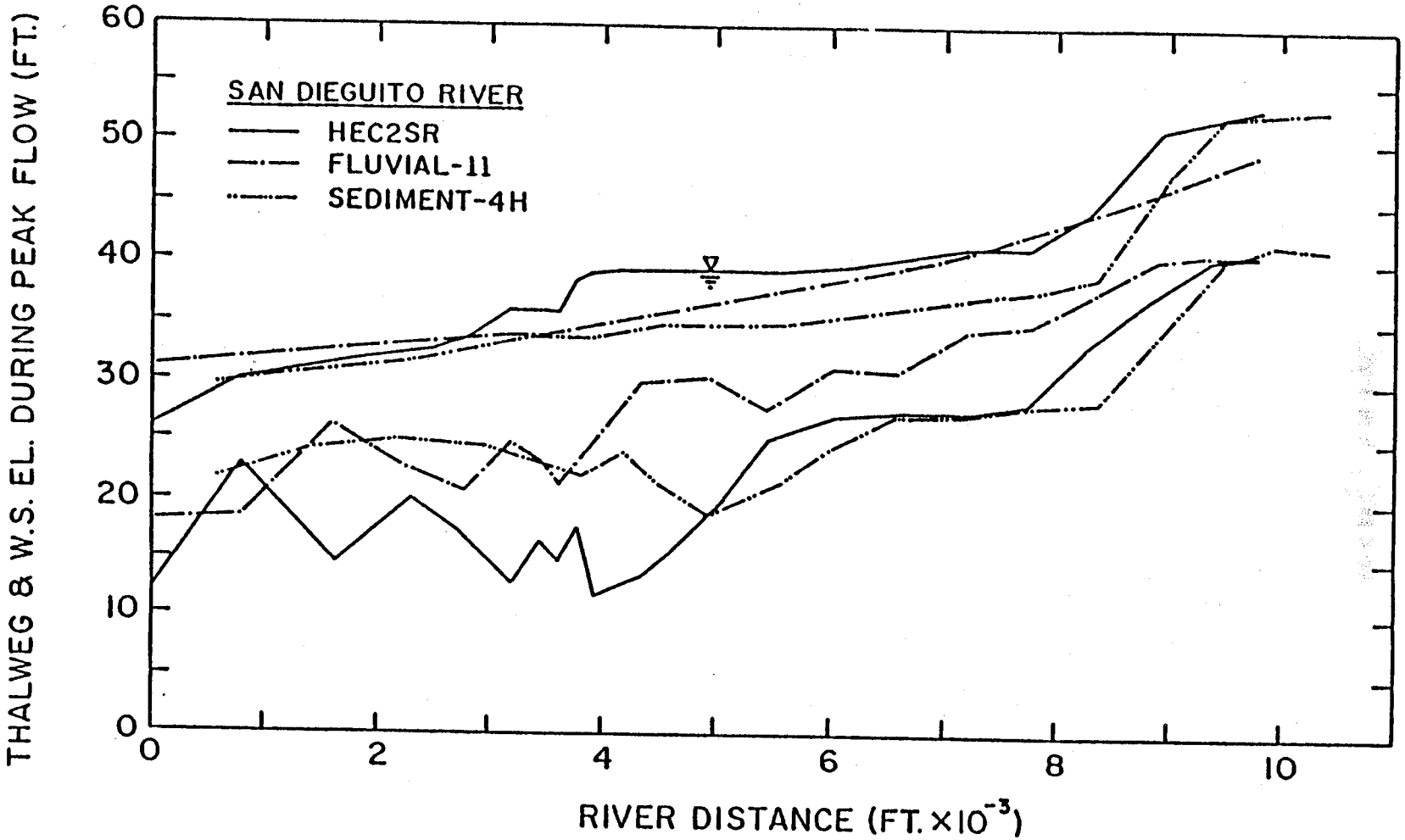

Figure 21 Comparison of thalweg and water-surface profiles at peak flow computed using the HEC2SR, FLUVIAL-11, and SEDIMENT-4H movable-bed models for the San Dieguito River

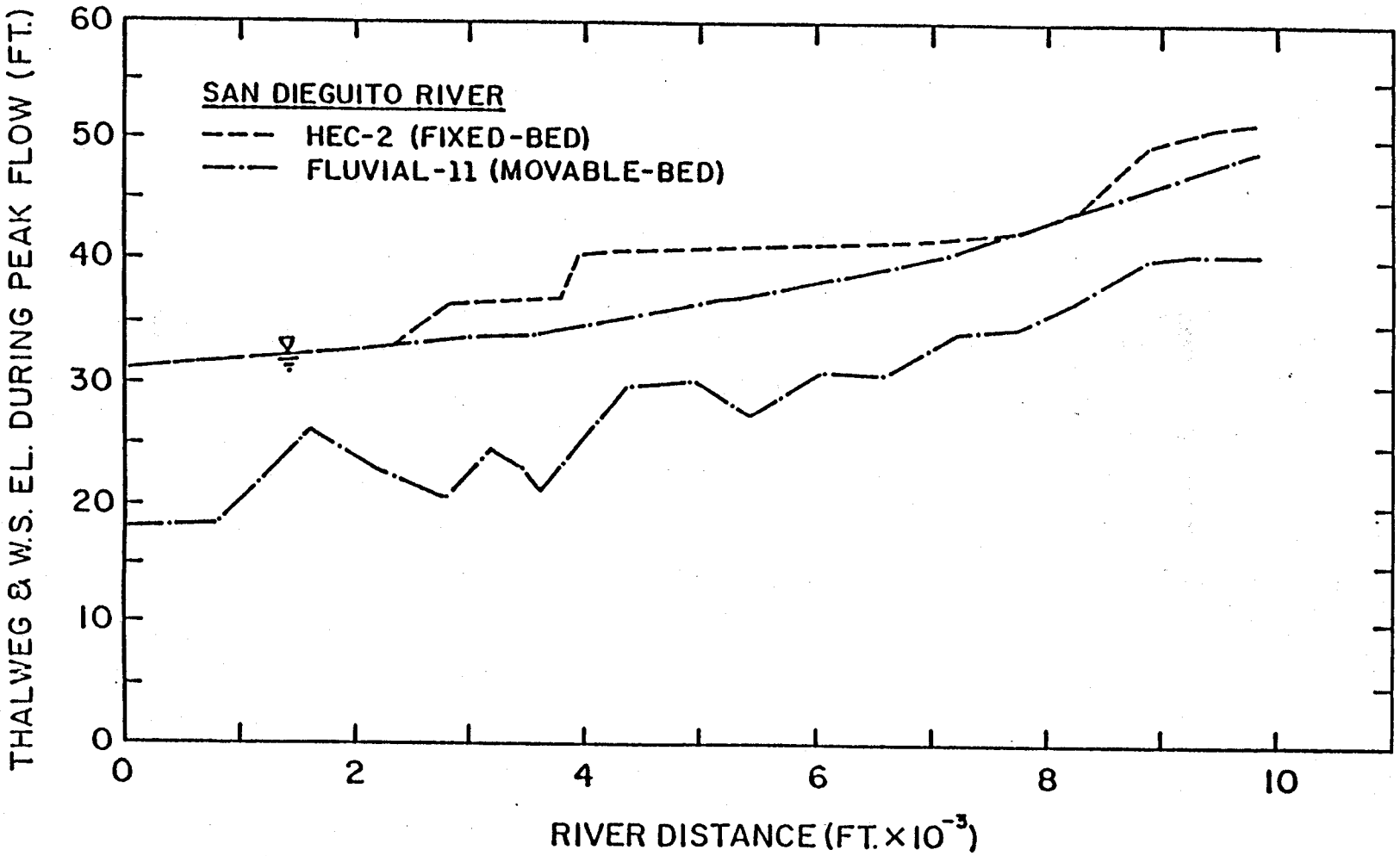

Figure 22 Comparison of water-surface profiles at peak flow computed by SDSU using HEC-2 and FLUVIAL-11 for the San Dieguito River

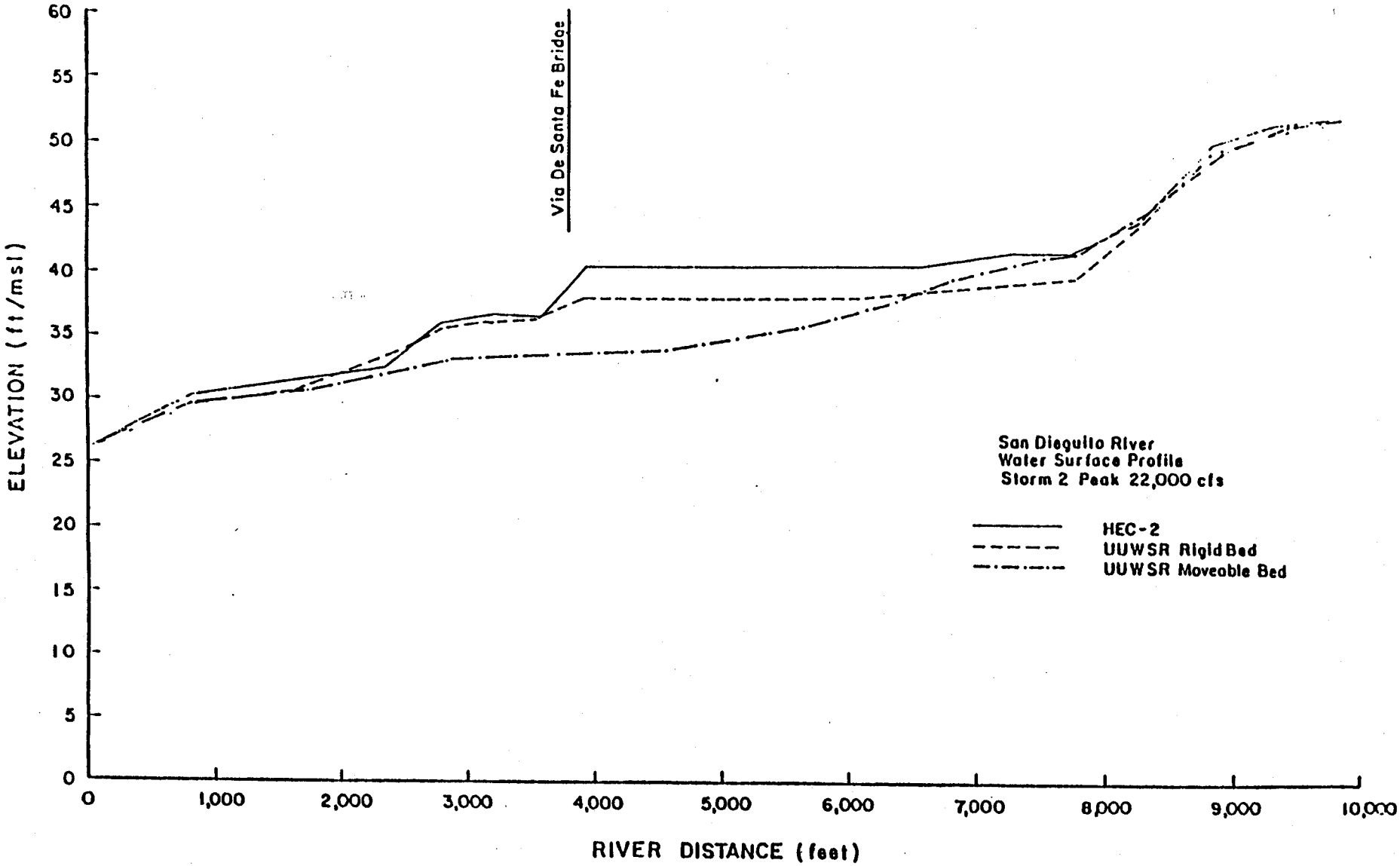

Figure 23 Comparison of water-surface profiles at peak flow computed by SLA using HEC-2, and the UUWSR fixed-bed and movable-bed models for the San Dieguito River

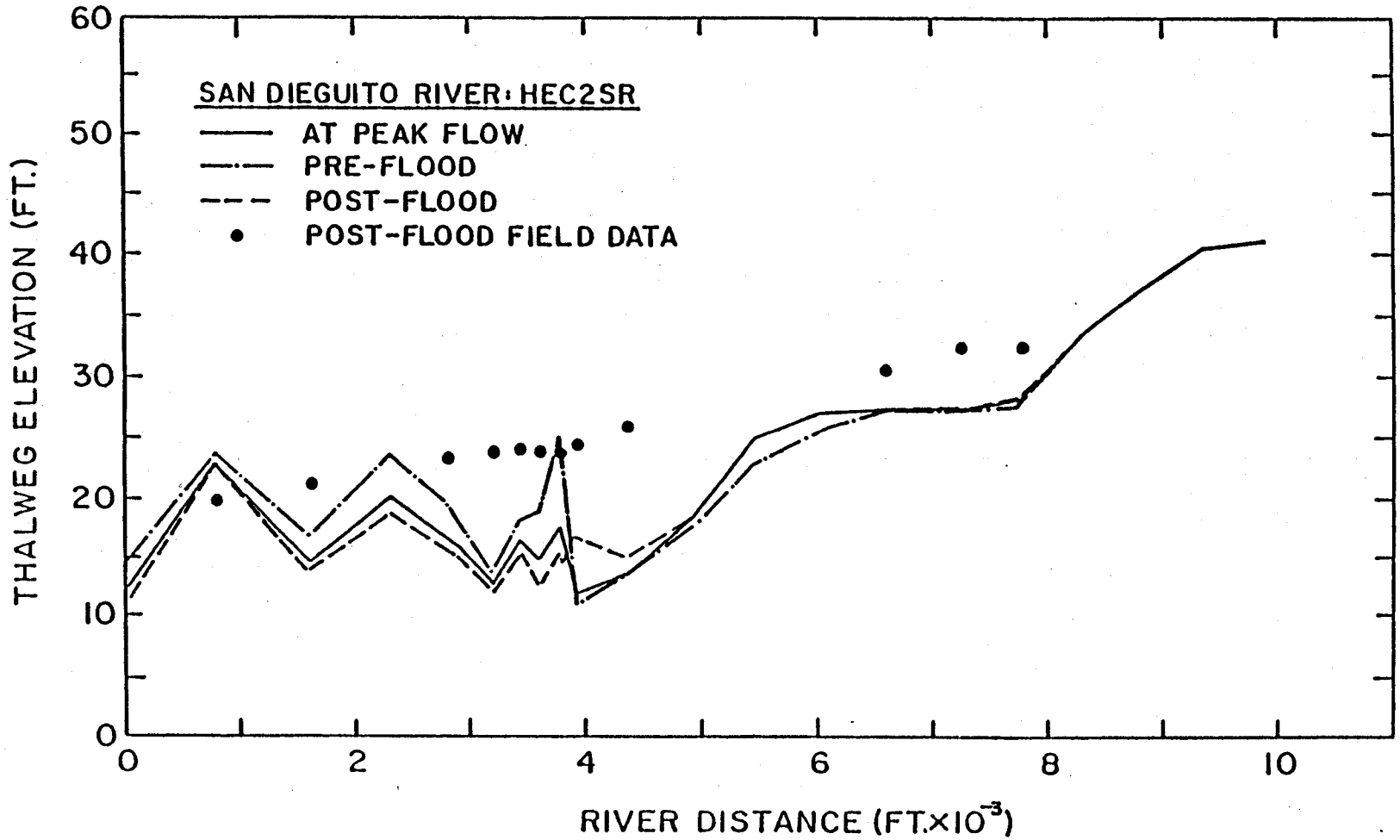

Figure 24 Thalweg profiles predicted by SLA using HEC2SR for the San Dieguito River

SAN DIEGUITO RIVER

X-SECTION ID	RIVER DISTANCE	OBSERVED THALWEG ELEVATION
	FT	FT
44	800	19.9
45	1610	21.4
47	2790	23.3
48	3190	23.8
49	3440	24.1
50	3600	23.8
50.1	3780	23.9
52	3930	24.4
53	4350	26.0
57	6590	30.4
58	7260	32.4
59	7770	32.4

NOTE: CROSS-SECTION DATA SHOWN WERE OBTAINED IN JUNE 1981 BY DEPARTMENT OF PUBLIC WORKS, COUNTY OF SAN DIEGO, CALIFORNIA.

THE HIGHEST WATER-SURFACE ELEVATION OBSERVED AT SECTION 52 (X = 3,930 FT) OF THE SAN DIEGUITO RIVER WAS APPROXIMATELY 36 FT ABOVE MSL.

Table 18 Thalweg elevations measured in June 1981 for the San Dieguito River

channel over the entire study reach, as seen in figure 25. FLUVIAL-11 predictions, shown in figure 26, indicate general deposition throughout the reach. It should be pointed out that FLUVIAL-11 allows for bank erosion, so variable river width is incorporated into the model, while UUWSR considers changes in cross-section profile for a fixed river width. Figure 27 shows the thalweg elevations predicted by SEDIMENT-4H. These profiles were plotted using output-summary tables submitted by RMA. As seen in the figure, the pre-flood, initial thalweg profile does not conform to the input data supplied to RMA (compare figure 27 with figure 24 or 26, for example, for the initial thalweg profile). It must be pointed out that because of RMA's failure to respond to requests for clarification, the results from SEDIMENT-4H presented in this report are based entirely on RMA's output summaries submitted to the Committee, and no modification or adjustment of their tabulated values could be made in spite of the fact that inconsistencies between the summarized values and computer output listings were detected and brought to their attention.

Longitudinal distributions of the mean flow velocity predicted by the HEC2SR, FLUVIAL-11, and SEDIMENT-4H movable-bed models are shown in figure 28. FLUVIAL-11 predicted gradual changes in the mean flow velocity between 3.8 ft/s and 8.5 ft/s; however, HEC2SR's predictions are seen to vary abruptly from cross section to cross section, with a variation range of 1.2 ft/s to 11.6 ft/s (see tables 15 and 16). The range of variation predicted by SEDIMENT-4H is seen to be between -1.8 ft/s and 12.2 ft/s (see table 17). Longitudinal variations of the water-surface width during the flood peak are presented in figure 29, in which the three models are seen to yield quite different results.

Table 19 lists total-load discharges during the peak flow and post-flood median bed-material sizes predicted by HEC2SR, FLUVIAL-11, and SEDIMENT-4H. The total-load predictions differ widely among these three models, as seen in figure 30. RMA's results were not included in the figure because of their small values. FLUVIAL-11 predicted extremely high total-load discharges with an almost linearly increase along the study reach. At a river distance of 9,815 ft, the total-load discharges predicted by HEC2SR, FLUVIAL-11, and SEDIMENt-4H were approximately 194,000 tons/day, 2,345,000 tons/day, and 7,

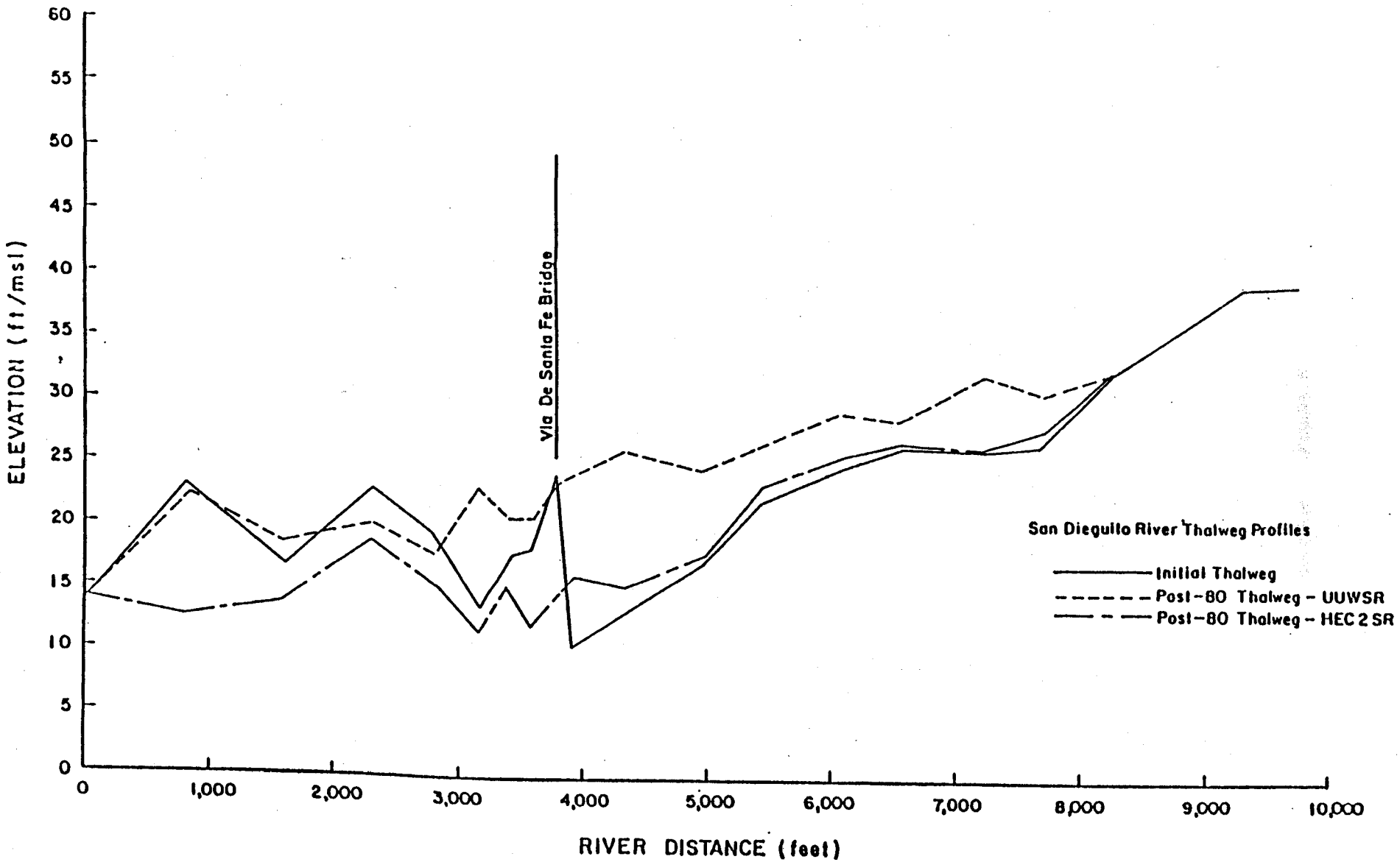

Figure 25 Comparison of post-flood thalweg profiles computed by SLA using UUWSR and HEC2SR for the San Dieguito River

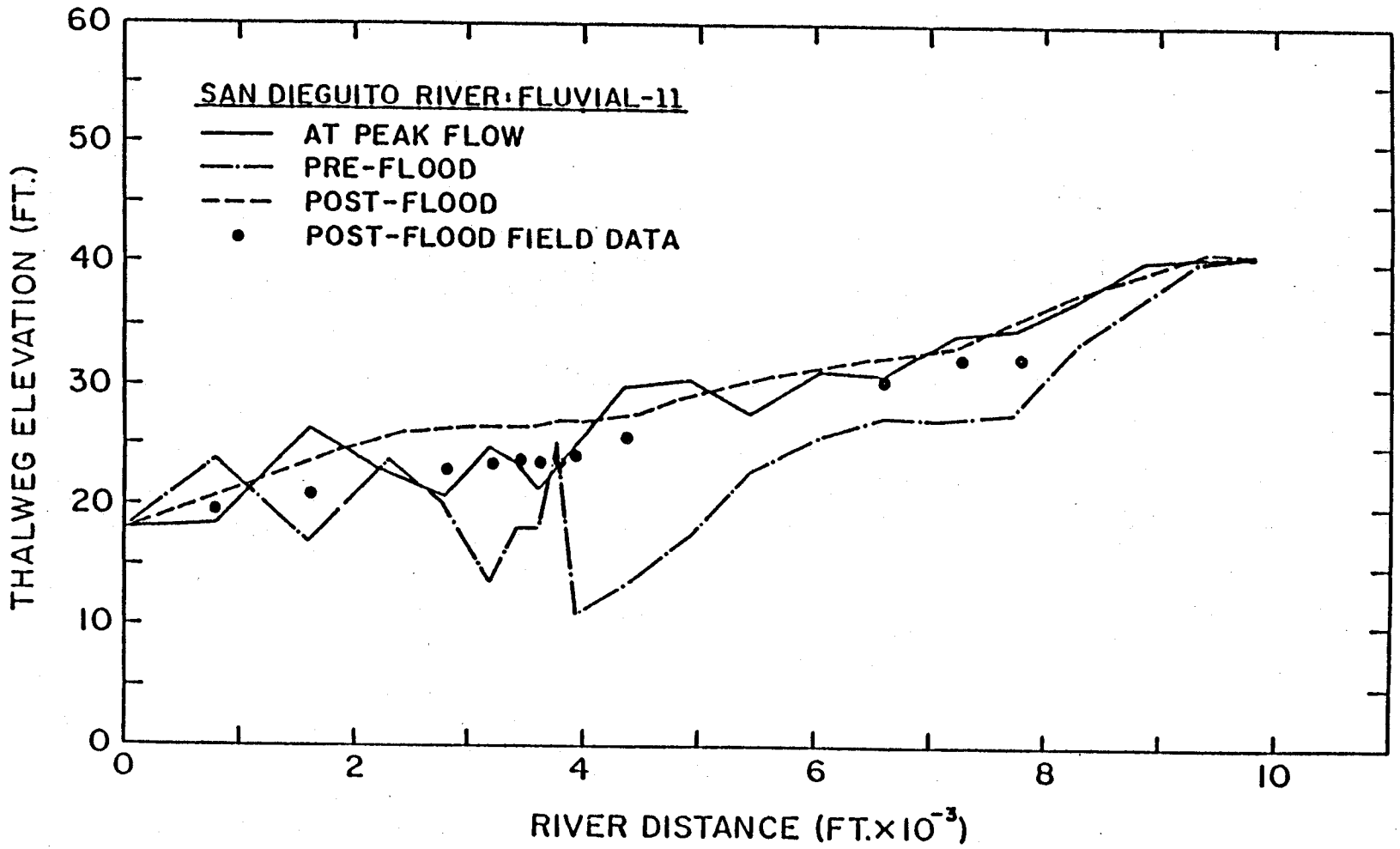

Figure 26 Thalweg profiles predicted by SDSU using FLUVIAL-11 for the San Dieguito River

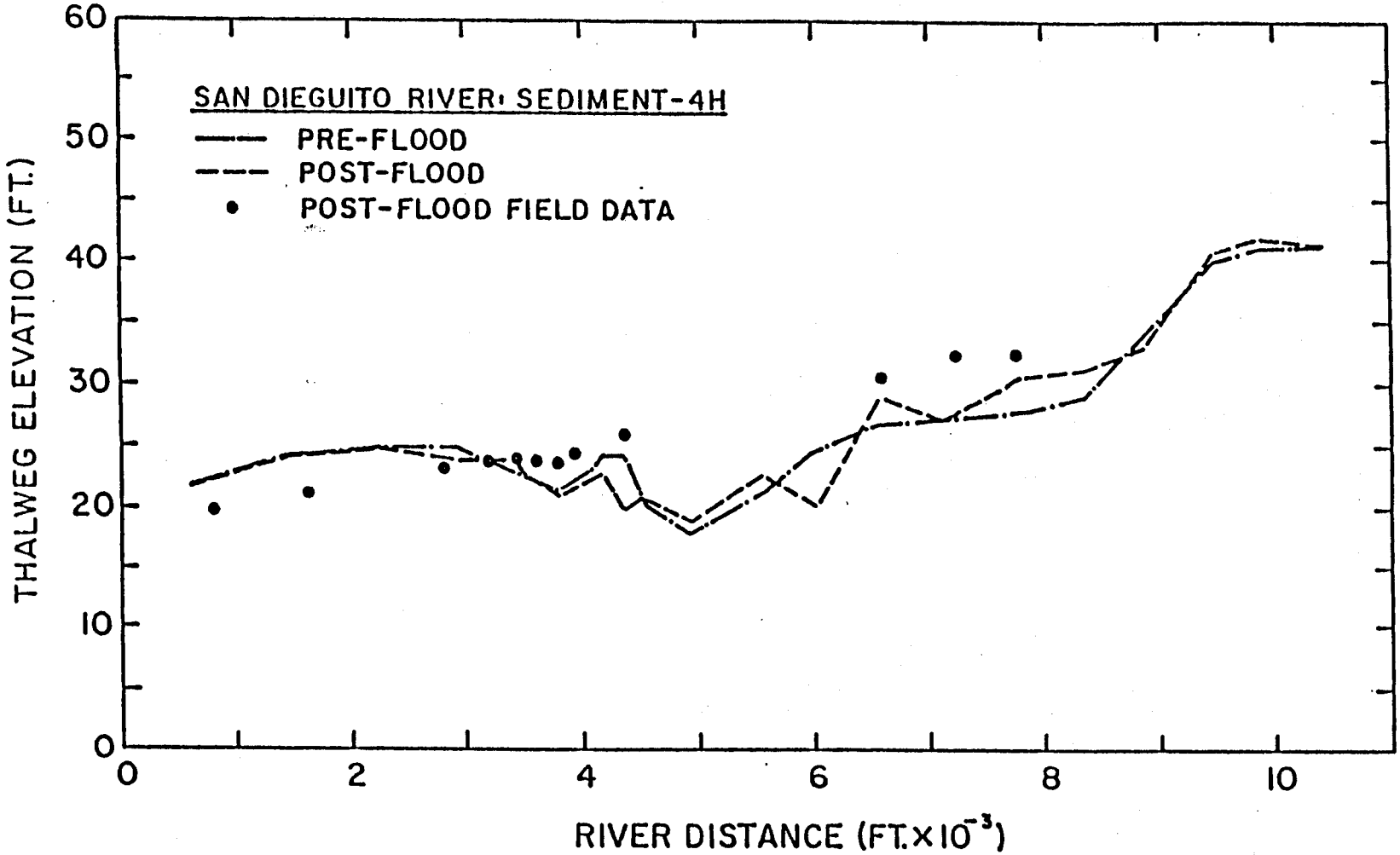

Figure 27 Thalweg profiles predicted by RMA using SEDIMENT-4H for the San Dieguito River

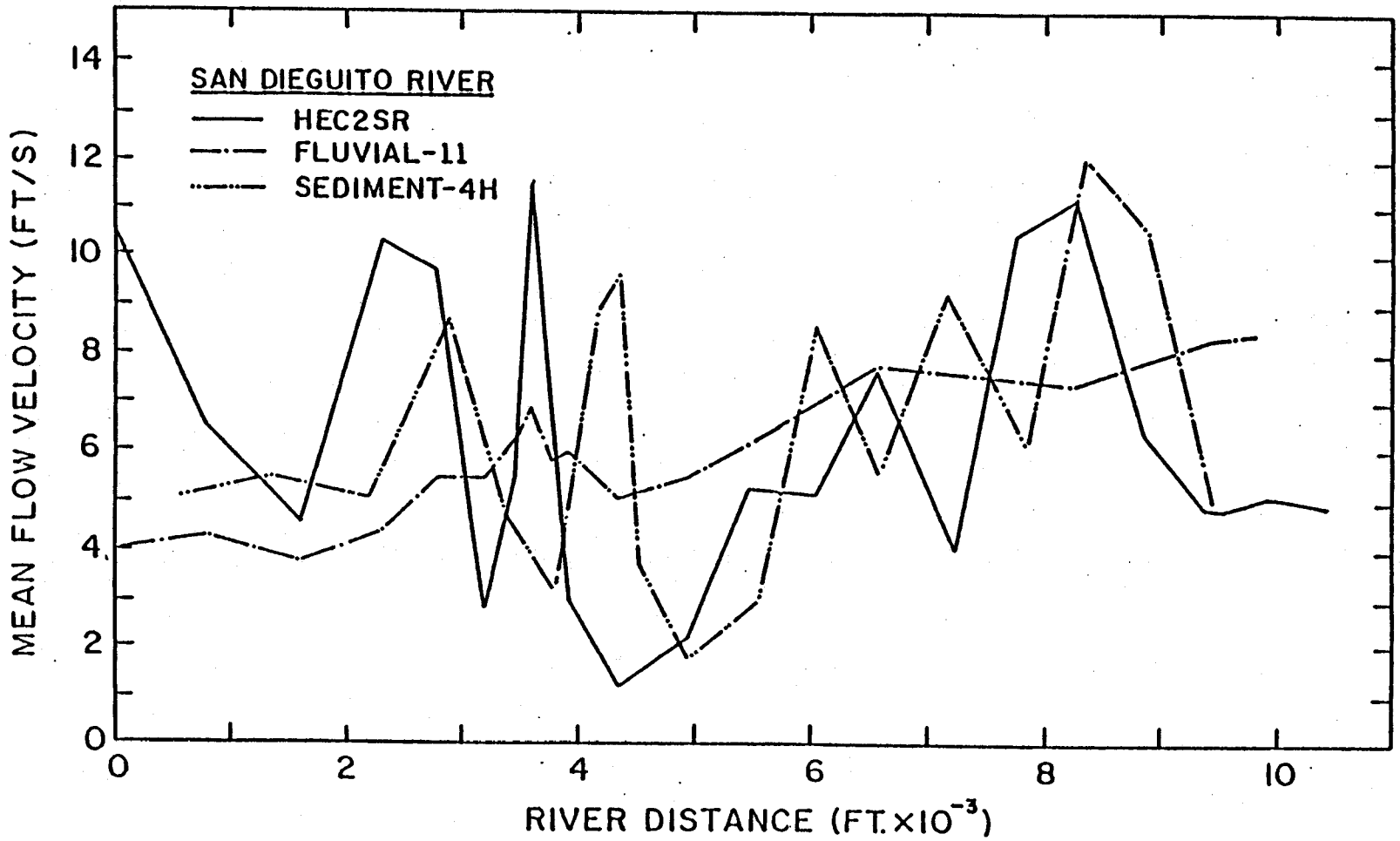

Figure 28 Longitudinal distributions of mean flow velocity at peak flow computed using the HEC2SR, FLUVIAL-11, and SEDIMENT-4H movable-bed models for the San Dieguito River

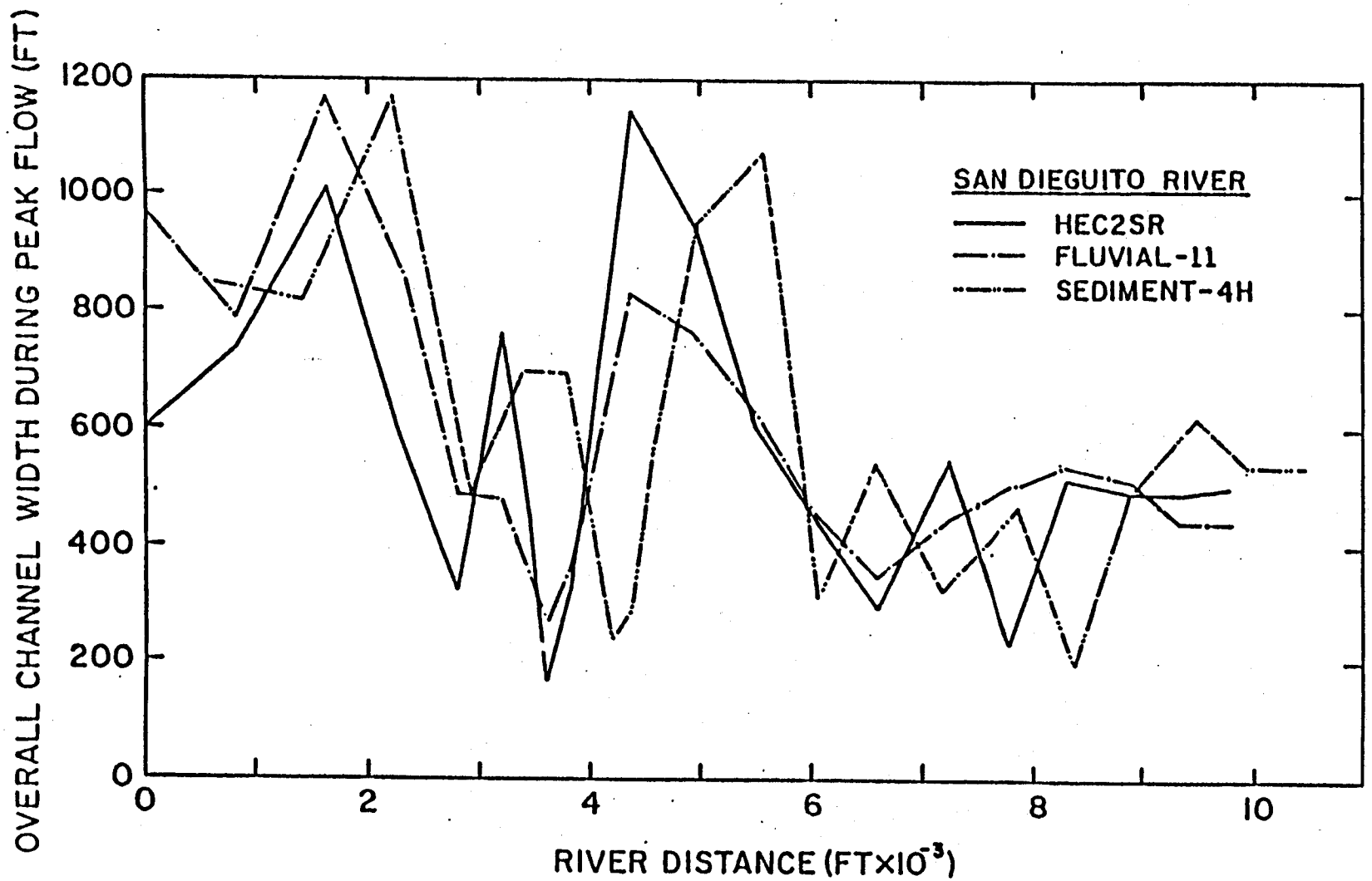

Figure 29 Water-surface widths at peak flow predicted by the HEC2SR, FLUVIAL-11, and SEDIMENT-4H movable-bed models for the San Dieguito River

SAN DIEGUITO RIVER			(FLUVIAL-11)		(HEC2SR)		(SEDIMENT-4H)		
ID	X	D50I	QT	D50F	QT	D50F	X	QT	D50F
	FT	MM	T/D	MM	T/D	MM	FT	T/D	MM
43	0	-	366360	0.23	204000	0.87	600	2670	0.46
44	800	0.46	373270	0.25	204000	0.87	1400	2760	0.46
45	1610	-	396320	0.25	204000	0.87	2210	3100	0.46
46	2310	-	518590	0.25	204000	0.87	2910	4150	0.46
47	2790	-	637080	0.25	204000	0.87	3390	3670	0.46
48	3190	-	645830	0.26	53940	0.92	3790	3130	0.46
49	3440	-	719270	0.27	53940	0.92	4040	3430	0.46
50	3600	-	811580	0.28	53940	0.92	4200	3940	0.46
51	3780	-	902600	0.28	23870	1.04	4380	4290	0.46
52	3925	-	896690	0.28	3820	0.30	4530	3140	0.46
53	4345	-	960950	0.30	3820	0.30	4950	1543	0.46
54	4945	-	1189820	0.33	42900	0.53	5550	2550	0.46
55	5455	-	1377560	0.36	42900	0.53	6060	3920	0.46
56	6055	-	1491140	0.40	42900	0.53	6600	3790	0.46
57	6585	-	1502880	0.46	180510	0.55	7190	3700	0.46
58	7255	-	1828820	0.54	180510	0.55	7860	3980	0.46
59	7765	0.70	1860140	0.58	180510	0.55	8370	4260	0.70
60	8285	-	1861060	0.58	194210	0.59	8890	4680	0.70
61	8065	-	2251690	0.67	194210	0.59	9470	5130	0.70
62	9365	-	2088720	0.81	194210	0.59	9920	7460	0.70
63	9815	-	2344990	0.85	194210	0.59	10420	9780	0.70

ID = SECTION I.D.
X = RIVER DISTANCE
D50I = INITIAL MEDIAN SIZE OF BED MATERIAL (PRE-FLOOD)
D50F = FINAL MEDIAN SIZE OF BED MATERIAL (POST-FLOOD)
QT = TOTAL-LOAD DISCHARGE AT PEAK-FLOW DISCHARGE OF 22,000 CFS

Table 19 Total-load discharges at peak flow and final median bed-material sizes computed by HEC2SR, FLUVIAL-11, and SEDIMENT-4H for the San Dieguito River

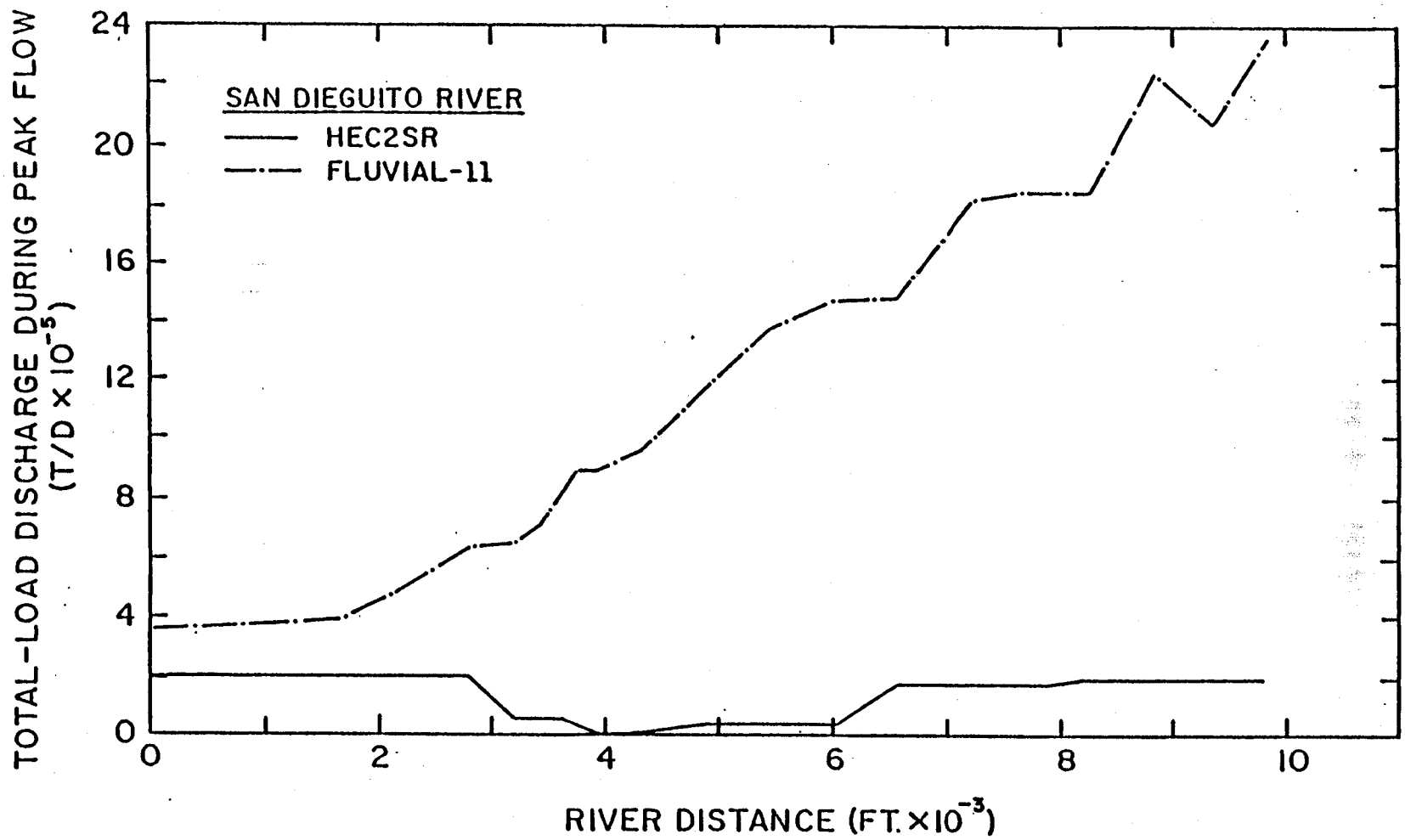

Figure 30 Total-load discharges at peak flow predicted by HEC2SR and FLUVIAL-11 for the San Dieguito River

tons/day, respectively; these values for a peak discharge of 22,000 cfs correspond to sediment concentrations of approximately 3,270 mg/l, 39,480 mg/l, and 120 mg/l, respectively. Longitudinal distributions of the median bed-material size at peak flow are shown in figure 31. Thalweg and water-surface elevations predicted by these three movable-bed models for the rising and falling limbs of the hydrograph are tabulated in tables 20, 21, and 22. During the falling stage, at a discharge of approximately 12,000 cfs, HEC2SR predicted generally much higher water-surface elevations, as seen in tables 20 and 21.

3. Salt River. Four movable-bed models, HEC2SR, HEC-6, FLUVIAL-11, and SEDIMENT-4H, were used to simulate a 100-yr flood with a peak discharge of 176,000 cfs; the principal hydraulic and sediment-transport parameters computed are summarized in tables 23, 24, 25, and 26, respectively. Note that additional water-surface elevations predicted by SDSU and RMA using the HEC-2 and SEDIMENT-4H fixed-bed models are also listed in tables 25 and 26, respectively. The peak-flow thalweg and water-surface elevations predicted by these four models are presented in figure 32. HEC2SR is seen to predict somewhat lower water-surface elevations in the middle reach than the other three models. At a river distance of 10,120 ft, the difference of the water-surface elevations between HEC2SR and FLUVIAL-11 amounts to 2.2 ft. Water-surface profiles predicted by HEC-6, FLUVIAL-11, and SEDIMENT-4H are seen to be similar to each other, while their thalweg-elevation predictions are quite different. As seen in tables 23 and 25, HEC2SR predicted a general trend of scour over the entire reach, while FLUVIAL-11 predicted deposition. Thalweg elevations predicted by HEC-6 and SEDIMENT-4H seem to fall between those of HEC2SR and FLUVIAL-11. At a river distance of 12,150 ft, FLUVIAL-11 predicted a thalweg elevation 9 ft higher than that of HEC2SR; however, the water-surface elevation predicted by FLUVIAL-11 was higher by only 1.8 ft. Similarly, at a river distance of 15,500 ft, the thalweg elevation obtained from FLUVIAL-11 was 11 ft higher than that computed by HEC2SR, but the water-surface elevations predicted by those models were almost identical (see tables 23 and 25). It should be pointed out that overall changes in thalweg elevations predicted by HEC2SR conformed quite well to those observed in the CSU movable-bed physical model (Anderson-Nichols, 1980) at a prototype discharge of 210,000 cfs.

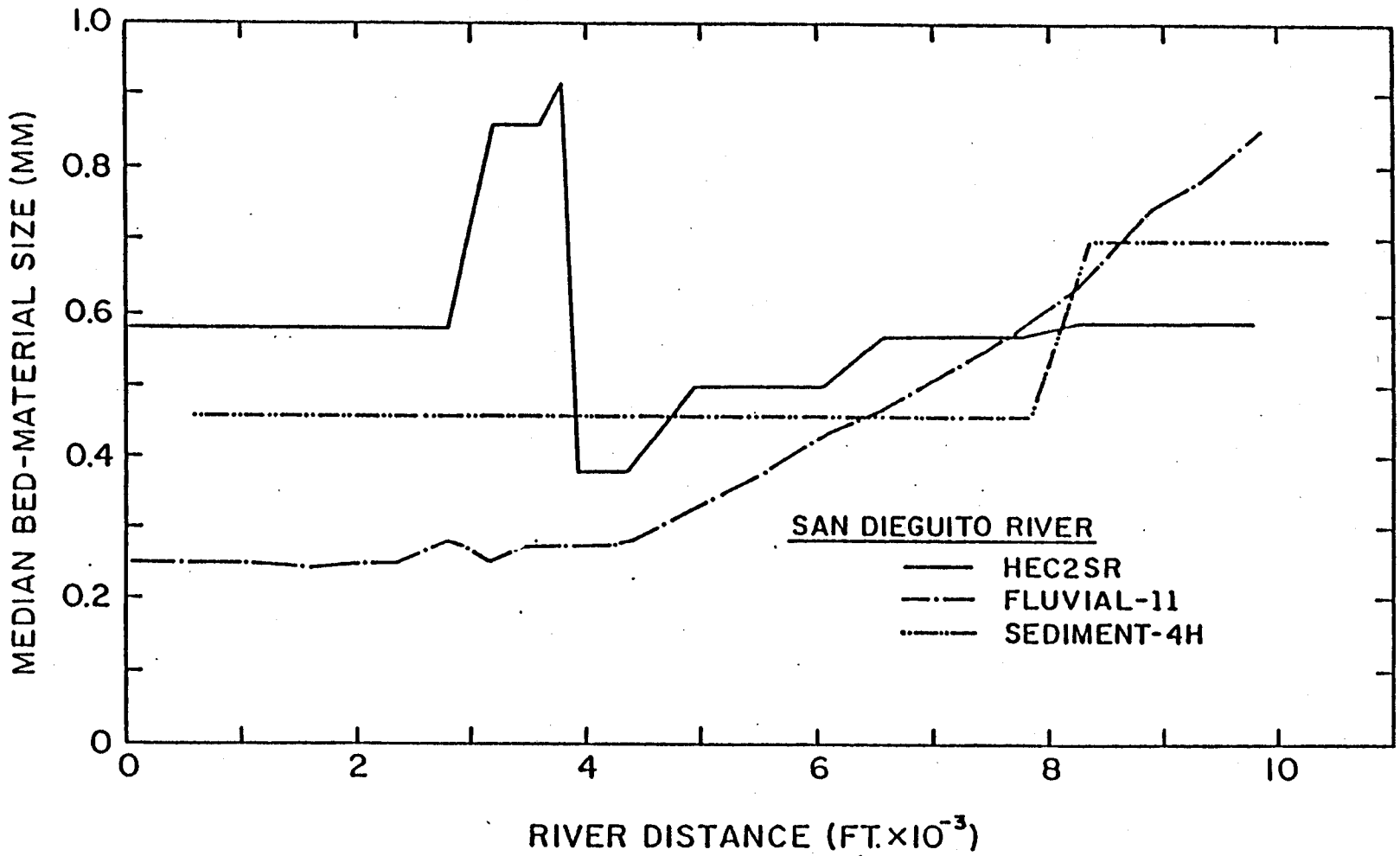

Figure 31 Longitudinal distributions of median bed-material size at peak flow computed using HEC2SR, FLUVIAL-11, and SEDIMENT-4H for the San Dieguito River

SAN DIEGUITO RIVER: HEC2SR

ID	X	YR	HR	YFA	HFA
	FT	FT	FT	FT	FT
43	0	13.6	23.2	11.2	24.3
44	800	23.4	27.1	22.6	28.1
45	1610	15.8	28.1	13.9	29.4
46	2310	22.1	29.0	19.0	30.2
47	2790	18.8	30.3	15.7	31.4
48	3190	13.9	30.7	11.9	32.3
49	3440	18.7	30.7	15.1	32.3
50	3600	19.6	30.7	12.5	32.3
50.1	3780	21.8	31.3	15.2	33.4
51.1	3805	21.8	31.3	14.6	33.4
52	3930	11.1	31.9	14.9	33.7
53	4350	13.4	31.9	14.4	33.9
54	4950	17.8	31.9	18.9	33.9
55	5460	23.2	31.9	25.7	34.2
56	6060	25.9	32.7	27.5	37.1
57	6590	27.3	33.1	27.6	37.4
58	7260	27.1	33.9	27.4	38.2
59	7770	27.9	34.0	28.4	38.2
60	8290	33.4	41.9	33.4	43.2
61	8070	37.3	46.6	37.3	48.7
62	9370	40.5	47.4	40.5	49.8
63	9820	40.9	47.7	40.9	50.3

ID =SECTION I.D.
X =RIVER DISTANCE
YR =THALWEG EL AT Q=5,000 CFS (RISING STAGE)
HR =W.S. EL AT Q=5,000 CFS (RISING STAGE)
YFA=THALWEG EL AT Q=12,000 CFS (FALLING STAGE)
HFA=W.S. EL AT Q=12,000 CFS (FALLING STAGE)

Table 20 Thalweg and water-surface elevations during rising and falling stages computed by HEC2SR for the San Dieguito River

SAN DIEGUITO RIVER: FLUVIAL-11

ID	X	YR	HR	YFA	HFA
	FT	FT	FT	FT	FT
43	0	18.0	25.7	18.0	27.8
44	800	19.2	26.8	20.5	28.9
45	1610	20.1	27.8	26.1	30.2
46	2310	20.1	28.5	24.6	31.2
47	2790	19.7	29.0	25.8	31.7
48	3190	19.0	29.2	25.5	32.2
49	3440	18.5	29.2	25.6	32.4
50	3600	18.5	29.3	25.6	32.6
51	3780	18.6	29.5	26.2	32.9
52	3925	10.9	29.7	26.6	33.0
53	4345	23.0	29.8	28.9	33.8
54	4945	24.6	29.8	29.6	34.9
55	5455	23.8	30.4	30.8	35.8
56	6055	27.9	31.7	31.3	36.9
57	6585	28.9	32.9	32.5	37.9
58	7255	29.9	34.9	34.7	39.5
59	7765	33.1	36.5	36.4	40.8
60	8285	35.6	38.5	37.8	42.2
61	8865	37.4	40.8	38.8	43.7
62	9365	39.5	43.1	41.3	45.5
63	9815	40.9	45.3	40.9	47.4

ID=SECTION I.D.
X =RIVER DISTANCE
YR =THALWEG EL AT Q=4,695 CFS (RISING STAGE)
HR =W.S. EL AT Q=4,695 CFS (RISING STAGE)
YFA=THALWEG EL AT Q=12,180 CFS (FALLING STAGE)
HFA=W.S. EL AT Q=12,180 CFS (FALLING STAGE)

Table 21 Thalweg and water-surface elevations during rising and falling stages computed by FLUVIAL-11 for the San Dieguito River

SAN DIEGUITO RIVER:SEDIMENT-4H

ID	X	YR	HR	YFA	HFA
	FT	FT	FT	FT	FT
43	600	20.0	26.1	19.9	28.2
44	1400	22.7	27.0	22.7	29.0
45	2210	23.6	28.0	23.5	29.9
46	2910	23.3	28.9	22.0	30.9
47	3390	20.1	29.6	20.2	31.6
48	3790	17.7	29.6	17.9	31.7
49	4040	18.8	29.7	18.3	31.8
50	4200	20.9	29.7	19.1	31.9
51	4380	20.9	30.1	16.4	32.0
52	4530	16.4	30.4	15.9	32.1
53	4950	14.2	30.4	14.6	32.2
54	5550	19.5	30.4	19.3	32.2
55	6060	24.9	30.7	24.2	32.6
56	6600	26.9	31.1	27.1	33.3
57	7190	27.2	32.0	26.9	34.4
58	7860	27.8	32.7	28.5	35.4
59	8370	29.1	33.3	27.6	36.1
60	8890	34.1	42.1	33.7	43.9
61	9470	39.9	50.4	40.3	51.4
62	9920	41.7	50.4	41.6	51.5
63	10420	41.4	50.4	40.8	51.6

ID =SECTION ID
X =RIVER DISTANCE
YR =THALWEG EL AT Q=4,360 CFS (RISING STAGE)
HR =W.S. EL AT Q=4,360 CFS (RISING STAGE)
YFA=THALWEG EL AT Q=12,940 CFS (FALLING STAGE)
HFA=W.S. EL AT Q=12,940 CFS (FALLING STAGE)

Table 22 Thalweg and water-surface elevations during rising and falling stages computed by SEDIMENT-4H for the San Dieguito River

SALT RIVER: HEC2SR

X	YO	YF	Y	H	W	Q	V	QB	QS	QT	DSO
FT	FT	FT	FT	FT	FT	CFS	FPS	T/D	T/D	T/D	MM
0	1079.2	1079.2	1079.2	1089.3	934	166320	17.8	-	-	2306810	49.0
150	1079.3	1079.3	1079.3	1091.4	912	166320	15.2	-	-	2306810	49.0
450	1079.6	1079.6	1079.6	1092.2	828	166320	16.2	-	-	2306810	49.0
800	1080.0	1080.2	1078.0	1094.0	749	166320	14.0	-	-	2306810	56.0
910	1080.0	1080.2	1078.0	1094.6	751	166320	13.5	-	-	2306810	56.0
1520	1080.7	1080.9	1078.6	1096.3	746	166320	12.8	-	-	2306810	56.0
1920	1081.1	1080.6	1082.7	1097.7	1122	166320	11.1	-	-	2321440	52.0
2520	1081.7	1081.2	1083.8	1098.5	1064	166320	12.6	-	-	2321440	52.0
3120	1084.5	1084.2	1086.5	1100.0	1176	166320	12.4	-	-	2321440	52.0
3520	1085.5	1084.4	1085.4	1100.9	1054	166320	12.4	-	-	2284790	79.0
4240	1087.3	1086.3	1087.3	1102.3	1025	166320	13.2	-	-	2284790	79.0
4840	1088.8	1087.8	1088.7	1104.1	1075	166320	12.3	-	-	2284790	79.0
5440	1090.4	1089.5	1090.4	1105.3	994	166320	13.7	-	-	2284790	79.0
6040	1092.0	1089.5	1089.1	1106.7	833	166320	13.8	-	-	2264580	106.0
6910	1094.2	1091.7	1091.3	1108.6	825	166320	14.2	-	-	2264580	106.0
7310	1095.3	1092.1	1090.3	1110.0	791	166320	13.0	-	-	2202860	126.0
7510	1095.8	1092.2	1090.3	1109.6	645	166320	15.6	-	-	2202860	126.0
7660	1096.2	1092.7	1090.8	1110.1	657	166320	15.4	-	-	2202860	126.0
7860	1096.7	1093.6	1091.7	1111.4	759	166320	13.4	-	-	2202860	126.0
8260	1097.7	1094.1	1095.0	1112.0	831	166320	14.3	-	-	2151420	154.0
8920	1099.4	1095.8	1096.7	1113.6	829	166320	14.4	-	-	2151420	154.0
9520	1101.0	1097.4	1098.3	1115.1	827	166320	14.5	-	-	2151420	154.0
10120	1102.6	1099.1	1099.9	1116.7	826	166320	14.4	-	-	2151420	154.0
10320	1103.1	1098.1	1099.6	1117.4	801	166320	14.0	-	-	2050060	120.0
10720	1104.6	1099.6	1101.1	1118.5	864	166320	13.5	-	-	2050060	120.0
11120	1106.0	1100.7	1102.5	1120.1	1060	166320	11.6	-	-	2050060	120.0
11320	1106.8	1101.6	1103.2	1120.3	1051	166320	12.1	-	-	2050060	120.0
11520	1107.5	1102.2	1103.8	1120.3	984	166320	13.4	-	-	2050060	120.0
11730	1108.3	1103.5	1104.9	1122.3	1415	166320	9.5	-	-	2050060	120.0
12150	1109.7	1104.6	1107.6	1122.8	1624	166320	9.7	-	-	1963050	108.0
12570	1111.2	1106.1	1109.0	1123.4	1574	166320	10.8	-	-	1963050	108.0
12990	1112.7	1107.6	1110.5	1124.6	1551	166320	11.3	-	-	1963050	108.0
13640	1117.7	1112.3	1115.5	1129.8	1513	166320	12.3	-	-	1963050	108.0
14440	1117.8	1113.9	1116.2	1132.9	2342	166320	7.6	-	-	1963050	108.0
15500	1118.5	1117.0	1118.0	1134.2	3529	166320	5.7	-	-	1940900	86.0
16620	1121.3	1120.5	1120.8	1135.1	2176	166320	10.0	-	-	1940900	86.0
17880	1126.3	1125.4	1125.7	1139.0	1623	166320	11.5	-	-	1940900	86.0
19520	1131.3	1132.6	1134.0	1143.8	2926	166320	7.9	-	-	1940190	6.6
20820	1129.7	1131.2	1132.5	1145.7	2960	166320	6.5	-	-	1940190	6.6
21820	1131.2	1131.2	1131.2	1146.6	1787	166320	8.1	-	-	2271650	49.0
22920	1129.0	1129.0	1129.0	1146.8	803	166320	14.5	-	-	2271650	49.0

ID=SECTION I.D.
X =RIVER DISTANCE
YO=INITIAL THALWEG EL
YF=FINAL THALWEG EL
Y =THALWEG EL AT PEAK FLOW
H =W.S. EL AT PEAK FLOW
W =TOP WIDTH AT PEAK FLOW

Q = WATER DISCHARGE AT PEAK FLOW
V = MEAN VELOCITY AT PEAK FLOW
QB = BED-LOAD DISCHARGE AT PEAK FLOW
QS = SUS-LOAD DISCHARGE AT PEAK FLOW
QT = TOTAL-LOAD DISCHARGE AT PEAK FLOW
DSO= MEDIAN DIAMETER OF BED MATERIAL AT PEAK FLOW

NOTE: VALUES OF QS & QB ARE NOT LISTED BECAUSE OF THE LIMITED SPACE.

Table 23 Principal results computed by HEC2SR for the Salt River

SALT RIVER: HEC-6

X	Y0	YF	Y	H	W	Q	V	QS	QT	DS0
FT	FT	FT	FT	FT	FT	CFS	FPS	T/D	T/D	MM
0	1079.2	1079.4	1079.3	1089.8	962	176000	18.1	579310	581320	15.5
150	1079.3	1078.6	1078.6	1092.0	955	176000	13.7	574560	575880	24.8
450	1079.6	1078.8	1078.9	1093.2	874	176000	14.9	486510	487680	20.4
800	1080.0	1078.8	1078.9	1093.9	785	176000	15.9	453570	454710	21.0
910	1080.0	1079.1	1079.2	1094.2	787	176000	15.8	419820	420080	20.4
1520	1080.7	1080.3	1080.3	1096.4	782	176000	14.7	347750	348690	23.8
1920	1081.1	1082.7	1082.0	1099.0	1187	176000	10.9	323080	323210	0.7
2520	1081.7	1084.2	1083.0	1099.7	1276	176000	11.9	326760	326930	0.7
3120	1084.5	1084.7	1084.5	1101.0	1377	176000	11.4	371560	372330	7.5
3520	1085.5	1085.4	1085.4	1101.4	1230	176000	11.9	384790	385960	16.5
4240	1087.3	1086.9	1087.0	1102.8	1264	176000	13.0	394720	396040	16.1
4840	1088.8	1088.7	1088.7	1104.5	1274	176000	12.1	411890	413210	12.6
5440	1090.4	1090.1	1090.0	1105.7	1189	176000	13.0	426360	427590	20.5
6040	1092.0	1090.5	1090.6	1106.2	1033	176000	19.0	350640	351480	20.7
6910	1094.2	1093.5	1093.9	1110.3	1040	176000	16.7	344520	345010	18.1
7310	1095.3	1094.2	1094.1	1111.5	1030	176000	16.2	374540	375020	19.1
7510	1095.8	1094.6	1094.0	1110.9	850	176000	19.3	379670	380180	24.8
7660	1096.2	1095.0	1094.7	1111.9	865	176000	18.5	333010	333550	21.7
7860	1096.7	1095.8	1095.7	1114.1	982	176000	15.4	329410	329860	17.3
8260	1097.7	1097.2	1097.7	1115.1	1046	176000	15.2	322510	322850	6.9
8920	1099.4	1098.8	1099.2	1116.4	1044	176000	15.4	326940	327330	8.9
9520	1101.0	1100.4	1100.7	1117.7	1043	176000	15.7	330790	331200	9.0
10120	1102.6	1101.8	1102.0	1119.1	1042	176000	15.7	334950	335420	12.6
10320	1103.1	1102.8	1103.1	1119.6	1042	176000	15.9	334650	335050	7.9
10720	1104.6	1103.0	1103.5	1121.2	1180	176000	14.1	335610	336380	17.0
11120	1106.0	1108.3	1106.8	1122.7	1533	176000	10.2	334360	334550	1.1
11320	1106.8	1105.9	1105.3	1122.9	1618	176000	12.6	336960	337640	21.2
11520	1107.5	1108.0	1106.9	1123.0	1630	176000	14.0	343880	344260	13.4
11730	1108.3	1107.2	1107.6	1124.4	2204	176000	10.8	369770	370610	13.0
12150	1109.7	1110.4	1110.0	1125.2	2615	176000	7.3	418790	419150	0.5
12570	1111.2	1111.8	1111.7	1125.7	2943	176000	7.7	563920	564380	0.5
12990	1112.7	1112.5	1112.5	1126.3	3267	176000	7.7	494610	495460	26.5
13640	1117.7	1115.4	1115.5	1130.1	3045	176000	16.4	433460	434370	28.4
14440	1117.8	1117.5	1117.6	1133.8	3201	176000	8.1	423170	424490	15.2
15500	1118.5	1124.7	1123.9	1135.2	6536	176000	7.0	418800	419060	0.4
16620	1121.3	1120.7	1120.8	1136.4	3927	176000	11.5	536850	537800	12.0
17880	1126.3	1125.5	1125.7	1139.8	4006	176000	11.5	581870	582850	13.6
19520	1131.3	1131.0	1131.2	1144.2	5252	176000	8.8	559590	560500	7.9
20820	1129.7	1130.8	1130.6	1145.7	4238	176000	6.8	593390	593660	0.4
21820	1131.2	1131.0	1131.1	1146.4	3960	176000	10.7	688020	689570	9.0
22920	1129.0	1129.2	1129.2	1147.6	2553	176000	14.7	713310	713840	4.7

X =RIVER DISTANCE
Y0=INITIAL THALWEG EL (T=0 HR)
YF=FINAL THALWEG EL (T=239 HRS)
Y =THALWEG EL AT PEAK FLOW
H =W.S. EL AT PEAK FLOW
W =TOP WIDTH AT PEAK FLOW
Q =WATER DISCHARGE AT PEAK FLOW
V =MEAN VELOCITY AT PEAK FLOW
QB =BED-LOAD DISCHARGE AT PEAK FLOW (=QT-QS)
QS =SUS-LOAD DISCHARGE AT PEAK FLOW
QT =TOTAL-LOAD DISCHARGE AT PEAK FLOW
DS0=MEDIAN DIAMETER OF BED MATERIAL AT PEAK FLOW

Table 24 Principal results computed by HEC-6 for the Salt River

SALT RIVER: FLUVIAL-11

X	Y0	YF	Y	H	H1	W	Q	V	QT	DS0
FT	FT	FT	FT	FT	FT	FT	CFS	FPS	T/D	MM
0	1079.2	1079.2	1079.2	1089.7	1089.7	962	176000	18.0	1539110	99.2
150	1079.3	1080.8	1080.0	1091.7	1091.8	958	176000	17.0	1539110	130.0
450	1079.6	1084.5	1080.8	1092.5	1092.5	892	176000	17.4	1556330	129.8
800	1080.0	1086.8	1082.8	1095.9	1093.1	1324	176000	14.5	1482100	121.8
910	1080.0	1086.9	1078.7	1097.4	1094.8	811	176000	12.1	1374360	93.6
1520	1080.7	1086.0	1081.5	1098.2	1097.8	868	176000	12.9	1348880	81.8
1920	1081.1	1087.5	1085.0	1100.2	1100.3	1253	176000	9.9	1311730	8.5
2520	1081.7	1087.8	1086.4	1100.8	1100.6	1307	176000	10.5	1333010	21.9
3120	1084.5	1087.7	1088.0	1101.7	1101.2	1368	176000	10.8	1372080	30.7
3520	1085.5	1088.3	1086.1	1102.1	1101.4	1163	176000	11.9	1391940	48.4
4240	1087.3	1087.8	1089.3	1103.5	1102.8	1264	176000	12.0	1404320	59.0
4840	1088.8	1089.2	1093.1	1104.8	1104.5	1288	176000	12.2	1408020	78.6
5440	1090.4	1089.8	1091.3	1106.1	1105.6	1153	176000	13.2	1414570	85.8
6040	1092.0	1091.2	1091.7	1107.3	1106.8	998	176000	14.3	1427380	96.9
6910	1094.2	1092.6	1092.9	1109.9	1110.4	991	176000	14.3	1415060	102.1
7310	1095.3	1094.3	1092.6	1110.9	1111.3	947	176000	14.5	1413850	101.2
7510	1095.8	1094.7	1096.9	1111.4	1110.5	857	176000	14.7	1415560	98.3
7660	1096.2	1095.6	1095.8	1111.9	1112.9	866	176000	14.5	1395000	96.2
7860	1096.7	1096.5	1098.5	1112.8	1114.7	979	176000	13.8	1387240	93.0
8260	1097.7	1097.0	1100.7	1114.0	1115.6	1046	176000	13.4	1376920	89.8
8920	1099.4	1098.7	1102.9	1115.7	1116.6	1047	176000	13.4	1370510	91.2
9520	1101.0	1100.7	1100.8	1117.1	1117.7	1012	176000	13.7	1361690	96.6
10120	1102.6	1102.4	1105.6	1118.9	1119.0	1044	176000	13.1	1331020	97.3
10320	1103.1	1103.3	1101.8	1119.2	1119.5	1005	176000	13.4	1335000	103.1
10720	1104.6	1105.4	1104.5	1120.9	1120.8	1179	176000	11.6	1303830	88.1
11120	1106.0	1107.7	1109.0	1122.2	1122.4	1532	176000	10.3	1311230	75.6
11320	1106.8	1108.5	1106.2	1122.6	1122.7	1584	176000	10.3	1320480	79.4
11520	1107.5	1108.9	1110.6	1123.2	1122.8	1647	176000	9.7	1292520	65.0
11730	1108.3	1110.3	1112.5	1123.9	1124.1	2202	176000	8.4	1297780	22.7
12150	1109.7	1111.6	1116.6	1124.6	1124.7	2617	176000	8.5	1342760	38.8
12570	1111.2	1113.8	1110.6	1125.4	1125.1	2951	176000	8.8	1348450	76.2
12990	1112.7	1115.8	1114.5	1126.5	1125.6	3256	176000	8.8	1345750	96.2
13640	1117.7	1118.9	1114.2	1128.4	1130.4	2921	176000	10.4	1432220	116.2
14440	1117.8	1123.3	1124.2	1131.6	1133.4	2931	176000	9.2	1357850	88.2
15500	1118.5	1129.1	1129.0	1134.7	1134.7	5919	176000	5.6	1275150	2.2
16620	1121.3	1130.0	1126.2	1136.3	1135.5	3663	176000	7.8	1439330	73.8
17880	1126.3	1130.8	1126.0	1139.4	1139.4	3208	176000	9.1	1478690	100.0
19520	1131.3	1135.2	1135.7	1144.0	1143.3	5468	176000	6.2	1446450	5.9
20820	1129.7	1139.1	1138.5	1146.0	1144.8	4443	176000	6.1	1448730	1.5
21820	1131.2	1135.8	1134.3	1147.3	1145.5	4044	176000	7.0	1578960	6.4
22920	1129.0	1129.0	1129.0	1149.3	1146.6	2881	176000	9.1	1689340	60.9

X =RIVER DISTANCE
Y0=INITIAL THALWEG EL
YF=FINAL THALWEG EL
Y =THALWEG EL AT PEAK FLOW
H =W.S. EL AT PEAK FLOW
H1=W.S. EL AT PEAK FLOW (HEC-2)
NOTE: QB & QS WERE NOT COMPUTED WITH FLUVIAL-11

W = TOP WIDTH AT PEAK FLOW
Q = WATER DISCHARGE AT PEAK FLOW
V = MEAN VELOCITY AT PEAK FLOW
QT = TOTAL-LOAD DISCHARGE AT PEAK FLOW
DS0= MEDIAN DIAMETER OF BED MATERIAL AT PEAK FLOW

Table 25 Principal results computed by FLUVIAL-11 for the Salt River

SALT RIVER: SEDIMENT-4H

ID	X	Y0	YF	Y	H	H1	W	Q	V	QT	DS0
	FT	FT	FT	FT	FT	FT	FT	CFS	FPS	T/D	MM
5	1300	1080.5	1079.4	1079.9	1099.7	1099.8	807	172124	11.3	818000	10.0
6	1950	1082.4	1083.6	1083.1	1100.9	1101.0	1958	172122	8.3	1004000	10.0
7	2500	1083.5	1084.5	1084.2	1101.4	1101.5	1632	172118	8.7	929000	10.0
8	3050	1084.6	1084.8	1084.8	1102.0	1102.0	1459	172114	9.2	963000	10.0
9	3600	1087.0	1086.4	1086.7	1102.7	1102.7	1263	172112	10.2	1005000	10.0
10	4200	1090.2	1089.4	1089.7	1103.7	1103.8	1388	172106	10.4	1018000	10.0
11	4850	1091.8	1091.0	1091.4	1104.8	1104.9	1325	172100	10.4	997000	10.0
12	5450	1093.2	1091.9	1092.5	1105.9	1106.2	1219	172094	11.3	949000	10.0
13	6200	1095.2	1093.3	1094.1	1107.9	1108.6	1066	172088	12.5	881000	10.0
14	6900	1097.5	1095.5	1096.4	1110.3	1111.3	1043	172081	12.6	826000	10.0
15	7500	1099.0	1096.4	1097.5	1112.1	1113.3	897	172077	13.2	796000	10.0
16	7850	1099.7	1097.8	1098.7	1113.2	1114.4	1009	172075	12.3	757000	10.0
17	8300	1100.8	1099.2	1100.0	1114.4	1115.5	1072	172071	11.8	697000	10.0
18	8900	1102.3	1100.6	1101.4	1115.8	1116.9	1069	172065	11.9	637000	10.0
19	9500	1104.1	1102.2	1103.1	1117.4	1118.4	1060	172060	11.9	579000	10.0
20	10150	1106.0	1104.2	1105.0	1119.0	1120.0	1088	172054	11.6	534000	10.0
21	10700	1107.8	1106.1	1106.9	1120.3	1121.3	1213	172051	11.3	497000	10.0
22	11050	1109.3	1107.9	1108.6	1121.2	1122.1	1533	172047	10.6	468000	10.0
23	11400	1110.6	1109.1	1109.8	1122.0	1122.8	1635	172043	10.6	450000	10.0
24	11750	1111.9	1110.9	1111.4	1122.7	1123.5	2201	172039	9.8	425000	10.0
25	12100	1113.3	1112.5	1113.0	1123.6	1124.2	2635	172034	9.3	403000	10.0
26	12550	1114.9	1114.0	1114.5	1124.5	1124.9	2963	172028	9.4	393000	10.0
27	13000	1116.5	1115.4	1116.0	1125.7	1125.9	3268	172022	9.6	386000	10.0
28	13450	1118.7	1116.8	1117.7	1127.1	1127.5	3264	172018	10.3	377000	10.0
29	14050	1120.3	1118.0	1119.0	1130.2	1131.3	2818	172016	11.3	339000	10.0
30	14600	1121.2	1120.3	1120.8	1133.1	1134.5	3081	172011	8.5	259000	10.0
31	15500	1123.1	1122.6	1122.9	1134.5	1135.4	5991	172002	7.0	199500	10.0
32	16600	1126.2	1125.9	1126.0	1136.6	1137.0	3988	171996	7.4	175900	10.0
33	17800	1130.3	1129.4	1129.8	1139.9	1140.3	3081	171996	8.2	129300	10.0
34	19100	1133.9	1134.0	1134.0	1142.3	1142.9	4438	171997	5.4	58230	10.0
35	19800	1135.5	1135.6	1135.5	1143.2	1143.6	4276	171997	5.3	36000	10.0
36	20800	1131.8	1132.0	1131.9	1144.7	1144.9	4302	171997	5.9	41800	10.0
37	21800	1131.3	1131.3	1131.3	1146.8	1146.9	3717	171999	7.5	46800	10.0
38	22900	1130.7	1129.9	1130.3	1149.8	1150.1	1404	172000	11.5	62700	10.0

ID = SECTION ID
X = RIVER DISTANCE
Y0 = INITIAL THALWEG EL
YF = FINAL THALWEG EL
Y = THALWEG EL AT PEAK FLOW
H = W.S. EL AT PEAK FLOW
H1 = W.S. EL AT PEAK FLOW COMPUTED USING FIXED-BED MODEL
W = TOP WIDTH AT PEAK FLOW
Q = WATER DISCHARGE AT PEAK FLOW (MAIN AND OVERBANK AREAS)
V = MEAN VELOCITY AT PEAK FLOW
QT = TOTAL-LOAD DIS. AT PEAK FLOW
D50= MEDIAN SIZE OF BED MATERIAL AT PEAK FLOW

NOTE: RESULTS SHOWN ARE FOR ENTIRE SECTION OF MAIN AND OVERBANK AREAS

Table 26 Principal results computed by SEDIMENT-4H for the Salt River

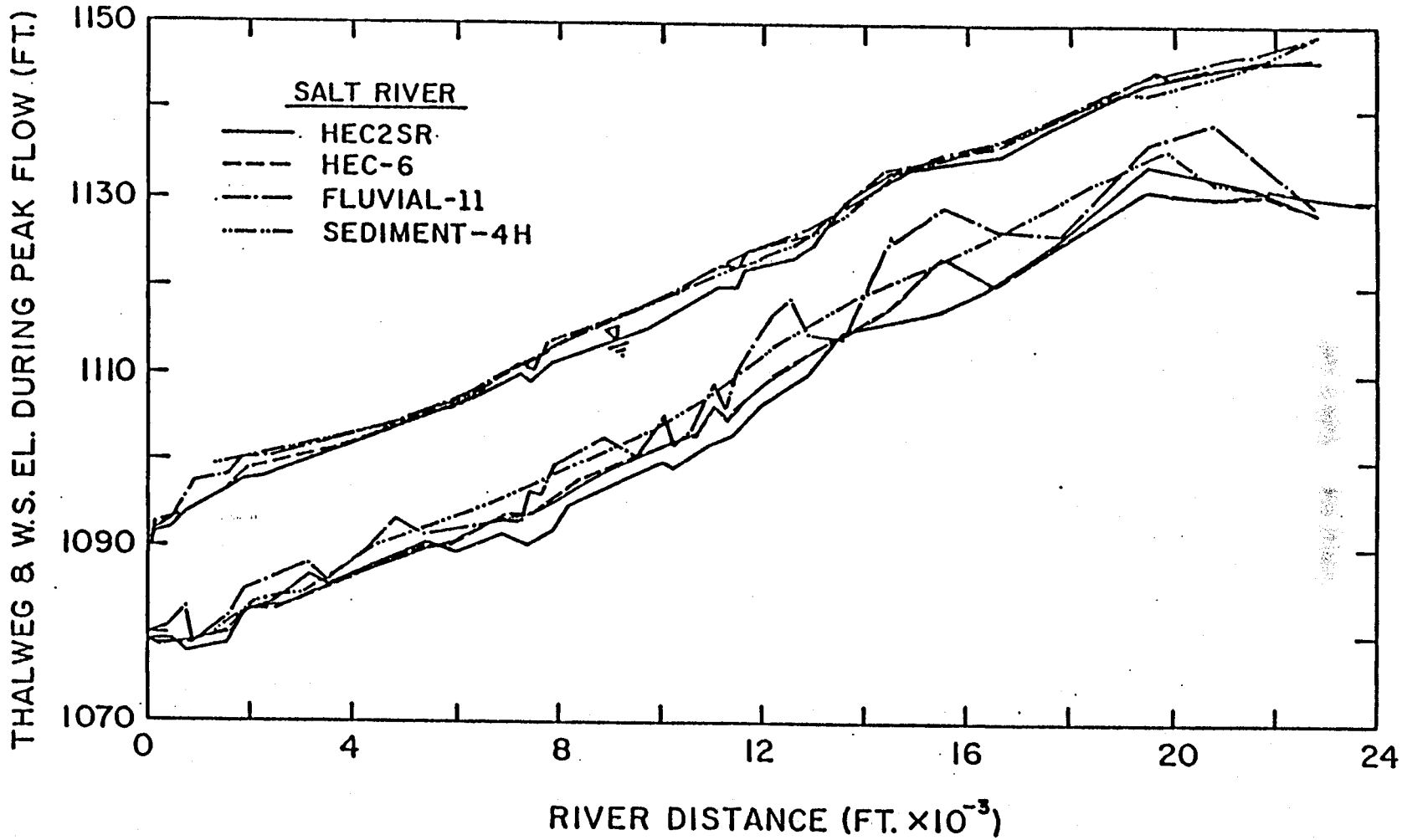

Figure 32 Comparison of thalweg and water-surface profiles at peak flow computed using the HEC2SR, HEC-6, FLUVIAL-11, and SEDIMENT-4H movable-bed models for the Salt River

Table 27 lists water-surface elevations at peak flow predicted by HEC using the HEC-6 movable-bed model, and the HEC-6 and HEC-2 fixed-bed models. The differences among these predictions of the three models are seen to be minute. It is of interest that in spite of cumulative bed deposition of 5.4 ft at a river distance of 15,500 ft, the water-surface elevation predicted by the HEC-6 movable-bed model was only 0.5 ft higher than that predicted by HEC-2, as seen in tables 24 and 27. Figure 33 shows two water-surface profiles at peak flow predicted by SDSU using HEC-2 and FLUVIAL-11; no significant differences are seen between them, although major thalweg degradation was predicted by FLUVIAL-11, as seen in table 25 (compare YO with Y).

Longitudinal distributions of mean flow velocities computed by the HEC-6, FLUVIAL-11, and SEDIMENT-4H movable-bed models are shown in figure 34. Since mean velocities of HEC2SR were very nearly equal to those of HEC-6, they are not plotted in the figure in order to simplify the graphic presentation. HEC-6 is seen to predict very high mean velocities in comparison with the other two models. The predicted total-load discharges at peak flow are compared in figure 35 (see table 28 also). Substantial differences among the predictions are seen. HEC-6 did not include transport of cobbles (sizes larger than 6 mm) or fines (finer than 0.125 mm) because of a program limitation for the former and a lack of measured data for the latter. Note that RMA tested two movable-bed cases for constant median bed-material diameters of 10 mm and 60 mm. Total-load discharges given in table 28 correspond to a median size of 60 mm according to their raw computer output, although in table 28 the median diameter is listed as 10 mm, the value reported by RMA. Post-flood median sizes predicted by HEC2SR, HEC-6, and FLUVIAL-11 are presented in table 28. Median sizes at peak flow predicted by these three models are shown in figure 36. HEC2SR and FLUVIAL-11 predicted armoring effects; however, finer sizes were predicted by HEC-6 because HEC-6 did not consider cobbles.

Finally, thalweg and water-surface elevations for rising and falling stages computed by HEC2SR, HEC-6, FLUVIAL-11 and SEDIMENT-4H are presented in tables 29, 30, 31, and 32, respectively. As can be seen in tables 29 and 30, water-surface elevations predicted by HEC2SR and HEC-6 for rising and falling stages at discharges of 95,040 cfs and 102,080 cfs, respectively, agree fairly well.

The computer model and computation time reported by each modeler are summarized in table 33.

SALT RIVER: HEC-6

X	H1	H2	H3	Q
FT	FT	FT	FT	CFS
0	1089.8	1089.7	1089.7	176000
150	1092.8	1092.0	1091.8	176000
450	1093.2	1092.7	1092.5	176000
800	1093.8	1093.7	1093.1	176000
910	1094.2	1095.0	1094.8	176000
1520	1096.4	1097.3	1097.8	176000
1920	1099.0	1099.9	1100.3	176000
2520	1099.7	1100.2	1100.6	176000
3120	1101.0	1101.0	1101.2	176000
3520	1101.4	1101.4	1101.4	176000
4240	1102.8	1102.8	1102.8	176000
4840	1104.5	1104.7	1104.5	176000
5440	1105.7	1105.8	1105.6	176000
6040	1106.2	1106.5	1106.8	176000
6910	1110.2	1111.0	1110.4	176000
7310	1111.5	1111.9	1111.3	176000
7510	1110.9	1111.1	1110.5	176000
7660	1111.9	1112.9	1112.9	176000
7860	1114.1	1115.0	1114.7	176000
8260	1115.1	1116.0	1115.6	176000
8920	1116.4	1117.0	1116.6	176000
9520	1117.7	1118.1	1117.7	176000
10120	1119.1	1119.5	1119.0	176000
10320	1119.6	1119.9	1119.5	176000
10720	1121.2	1121.3	1120.8	176000
11120	1122.7	1123.2	1122.4	176000
11320	1122.9	1123.2	1122.6	176000
11520	1123.0	1123.3	1122.8	176000
11730	1124.4	1124.7	1124.1	176000
12150	1125.2	1125.4	1124.7	176000
12570	1125.6	1125.8	1125.1	176000
12990	1126.3	1126.4	1125.6	176000
13640	1130.1	1130.2	1130.4	176000
14440	1133.8	1134.0	1133.4	176000
15500	1135.2	1135.1	1134.7	176000
16620	1136.4	1136.0	1135.5	176000
17080	1139.8	1140.1	1139.4	176000
19520	1144.2	1144.2	1143.3	176000
20820	1145.7	1145.7	1144.8	176000
21820	1146.4	1146.3	1145.4	176000
22920	1147.6	1147.6	1146.6	176000

X =RIVER DISTANCE
H1=W.S. EL. BY HEC-6 (MOVABLE BED)
H2=W.S. EL. BY HEC-6 (FIXED BED)
H3=W.S. EL. BY HEC-2 (FIXED BED)
Q =PEAK FLOW WATER DISCHARGE

Table 27 Water-surface elevations computed by the HEC-6 movable-bed and fixed-bed models and HEC-2 for the Salt River

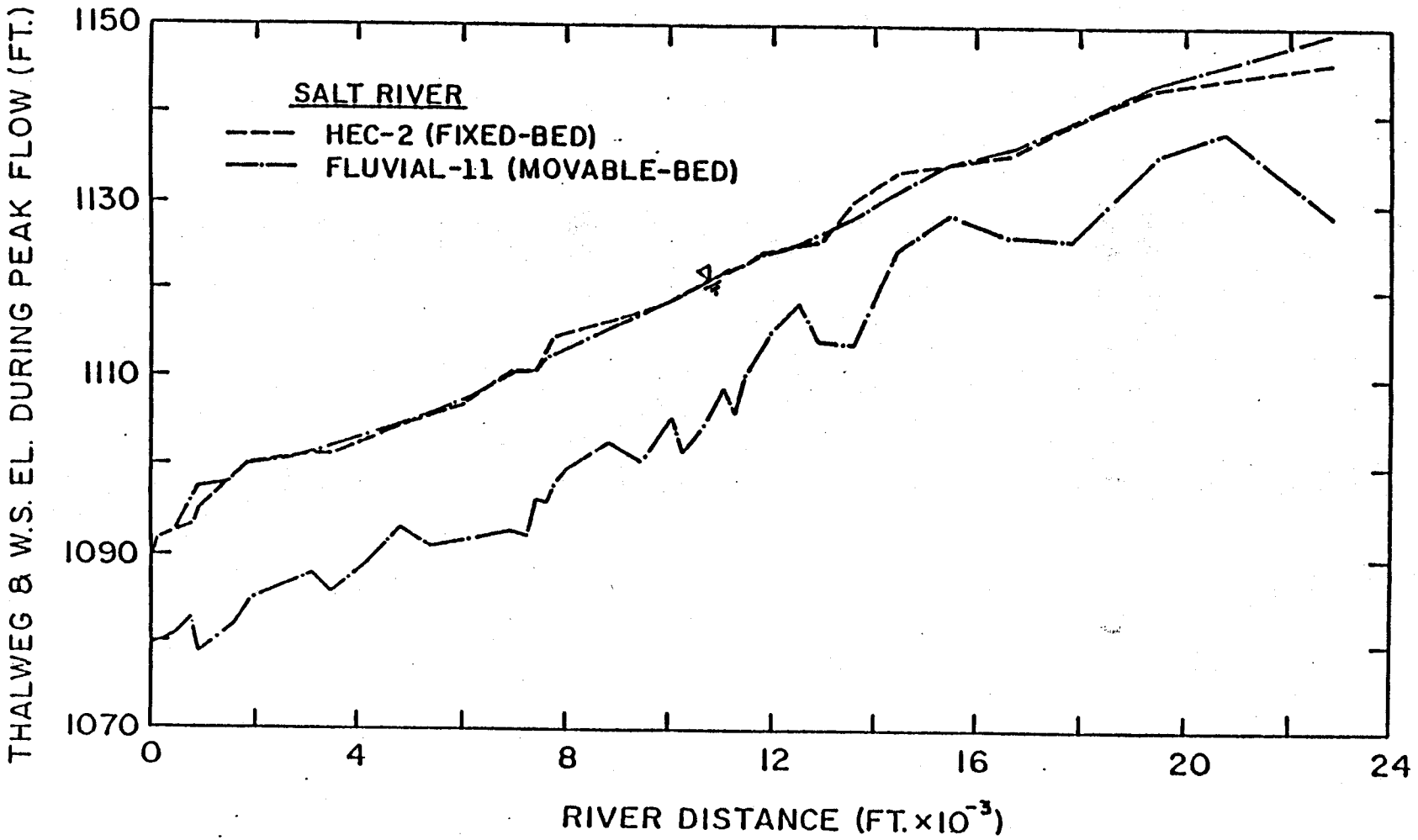

Figure 33 Comparison of water-surface profiles at peak flow computed by SDSU using HEC-2 and FLUVIAL-11

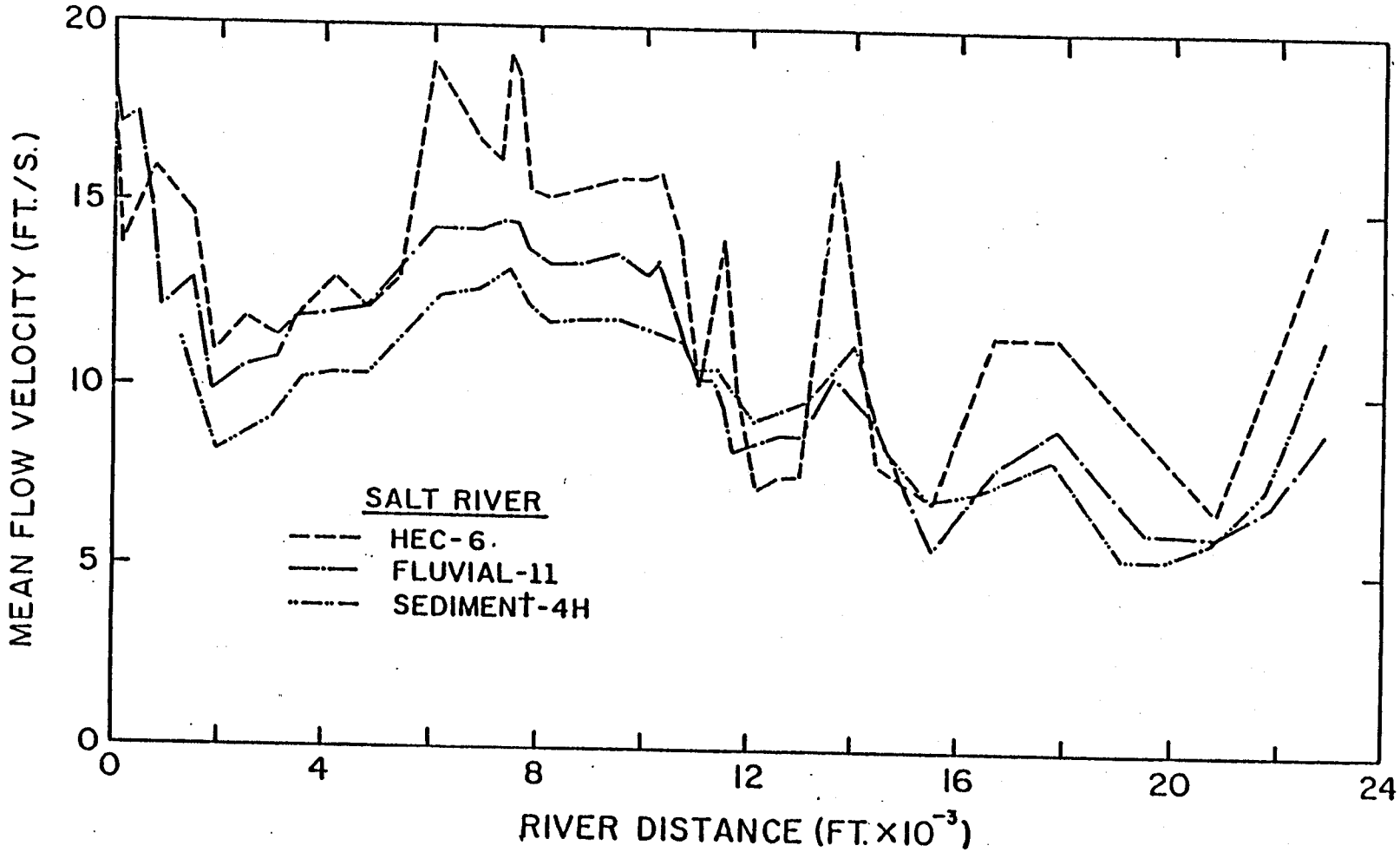

Figure 34 Longitudinal distributions of mean flow velocity at peak flow computed using the HEC-6, FLUVIAL-11, and SEDIMENT-4H movable-bed models for the Salt River

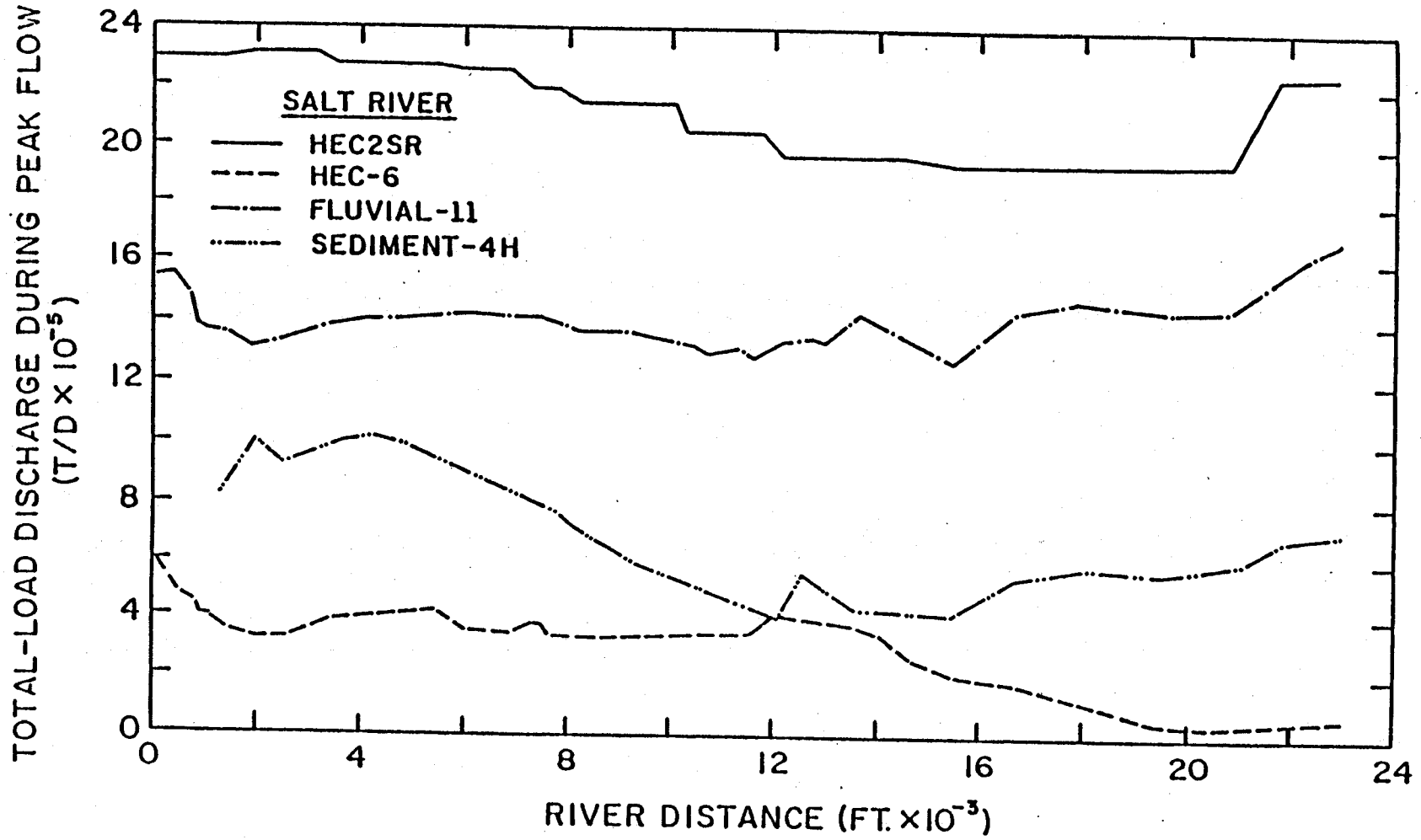

Figure 35 Total-load discharges at peak flow predicted by HEC2SR, HEC-6, FLUVIAL-11, and SEDIMENT-4H for the Salt River

SALT RIVER		(HEC-6)		(FLUVIAL-11)		(HEC2SR)		(SEDIMENT-4H)		
X	DS0I	QT	DS0F	QT	DS0F	QT	DS0F	X	QT	DS0F
FT	MM	T/D	MM	T/D	MM	T/D	MM	FT	T/D	MM
0	64.0	581320	35.48	1539110	144.89	2306010	49	1300	818000	10.0
150	64.0	575880	31.59	1539110	163.14	2306010	49	1950	1004000	10.0
450	64.0	487680	15.59	1556330	163.43	2306010	49	2500	929000	10.0
800	64.0	454710	19.89	1482100	161.38	2306010	47	3050	963000	10.0
910	64.0	420080	1.45	1374360	159.55	2306010	47	3600	1005000	10.0
1520	64.0	348690	14.32	1348880	2.17	2306010	47	4200	1018000	10.0
1920	64.0	323210	21.61	1311730	2.59	2321440	87	4850	997000	10.0
2520	64.0	326930	2.29	1333010	4.40	2321440	87	5450	949000	10.0
3120	64.0	372330	7.25	1372080	13.18	2321440	87	6200	881000	10.0
3520	64.0	385960	11.61	1391940	19.04	2284790	20	6900	826000	10.0
4240	64.0	396040	16.25	1404320	26.68	2284790	20	7500	796000	10.0
4840	64.0	413210	19.86	1408020	45.02	2284790	20	7850	757000	10.0
5440	64.0	427590	19.78	1414570	48.09	2284790	20	8300	697000	10.0
6040	64.0	351480	22.01	1427380	73.88	2264580	94	8900	637000	10.0
6910	64.0	345010	25.84	1415060	95.85	2264580	94	9500	579000	10.0
7310	64.0	375020	18.59	1413850	92.44	2202860	84	10150	534000	10.0
7510	64.0	380180	3.77	1415560	107.22	2202860	84	10700	497000	10.0
7660	64.0	333550	17.85	1395000	101.46	2202860	84	11050	468000	10.0
7860	64.0	329860	24.47	1387240	100.00	2202860	84	11400	450000	10.0
8260	64.0	322850	26.37	1376920	69.84	2151420	54	11750	425000	10.0
8920	64.0	327330	26.19	1370510	77.11	2151420	54	12100	403000	10.0
9520	64.0	331200	26.69	1361690	82.74	2151420	54	12550	393000	10.0
10120	64.0	335420	28.91	1331020	104.41	2151420	54	13000	386000	10.0
10320	64.0	335051	31.47	1335000	103.92	2050060	26	13450	377000	10.0
10720	64.0	336300	35.37	1303830	94.37	2050060	26	14050	339000	10.0
11120	64.0	334550	27.71	1311230	90.92	2050060	26	14600	259000	10.0
11320	64.0	337640	24.77	1320480	94.71	2050060	26	15500	199500	10.0
11520	64.0	344260	1.22	1292520	105.41	2050060	26	16600	175900	10.0
11730	64.0	370610	3.33	1297780	98.72	2050060	26	17800	129300	10.0
12150	64.0	419150	8.63	1342760	116.40	1963050	46	19100	58230	10.0
12570	64.0	564380	24.23	1348450	105.89	1963050	46	19800	36000	10.0
12990	64.0	495460	27.61	1345750	118.31	1963050	46	20800	41800	10.0
13640	64.0	434370	30.08	1432220	103.63	1963050	46	21800	46800	10.0
14440	64.0	424490	29.47	1357850	107.23	1963050	46	22900	62700	10.0
15500	64.0	419060	9.11	1275150	112.37	1940900	17	-	-	-
16620	64.0	537800	25.96	1439330	70.51	1940900	17	-	-	-
17880	64.0	582850	24.05	1478690	88.45	1940900	17	-	-	-
19520	64.0	560500	27.46	1446450	144.83	1940190	33	-	-	-
20820	64.0	593660	2.76	1448730	16.81	1940190	33	-	-	-
21820	64.0	689570	25.93	1578960	31.87	2271650	49	-	-	-
22920	64.0	713840	24.72	1689340	60.89	2271650	49	-	-	-

ID = SECTION I.D.
X = RIVER DISTANCE
DS0I = INITIAL MEDIAN SIZE OF BED MATERIAL (PRE-FLOOD)
DS0F = FINAL MEDIAN SIZE OF BED MATERIAL (POST-FLOOD)
QT = TOTAL-LOAD DISCHARGE AT PEAK-FLOW DISCHARGE OF 176,000 CFS

Table 28 Total-load discharges at peak flow and final median bed-material sizes computed by HEC2SR, HEC-6, FLUVIAL-11, and SEDIMENT-4H for the Salt River

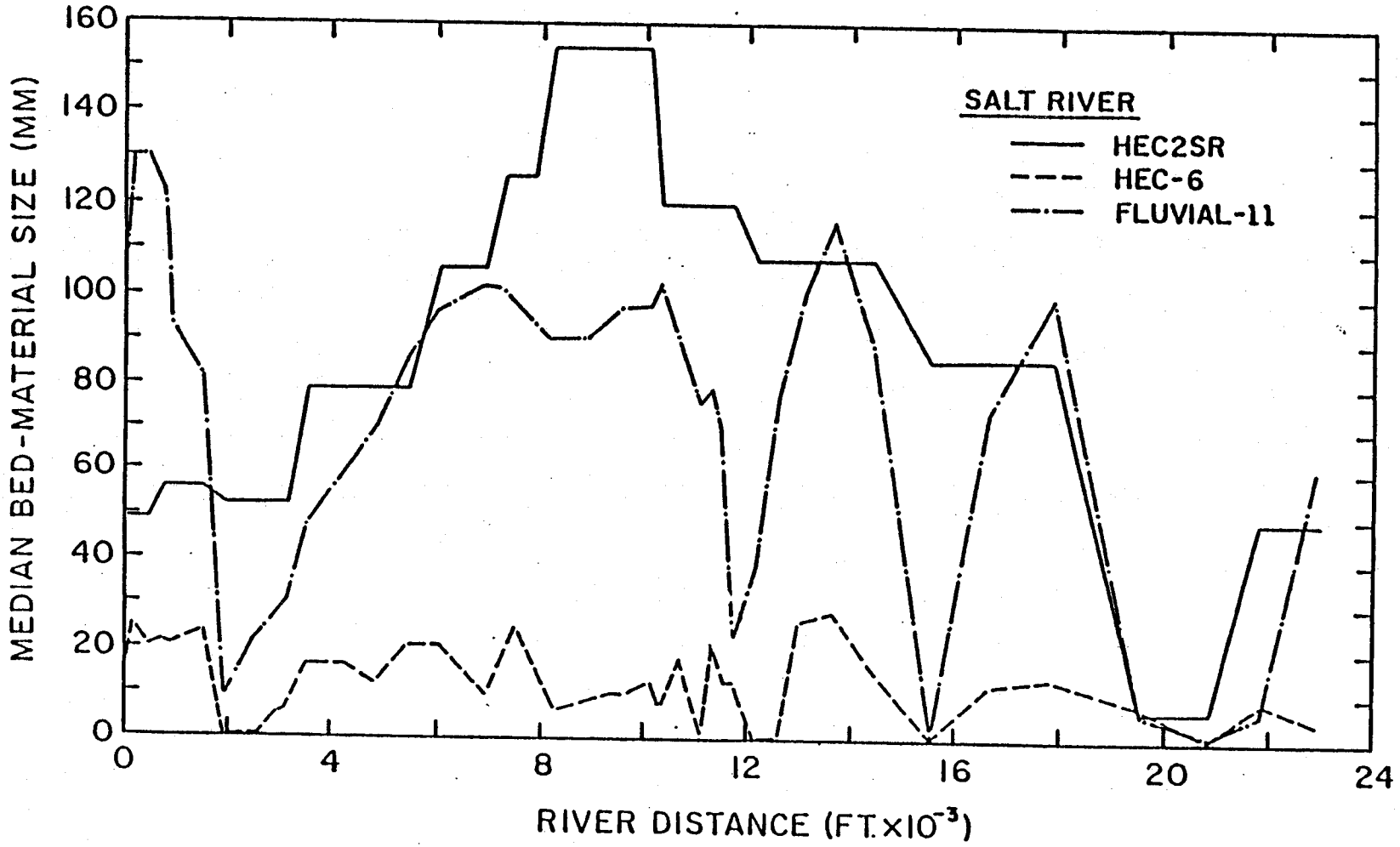

Figure 36 Longitudinal distributions of median bed-material size at peak flow computed using HEC2SR, HEC-6, and FLUVIAL-11 for the Salt River

SALT RIVER: HEC2SR

X	YR	HR	YFA	HFA
FT	FT	FT	FT	FT
0	1079.2	1086.2	1079.2	1086.5
150	1079.3	1088.2	1079.3	1088.5
450	1079.6	1089.0	1079.6	1089.4
800	1079.1	1090.2	1078.4	1090.8
910	1079.1	1090.6	1078.4	1091.2
1520	1079.8	1092.2	1079.1	1092.4
1920	1081.7	1093.5	1081.8	1093.4
2520	1082.8	1094.1	1082.8	1094.3
3120	1085.5	1095.5	1085.6	1096.2
3520	1085.3	1096.5	1084.9	1097.4
4240	1087.1	1098.5	1086.8	1098.9
4840	1088.6	1100.6	1088.2	1100.9
5440	1090.2	1101.8	1089.9	1102.1
6040	1090.8	1103.2	1088.9	1103.7
6910	1093.0	1105.8	1091.1	1105.2
7310	1093.1	1106.9	1090.3	1106.3
7510	1093.4	1106.8	1090.4	1106.3
7660	1093.9	1107.5	1090.8	1106.5
7860	1094.5	1108.7	1091.7	1107.2
8260	1096.8	1109.4	1094.5	1107.7
8920	1098.5	1111.1	1096.2	1109.8
9520	1100.1	1112.7	1097.8	1111.3
10120	1101.7	1114.3	1099.5	1113.0
10320	1100.6	1115.3	1098.3	1113.9
10720	1102.2	1115.8	1099.8	1114.4
11120	1103.4	1116.5	1101.2	1115.1
11320	1104.1	1116.7	1101.9	1115.7
11520	1104.8	1117.2	1102.5	1116.6
11730	1105.7	1119.2	1103.8	1118.3
12150	1107.7	1119.6	1106.9	1119.7
12570	1109.2	1121.2	1108.4	1121.2
12990	1110.7	1122.9	1109.9	1123.0
13640	1115.6	1128.1	1114.9	1128.2
14440	1116.3	1130.8	1115.8	1130.9
15500	1118.0	1131.8	1117.9	1131.9
16620	1120.8	1133.3	1120.7	1133.5
17880	1125.7	1136.7	1125.6	1136.9
19520	1132.3	1140.9	1134.1	1142.1
20820	1130.7	1142.5	1132.6	1144.3
21820	1131.2	1143.2	1131.2	1145.0
22920	1129.0	1144.4	1129.0	1145.4

X =RIVER DISTANCE
YR =THALWEG EL AT Q=95,040 CFS (RISING STAGE)
HR =W.S. EL AT Q=95,040 CFS (RISING STAGE)
YFA=THALWEG EL AT Q=102,080 CFS (FALLING STAGE)
HFA=W.S. EL AT Q=102,080 CFS (FALLING STAGE)

Table 29 Thalweg and water-surface elevations during rising and falling stages computed by HEC2SR for the Salt River

SALT RIVER: HEC-6

X	YR	HR	YFA	HFA
FT	FT	FT	FT	FT
0	1079.3	1086.3	1079.3	1086.6
150	1079.1	1088.5	1078.6	1089.2
450	1079.4	1089.2	1078.7	1089.7
800	1079.8	1090.1	1078.7	1090.4
910	1079.8	1090.7	1079.0	1090.6
1520	1080.6	1092.5	1080.3	1092.1
1920	1082.9	1093.9	1083.0	1093.8
2520	1082.3	1095.0	1083.8	1095.0
3120	1084.4	1095.9	1084.7	1097.0
3520	1085.4	1096.8	1085.4	1097.7
4240	1087.1	1098.8	1086.9	1099.3
4840	1088.8	1100.9	1088.7	1101.1
5440	1090.3	1102.2	1090.0	1102.5
6040	1091.0	1103.1	1090.4	1103.2
6910	1093.9	1106.3	1094.0	1106.3
7310	1094.5	1107.4	1094.1	1107.8
7510	1094.6	1107.4	1093.8	1107.9
7660	1095.3	1107.9	1094.5	1108.2
7860	1096.3	1109.3	1095.5	1109.4
8260	1097.9	1110.4	1097.7	1110.3
8920	1099.3	1112.0	1099.1	1112.2
9520	1100.7	1113.4	1100.7	1113.6
10120	1102.2	1114.9	1101.9	1115.2
10320	1103.2	1115.4	1103.1	1115.6
10720	1104.1	1116.7	1103.1	1117.0
11120	1106.2	1118.4	1107.5	1118.0
11320	1105.5	1118.4	1105.3	1118.9
11520	1106.5	1118.4	1106.6	1118.9
11730	1107.6	1119.9	1106.9	1120.3
12150	1109.7	1121.2	1110.3	1121.4
12570	1111.2	1122.1	1112.0	1122.5
12990	1112.6	1123.4	1112.5	1123.9
13640	1116.0	1128.5	1115.4	1128.6
14440	1117.7	1131.2	1117.5	1131.4
15500	1120.3	1132.2	1127.1	1132.8
16620	1120.7	1133.7	1120.8	1134.8
17880	1125.9	1137.2	1125.6	1137.3
19520	1131.1	1141.4	1131.1	1141.7
20820	1129.7	1142.9	1130.9	1143.3
21820	1131.1	1143.1	1131.0	1143.7
22920	1129.0	1145.3	1129.2	1145.6

X =RIVER DISTANCE
YR =THALWEG EL AT Q=95,040 CFS (RISING STAGE)
HR =W.S. EL AT Q=95,040 CFS (RISING STAGE)
YFA=THALWEG EL AT Q=102,080 CFS (FALLING STAGE)
HFA=W.S. EL AT Q=102,080 CFS (FALLING STAGE)

Table 30 Thalweg and water-surface elevations during rising and falling stages computed by HEC-6 for the Salt River

SALT RIVER: FLUVIAL-11

X	YR	HR	YFA	HFA
FT	FT	FT	FT	FT
0	1079.2	1086.2	1079.2	1086.7
150	1079.6	1088.4	1080.2	1088.2
450	1080.7	1089.0	1081.2	1089.6
800	1082.4	1090.3	1083.1	1092.3
910	1079.3	1093.5	1082.3	1093.7
1520	1080.3	1094.2	1083.8	1095.6
1920	1083.9	1095.2	1086.3	1097.2
2520	1085.1	1095.6	1086.9	1097.8
3120	1085.0	1096.6	1087.7	1098.6
3520	1086.8	1097.3	1086.1	1099.0
4240	1090.0	1099.1	1087.4	1100.4
4840	1092.9	1100.7	1088.4	1101.6
5440	1091.3	1102.1	1089.3	1102.8
6040	1092.1	1103.6	1091.2	1104.1
6910	1096.8	1106.3	1092.3	1106.2
7310	1096.3	1107.4	1093.0	1107.3
7510	1094.8	1107.7	1097.1	1108.3
7660	1096.4	1108.4	1096.4	1108.6
7860	1096.8	1109.3	1096.2	1109.1
8260	1100.3	1110.4	1096.6	1110.2
8720	1100.0	1111.9	1098.3	1111.9
9520	1100.8	1113.3	1101.1	1113.4
10120	1102.2	1114.8	1104.9	1115.0
10320	1102.8	1115.3	1102.6	1115.4
10720	1104.3	1116.5	1104.3	1116.8
11120	1107.9	1117.8	1107.1	1117.9
11320	1106.2	1118.3	1107.8	1118.4
11520	1106.5	1118.8	1110.9	1119.0
11730	1110.4	1119.7	1111.4	1119.8
12150	1115.5	1120.8	1112.7	1121.3
12570	1117.6	1122.0	1114.1	1122.8
12990	1114.2	1123.5	1116.4	1124.5
13640	1114.2	1127.0	1114.2	1126.8
14440	1120.2	1130.7	1124.0	1129.5
15500	1122.0	1132.3	1129.2	1132.8
16620	1125.9	1134.0	1129.2	1135.1
17880	1126.0	1137.2	1126.6	1137.5
19520	1132.9	1141.5	1135.8	1141.6
20820	1134.7	1143.1	1139.2	1144.2
21820	1132.1	1144.1	1134.8	1145.6
22920	1129.0	1145.8	1129.0	1147.4

X =RIVER DISTANCE
YR =THALWEG EL AT Q=94,400 CFS (RISING STAGE)
HR =W.S. EL AT Q=94,400 CFS (RISING STAGE)
YFA=THALWEG EL AT Q=106,400 CFS (FALLING STAGE)
HFA=W.S. EL AT Q=106,400 CFS (FALLING STAGE)

Table 31 Thalweg and water-surface elevations during rising and falling stages computed by ELUVIAL-11 for the Salt River

SALT RIVER: SEDIMENT-4H

ID	X	YR	HR	YFA	HFA
	FT	FT	FT	FT	FT
5	1300	1080.5	1095.3	1079.3	1095.8
6	1950	1081.0	1095.9	1080.0	1096.4
7	2500	1082.2	1096.5	1081.4	1097.2
8	3050	1084.0	1097.1	1083.1	1097.9
9	3600	1085.4	1097.9	1084.1	1098.7
10	4200	1087.1	1099.2	1085.4	1099.7
11	4850	1088.7	1100.5	1087.1	1100.8
12	5450	1090.0	1101.9	1087.9	1102.0
13	6200	1092.0	1104.2	1089.1	1103.7
14	6900	1094.3	1106.9	1091.2	1105.8
15	7500	1095.8	1108.7	1092.5	1107.3
16.	7850	1096.5	1109.7	1093.8	1108.3
17	8300	1097.7	1110.8	1095.2	1109.5
18	8900	1099.1	1112.1	1096.5	1111.0
19	9500	1100.9	1113.7	1098.1	1112.7
20	10150	1102.7	1115.3	1100.3	1114.2
21	10700	1104.4	1116.6	1102.3	1115.5
22	11050	1105.8	1117.7	1103.7	1116.7
23	11400	1107.1	1118.6	1104.9	1117.8
24	11750	1108.2	1119.5	1106.3	1118.9
25	12100	1109.6	1120.6	1107.7	1120.4
26	12550	1111.0	1121.8	1109.0	1122.1
27	13000	1112.6	1123.2	1110.1	1123.8
28	13450	1115.4	1125.1	1111.8	1125.6
29	14050	1117.5	1128.4	1114.3	1128.6
30	14600	1118.0	1131.0	1116.1	1131.2
31	15500	1119.6	1132.2	1118.4	1132.5
32	16600	1122.8	1134.2	1122.0	1134.5
33	17800	1126.9	1137.7	1125.3	1137.4
34	19100	1130.6	1140.2	1130.5	1139.7
35	19800	1132.0	1140.9	1132.1	1140.8
36	20800	1131.8	1142.0	1132.0	1142.3
37	21800	1131.3	1143.7	1131.3	1144.3
38	22900	1130.6	1146.0	1129.6	1146.3

ID = SECTION ID
X = RIVER DISTANCE
YR = THALWEG EL AT Q=92,110 CFS (RISING STAGE)
HR = W.S. EL AT Q=92,110 CFS (RISING STAGE)
YFA= THALWEG EL AT Q=104,530 CFS (FALLING STAGE)
HFA= W.S. EL AT Q=104,530 CFS (FALLING STAGE)

Table 32 Thalweg and water-surface elevations during rising and falling stages computed by SEDIMENT-4H for the Salt River

MODEL	MODE	COMPUTER MODEL	CPU TIME (SEC)
(SAN LORENZO RIVER)			
HEC2SR	MOVABLE-BED	CDC CYBER 172	800.0
KUWASER	MOVABLE-BED	CDC CYBER 172	117.1
UUWSR	MOVABLE-BED	CDC CYBER 172	210.0
HEC-6	MOVABLE-BED	CDC 7600	13.5
HEC-6	MOVABLE-BED	HARRIS 500	199.1
HEC-6	FIXED-BED*	CDC 7600	0.3
HEC-6	FIXED-BED*	HARRIS 500	9.7
HEC-2	FIXED-BED*	CDC 7600	0.5
HEC-2	FIXED-BED*	HARRIS 500	14.3
FLUVIAL-11	MOVABLE-BED	VAX 11/780	606.0
SEDIMENT-4H	MOVABLE-BED	PRIME 550	7,200.0
(SAN DIEGUITO RIVER)			
HEC2SR	MOVABLE-BED	CDC CYBER 172	526.5
UUWSR	MOVABLE-BED	CDC CYBER 172	209.1
FLUVIAL-11	MOVABLE-BED	VAX 11/780	1,291.0
SEDIMENT-4H	MOVABLE-BED	PRIME 550	7,200.0
(SALT RIVER)			
HEC2SR	MOVABLE-BED	CDC CYBER 172	530.0
HEC-6	MOVABLE-BED	CDC 7600	17.6
HEC-6	FIXED-BED*	CDC 7600	0.4
HEC-2	FIXED-BED*	CDC 7600	0.6
FLUVIAL-11	MOVABLE-BED	VAX 11/780	831.0
SEDIMENT-4H	MOVABLE-BED	PRIME 550	7,200.0

*: FOR A PEAK DISCHARGE ONLY

Table 33 List of computer models used in the present study and their computing times

V. LIMITATIONS OF ALLUVIAL-RIVER-FLOW MODELS

The computer-based alluvial-river flow models utilized in this study account for the effects of changes in river-bed elevation on flood stages. Degradation or aggradation occurs in a subreach when the sediment-transport capacity of the flow at the upstream boundary of a reach differs from that at the downstream boundary. Degradation results when the sediment output across the downstream boundary of the reach exceeds the sediment input into the upstream end of the reach, while aggradation occurs when the sediment input exceeds the output. These sediment-transport imbalances occur along the river reach when there is a change in flow characteristics or the sediment input to the reach is changed without accompanying changes in the sediment-transport capacity. Alluvial-river-flow models compute changes in river-bed elevation (degradation or aggradation) by means of the sediment-continuity equation, and determine the new flow field on the basis of the altered bed elevation and slope using the flow-continuity and the flow-momentum or flow-energy equations. Interaction or feedback between changing river bed and flow characteristics is handled by the numerical schemes described in Chapter II. Common to all alluvial-river-flow models are requirements for input data on channel geometry, sediment, and hydrologic characteristics. The input-data requirements for the individual models tested in the present study are summarized in Chapter II. Even if adequate data are provided for a study river, there still remains a need to calibrate and verify the model by means of field data. In most natural rivers, only extremely limited geometric, sediment, and hydrologic field data are available for high flood stages, and, consequently, adequate calibration or verification of the models usually cannot be obtained.

The limitations of the individual models tested are described in Chapter II, and attention here will be focused on several important considerations that may explain some of the discrepancies among the computed results presented in Chapter IV. First, it should be pointed out that the initial channel-geometry condition is in general not completely known. Strictly speaking, the initial condition must be specified at the time a 100-year-flood simulation is initiated. In most practical cases, rather old river cross-

section profiles are provided as input data; however, the river geometry may in reality be undergoing changes in a somewhat random manner as a consequence of floods during the period between the time of cross-section surveys and the 100-year flood. This means that a movable-bed model should have the capability of predicting the random initial condition by statistical means using flood-frequency records. Randomness of the initial conditions has not been incorporated into any of the available models.

Second, the bed-armoring process during channel degradation is not well understood, and has not been adequately formulated. Armoring and the result coarsening of the bed-material size have a direct effect on the sediment-discharge capacity and the channel roughness or bed friction factor, and, thereby, impact on the velocity, depth, and energy slope of the flow. Moreover, bed armoring greatly impedes degradation. Finally, the field data available on the horizontal and vertical distributions of bed-material size generally are inadequate to make use of even the imperfect armoring formulations available. Many of the seeming anomalies and discrepancies in the results computed by the various models presented in Chapter IV may have resulted from the differences among the armoring and bed-material sorting formulations utilized. In order to stress this point, the median-bed sizes predicted by different models at narrow and wide cross sections during peak flow are summarized in table 34 for SDR and SR. At narrow, constricted cross sections, channel degradation and attendant armoring (or coarsening of the bed-material size) are generally expected during peak flow. However, as seen in table 34, only HEC2SR predicted the coarsening at the narrower sections for both SDR and SR. However, the final SDR post-flood median bed-material size predicted by HEC2SR at a river distance of 3,600 ft is coarser than that computed during peak flow. FLUVIAL-11 predicted the coarser post-flood bed-material sizes at the narrower sections for both SDR and SR. Because each sediment-transport function has its own independent variables, the characteristics of the sediment-transport formula in an alluvial-river-flow model have a strong effect on the flow characteristics and the sediment-discharge prediction. As has been pointed out in Chapter IV, greatly different sediment discharges were predicted by the models tested in this study.

MODEL	X FT	W FT	V FT/S	D50 MM	D50F MM
SAN DIEGUITO RIVER					
HEC2SR	3,600	170	11.6	0.86	0.92
	4,350	1,143	1.2	0.38	0.30
FLUVIAL-11	3,600	266	6.9	0.27	0.28
	4,350	829	5.1	0.28	0.30
SEDIMENT-4H*	4,200	237	9.0	0.46	0.46
	4,950	944	1.8	0.46	0.46
SALT RIVER					
HEC2SR	7,510	645	15.6	126.0	84.0
	13,640	1,513	12.3	108.0	46.0
HEC-6**	7,510	850	19.3	24.8	3.8
	13,640	3,045	16.4	28.4	30.1
FLUVIAL-11	7,510	857	14.7	98.3	107.2
	13,640	2,921	10.4	116.2	103.6
SEDIMENT-4H*	7,500	897	13.2	10.0	10.0
	13,450	3,264	10.3	10.0	10.0

X = RIVER DISTANCE
W = COMPUTED TOP WIDTH AT PEAK FLOW
D50 = COMPUTED MEDIAN DIAMETER OF BED MATERIAL AT PEAK FLOW
D50F = COMPUTED POST-FLOOD MEDIAN DIAMETER OF BED MATERIAL
* = SEDIMENT-4H DOES NOT CONSIDER SEDIMENT SORTING
** = HEC-6 DID NOT CONSIDER TRANSPORT OF COBBLES (COARSER THAN 64 MM) OR WASH LOAD (FINER THAN 0.125 MM) FOR SR

Table 34 Typical median bed-material sizes computed during peak flow and post-flood bed-material sizes for the San Dieguito and Salt Rivers

Third, it should be pointed out that the boundary conditions applied to alluvial-river-flow models play important roles in their simulations. For example, if the upstream sediment input is a boundary condition and is greater than the computed sediment-transport capacity of the flow at the first cross section, the first subreach will aggrade until the bed slope increases until the imposed sediment discharge is transported by the resulting increased flow velocity. The local aggradation propagates downstream until the entire reach is sufficiently steep to produce a velocity that is competent to pass the imposed sediment discharge through the system. The boundary condition used to account for erodible banks is also extremely important in cases where banks are susceptible to erosion during floods. Unless some computational means are employed to account for changing movable-bed width, predicted flood levels in rivers with very erodible banks become less reliable. FLUVIAL-11 is the only model among the models tested in this study that incorporates width variations.

Finally, the effects of uncertainty surrounding variations in the channel roughness or friction factor on flooded stages are not well understood. Because of the strong dependence of the friction factor on the sediment discharges, the effects of suspended- and bed-load sediment on the friction factor should be accounted for.

VI. SUMMARY, CONCLUSIONS, AND RECOMMENDATIONS

The report summaries that were prepared and submitted in letter form to the Committee by the individual modelers are first quoted, in order to present their views regarding their modeling experience in the present study.

1. SLA. "In general, the conventional rigid-boundary flood analysis based on HEC-2 is adequate for a river system experiencing adequate armoring control, equilibrium or near equilibrium conditions. However, this method of analysis underestimates or overestimates the flood level in a reach that has experienced significant aggradation or degradation before the flood peak. The results of application of HEC2SR, KUWASER, and UUWSR to the study reaches are very similar. Minor differences are a product of the various assumptions associated with the individual models. While each model is especially applicable to specific situations, we recommend adoption of HEC2SR. The primary advantage of this model is its compatibility with HEC-2. This feature would expedite application of HEC2SR to flood insurance studies."

2. HEC. "With regard to the subject of the study, it should be noted that, as the hydraulic computations in both HEC-2 and HEC-6 are steady state, neither one can be accurately termed a "flood routing model". In general, the computed water surface profiles for the peak flood discharges differed little between the fixed-bed and movable-bed simulations. This may be due to certain peculiarities of the data sets. The Salt River data set, as provided, included no information on inflowing sediment load, an essential ingredient of movable bed river modeling. The inflowing load had to be assumed to be in equilibrium with the bed material throughout the range of discharges on the flood hydrograph. Therefore, little scour or deposition would be expected, as is seen in the simulation results. The San Lorenzo River flood event was of very short duration. It appears that this factor, plus local hydraulic control at the tidal downstream boundary condition, minimizes any overall bed elevation changes. Furthermore, we have not previously applied HEC-6 to short-term, single flood event simulations. We certainly would not conclude that fixed and movable boundary simulations will always produce similar water surface profiles as these results indicate. Because no data were provided for model calibration, these results should not be considered to be an engineering analysis of water surface profiles. Use of these results should be limited to intermodel comparisons".

3. SDSU. "If a river channel is in the state of approximate equilibrium, river-channel changes during floods are usually not sufficiently significant to result in major differences in the flood level. Such are the cases for the San Lorenzo River and the Salt River. However, if the natural equilibrium of a river is significantly distorted, river-channel changes during floods are such that major differences in the flood level can be expected. Such is the case for the San Dieguito River, for which

the water-surface profile as well as special variations in velocity obtained using the fixed-bed model are shown to be unrealistic; the computed flood level is not substantiated by measured data. On the other hand, the FLUVIAL-11 results are supported by measured data. Since a small difference in flood level may involve a large difference in the inundated area, the accuracy of flood-level prediction is of major importance in flood-plain management. River-channel changes may include channel-bed aggradation and degradaton, width variation, and lateral migration in channel bends. These changes are interrelated as they may occur concurrently. Changes in channel-bed elevation are inseparable from changes in channel width because a channel tends to become narrower during degradation while it tends to widen during aggradation. Therefore, a hydrodynamic model for erodible channels must include these variables."

4. RMA. "The accuracy of model simulations depend on the accuracy with which initial conditions, sediment properties, etc., are specified. In all of the cases we modeled, the data available were sparse and certainly insufficient for using model results for design. We have been able to demonstrate here, however, the significance of accounting for bottom changes in flood routing."

The principal conclusions and recommendations arrived at by the Committee in this study may be summarized as follows:

1. None of the movable-bed models evaluated was found to yield wholly satisfactory results. However, all of the models seem to make reasonably accurate predictions of flood water-surface profiles provided appropriate friction factors are utilized in the computations. This conclusion is attested to by the fact that the HEC2SR, HEC-6, FLUVIAL-11, and SEDIMENT-4H movable-bed models all predicted closely the water-surface profiles for the lower reach of SLR (X = 0 - 10,150 ft), for which Manning's n values obtained from the February 1980 flood records were provided in the input. At over one-half of the stations in this reach, the difference between the highest and lowest stages predicted by the four models were not more than two feet. However, water-surface profiles predicted by the same models for the upper reach of this study section deviated widely, apparently because the available field data were inadequate to determine n values. It is concluded, therefore, that a major deficiency of all movable-bed models is their inability to accurately predict channel roughness or friction factor from the input variables provided. Because the friction factor has a major effect on river stages, this deficiency is a major one.

2. The effects of uncertainty surrounding variations in the channel roughness on flood stages are far greater than the effects of bed erodibility and the attendant degradation/aggradation. Accordingly, until models are developed which include better friction-factor or channel-roughness predictors, and then except in situations in which extensive input and calibration data on channel geometry, bed-material composition, water and sediment hydrographs, etc. are available, the added cost of utilizing movable-bed rather than fixed-bed models is not justified in most cases.

3. An exception to the recommendation set forth in item 2, above, arises in the case of severely disturbed rivers (e.g., by channel straightening or aggregate mining), or channels in very unstable conditions. If adequate input and calibration data are available, erodible-bed models should be utilized in these cases, because the large-scale geometry changes occurring during a flood can have significant flood-stage effects. It is repeated, for emphasis, that localized channel-bed degradation/aggradation has such minor effects on flood-stage elevations that this feature of channel change is masked by uncertainties about the channel roughness and friction factor, initial conditions, and sediment input to the study reach.

4. In order to instill more confidence in fixed-bed models, and to provide guidance concerning the extent and accuracy of the input data required to achieve a specified level of precision, there is a need to undertake a detailed sensitivity analysis of the results to such input variables as channel roughness, channel slope, cross-section geometry, and input hydrograph characteristics (including unsteadiness). In the HEC study of Line Creek, Mississippi (HEC, 1970), HEC-2 was found to be very sensitive to these variables. In particular, the findings of this study showed that the increases in water-surface levels attendant to larger values of Manning's n tend to increase as channel slope decreases; the influence of inaccuracies in channel cross-section geometry tends to increase as channel slope increases; and the influence of discharge errors decreases with increasing channel slope.

5. Because degradation and aggradation are the result of streamwise gradients in the sediment-transport capacity of streams, a very reliable sediment-transport relation is a prerequisite to reliable estimates of channel-geometry changes. It is in the calculation of sediment-discharge

capacities that the various models examined differed most widely. The SLA approach of expressing sediment-transport capacity as a power-law function of local mean velocity and flow depth seems to be reasonable, provided that adequate data are available for the stream being modeled to evaluate the coefficient and exponents appearing in the transport relation. As presently utilized, however, this approach does not make an adequate accounting of the critically important effects of bed armoring.

6. A conspicuous stumbling block in making predictions of channel degradation is the poor understanding and formulation of the bed-armoring process, and the effect of armoring on channel roughness and the sediment-discharge capacity of the flow. Until the formulation of these phenomena are improved, all movable-bed models are likely to be somewhat unreliable in predicting thalweg-elevation changes. Improved formulation of these phenomena must, in turn, await further research.

7. Future alluvial-channel modeling efforts should be directed toward improved incorporation of channel-width changes and channel-pattern migration. There is also a need to improve the formulation of large-scale, abrupt, tributary-sediment inputs to rivers. The approach utilized by SDSU in incorporating these features appears to be in the right direction.

8. It is unlikely that a movable-bed model will be forthcoming that is applicable to all types of rivers. Instead, each model will be more dependable for rivers of the type for which it was developed. Accordingly, there is a need to undertake an effort to classify natural rivers in terms of their hydraulic and geomorphological characteristics to provide for selection and application of appropriate models that use appropriate, constituent formulations for sediment discharge, channel roughness, bank erodibility, etc.

APPENDIX: BIOGRAPHICAL SKETCHES OF COMMITTEE MEMBERS AND CONSULTANT

JOHN F. KENNEDY is Director of the Iowa Institute of Hydraulic Research and Carver Distinguished Professor in the Energy Engineering Division of The University of Iowa. He studied Civil Engineering at Notre Dame University where he received the BSCE in 1955. He entered graduate school at California Institute of Technology, where he received his M.S. in 1956 and, after a period of service as a Second Lieutenant in the U.S. Army Corps of Engineers, his Ph.D. in 1960, both in Civil Engineering. He was a Research Fellow at Caltech from 1960 to 1961, when he became Assistant Professor at Massachusetts Institute of Technology, where he was promoted to the rank of Associate Professor in 1964. In 1966 he accepted the position of Director of the Iowa Institute of Hydraulic Research and Professor of Fluid Mechanics at The University of Iowa. From 1974 to 1976 he also served as Chairman of UI's Division of Energy Engineering, and in July 1981 was named Carver Distinguished Professor. He has received many awards; among these was his election to membership in the National Academy of Engineering in 1973; receipt of ASCE's Stevens (in 1961), Huber (in 1964), and Hilgard (in 1974 and 1978) prizes; selection as ASCE's Hunter Rouse Lecturer in 1981; and his election to the Presidency of the International Association for Hydraulic Research in 1980. He was re-elected to that office in 1982 and currently is serving his second two-year term. His principal technical interests include river hydraulics, ice engineering, cooling-tower technology, and density-stratified flows.

DAVID R. DAWDY is a hydrologic consultant in San Francisco, California. He received his B.A. in History in 1948 from Trinity University in San Antonio, Texas, and his M.S. in Statistics in 1962 from Stanford University. He served 25 years in the United States Geological Survey, where he did research in statistical flood frequency analysis, stochastic simulation of streamflows, rainfall-runoff modeling, and resistance to flow and sediment transport in alluvial streams. For the last 6 years he has been in private consulting, involved with the National Flood Insurance Program, design storm analysis for major dams in South America,

and scour at river crossings. He is Chairman, U.S. National Committee for International Association of Hydrological Sciences; member, U.S. National Committee for International Union of Geodesy and Geophysics; and Adjunct Professor of Civil Engineering, University of Mississippi.

CARL F. NORDIN is a research hydrologist with the U.S. Geological Survey in Denver, Colorado. He received his B.S. and M.S. in Civil Engineering from the University of New Mexico and his Ph.D. from Colorado State University. He is a specialist on sediment transport in rivers, and on stochastic processes in hydraulics and hydrology. He has served on committees of the American Society of Civil Engineers, American Geophysical Union, International Association for Hydraulic Research, and the National Research Council.

JOHN C. SCHAAKE, Jr., is presently responsible for the river and flood forecast operations of the National Weather Service. His position is Chief, Hydrologic Services Division and he also serves as NWS Deputy Associate Director for Hydrology. He first joined the NWS in 1974 as Deputy Director, Hydrologic Research Laboratory. From 1968 to 1974, he was a member of the MIT Civil Engineering Faculty. Prior to that he held joint appointments at the University of Florida in Environmental Engineering and in Industrial and System Engineering. He received B.E.S. and Ph.D. degrees from the John Hopkins University, and held a Post-Doctoral Fellowship at Harvard University. Throughout his career, he has been involved in areas of consulting engineering practice associated with his research in urban hydrology, water resources planning and in both stochastic and determining modeling of hydrologic systems.

STANLEY A. SCHUMM is Professor of Geology at Colorado State University, Fort Collins, Colorado. He received his B.A. in Geology from Upsala College in 1950 and Ph.D. in Geomorphology from Columbia University in 1955. He served 12 years as a geologist for the U.S. Geological Survey. He was a Visiting Lecturer at the University of California, Berkeley from 1959 to 1960; and a Visiting Fellow at the University of Sydney, Australia, from 1964 to 1965. In 1967, he accepted his present position with Colorado

State University and during 1972-1973 was Acting Associate Dean for Research. He received the Horton Award in 1957 from the American Geophysical Union, and in 1970 he received "Honorable Mention" for his paper "Geomorphic Approach to Erosion Control in Semiarid Regions" from the American Society of Agricultural Engineers. In 1979, he received the Kirk Bryan Award of the Geological Society of America for his book "The Alluvial System." In 1980, he received the Distinguished Alumni Award for scientific contributions from Upsala College and the L.W. Durrell Award for research and creativity from Colorado State University. He is presently a member of the NAS-NRC Committee on Disposal of Excess Spoil. He also has served on other technical and advisory Committees of the National Research Council, Geological Society of America, American Geophysical Union, International Geographical Union, American Society of Civil Engineers, U.S. Forest Service and National Park Service.

VITO A. VANONI is Professor of Hydraulics Emeritus, California Institute of Technology (Caltech), Pasadena, California. Since retiring in 1974, he has been active in consulting on sedimentation problems. All of his academic training was at Caltech where he received B.S., M.S., and Ph.D. degrees in Civil Engineering in 1926, 1932, and 1940, respectively. He started his research in sedimentation with the U.S. Soil Conservation Service in 1935 and continued it without interruption while on the Caltech faculty, which he joined in 1947. His research has been experimental in nature and has dealt mostly with the mechanics of sediment suspension, flow resistance, temperature effects, and alluvial bed forms. He has been active for many years consulting on river problems. Among his clients have been the U.S. Army Corps of Engineers, the California Division of Water Resources, and the Bechtel Corporation. He has lectured on sedimentation and consulted on river problems in several countries in Latin America. He was awarded the ASCE Hilgard prizes in 1949 and 1976 for his ASCE paper on suspended-sediment transport mechanics and for his editing of the ASCE monograph "Sedimentation Engineering", respectively. He was elected to the National Academy of Engineering in 1977.

TATSUAKI NAKATO is a Research Scientist at the Iowa Institute of Hydraulic Research of The University of Iowa. He received his B.S. and M.S. degrees in Civil Engineering at Nagoya University, Nagoya, Japan in 1966 and 1968; and his Ph.D. degree in Mechanics and Hydraulics at The University of Iowa in 1974. Since 1975, he has conducted research in sediment-transport processes and been engaged in numerous hydraulic-model investigations at the Iowa Institute of Hydraulic Research.

LIST OF REFERENCES

Amein, M., and Chu, H.L., "Implilcit numerical modeling for unsteady flows," Journal of the Hydraulics Division, ASCE, Vol. 101, No. HY6, June 1975.

Anderson-Nichols/West, "Design review of the Salt River channelization project," prepared by Roberts, B.R., et al., for Corps of Engineers, Sacramento, Californnia, November 1980.

Ariathurai, R., "Erosion and sedimentation downstream from Harry S. Truman Dam as a result of hydropower operations," prepared for Corps of Engineers, Kansas City, Missouri, May 1980.

Brown, C.B., "Sediment transportation," Engineering Hydraulics, H. Rouse ed., John Wiley and Sons, Inc., New York, N.Y., 1950.

Chang, H.H., and Hill, J.C., "Computer modeling of erodible flood channels and deltas," Journal of the Hydraulics Division, ASCE, Vol. 102, No. HY10, October 1976.

Chang, H.H., and Hill, J.C., "Minimum stream power for rivers and deltas," Journal of the Hydrauulic division, ASCE, Vol. 103, No. hY12, December 1977.

Chang, H.H., "Mathematical model for erodible channels," Journal of the Hydraulics Division, ASCE, Vol. 108, No. HY5, May 1982.

Colby, B.R., "Relationship of unmeasured sediment discharge to mean velocity," Transactions, American Geophysical Union, Vol. 38, No. 5, October 1957.

Engelund, F. and Hansen, E., "A monograph on sediment transport in alluvial streams," Teknisk Vorlag, Copenhagen, Denmark, 1967.

Gessler, J., "Beginning and ceasing of sediment motion," River Mechanics, Vol. 1, Colorado State University, Fort Collins, Colorado, 1971.

Graf, W.H., "Hydraulics of sediment transport," McGraw-Hill Book Co., Inc., New York, N.Y. 1971.

Hydrologic Engineering Center, "National Academy of Sciences study of computer based flood and sediment routing models, San Lorenzo River, California and Salt River, Arizona," prepared by MacArthur, R.C., and Gee, M.D., Corps of Engineers, Davis, California, January 1982.

Hydrologic Engineering Center, "Sensitivity analysis of factors that influence water surface profiles: HEC-2," Corps of Engineers, Davis, California, October 1970.

Hydrologic Engineering Center, "Scour and deposition in rivers and reservoirs," Computer Program HEC-6, Corps of Engineers, Davis, California, March 1977.

Jennings, M.E., and Land, L.F., "Simulation studies of flow and sediment transport using a mathematical model, Atchafalaya River basin, Louisiana," U.S.G.S. Water-Resources Investigation 77-14, May 1977.

Jones-Tillson & Associates, et al., "San Lorenzo River study, stage II, field and simulation studies," prepared for Corps of Engineers, San Francisco, California, September 1980.

Laursen, E.M., "The total sediment load of streams," Journal of the Hydraulics Division, ASCE, Vol. 54, February 1958.

Nakato, T., and Vadnal, J.L., "Field study and tests of several one-dimensional sediment-transport computer models for Pool 20, Mississippi River," IIHR Report No. 237, Iowa Institute of Hydraulic Research, The University of Iowa, July 1981.

Prasuhn, A.L., and Sing, E.F., "Modeling of sediment transport in Cottonwood Creek," Proceedings of the Specialty Conference on Computer and Physical Modeling in Hydraulic Engineering, ASCE, Chicago, Illinois, August 1980.

Resource Management Associates, "Flood routing with movable bed," prepared by Ariathurai R., and Smith, D.J., March 1982.

Rouse, H., "Modern conception of the mechanics of fluid turbulence," Transactions, ASCE, Vol. 102, Paper No. 1965, 1937.

San Diego State University, "Computer-based flood and sediment routing model: case studies of San Dieguito River, California; San Lorenzo River, California; and Salt River, Arizona," prepared by Chang, H.H., and Hill, J.C. for National Research Council, January 1982.

Simons, Li & Associates, Inc., "Erosion, sedimentation, and debris analysis of Boulder Creek (24th Street Bridge to 30th Street Bridge), Boulder, Colorado," prepared for URS Company, Denver, Colorado, 1980.

Simons, Li & Associates, Inc., "Scour and sedimentation analysis of the proposed channelization of the Salt River for protecting the Sky Harbor International Airport in Phoenix, Arizona," prepared for HNTB, Kansas City, Missouri, December 1980.

Simons, Li & Associates, Inc., "River response analysis associated with Rio Nuevo-Santa Cruz River flood control and channelization project, Tucson, Arizona," prepared for Cella Barr Associates, 1981.

Simons, Li & Associates, Inc., "Cañada del Oro Wash flood control project - Oro Valley, Pima County, Arizona," prepared for Department of Water Resources, Phoenix, Arizona, 1981.

Simons, Li & Associates, Inc., "Sediment transport analysis of Rillito River and tributaries for regional flood control element of the Tucson urban study," 1981.

Simons, Li & Associates, Inc., "Application of hydrodynamic computer models to flood analysis," prepared for National Research Council, February 1982.

Simons, D.B., Li, R.M., and Brown, G.O., "Sedimentation study of the Yazoo River basin-user manual for Program KUWASER", Report No. CER79-80DBS-R, Colorado State University, August 1979.

Simons, D.B., et al., "A geomorphic study of Pools 24, 25, and 26 in the Upper Mississippi and Lower Illinois Rivers," Report No. CER74-75DBS-SAS-MAS-YHC-PFL8, Colorado State University, March 1975.

Simons, D.B., and Chen, Y.H., "A mathematical model study of Pool 4 in the Upper Mississippi and Lower Chippewa Rivers," Report No. CER76-77DBS-YHC-8, Colorado State University, October 1976.

Simons, D.B., and Chen, Y.H., "Investigation of the effects of Chippewa River erosion and silt reduction measures," Report No. CER76-DBS-YHC-54, Colorado State Univesity, 1977.

Simons, D.B., Chen, Y.H., and Saez-Benito, J.M., "A mathematical model of Pools 5 through 8 in the Upper Mississippi River system," Report no. CER79-80DBS-YHC-JMS21, Colorado State University, December 1979.

Simons, D.B., and Chen, Y.H., "A mathematical model of the Lower Chippewa River network system," Report No. CER78-79-DBS-YHC58, Colorado State University, June 1979.

Simons, D.B., and Chen, Y.H., "Assessment of hydraulic impacts of the Atchafalaya River flood control program on the Lower Mississippi River," Report No. CER77-78DBS-YHC38, Colorado State University, August 1978.

Thomas, W.A., and Prasuhn, A.L., "Mathematical modeling of scour and deposition," Journal of the Hydraulics Division, ASCE, Vol. 103, No. HY8, August 1977.

Toffaleti, F.B., "A procedure for computation of the total river sand discharge and detailed distribution, bed to surface," Technical Report No. 5, Committee on Channel Stabilization, Corps of Engineers, Vicksburg, Mississippi, November 1968.

Williams, D.T., "Effects of dam removal: an approach to sedimentation," Technical Paper No. 50, Hydrologic Engineering Center, Corps of Engineers, Davis, California, October 1977.

Yang, C.T., "Incipient motion and sediment transport," Journal of the Hydraulics Division, ASCE, Vol. 99, No. HY10, October 1973.

COMPUTATIONAL HYDRAULICS

AT THE

IOWA INSTITUTE OF HYDRAULIC RESEARCH

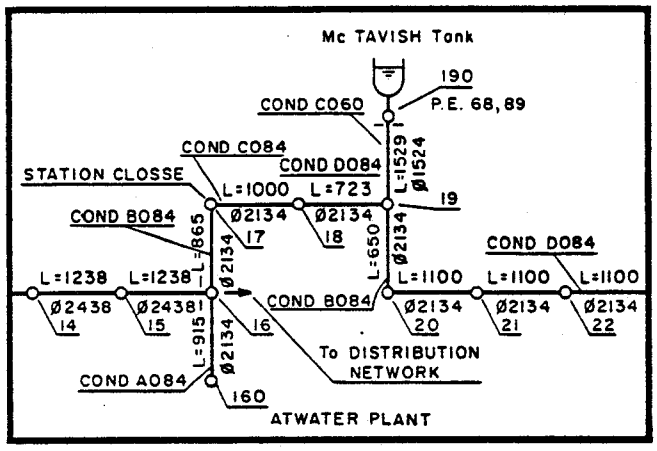

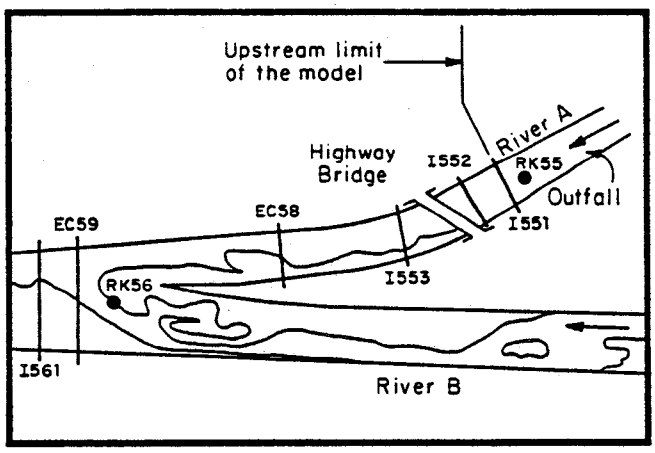

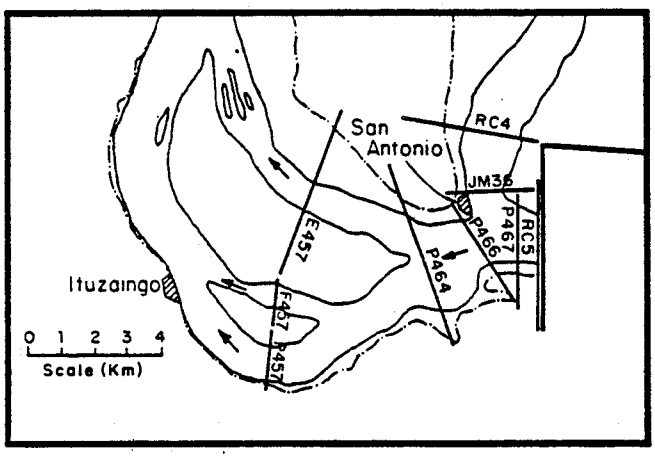

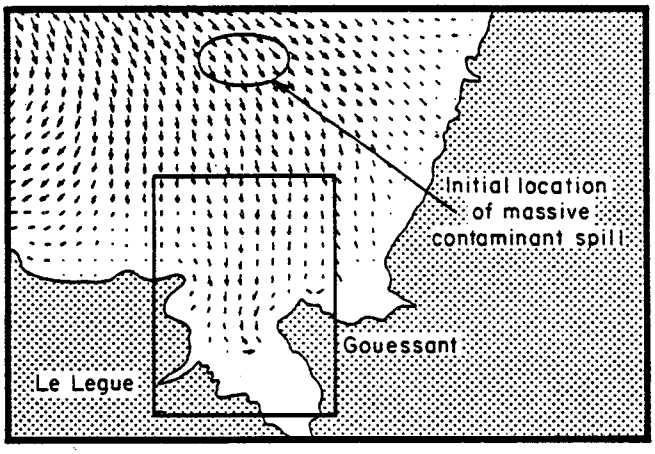

THE UNIVERSITY OF IOWA
IOWA CITY, IOWA

OCTOBER 1985

COMPUTATIONAL HYDRAULICS

AT THE

IOWA INSTITUTE OF HYDRAULIC RESEARCH

A Summary of Capabilities

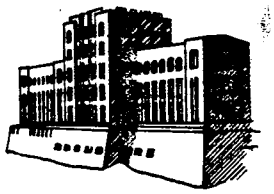

Iowa Institute of Hydraulic Research
The University of Iowa
Iowa City, Iowa 52242

October 1985

TABLE OF CONTENTS

Page

I. Introduction.....1

II. Computational Hydraulics Staff.....2

III. Brief Descriptions of Computer Programs.....18

ARGOS (Pollutant dispersion in 2-D flow).....19

BRALLUVIAL (Quasi-steady water and sediment routing in multiply connected channel networks).....23

CAREDAS (Unsteady flow in looped storm sewer networks)...27

CAREMUSK (Unsteady flow in branched storm sewers).....32

CARIMA (Unsteady flow in river and canal systems).....35

CERTITUDE (Water hammer in pipe networks).....40

CHAR II (Water and sediment routing in rivers).....44

CHARIMA (Fully unsteady water and sediment routing in multiply connected channel networks).....49

CYTHERE-ES1 (Unsteady flow in two dimensions).....50

IALLUVIAL (Water and sediment routing in rivers).....54

POLDER (Pollutant dispersion in rivers).....57

PROCEDURE (Flow in looped water distribution networks)...61

SEDRES (Sedimentation in reservoirs).....67

CONDOR (Unsteady contaminant dispersion in river and canal networks).....70

IV. Additional Programs Available at IIHR.....74

V. Selected Additional Programs Available at SOGREAH.....74

I. INTRODUCTION

The purpose of this brochure is briefly to describe the computational hydraulics capabilities of the Iowa Institute of Hydraulic Research (IIHR). These capabilities consist of two basic elements:

* Computational hydraulics personnel (see Section II)
* Available software (see Sections III, IV, and V)

The software described consists of proven, well documented, industrialized program systems for the solution of a broad range of engineering hydraulics problems using mathematical modeling techniques. When a particular problem is not susceptible to study using these existing programs, the needed extensions or innovations can be developed by the computational hydraulics staff, drawing on the experience and technical expertise available at the Institute.

Many of the programs described in Sections III and IV are available through agreement with SOGREAH Ingenieurs Conseils, Grenoble, France. SOGREAH has been heavily involved in computational hydraulics development since the early beginnings of this discipline in the 1950's. As a consulting engineering firm with projects throughout the world, SOGREAH has developed a broad range of computational hydraulics programs which have had to be responsive to the needs of clients while being economical, reliable, and usable by engineers other than the originators. The Institute is indeed fortunate to be able to draw upon the computational hydraulics tradition, experience, and technical expertise of SOGREAH.

II. COMPUTATIONAL HYDRAULICS STAFF

The individuals listed below and whose abridged curriculum vitae appear in the following pages are the IIHR professional staff members whose activities include computational hydraulics. These engineers have the responsibility of operating the program systems described in this brochure, as well as of developing new software for clients' particular problems as required.

Name	Address	Telephone	Telex	Bitnet ID
F. M. Holly	Room 301A, Hydraulics Lab The University of Iowa Iowa City, Iowa 52242	319-353-5896	756569	AEGCRAPA@UIAMVS
J. F. Kennedy	Room 403A Hydraulics Lab The University of Iowa Iowa City, Iowa 52242	319-353-4679	756569	AEGCRAPA@UIAMVS
T. Nakato	Room 308B1 Hydraulics Lab The University of Iowa Iowa City, Iowa 52242	319-353-5016	756569	AEGCRAPA@UIAMVS
S. C. Jain	Room 200D Hydraulics Lab The University of Iowa Iowa City, Iowa 52242	319-353-3358	756569	AEGCRAPA@UIAMVS
A. J. Odgaard	Room 200A Hydraulics Lab The University of Iowa Iowa City, Iowa 52242	319-353-4194	756569	AEGCRAPA@UIAMVS
J. L. Schnoor	Room 2134 Engineering Bldg The University of Iowa Iowa City, Iowa 52242	319-353-7262	756569	AEGCRAPA@UIAMVS
M. F. Karim	Room 307B Hydraulics Lab The University of Iowa Iowa City, Iowa 52242	319-353-5838	756569	AEGCRAPA@UIAMVS
K. P. Georgakakos	Room 307A Hydraulics Lab The University of Iowa Iowa City, Iowa 52242	319-353-4034	756569	AEGCRAPA@UIAMVS

Abridged Curriculum Vitae

for

Forrest M. Holly, Jr.

October 1985

Present Position:

Associate Professor, Department of Civil and Environmental Engineering, and Research Engineer, Institute of Hydraulic Research, The University of Iowa

Areas of Research Interest:

Computational Hydraulics; Turbulent Dispersion in Natural Waters; Sediment Transport

Higher Education:

B.S. (Civil Engineering), 1968, Stanford University

M.S. (Civil Engineering), 1969, University of Washington

Ph.D. (Civil Engineering), 1975, Colorado State University

Employment Record:

04/69-08/69	Engineer Trainee, U.S. Corps of Engineers, Seattle, WA
08/69-01/70	Jr. Civil Engineer, County of San Diego, CA
04/70-03/72	Research Engineer, U.S. Corps of Engineers, Vicksburg, MS
08/73-12/73	Engineer, Northwest Hydraulics Consultants, Ltd., Edmonton, Alberta
07/75-12/75	Engineer, Dames and Moore, Washington, D.C.
02/76-06/81	Engineer, SOGREAH, Grenoble, France
08/81-06/82	Visiting Research Scientist, University of Reading, England
06/82-pres.	Associate Professor and Research Engineer, The University of Iowa, Iowa City, IA

Professional Affiliations and Registration:

American Society of Civil Engineers (Member)

International Association for Hydraulic Research (Member)

Society of Sigma Xi (Member)

American Geophysical Union (Member)

Registered Professional Engineer: Iowa, Colorado, Alberta

Recognitions:

Arthur T. Ippen Award, IAHR, 1983

University of Iowa Faculty Scholar, 1985-88

Abridged Curriculum Vitae

for

John F. Kennedy

October 1985

Present Position:

Carver Distinguished Professor of Fluid Mechanics and Director, Institute of Hydraulic Research, The University of Iowa

Research Specialization:

Hydraulic structures, pump intakes, sediment transport, coastal processes, arctic engineering, cooling tower technology, management of waste heat from steam generation of electrical power, turbulent mixing

Higher Education:

B.S. (Civil Eng'g, magna cum laude), 1955, Univ. of Notre Dame
M.S. (Civil Eng'g), 1956, California Institute of Technology
Ph.D. (Civil Eng'g), 1960, California Institute of Technology

Employment Record:

09/56-06/56	Teaching Assistant, California Institute of Technology, Pasadena, CA
06/56-03/57	Stress Analyst, Sandia Corporation, Albuquerque, NM
09/57-06/60	Active Duty, 2nd Lt., U.S. Army Corps of Engineers, Ft. Belvoir, VA
09/60-08/61	Postdoctoral Fellow, California Institute of Technology, Pasadena, CA
09/61-06/64	Assistant Professor, Massachusetts Institute of Technology, Cambridge, MA
07/64-06/66	Associate Professor, Massachusetts Institute of Technology, Cambridge, MA
07/74-06/76	Chairman, Energy Engineering Division, The University of Iowa, Iowa City, IA

07/66-07/81 Professor of Fluid Mechanics and Director, Institute of Hydraulic Research, The University of Iowa, Iowa City, IA

07/81-Pres. Carver Distinguished Professor and Director, Institute of Hydraulic Research, The University of Iowa, Iowa City, IA

Professional Affiliations and Registration:

National Academy of Engineering (Member)

International Association for Hydraulic Research (Member and President)

American Society of Civil Engineers (Member)

American Society of Mechanical Engineers (Member)

Society of Sigma Xi (Member)

American Society of Engineering Education (Member)

Registered Professional Engineer: California

Recognitions:

Elected to National Academy of Engineering, 1973; J.C. Stevens Award for Outstanding Discussion (ASCE), 1964; Huber Prize for Outstanding Research (ASCE), 1964; Hilgard Hydraulic Prize (ASCE), 1974 and 1978; Notre Dame University Engineering Honor Award, 1978; Elected President of International Association for Hydraulic Research, (1980-82 term; re-elected for 1982-84 term); Hunter Rouse Hydraulic Engineering Lecture Award (ASCE), 1981; Named Carver Distinguished Professor, The University of Iowa, 1981; Iowa Governor's Medal for Science Application, 1983; Elected Honorary Member of Hungarian Hydrological Society (first American so honored), 1983; Elected Honorary Fellow, Institute of Water Conservancy and Hydroelectric Power Research (Beijing, China)(first foreign scholar so honored), 1985; Named Honorary Professor, East China Technical University of Water Resources (Nanjing, China), 1985.

Abridged Curriculum Vitae

for

Tatsuaki Nakato

October 1985

Present Position:

Adjunct Assistant Professor, Division of Energy Engineering, and Research Scientist, Institute of Hydraulic Research, The University of Iowa

Areas of Research Interest:

Sedimentation engineering, experimental hydraulics, hydraulic structures

Higher Education:

B.S. (Civil Engineering), 1966, Nagoya University, Japan

M.S. (Civil Engineering), 1968, Nagoya University, Japan

Ph.D. (Mechanics and Hydraulics), 1974, The University of Iowa

Employment Record:

1974-76	Assistant Research Scientist, The University of Iowa, Iowa City, IA
1976-78	Adjunct Assistant Professor & Associate Research Scientist, The University of Iowa, Iowa City, IA
1978-pres.	Adjunct Assistant Professor & Research Scientist, The University of Iowa, Iowa City, IA

Professional Affiliations and Registration:

Japan Society of Civil Engineers (Member)

American Society of Civil Engineers (Member)

Society of Sigma Xi (Member)

International Association for Hydraulic Research (Member)

Abridged Curriculum Vitae

for

Subhash C. Jain

October 1985

Present Position:

Professor, Civil and Environmental Engineering, and Research Engineer, Institute of Hydraulic Research, The University of Iowa

Research Specialization:

Hydraulic structures, thermal hydraulic model studies, river mechanics, air entrainment

Higher Education:

B.Sc. (Phy., Chem., Math.), 1957, Agra University (India

B.S. (Civil Engineering), 1960, University of Roorkee (India)

M.E. (Civil Engineering), 1966, University of Roorkee (India)

Ph.D. (Mechanics and Hydraulics), 1971, The University of Iowa

Employment Record:

09/61-09/67	Lecturer, M.N.R. Engineering College, Allaharsad, India
10/70-09/73	Postdoctoral Research Engineer, The University of Iowa, Iowa City, IA
09/73-11/73	Reader, University of Roorkee, Roorkee, India
11/73-03/74	Professor, Birla Institute of Technology and Science, Birla, India
09/71-08/77	Assistant Professor & Research Engineer, The University of Iowa, Iowa City, IA
08/77-08/82	Associate Professor & Research Engineer, The University of Iowa, Iowa City, IA
08/82-pres.	Professor & Research Engineer, The University of Iowa, Iowa City, IA

Professional Affiliations and Registration:

Society of Sigma Xi (Member)

International Association for Hydraulic Research (Member)

American Society of Civil Engineers (Member)

American Geophysical Union (Member)

Recognitions:

Gold medal for obtaining highest marks in Math in B.E., 1960

C.S. Yih award for the best Ph.D. thesis of the year, 1971

Abridged Curriculum Vitae

for

A. Jacob Odgaard

October 1985

Present Position:

Associate Professor, Civil and Environmental Engineering, and Research Engineer, Institute of Hydraulic Research, The University of Iowa

Areas of Research Interest:

River Mechanics, Hydraulic Structures, Environmental Fluid Mechanics, Experimental Methods, Coastal Engineering

Higher Education:

M.S. (Civil and Structural Engineering), 1966, The Technical University of Denmark

Ph.D. (Civil and Structural Engineering), 1970, The Technical University of Denmark

Employment Record:

1966-72	Research Engineer, Technical University of Denmark
1972-73	U.N. Assignment in Brazil
1973-74	Post-Doctoral Scholar, University of Cambridge, England
1974-77	Senior Research Engineer, Danish Hydraulic Institute
1977-80	Adjunct Assistant Professor & Research Scientist, The University of Iowa, Iowa City, IA
1980-84	Assistant Professor & Research Engineer, The University of Iowa, Iowa City, IA
1984-pres.	Associate Professor & Research Engineer, The University of Iowa, Iowa City, IA

Professional Affiliations and Registration:

American Society of Civil Engineers (Member)

International Association for Hydraulic Research (Member)

National Society of Professional Engineers (Member)

Iowa Engineering Society (Member)

Sigma Xi (Member)

Registered as Professional Engineer in Iowa

Recognitions:

British Council Scholarship, 1973

Abridged Curriculum Vitae

for

Jerald L. Schnoor

October 1985

Present Position:

Professor and Chairman, Department of Civil and Environmental Engineering, and Research Engineer, Institute of Hydraulic Research, The University of Iowa

Areas of Research Interest:

Water Quality Modelling, Toxic Chemicals, Acid Rain, Groundwater Quality and Hazardous Wastes

Higher Education:

B.S. (Chemical Engineering), 1972, Iowa State University

M.S. (Environmental Health Engineering), 1974, University of Texas

Ph.D. (Civil Engineering), 1975, University of Texas

Employment Record:

1975-76	NSF Postdoctoral Fellow, Manhattan College, New York, NY
1977-80	Assistant Professor and Research Engineer, The University of Iowa, Iowa City, IA
1980-83	Associate Professor and Research Engineer, The University of Iowa, Iowa City, IA
1982	Visiting Professor, Swiss Federal Institute of Technology (EAWAG), Zurich, Switzerland
1982-83	Visiting Professor, Swiss Federal Institute of Technology, EAWAG, ETH
1983-pres.	Professor and Research Engineer

Professional Affiliations and Registration:

Water Pollution Control Federation (Member)

American Institute of Chemical Engineers (Member)

American Water Works Association (Member)

American Society of Civil Engineers (Member)

Society of Environmental Toxicology and Chemisty (Member)

Association of Environmental Engineering Professors (Member)

Tau Beta Pi, Omega Chi Epsilon, Chi Epsilon (Member)

Recognitions:

Water L. Huber Research Prize, American Society of Civil Engineers, 1985

President, Iowa Groundwater Association, 1984-85

Associate Editor, Water Resources Research, 1985-

Editorial Board, Environmental Toxicology and Chemistry, 1982-

Editorial Board, Ecological Modeling, 1983-85

Editorial Board, Environmental Professional, 1984

NRC/NAS Panel on Lake Acidification Processes, 1984

University of Iowa Faculty Scholar, 1980-83

U.S. Delegate to USSR, 1981

Merit Award, American Chemical Society, Environmental Division, 1981

Best Paper Award, ASTM Aquatic Toxicology, 1980

Abridged Curriculum Vitae

for

M. Fazle Karim

October 1985

Present Position:

Assistant Research Scientist, Institute of Hydraulic Research, The University of Iowa

Areas of Research Interest:

Mechanics of alluvial river processes including sediment transport, friction factor, and bed configuration; computer-based mathematical modelling of nonequilibrium river processes; water and sediment routing in open-channel flows; sedimentation in natural and impounded lakes.

Higher Education:

B.E. (Civil Engineering), 1967, University of Calcutta, India

M.S. (Environmental Engineering), 1972, Harvard University/M.I.T.

Ph.D. (Mechanics and Hydraulics), 1981, The University of Iowa

Employment Record:

00/67-00/68	Louis Burger, Inc., Consulting Engineers, Ltd., Dacca, Bangladesh
00/68-00/70	Water and Power Development Authority, Dacca, Bangladesh
00/70-00/72	Studied at Harvard University and M.I.T.; worked part-time at the Center for Population Studies, Harvard University
00/72-00/75	Bangladesh Water Development Board
00/75-00/85	Iowa Institute of Hydraulic Research, The University of Iowa

Professional Affiliations and Registration:

Associate Member, American Society of Civil Engineers

Member, International Association for Hydraulic Research

Abridged Curriculum Vitae

for

Konstantine P. Georgakakos

October 1985

Present Position:

Assistant Professor, Department of Civil and Environmental Engineering, and Research Engineer, Institute of Hydraulic Research, The University of Iowa

Areas of Research Interest:

Modeling of physical systems under uncertainty; Coupling of stochastic, physically based models of precipitation, soil moisture-groundwater, channel routing; Flash-flood forecasting; Modeling of mesoscale precipitation processes under uncertainty; Parameter estimation for large scale hydrologic models; Filtering theory for large scale nonlinear physical systems; Decomposition-theory applications to Water Resources Systems Planning and Operation; Spatial variability of physical properties from sparse data; Conditional inference; Numerical methods applied to water resources systems

Higher Education:

Sc.D. (Civil Engineering), 1982, Massachusetts Institute of Technology
M.S. (Civil Engineering), 1980, Massachusetts Institute of Technology
Diploma (Civil Engineering), 1977, National Technical University of Athens, Greece

Employment Record:

09/80-01/81	Teaching Assistant, Massachusetts Institute of Technology, Cambridge, MA
06/77-06/82	Research Assistant, Massachusetts Institute of Technology, Cambridge, MA
06/82-08/85	Research Associate, National Oceanic and Atmospheric Administration, Silver Spring, MD

08/85-01/86 Research Hydrologist, Hydrologic Research Laboratory
National Weather Service, NOAA, Silver Spring, MD

Professional Affiliations and Registration:

American Geophysical Union (Member)

Institute of Electrical and Electronics Engineers (Member)

Sigma Xi (Member)

American Association for Advancement of Science (Member)

Greek Technical Chamber (Member)

III. BRIEF DESCRIPTIONS OF COMPUTER PROGRAMS

The following descriptions of computational-hydraulics software are intended to give a general idea of their scope of application, technical basis, and typical results. Additional information in the form of brochures and descriptive reports is available on request, as noted for each program.

The additional programs listed in Section IV are either more research oriented (CHAR I, CHAR III, CHAR IV, MEK002) or less industrialized (ITRM, DWM, ICOOL, JECHAU, PANACHE, THERMO) than those described in this section.

The programs listed in Section V are best employed by their originators at SOGREAH. The Institute can, however, provide additional information and liaison with SOGREAH regarding these programs; most of them are immediately available at SOGREAH or could be transferred to the Institute's computing center for a specific study.

POLLUTANT DISPERSION IN TWO-DIMENSIONAL FLOW

Program Name: ARGOS

Origin: Developed by F. Holly at the University of Reading, England, and A. Preissmann, SOGREAH, in 1981-82. Available by agreement with SOGREAH.

General Description: ARGOS computes the dispersion of one or several conservative, neutrally buoyant, vertically mixed tracers (pollutants) in two-dimensional unsteady flow. This dispersion is due to the combined effects of differential advection by currents and turbulent diffusion. Use of ARGOS requires detailed information on water depths and current speed and direction as a function of time; these are usually obtained from a hydrodynamic mathematical model such as CYTHERE-ES1. The tracer distribution in the model at the beginning of the simulation (usually zero concentration everywhere, otherwise a known or assumed starting condition), and a time-variation of tracer concentration at inflow boundaries (clean water or known pollutant inflow) or from outfalls, complete the data needed for a computation. Results consist of tracer concentrations as a function of time at the points where depths and currents are defined. A special procedure computes the initial stages of growth of tracer clouds of small spatial extent. ARGOS is used for

* determining the zones of influence of, and concentration fields resulting from, pollutant sources such as outfalls, shoreline activity, littoral streams, etc;
* studying the effects of bathymetric modification and structures on existing capacity to disperse pollutants;
* determining the level of treatment needed to meet water quality standards at a particular site.

Particular Features: In each time increment, ARGOS uses a split operator approach in which differential advection is computed by a characteristics method using highly accurate interpolation, and turbulent diffusion is computed using an implicit finite difference scheme. This procedure ensures that very little artificial diffusion is introduced in the advection. The

turbulent mixing is modeled as a gradient diffusion process, with diffusivities evaluated using Elder's formulation; however local values of depth, shear velocity, and dimensionless cross-stream and streamwise diffusivity are employed. The initial growth of small clouds is computed by assuming a jointly Gaussian distribution which is deformed by differential advection and diffusion along the trajectory defined by the current field. These clouds can be superimposed to reproduce a continuous source.

Restrictions: Buoyancy effects and vertical non-homogeneity are excluded in the two-dimensional formulation. The restriction to conservative tracers can easily be removed by incorporating biological and/or chemical decay.

Published References:

Holly, F.M. Jr and Usseglio-Polatera, J.M., "Dispersion Simulation in Two-Dimensional Tidal Flow", Journal of Hydraulic Engineering, ASCE, Vol. 110, No. 7, July, 1984, pp. 905-926.

Example of Application: Figure 1 shows the tidal currents computed by CYTHERE-ESI in the Bay of Saint-Brieuc, France. A large contaminant spill was placed in the bay at high water slack tide as shown; during the following tidal cycle it was swept out nearly to the seaward boundary, then back again very close to its starting position. Figure 2 shows a cross-section of the concentration profile after one tidal cycle, along with a "small cloud" computation of the same spill for comparison. Figure 3 shows the evolution of another authentically small cloud in the lower part of the Bay, during the same tidal cycle.

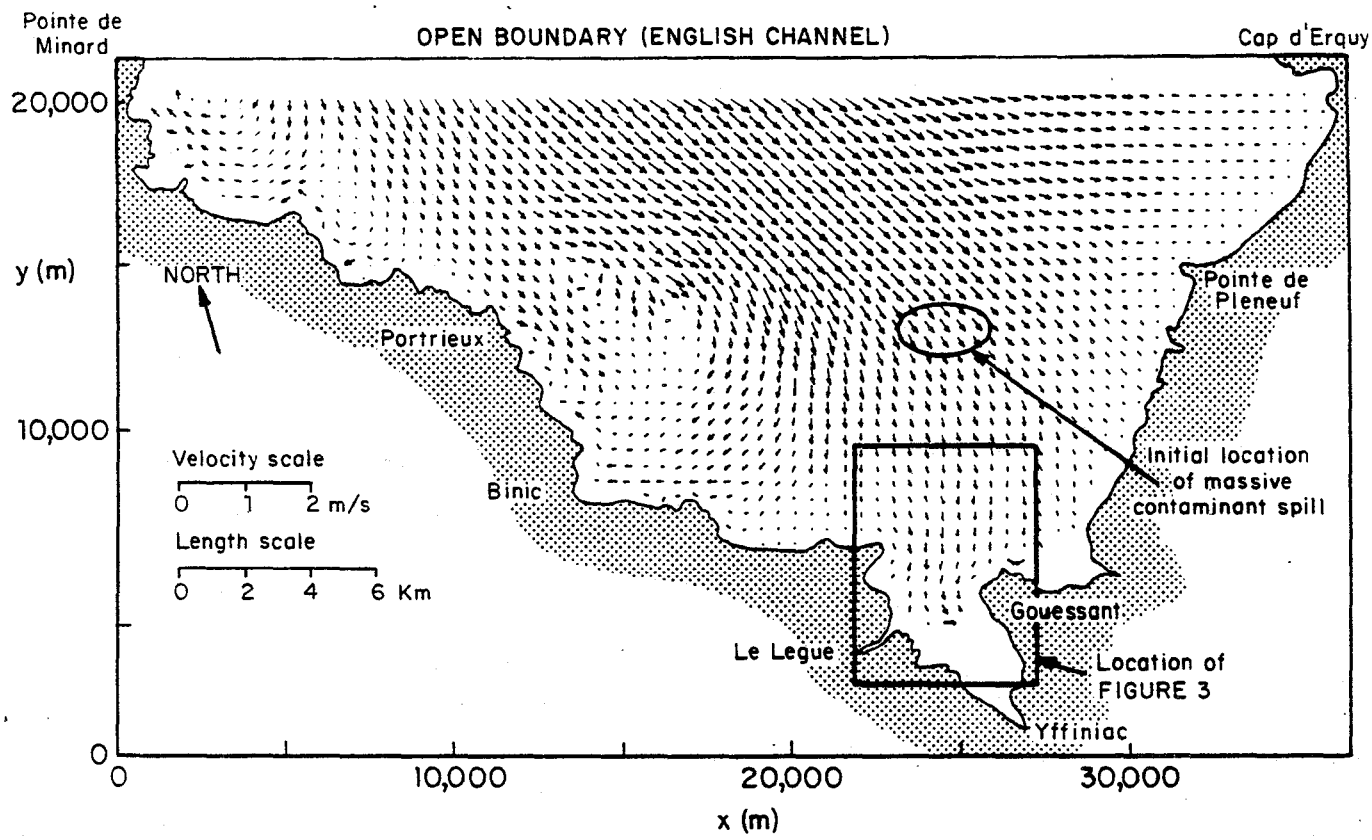

Figure 1. Tidal currents in the bay of Saint-Brieuc.

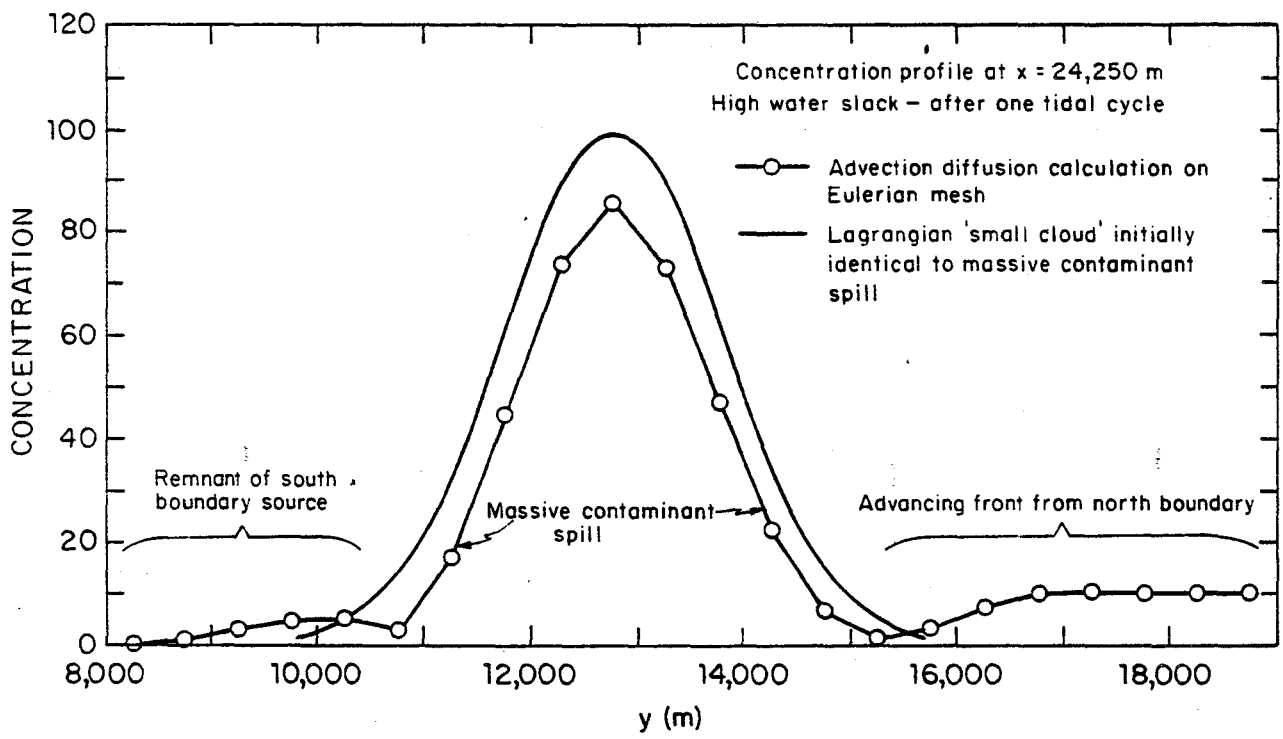

Figure 2. Computed concentration profiles in the bay of Saint-Brieuc.

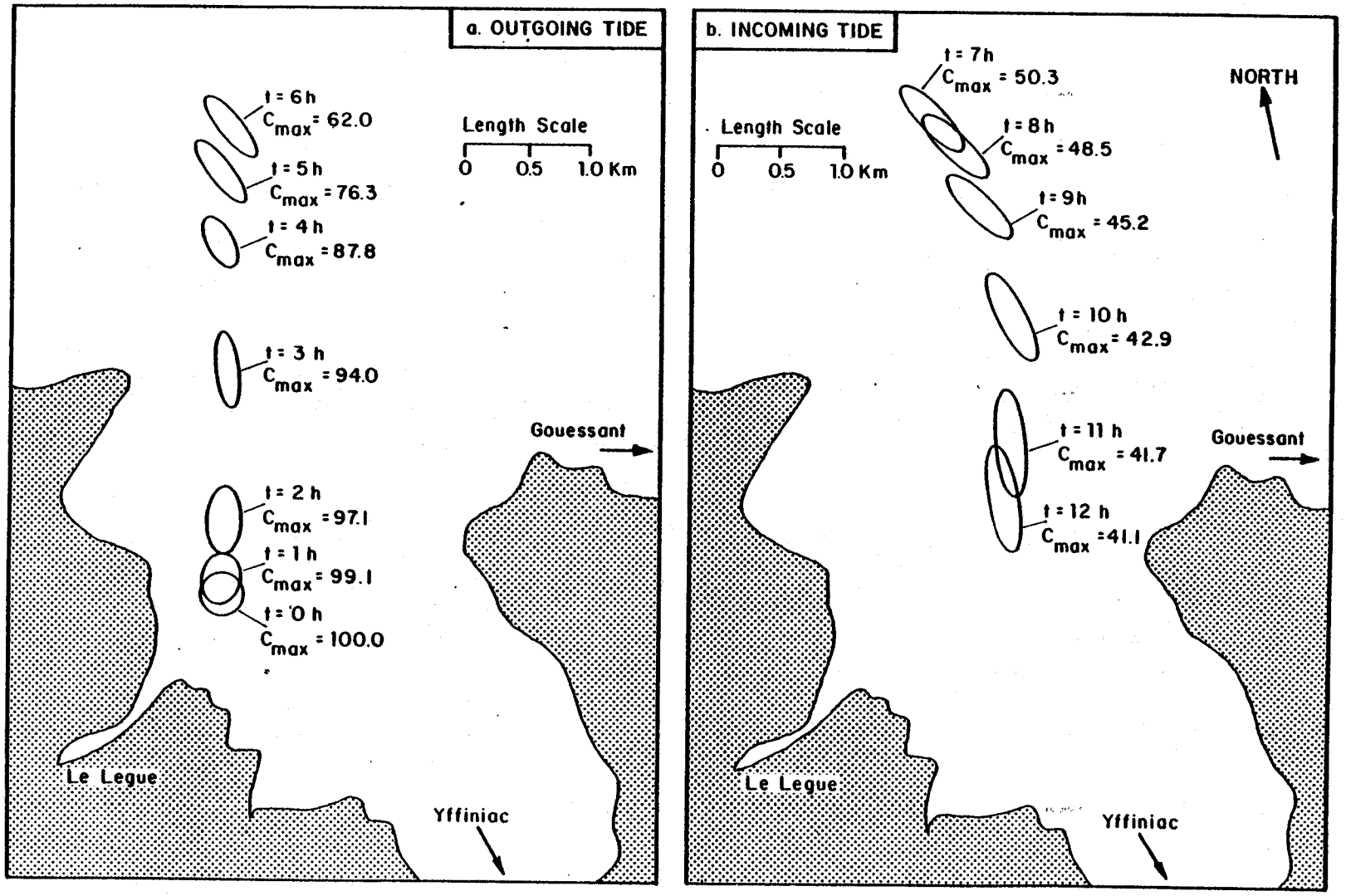

Figure 3. Computed dispersion of Lagrangian "small cloud."

QUASI-STEADY WATER AND SEDIMENT ROUTING IN MULTIPLY CONNECTED CHANNEL NETWORKS

Program Name: BRALLUVIAL

Origin: Developed by F. Holly, J.C. Yang, and M. Spasojevic at the Iowa Institute of Hydraulic Research, The University of Iowa, 1984-85.

General Description: BRALLUVIAL computes long-term bed evolution in multiply connected (looped, braided) networks of one-dimensional channels having non-uniform bed sediment. Bed armoring and sorting effects are specifically taken into account through simulation of the constituent processes. Application of BRALLUVIAL to a braided river requires the implicit assumption that the plan-form geometry of the channels does not change for the duration of the simulation. Boundary conditions comprise water-inflow hydrographs at any interior or exterior computational node, sediment-inflow hydrographs at exterior nodes, and a stage hydrograph at the downstream limit of the model. Output includes the water-flow distribution among the various channels, all hydraulic parameters at each point of the model, current and accumulated bed-level changes at any point, and bed-sediment distributions, including armoring factors, at any point. Tributaries are treated as a natural part of the multiply connected topology. Although the code is designed for complex multiply connected networks, it can equally well be applied to branched or single-channel systems.

Particular Features: BRALLUVIAL incorporates the armoring and sorting algorithms of the single-channel IALLUVIAL code described elsewhere in this brochure. BRALLUVIAL also uses a quasi-steady water flow assumption, whereby the energy equation and node-continuity equation are used to find a mutually compatible set of discharge distributions and water levels throughout the model, in any time step. Total-load sediment transport is normally computed with the same TLTM predictor used in IALLUVIAL, but with empirical coefficients adjusted, if necessary, using site-specific calibration data. Other total-load formulae (e.g. Engelund-Hansen, etc.) are programmed and can be used by option; in all cases, transport-dependent friction factors are

iteratively coupled with the transport formula adopted. The code avoids inversion of large matrices by using both channel and matrix double-sweep procedures, guided by a simple node-link identification system in the input data.

The techniques of BRALLUVIAL are currently being generalized for fully unsteady flow (see the CHARIMA program described elsewhere in this brochure).

Restrictions: Wave-propagation and reversing-flow effects are ignored in this quasi-steady formulation. In a braided river, no attempt is made to simulate lateral channel migration or new-channel formation.

Published References:

Holly, F.M. Jr. and Yang, J.C., "Numerical Simulation of Bed Evolution in Braided Channel Systems", Proceedings Hydraulic Division Specialty Conference, ASCE, Orlando, Aug. 1985.

Holly, Forrest M. Jr., "Computer-Based Simulation of Transport of Non-Uniform Sediments in Braided Channel Systems", EUROMECH 192, Transport of Suspended Solids in Open Channels, Munich, 11-15 June 1985.

Holly, F.M. Jr., Schneider, K., and Mellema, W., "Alluvial Computations in Complex River Networks", Proceedings Interagency Sediment Conference, Las Vegas, 1 April 1986.

Holly, F.M., Jr., "Computation of Non-Uniform Sediment Transport and Bed Evolution in Looped River Systems", Proceedings Second International Workshop on Alluvial River Problems, Roorkee, India, October, 1985.

Example of Application: Figure 4 shows the computational network of a complex gravel-bed braided river reach in Alaska. This model was used to predict the long-term effects of upstream flow regulation on channel stability and gravel deposits in the upper portion of the reach. Current activity on this study

includes use of BRALLUVIAL's weir-type links to simulate cross-channel water exchange at high flows, when gravel bars separating braided channels become fully submerged.

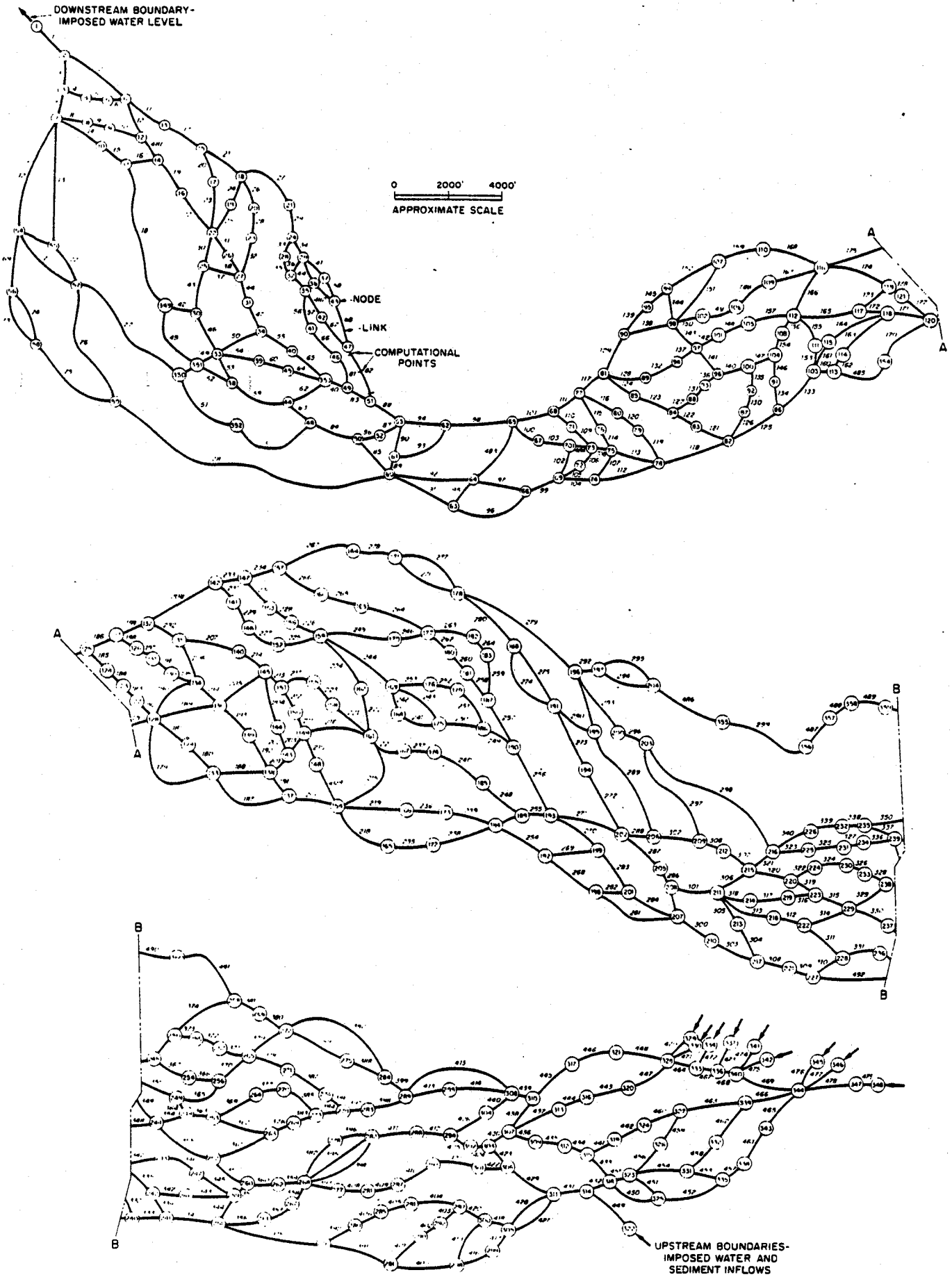

Figure 4. Discretized braided-channel system for BRALLUVIAL application.

UNSTEADY FLOW IN LOOPED STORM SEWER NETWORKS

Program Name: CAREDAS

Origin: Developed by G. Chevereau, A. Preissmann, and J.A. Cunge at SOGREAH, 1973-74. Improved by B. Mazaudou and A. Preissmann at SOGREAH, 1979-80. Available by agreement with SOGREAH.

General Description: CAREDAS computes one-dimensional steady or unsteady flow in branched or looped networks of pipes, closed conduits, and canals. Hydraulic works and control structures such as weirs, inverted siphons, manholes, retention basins, and pumping stations are included as standard features. Given input hydrographs of surface runoff from urban catchments (which can be computed by CAREDAS itself if desired), and a topographic, hydraulic, and topological description of the network, CAREDAS computes the time variation of water levels (or piezometric heads), velocities, and discharges at designated computational points. A separate program in the CAREDAS system uses these results to compute pollutant propagation in the network, if desired. Typical uses include:

* analysis of flow distribution in complex networks, for the optimization of pipe sizes;
* sizing of retention basins;
* design of real-time operating systems for control of flow regulation structures;
* verification of overall network design;

Particular Features: The de St. Venant equations for one-dimensional, free surface unsteady flow are solved using an implicit finite difference scheme with a special double-sweep algorithm for looped flow paths. Pressurized flow is computed using the same method, the piezometric head corresponding to the free surface level in a thin slot, or chimney, running longitudinally above each closed conduit. The transition between channel and pressurized flow is smoothed, when necessary, by iterative corrections in the numerical algorithm during one time increment. Backwater effects, flow reversal, and the effects

of in-pipe storage capacity are all naturally included in the de St. Venant formulation. Although CAREDAS includes an optional general routine for generating surfae runoff hydrographs, any method or program valid for local conditions can be used in its place.

Restrictions: In assuming incompressible flow and inelastic conduits, CAREDAS is not designed for waterhammer computation (see CERTITUDE description).

Published References:

Brandstetter, A., "Assessment of Mathematical Models for Storm and Combined Sewer Management", Environmental Protection Agency, Cincinnati, Ohio, 45268, 1975.

Chevereau, G. and F.M. Holly, Jr., "Conception of a Comprehensive Urban Drainage Simulation Program and its Application to a Prototype Case," International Symposium on Urban Storm Water Management, University of Kentucky, Lexington, 1975, pp. 55-61.

Holly, F., B. Chevereau, and B. Mazaudou, "Numerical Simulation of Unsteady Flow in Storm Sewer Systems Using a Complete and Simplified Flow Equations", International Conference on Numerical Modelling of River, Channel, and Overland Flow for Water Resources and Environmental Applications, Bratislava, Czechoslovakia, May, 1981.

Cunge, J.A., F.M. Holly, Jr., and A. Verwey, Practical Aspects of Computational River Hydraulics, Chapter 9, Pitman Publishing Ltd., 1980.

Additional Information Available: Descriptive brochure.

Example of Application: Fig. 5 shows the main components of the combined sewer system in the Seine St. Denis Department, adjacent to Paris, France. CAREDAS was used to identify deficiencies in the existing system in view of future urbanization, and to select new collector sizes and layout for

alleviation of local flooding. Figure 6 shows the hydrographs at selected outfalls into the Seine, for a 10-year storm. The model has been installed at the drainage authority's operations center, and is used regularly in the planning and design of network additions. A special version of CAREDAS which incorporates automatic control structures and their real-time centralized command/surveillance post is being used in the planning and design of a fully automatic network operating system.

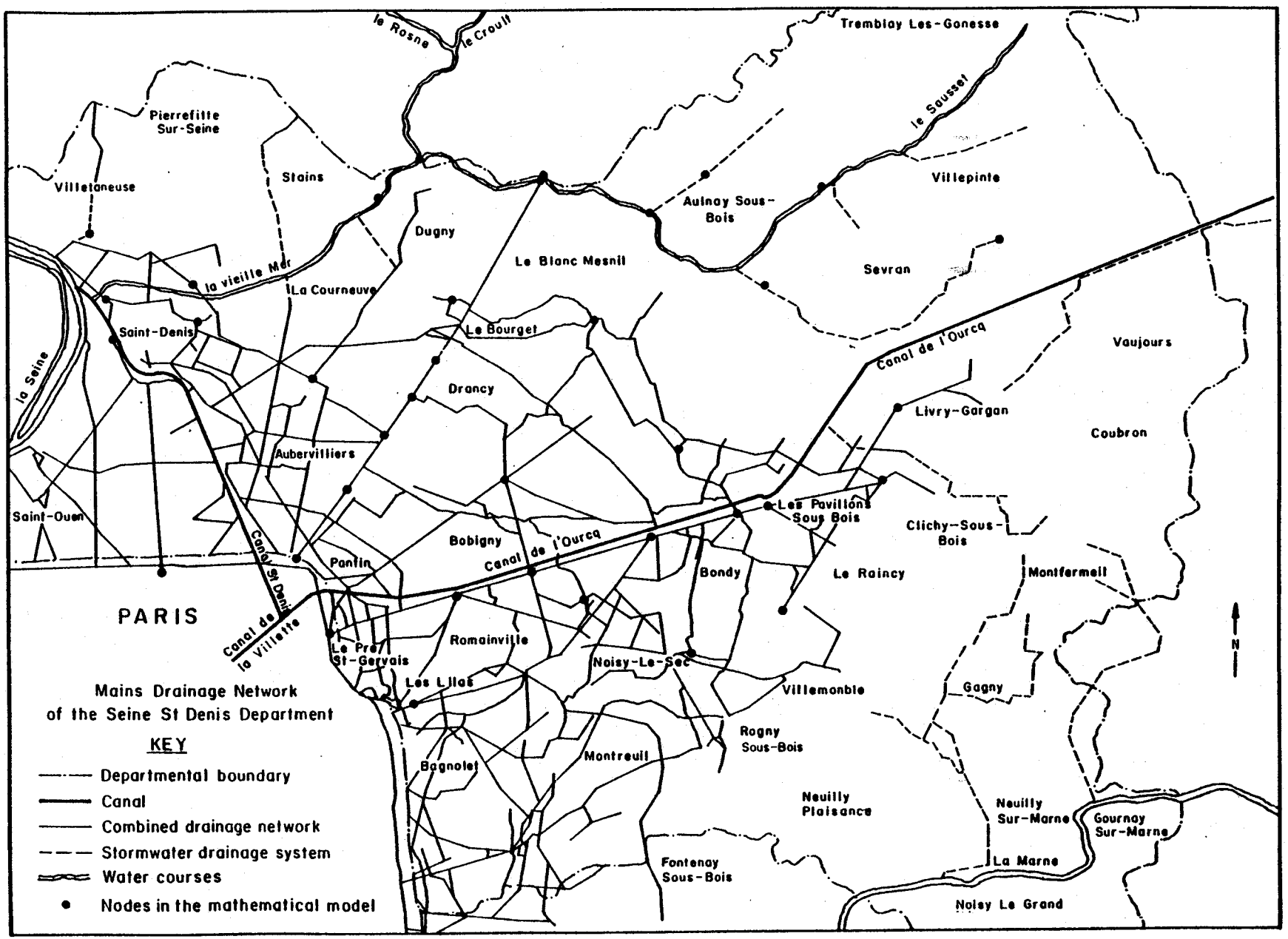

Figure 5. General layout of the Seine-St. Denis drainage network.

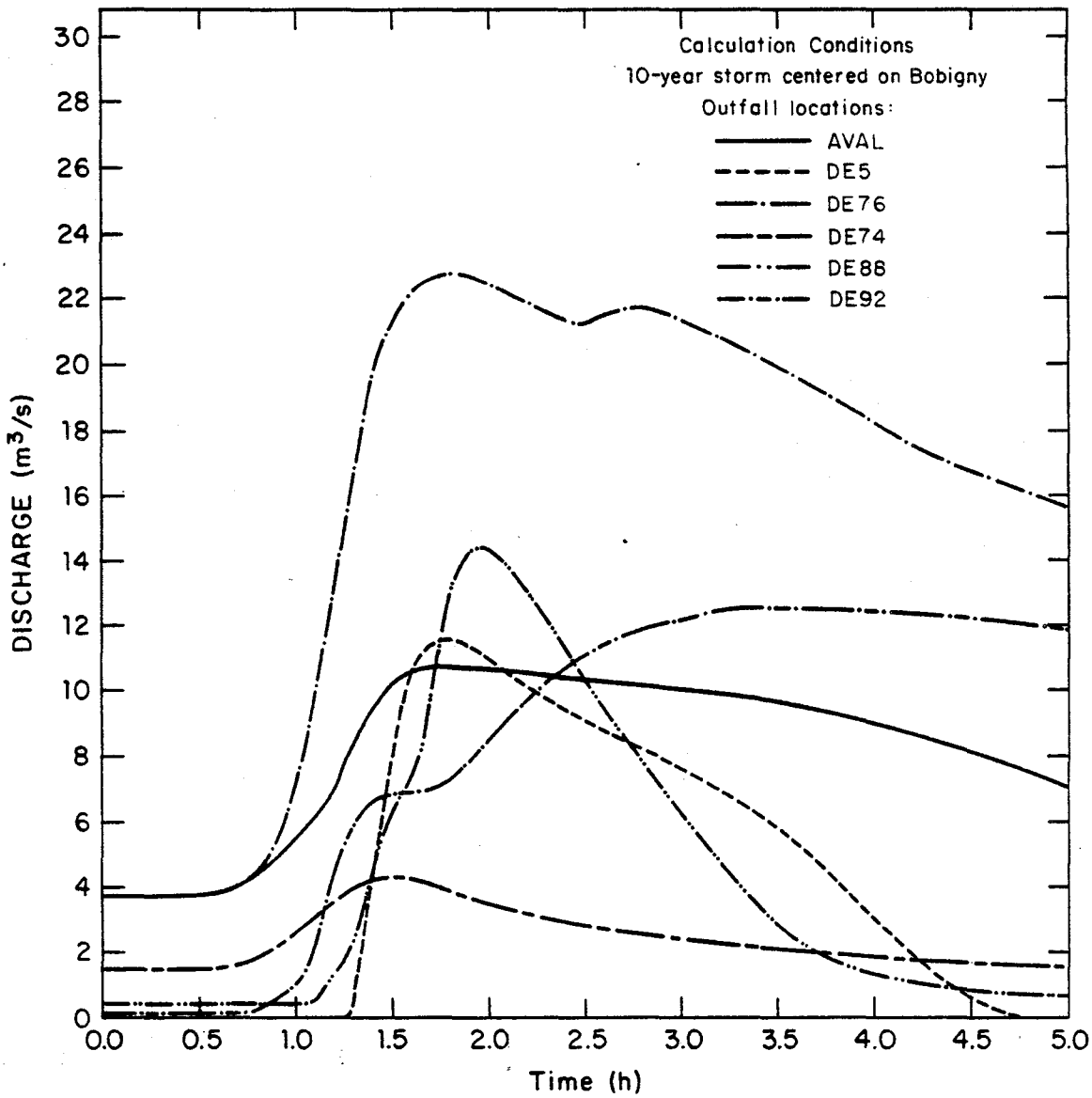

Figure 6. Computed outfall hydrographs at various locations.

UNSTEADY FLOW IN BRANCHED STORM SEWERS

Program Name: CAREMUSK

Origin: Developed at SOGREAH in 1979-1980 by B. Mazaudou and F. Holly. Available by agreement with SOGREAH.

General Description: CAREMUSK is designed for use in branched, non-pressurized, relatively steep slope storm sewer networks where the full dynamic approach of CAREDAS (see description) is not required. Based on a simplified form of the flow equations, CAREMUSK is less demanding of computer resources and can be operated by less specialized personnel. Since it uses exactly the same description of network components as CAREDAS, transition from one program to the other, if necessary, involves minimal time and effort. Alternatively, CAREMUSK can be used to achieve preliminary routing of urban catchment hydrographs from the extremities of a network (often branched, steep slopes) to main collectors (often looped, milder slopes, occasionally pressurized) where CAREDAS must be used. Given the characteristics of the pipes of the network and their topological links, and input hydrographs from urban catchments, CAREMUSK furnishes the time-variation of discharge and unused pipe capacity at all designated computational nodes.

Particular Features: CAREMUSK is based on the Cunge-Muskingum method, which is a finite-difference approximation to the diffusion-analogy form of the one-dimensional unsteady flow equations. As such the method allows for variable wave celerity and damping based on physical principles. On the other hand it cannot take into account downstream influences, thus precluding its use when backwater effects, reversing flow, etc. are important.

Restrictions: As stated above, CAREMUSK must defer to CAREDAS when backwater effects exist, flow can become locally pressurized, or closed loops exist in the network.

Published References:

Holly, F., G. Chevereau, and B. Mazaudou, "Numerical Simulation of Unsteady Flow in Storm Sewer Systems Using Complete and Simplified Flow Equations", International Conference on Numerical Modelling of River, Channel, and Overland Flow for Water Resources and Environmental Applications, Bratislava, Czechoslovakia, May, 1981.

Example of Application: Figure 7 shows a branched portion of a storm sewer network in Germany. For given urban runoff inputs from a 10-minute storm, the outflow hydrograph was computed using both CAREDAS (full dynamimc equations) and CAREMUSK. It can be seen from the Figure that only near the peak discharge are the two hydrographs significantly different. Flow became slightly pressurized in the CAREDAS calculation, whereas CAREMUSK had to spill this water, resulting in a slightly lower peak discharge.

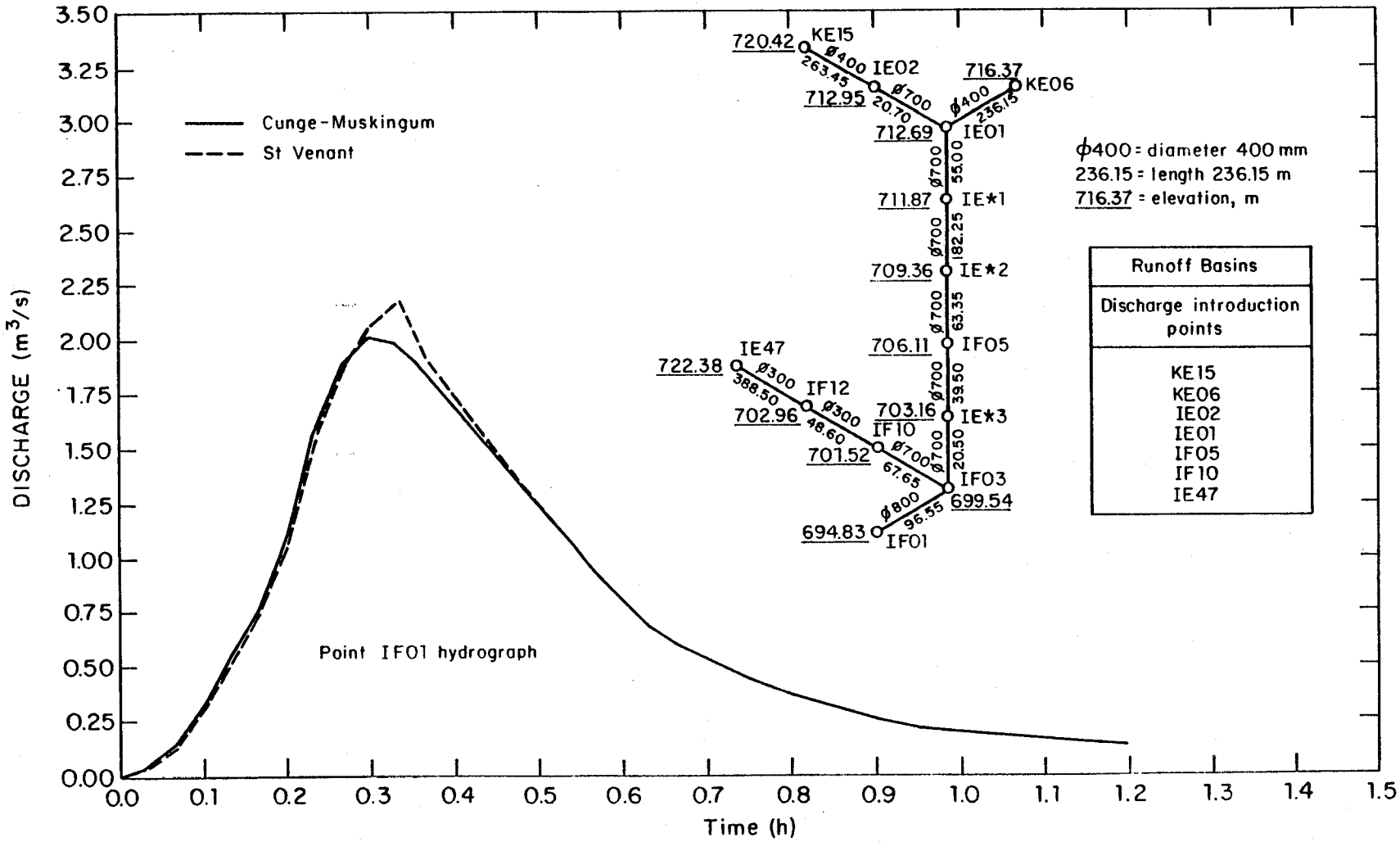

Figure 7. Computed outfall hydrographs using Cunge-Muskingum and de St. Venant equations.

UNSTEADY FLOW IN RIVER AND CANAL SYSTEMS

Program Name: CARIMA

Origin: Developed by F.M. Holly, Jr., G. Chevereau, A. Preissmann and J.A. Cunge at SOGREAH, 1976-1978. Available by agreement with SOGREAH.

General Description: CARIMA computes one-dimensional steady or unsteady flow in fixed-bed channels, and quasi-two-dimensional unsteady flow on flooded plains. There is no restriction on the way channel and flood-plain flow paths are connected; branched or looped systems are accepted. Hydraulic works such as weirs, gated flow control structures, culverts, irrigation canal control systems, etc., are included in the standard program. CARIMA is typically used for:

* studies of flood propagation for protection works design and flood area delineation;
* evaluation of effects of local flow modification (structures, cutoffs, etc) on water levels and flood propagation;
* design of operating systems for run-of-river hydropower installations;
* design of irrigation canal flow control devices and operating systems;
* evaluation of effects of peaking hydropower releases on downstream navigation;

For a given topographical and hydraulic description of a channel/flood-plain network, CARIMA computes the time-variation of water level, discharge, and velocity at designated computational points.

Particular Features: Unsteady flow in channels is computed using an implicit finite difference approximation of the de St. Venant flow equations. Unsteady flow on the flood plain is computed using non-inertial, simplified flow relationships between adjacent flood plain cells, whose submergeable boundaries correspond to natural obstacles to flow such as road embankments,

railroads, beams, etc. These relations between cells, when linearized, discretized, and combined with the finite difference equations for channel flow, form an algebraic system which is solved in each time step using a looped double-sweep algorithm.

Restrictions: The de St. Venant hypotheses for one-dimensional flow must be satisfied in channels. Inertial effects must be of small importance on the flood plain.

Published References:

Cunge, J.A., F.M. Holly Jr. and A. Verwey, Practical Aspects of Computational River Hydraulics, Chapter 3 and 4, Pitman Publishing Ltd., 1980.

Cunge, J.A., Lara, A., Major, T., Nerat, G., and Holly, F.M. Jr., "Mathematical Modelling of Yacyreta-Apipe Scheme on Rio Parana: Natural Floods and Power Releases", article submitted to La Houille Blanche, June 1982.

Gueguen, A. and F.M. Holly, Jr., "Use of Mathematical Modelling in the Design of Automatic Regulation for Upper Rhone River Hydroelectric Installations," International Conference on Numerical Modelling of River, Channel and Overland Flow for Water Resources and Environmental Applications, Bratislava, Czechoslovakia, May 1981.

Additional Information Available: Descriptive report.

Example of Application: Fig. 8 shows a 180 km reach of the Parana River on the Argentina-Paraguay border. The proposed Yacyreta Dam is to be used primarily for peak power production. The resulting surges propagated downstream could be detrimental to navigation. Accordingly CARIMA was used to simulate the surges produced by various turbine operating strategies, in order to eliminate those which result in excessive velocities and water surface slopes in the 50 km reach below the dam. Fig. 9 shows a typical output plot

of velocities at various points in the looped channel system, for a given operating strategy.

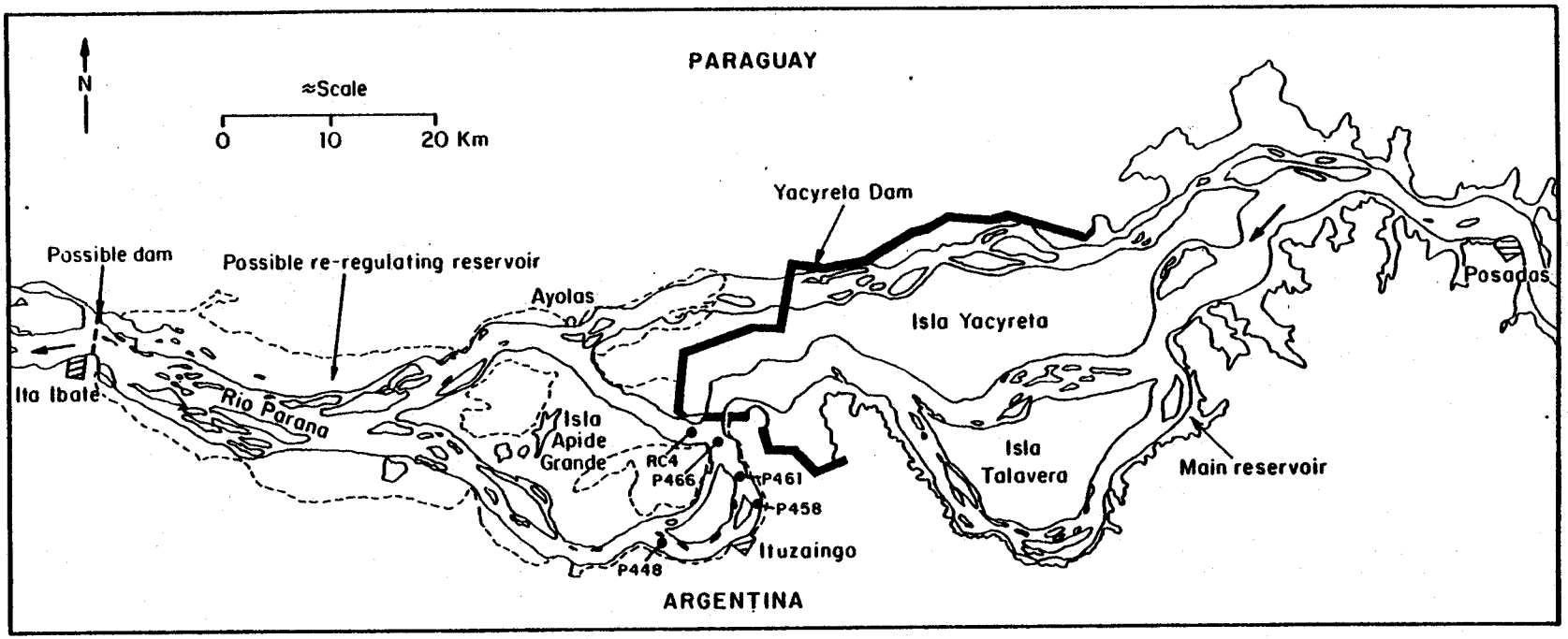

Figure 8. Portion of Parana River included in Yacyreta Dam mathematical model.

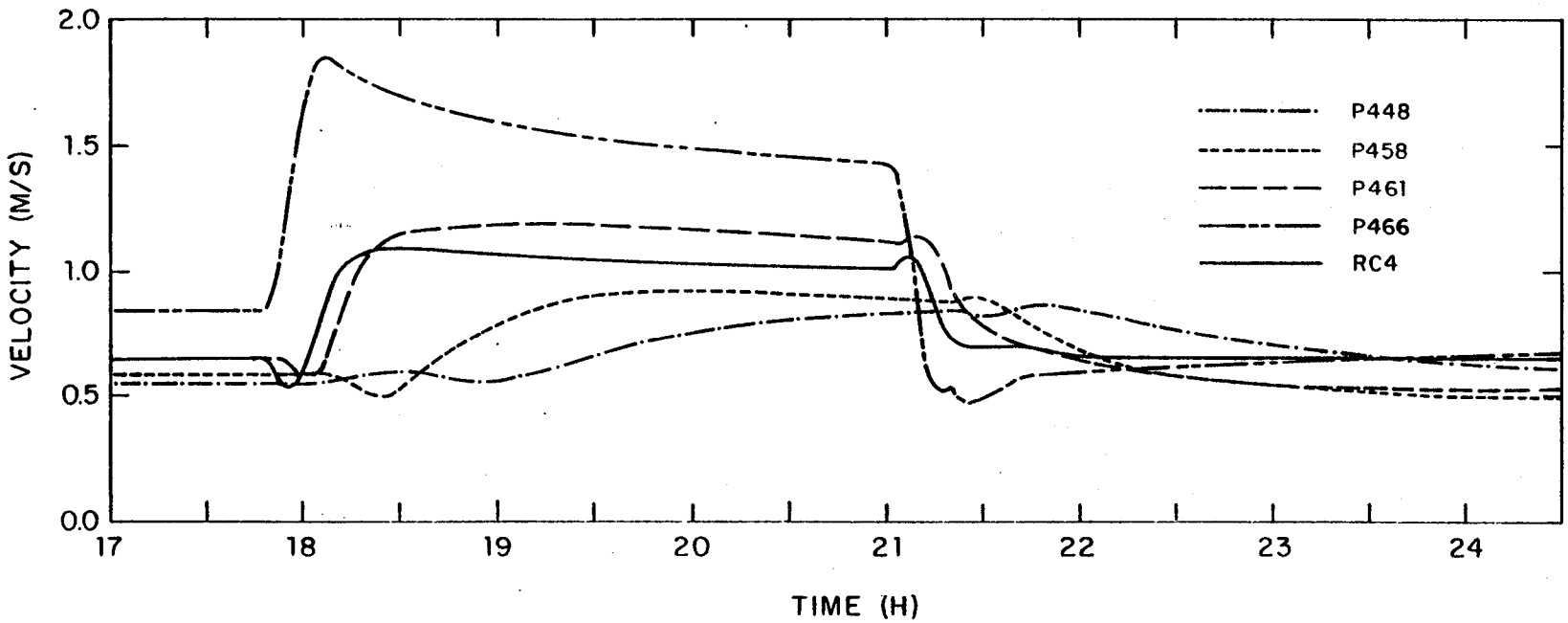

Figure 9. Computed velocity variations with time at various points.

WATER HAMMER IN PIPE NETWORKS

Program Name: CERTITUDE

Origin: First version developed in 1957 at SOGREAH, subsequent improvements and generalizations by A. Preissmann, J. Zaoui, and others. Available by agreement with SOGREAH.

General Description: CERTITUDE computes pressure transients due to sudden valve closures, pump start-up, failure of a protective device, etc., in a pipe network. A network is described by furnishing geometrical, topological, and hydraulic descriptions of all conduits and devices, for example head tanks, hydrants, weirs, orifices, flow regulators, pumps, valves, turbines, surge tanks, air tanks, check valves, etc. Once the model is constructed, the program computes pressures and discharges at all nodes of the system following the anamalous incident under study. Analysis of the pressure records thus obtained enables the engineer to design his system against failure under extreme conditions, optimize his specification of pipe and device configurations, identify needs for additional protection, etc. Optional harmonic analysis of pressures can be used in designing against failure due to resonance.

Particular Features: CERTITUDE employs a numerical solution method which involves pressure corrections at each node and disturbance propagation by the method of characteristics. The inertia of rotating machinery and check valves is taken into account. Both positive and negative surges are computed.

Restrictions: The fluid is assumed to be incompressible.

Previous Studies: Since 1957 CERTITUDE has been employed hundreds of times for studying a broad range of facilities, such as the following:

* municipal water supply systems (Montreal, Canada; Marseille, France; Rabat-Casablanca, Morocco; etc.)

* industrial water supply (Nekoosa-Edwards, Nepco, Wisconsin; Phenix Fast Breeder reactor, French Atomic Energy Commission; etc.)

* Sprinkler Irrigation Networks (Cariaco, Venezuela; Thessaly, Greece; etc.)

* Hydroelectric Projects (Mahaweli, Sri-Lanka; Emosson, France; Ahrzerouftis, Algeria; etc.)

* Airport Fuel Distribution Systems (Orly and Roissy airports, Paris; Moscow and Kiev, USSR; Tripoli, Libya)

Additional Information Available: Descriptive brochure.

Examples of Application: Figure 10 shows two network layouts for actual studies performed using CERTITUDE. Figure 11 shows a pressure time-history computed for the Caracas (Venezuela) water supply system.

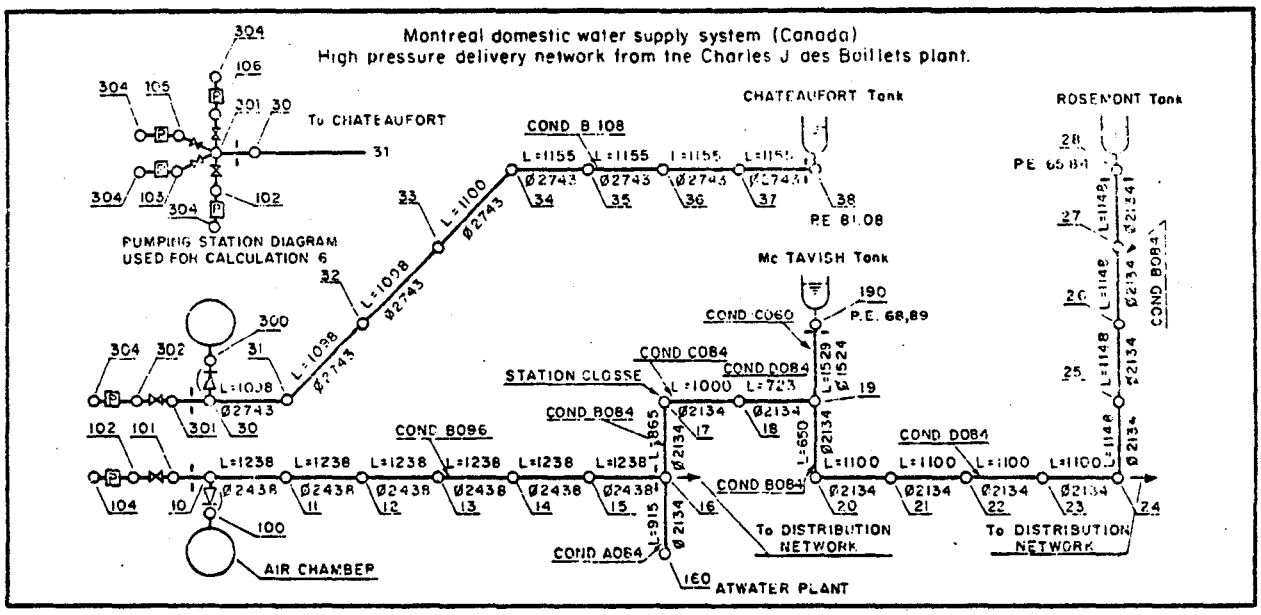

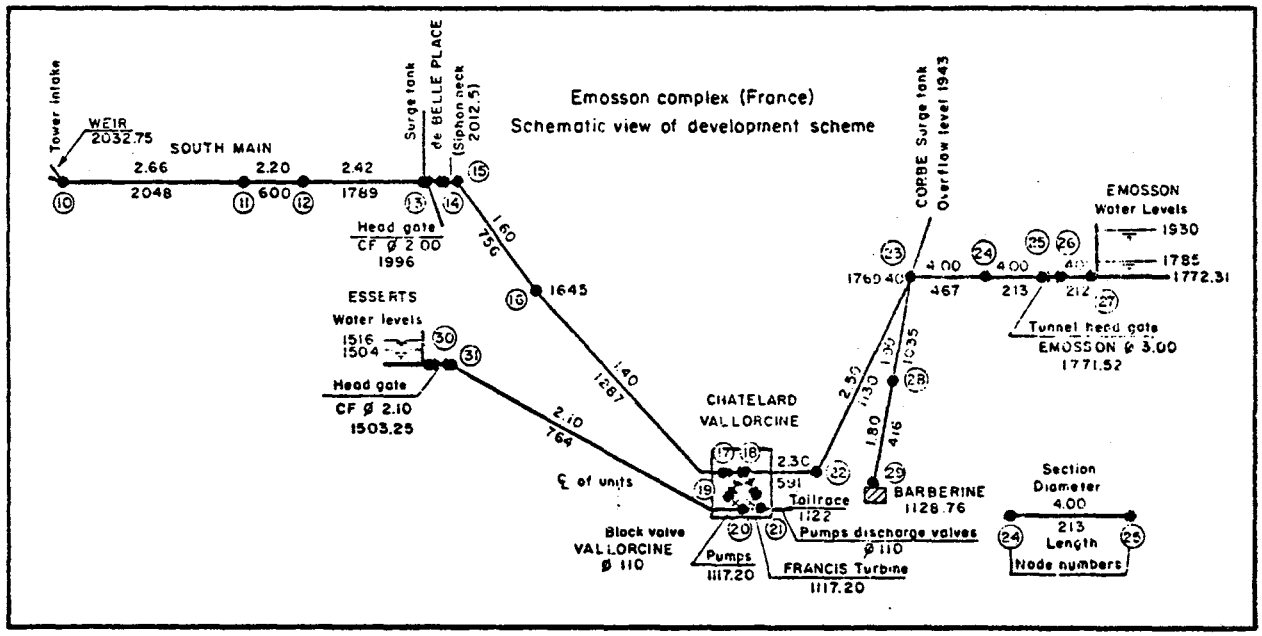

Figure 10. Network layouts for Montreal and Emosson models.

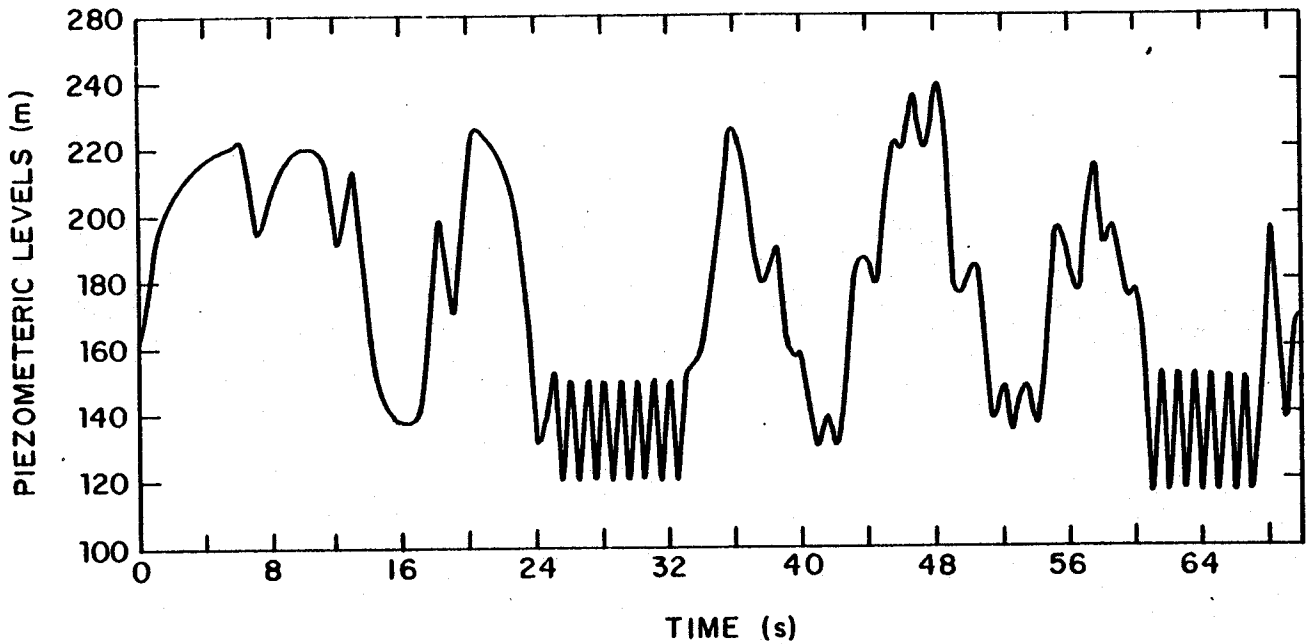

Figure 11. Computed piezometric level variations upstream of a pumping station in the Caracas water supply system.

WATER AND SEDIMENT ROUTING IN RIVERS

Program Name: CHAR II

Origin: Developed at SOGREAH in 1975-76 by J.A. Cunge and A. Preissmann. Available by agreement with SOGREAH.

General Description: CHAR II belongs to a family of four programs for the computation of one-dimensional unsteady water and sediment flow in rivers. In treating the water flow unsteadiness as a sequence of steady flows at different discharges, CHAR II is designed for the simulation of long term bed evolution (such as over a period of several years) in response to changes in water and sediment input and channel modification. Both the mainstem channel and tributaries can be included in the simulation model; check dams, reservoirs, and diversions are routinely accepted by the program. Given topographic and hydraulic descriptions of the river and its tributaries; water and sediment hydrographs for the upstream limits of all channels, local inflows, and diversions; downstream water level as a function of time; initial bed configuration; and median sediment size, CHAR II computes the water level, velocity, total sediment load, and bed elevation as a function of time at all computational nodes.

Particular Features: Energy loss due to bed resistance is assumed to be described by a simple Manning-Strickler equation. Sediment transport capacity is obtained from flow depth and velocity using the Meyer-Peter, Engelund-Hansen, DuBoys, Einstein-Brown, or user-furnished method. The water flow (backwater) equation is solved using Newton-Raphson iterations to supply water surface elevations and velocities for each steady discharge. Then the sediment continuity equation is solved by an implicit finite difference procedure for the duration of the steady discharge.

Restrictions: CHAR II does not take into account bed sediment sorting or armouring, changing resistance due to bed form evolution, or supercritical flow.

Published References:

Cunge, J.A. and Perdreau, N., "Mobile Bed Fluvial Mathematical Models", La Houille Blanche, No. 7, 1973.

Cunge, J.A., Holly, F.M. Jr., and A. Verwey, Practical Aspects of Computational River Hydraulics, Chapt 7, Pitman Publishing Ltd., 1981.

Nakato, T. and Vadnal, J., "Field Study and Tests of Several One-dimensional Sediment-Transport Computer Models for Pool 20, Mississippi River", IIHR Report No. 237, University of Iowa, July 1981.

Additional Information Available: Descriptive report.

Example of Application: Figure 12 shows the confluence of a river and its tributary, and a dam built 56 km downstream of the confluence at point D. In order to forestall the loss of useful reservoir capacity due to sediment deposition, three possible projects were considered:

1) a new dam at C to trap sediments before they enter the reservoir;

2) new dams at A and B to form sedimentation reservoirs;

3) low level flushing operations at the main dam D to remove trapped sediments.

CHAR II was used to simulate the three alternatives. Cross sections and annual water and sediment input hydrographs are shown on Fig. 12. First the previous five years were simulated for existing conditions, to establish a starting bed profile. Then three years of future bed elevation were simulated for existing conditions and for the three proposed projects. Figure 13 shows the bed profile after three years for project (2), and Figure 14 shows the profile for project (3). On the basis of comparisons such as these, the low-level flushing of project (3) was finally chosen as the most effective method of preserving reservoir capacity.

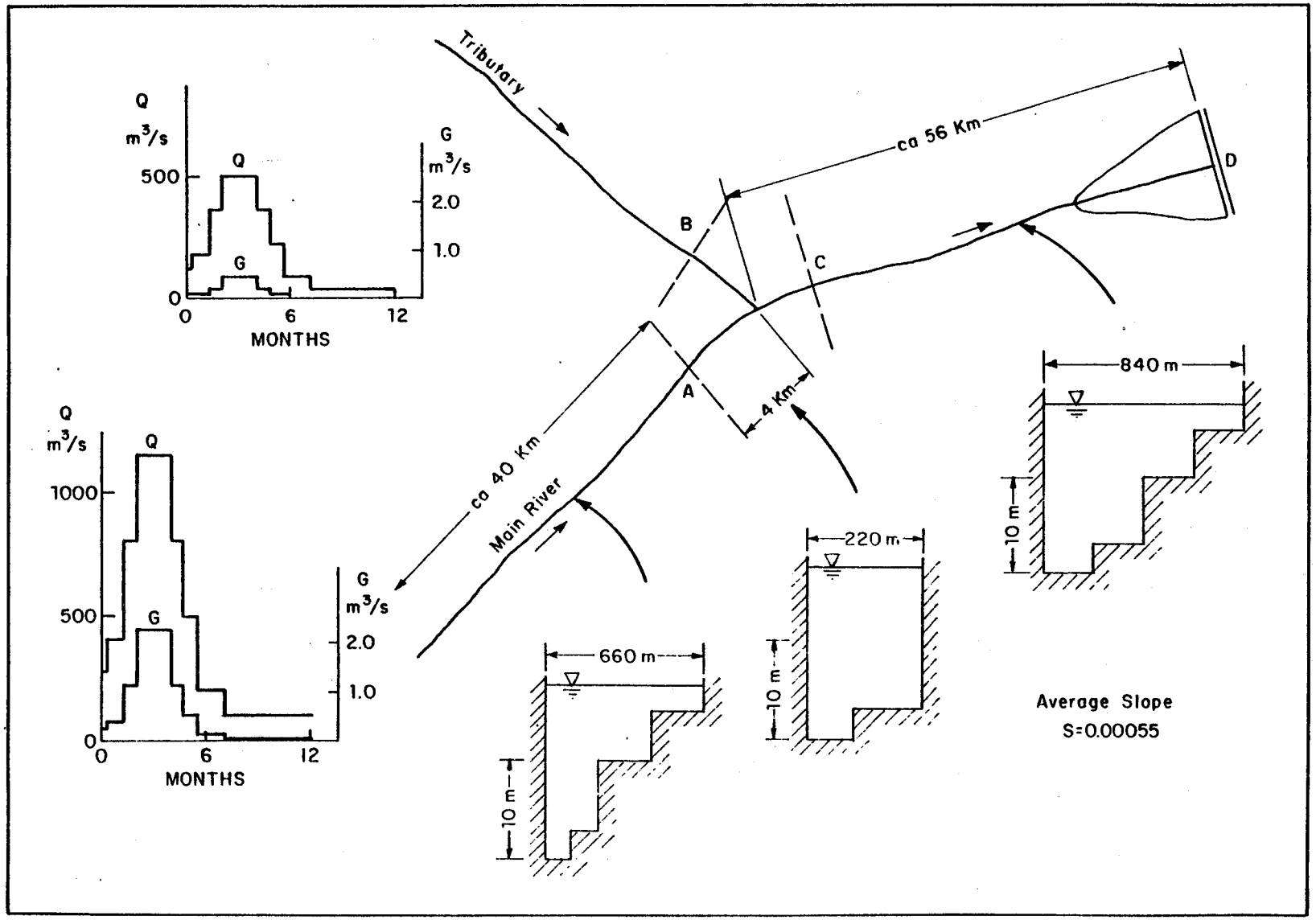

Figure 12. General model layout, cross-sections, and boundary conditions for CHAR-II bed evolution model.

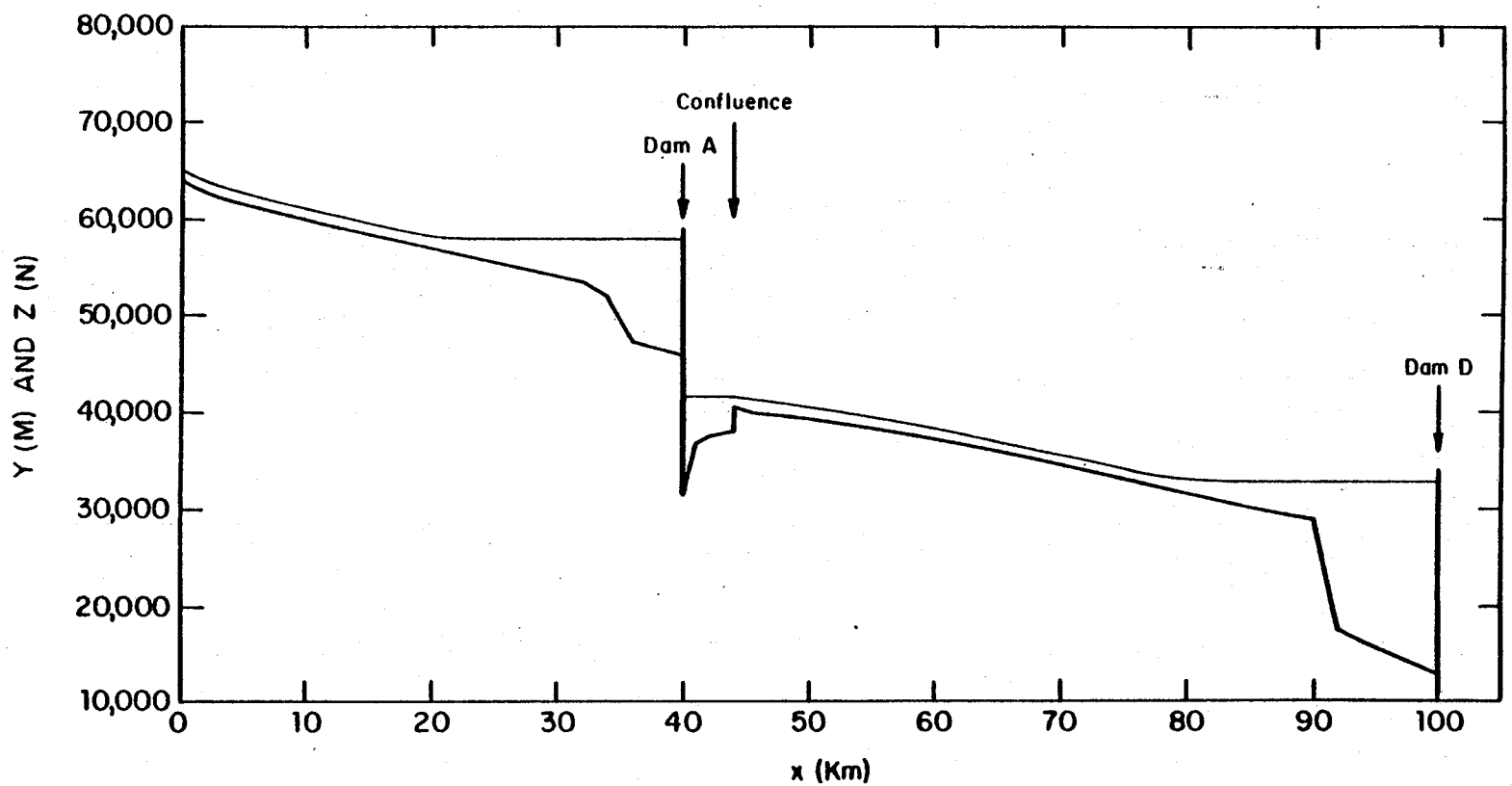

Figure 13. Computed water surface and bed profiles at 1093 days, Project 2.

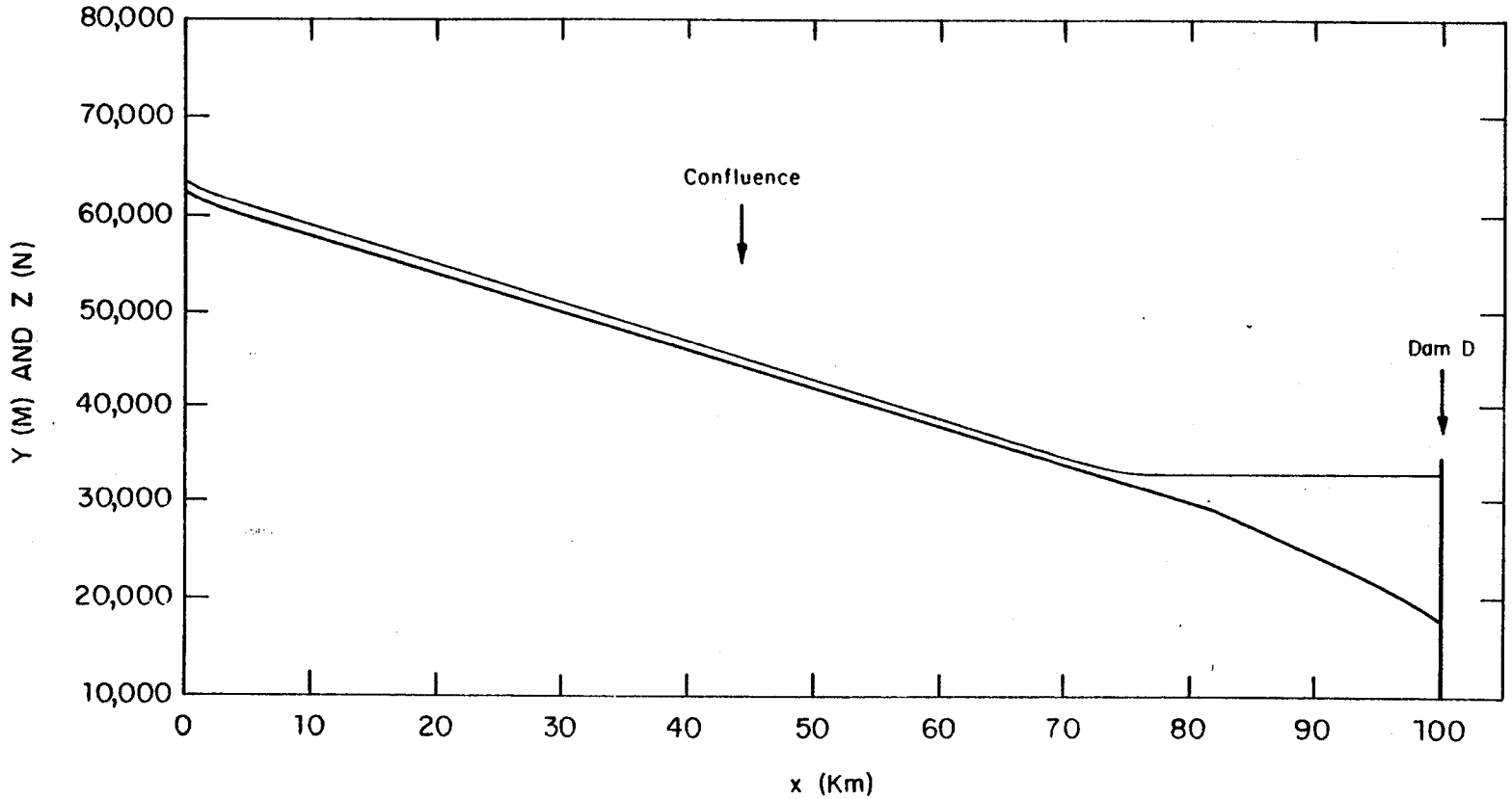

Figure 14. Computed water surface and bed profiles at 1093 days, Project 3.

FULLY UNSTEADY WATER AND SEDIMENT ROUTING IN MULTIPLY CONNECTED CHANNEL NETWORKS

Program Name: CHARIMA

Origin: Currently under development at Iowa Institute of Hydraulic Research by F.M. Holly Jr. and J.C. Yang (Fall 1985).

General Description: The CHARIMA code is a generalization of BRALLUVIAL (described elsewhere in this brochure) in which the latters' quasi-steady flow assumption is relaxed through use of the fully unsteady de St. Venant flow equations. This enables CHARIMA to treat flows in which shallow water-wave propagation effects are important, as in tidal estuaries with reversing flow.

Particular Features: The unsteady water-flow computation of CHARIMA is similar to that of CARIMA (described elsewhere in this report), in which Preissmann's four-point implicit scheme is used to solve the de St. Venant equations in multiply connected networks. Water and sediment operations are coupled, if necessary, through global iterations in each time step. Steady-flow situations such as those modelled using BRALLUVIAL can be simulated through judicious management of "time" steps as iteration parameters; in this sense, BRALLUVIAL is a subset of CHARIMA.

Restrictions: See BRALLUVIAL

Published References: None (code currently under development, Fall 1985)

UNSTEADY FLOW IN TWO DIMENSIONS

Program Name: CYTHERE-ES1

Origin: Developed by J.P. Benque, A. Hauguel, and J. Feuillet of LNH-Chatou, France; and by J. Cunge and A. Preissmann of SOGREAH, 1978-1981. Available by agreement with SOGREAH.

General Description: CYTHERE-ES1 computes time-dependent water surface elevations and depth-averaged velocities in well-mixed estuaries, coastal bays and inlets, ports, lakes, and reservoirs. A bathymetric description of the area to be modeled, along with specified water surface or discharge evolution with time along open boundaries, are used with the two-dimensional shallow water wave equations to obtain depths and current speeds and direction at any point in the model as a function of time. Coriolis acceleration, surface wind shear, non-uniform/non-isotropic bed roughness, and tidal flat flooding and exposure are routinely incorporated in the numerical solution of the wave equations. CYTHERE-ES1 is used for:

* generation of current fields for water quality studies;
* simulation of effect of structures and major bathymetric change on circulation and current fields;
* study of protective measures against erosion and sediment deposition;
* study of power plant cooling pond recirculation (when stratification is unimportant)

Particular Features: CYTHERE is based on the complete shallow water wave equations with additional terms for gradient-diffusion of horizontal momentum. The equations are solved in each time step using three distinct approximate methods:

a) Method of characteristics for momentum advection;
b) Implicit finite differences for momentum diffusion and Coriolis force;

c) Iterative implicit finite differences for water continuity, wind shear, and wave propagation.

This split-operator approach has made it possible to use numerical methods best suited for the different components of the problem. In particular, it computes momentum advection with very little numerical damping, and successfully computes wave propagation at large Courant numbers. Thus jet-type effects are faithfully reproduced, and waveforms undergo little or no distortion on non-uniform computational grids. A non-uniform, cartesian computational grid is usually employed, although an orthogonal curvilinear system is used when necessary to better fit the shape of the modeled area.

Restrictions: Vertical accelerations are neglected, precluding the computation of short-waves (refraction, diffraction, harbor resonance). Vertical homogeneity is assumed (precludes use in strongly stratified estuaries).

Published References:

Benque, J.P., Cunge, J.A., Feuillet, J., Hauguel, A., and Holly, F.M., "New Method for Tidal Current Computation", Journal of the Waterway, Port, Coastal and Ocean Division, ASCE, Vol. 108, No. WW3, Aug., 1982, pp. 396-417.

Cunge, J.A., Holly, F.M. Jr., and Schwartz, S., "Mathematical Modelling Study of Pollution Transport in the Bay of Saint-Brieuc, France", Symposium Engineering in Marine Environment, Brugge, Belgium, 1982.

Additional Information Available: Descriptive brochure.

Example of Application: Figure 15 shows the English channel, in which tidal currents and elevations were computed several years ago using a predecessor to CYTHERE-ES1; the 10-m grid shown was used at that time. The present example

concerns the Bay of Saint-Brieuc on France's north Brittany coast as shown on the Figure. The object of the study was to compute tidal currents in the Bay, then use them to determine the zones of influence of several municipal sewage outfalls in the vicinity of sensitive oyster beds. CYTHERE-ES1 was used to construct first a regional model with a uniform 2.5 km grid, then a detailed model with a uniform 0.5 km grid, using the previous model for the entire channel to obtain flow conditions at the seaward boundary. Figure 16 shows the computed tidal currents 3 hours before slack high water spring tide; the extensive tidal flats on the south shore are being flooded, and the rock outcrops near Portrieux have just been submerged by the rising waters. The tidal range in this area is about 10 m.

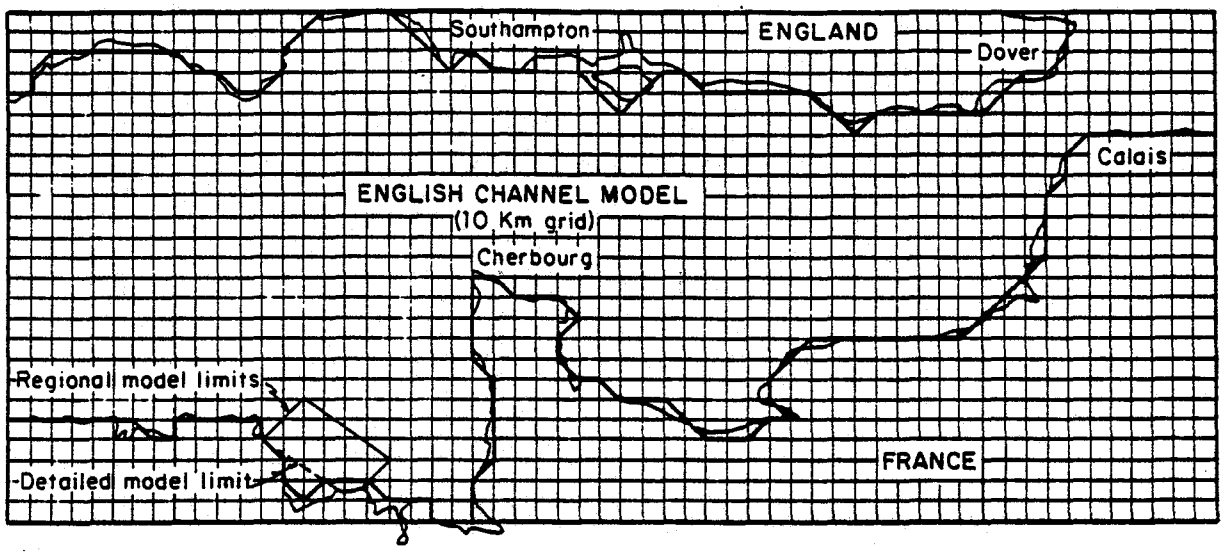

Figure 15. Model layouts used for bay of Saint-Brieuc study.

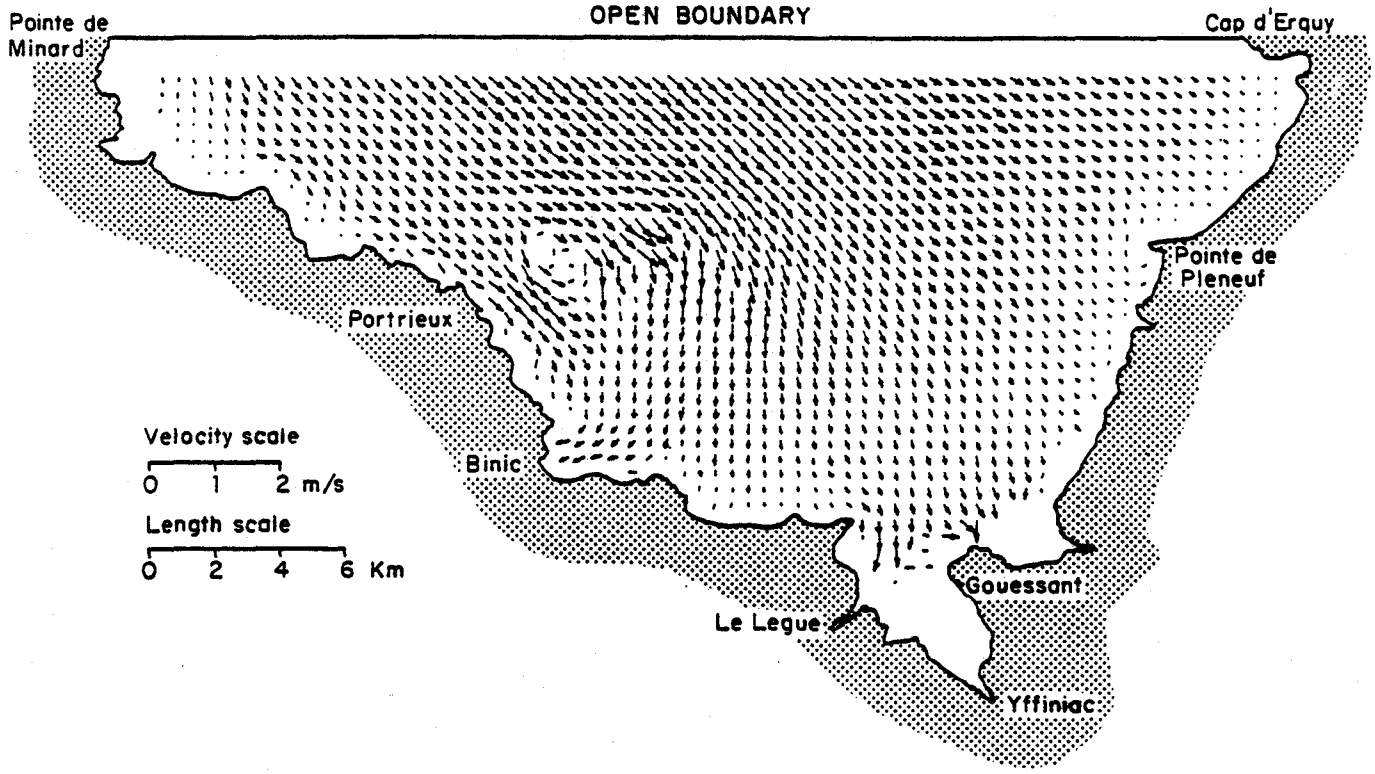

Figure 16. Computed tidal currents in the bay of Saint-Brieuc.

WATER AND SEDIMENT ROUTING IN RIVERS

Program Name: IALLUVIAL

Origin: Developed by Karim, M.F., Silva, J.M., and Kennedy, J.F. at the Iowa Institute of Hydraulic Research (IIHR), University of Iowa, 1980-82.

General Description: IALLUVIAL (or IAL) computes one-dimensional water and sediment flows in alluvial channels. IAL is specially designed to simulate long-term evolution of bed-elevation changes in rivers in response to changes in water and sediment inputs and channel cross-sections and alignments. For given initial channel and sediment characteristics, water discharge and sediment-discharge hydrographs at the upstream boundary, and a stage hydrograph at the downstream boundary, IAL computes flow depth and velocity, sediment discharge, water surface and bed elevations, and changes in bed-material size distribution at all computational points for each time interval. Armoring of the bed surface and its effect on sediment discharge, friction factor and degradation is an integral part of the computation. Tributary inflows of water and sediment, as well as the depth-variation of parent bed material size distribution, are taken into account.

Particular Features: IAL Utilizes the Total Load Transport Model (TLTM), an integrated sediment-discharge and friction-factor predictor recently developed at the Iowa Institute of Hydraulic Research. TLTM considers the interdependence between sediment discharge and friction factor, which allows the determination of friction factor internally in the program; this eliminates the need for external specification of flow resistance. The variation of friction factor with changes in water and sediment discharge, stage, and sediment characteristics is thus automatically computed in IAL. Another special feature of the program is a determination of the appropriate time step based on a physical examination of the degradation/aggradation process.

Restrictions: IAL does not compute water wave propagation, as it assumes steady water flow in the entire computational reach during a time increment. The annual hydrograph is taken to be a succession of steady flows at varying discharges.

Published References:

Karim, M.F. and Kennedy, J.F., "IALLUVIAL: A Computer-Based Flow- and Sediment-Routing Model for Alluvial Streams and its Application to the Missouri River", Iowa Institute of Hydraulic Research, Report No. 250, August 1982.

Silva, J.M., "A Numerical Model of Bed Degradation Along the Missouri River Between Yankton (South Dakota) and Omaha (Nebraska)", Master of Science Thesis, Civil and Environmental Engineering, Graduate College, University of Iowa, July 1982.

Karim, M.F. and Kennedy, J.F., "Computer-Based Predictors for Sediment Discharge and Friction Factor of Alluvial Streams", Iowa Institute of Hydraulic Research, Report No. 242, December 1981.

Holly, F.M. Jr., Yang, J.C., and Karim, M.F., "Computer-Based Prognosis of Missouri-River Bed Degradation; Refinement of Computational Procedures", Iowa Institute of Hydraulic Research, Report No. 281, August 1984.

Additional Information Available: Descriptive report

Example of Application: IAL was applied to the Missouri River to simulate the changes in bed and water surface elevations and the process of bed armoring in the 200-mile reach between the Gavins Point Dam and Omaha, Nebraska following construction of the dam in 1955. Computed changes in bed and water surface elevations after 20 years of simulation were found to be in good agreement with the measured values, as shown in Figure 17.

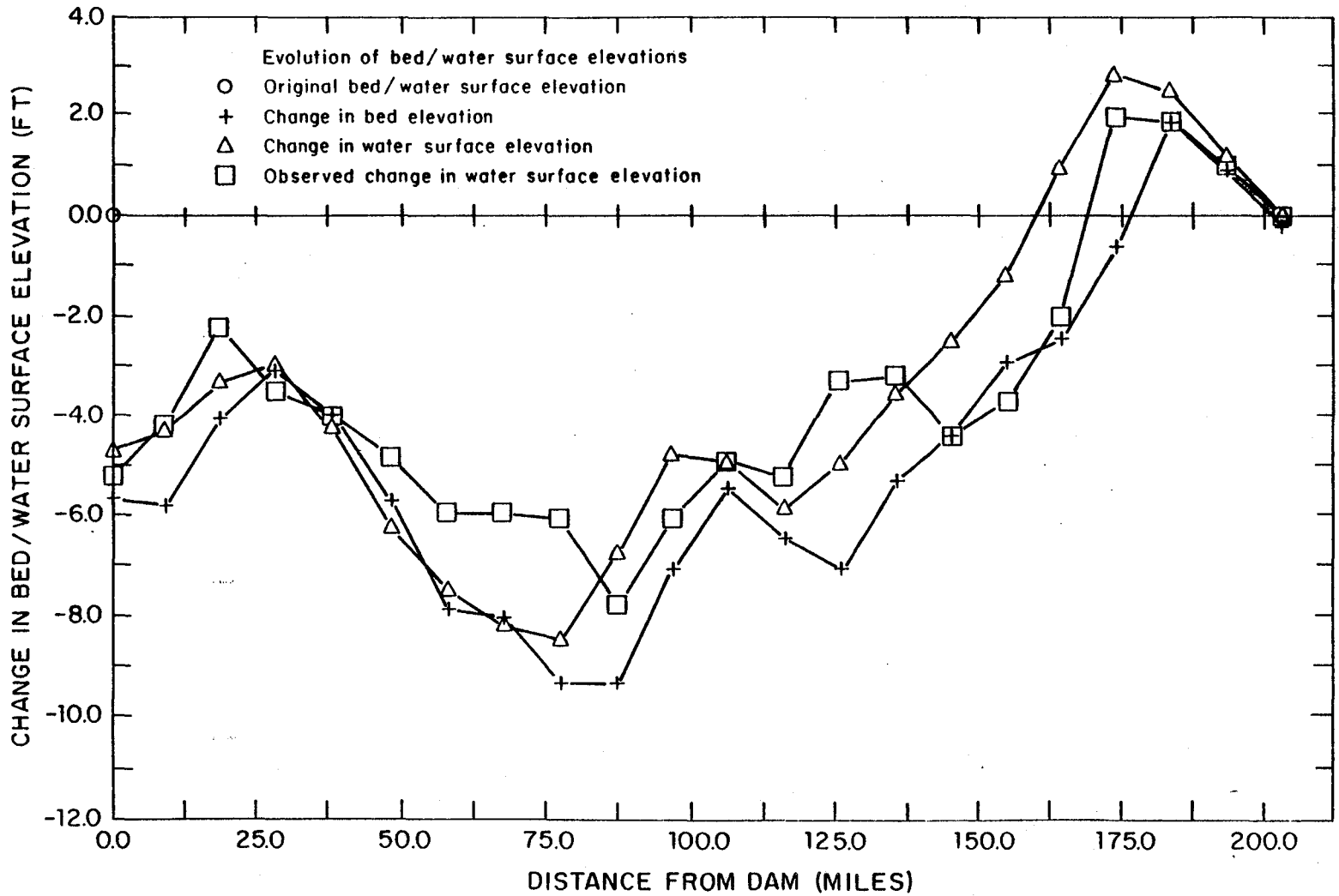

Figure 17. Computed changes in bed and water surface elevations after 20 years, Sioux City to Omaha.

POLLUTANT DISPERSION IN RIVERS

Program Name: POLDER

Origin: Developed by F.M. Holly Jr. and J.A. Cunge at Colorado State University, 1973-75. Subsequently improved and generalized by Holly at SOGREAH, 1976-77. Available by agreement with SOGREAH.

General Description: POLDER computes the time-dependent mixing of a neutrally buoyant, conservative tracer (pollutant) in steady but nonuniform river flow. The tracer is assumed to be mixed uniformly over the depth, but may be fully or partially mixed across the channel width depending on the type of tracer source under study. Possible sources include:

* continuous or time-varying injection at any point in the cross-section at the upstream model limit (sewage outfalls, diffusers, industrial effluents)
* sudden spills within all or part of the cross-section (barge accidents, spillage at bank)

The program predicts the time-variation of tracer concentration at any point downstream from the injection site.

Particular Features: Quasi-two-dimensional mixing (in plan) is computed relatively inexpensively using the cumulative discharge, or stream tube, approach. The period of time to be simulated is divided into short increments, or time steps, within each of which three mixing processes are separately computed:

1) Longitudinal convection in each stream tube, using a recently developed characteristics method which virtually eliminates artifical damping and phase error;

2) Longitudinal diffusion in each stream tube, using an implicit finite difference method;

3) Transverse diffusion between adjacent stream tubes, using an implicit finite difference method.

Restrictions: Step (3) above requires an estimate and/or calibration of the non-dimensional transverse mixing coefficient; when secondary flows are important (as in sharp bends), calibrated values may not be valid for use in flow conditions for which they were not specifically adjusted.

Published References:

Holly, Forrest M. Jr., "Two Dimensional Mass Dispersion in Rivers", Hydrology Paper No. 78, Colorado State University, Ft. Collins, Colorado, Nov. 1975.

Cunge, J.A., F.M. Holly, Jr. and J. Verwey, Practical Aspects of Computational River Hydraulics, Ch. 8, Pitman Publishing Ltd., 1980.

Holly, F.M. Jr. and G. Nerat, "Field Calibration of a Stream-Tube Dispersion Model", Journal of Hydraulic Engineering, ASCE, Vol. 109, No. 11, November, 1983, pp. 1455-1470.

Additional Information Available: Descriptive report.

Example of Application: Fig. 18 shows a 4 km reach of river at the upper limit of which an industrial outfall injects a low-concentration toxic waste as shown. POLDER was used to determine the effect of a proposed dam 4 km downstream on the mixing of the contaminant in the reach. Fig. 19 shows the dam's effect on depths, velocities, and concentrations at the dam site. The maximum concentration remains essentially the same before and after dam construction for these flow conditions.

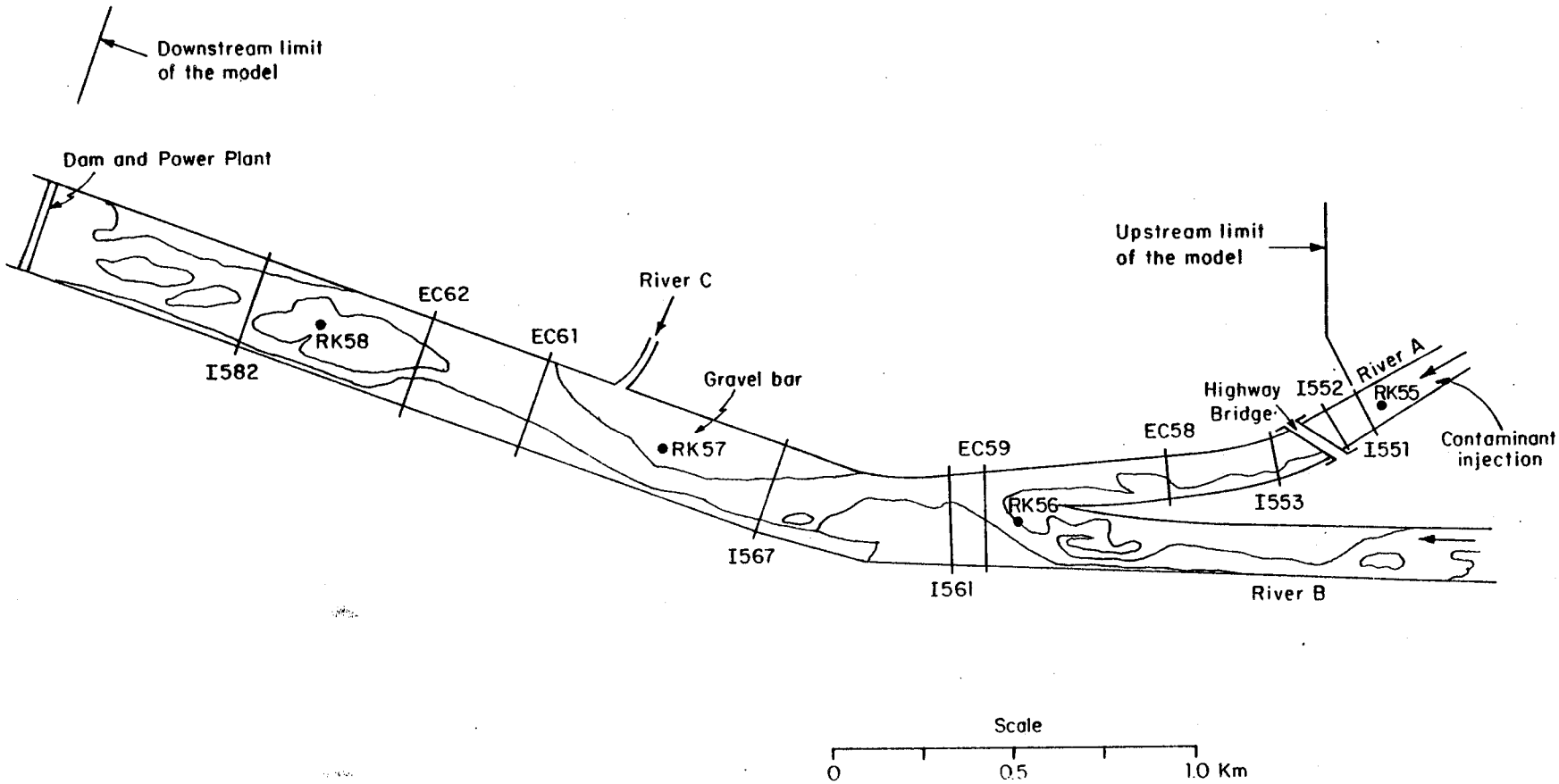

Figure 18. General layout of stream tube dispersion model.

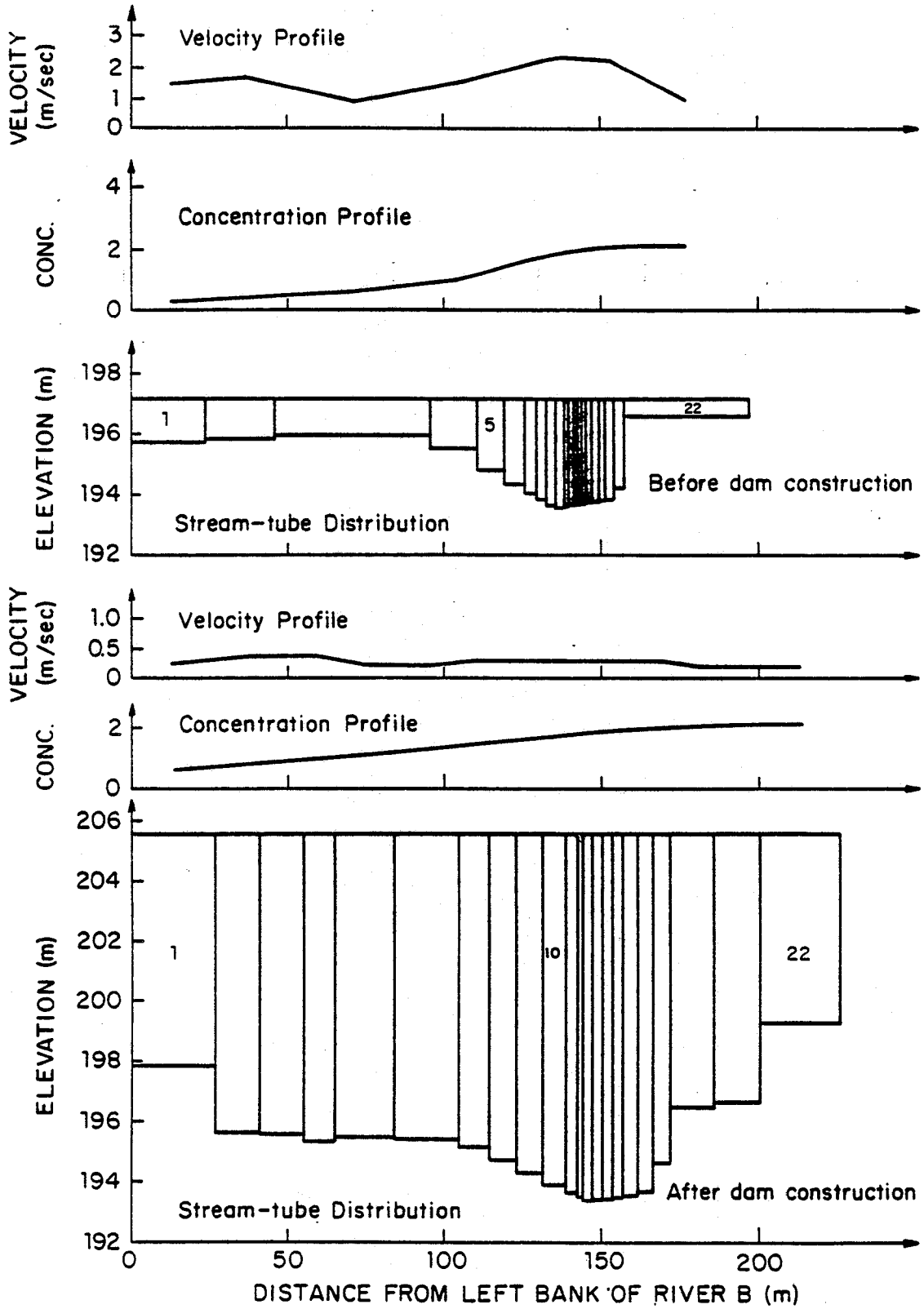

Figure 19. Computed velocity and concentration profiles at dam site, before and after dam construction.

FLOW IN LOOPED WATER DISTRIBUTION NETWORKS

Program Name: PROCEDURE

Origin: Developed at SOGREAH in the 1960's under the direction of A. Preissmann. Available by agreement with SOGREAH.

General Description: PROCEDURE computes the time-variation of discharges and pressures in a looped distribution network subject to fluctuating supply and demand. It is designed to simulate network flows over a period of, say, 24 hours, in order to: a) verify that a proposed network design can supply required discharges at minimum pressures; and/or b) identify specific problem areas in a proposed design. Thus PROCEDURE should be thought of as a simulation tool which aids the engineer in arriving at an optimum network design. The program routinely handles such appurtenances as control valves, check valves, reservoirs, pumps, booster stations, etc.

Particular Features: In order to allow for flow path closure and reopening when a check valve exists, PROCEDURE is based on a numerical method which abandons the traditional Hardy-Cross approach. Instead, an iterative nodal continuity method with periodic solution of the entire linear system to speed convergence is employed. This approach allows programmed water consumption to be reduced when available pressure is too low, removing another restriction of the Hardy-Cross method.

Restrictions: PROCEDURE does not simulate unsteady flow within the network (see CAREDAS). Unsteady behavior is taken into account only insofar as the boundary conditions (water levels or discharges at network inflow/outflow points) are allowed to vary during the day. By the same token, waterhammer is not simulated (see CERTITUDE).

Principal References for Previous Studies:

Project and Country	Project Authority Date	Services supplied by Sogreah
Toulouse water distribution system France	Toulouse Municipality 1963	Computer study of the distribution flow net, in terms of various hypotheses as to population (350,000 to 530,000 inhabitants; discharge 130,000 m3 daily)
Malacca water supply system Malaysia	Etablissements Degremont 1964-1965	Computer study of a distribution network for a population of 205,000 inhabitants in 1975 giving a discharge of 7.8 MGD - Determination of pipe dimensions - Determination of balance reservoir settings and storage capacities
City of Lyons water supply for the year 2000 France	Lyons Municipal Authorities 1965	Computer study of the extension of the water distribution network to deliver 10 m3/s to a population of 700,000 inhabitants. Application of the PROCEDURE program to the 1985 loop network comprising 255 sections
Grenoble water distribution system France	Service des Eaux de Grenoble 1969-1970	Verification of the operation of the present installations and projects for improvement of distribution. Operational simulation on an IBM 350/54 computer. Application of the PROCEDURE program to the 1970, 1975 and 1985 systems (188, 194, and 217 sections respectively). Optimization tests for 1975 by PROPRETE program.

Toulon water distribution system France	Service des Eaux de Toulon 1971-1972	Study of the operation of existing and planned municipal water distribution arrangements. Local measurements and a mathematical model simulation on an IBM 360-65 computer. Application of the PROCEDURE program to the networks for 1971 and 1985 (400 and 450 sections respectively). Optimization test for 1985.
Abidjan water supply system Ivory Coast	World Health Organization 1971-1972	Preliminary studies for a water supply Master Plan for the year 2000, using the PROCEDURE program, and including a survey of water resources, water requirements and existing distribution networks for a population of 2,000,000 inhabitants.
Economic study of water distribution system interconnection in the greater Paris area France	Agence de Bassin Seine Normandie 1972-1976	Study of water requirements in 1985 for 600 communes. Design, adjustment and operation of a mathematical model of existing water distribution loop networks (IBM 360/65). Definition and optimization of various interconnection alternatives for future requirements by the PROCEDURE program. (2,000 sections. Population of area 10 million).
Greater Tunis water distribution system Tunisia	SONEDE 1976	Study of a water distribution master plan for the year 2000 concerning 500 km of pipes, 300,000 m3 of reservoir capacity and 2,000,000 inhabitants. Application of the PROCEDURE program.

Water distribution systems for the new towns of Marne-la Vallee, Cergy-Pontoise and the Northern Paris-Roissy axis France	Agence Financiere de Bassin Seine-Normandie 1977	Definition of the drinking water distribution structures to be subsidized by the AFB in the interests of safety. Application of the PROCEDURE program.

Additional Information Available: Descriptive brochure

Example of Application: Figure 20 shows a portion of the water distribution network in the Paris metropolitan region. PROCEDURE was used to study optimum interconnections of several separate networks, to meet future needs. Figure 21 shows the typical computed variations in water levels and piezometric heads in several reservoirs and pipes, over a 24-hour period.

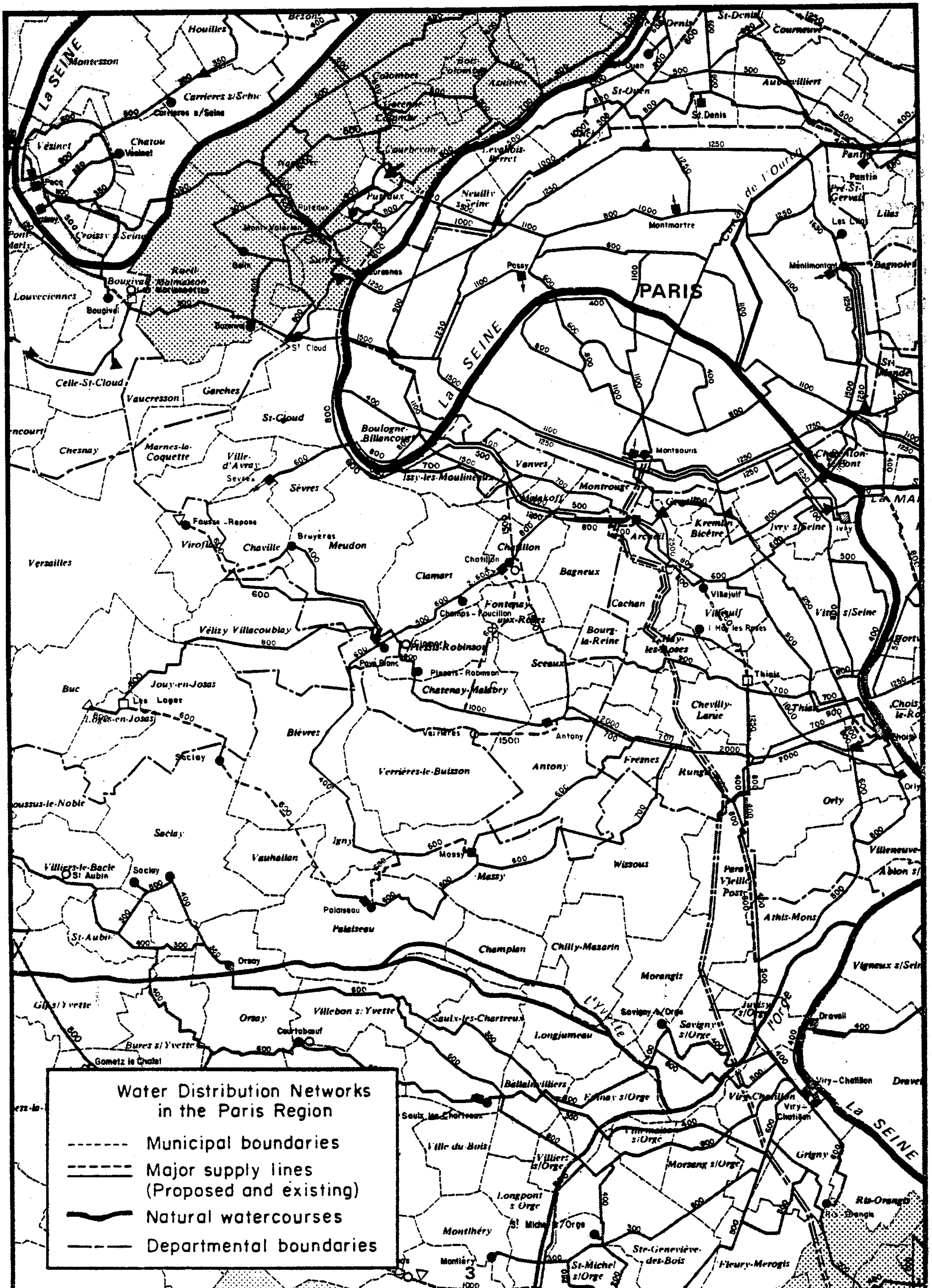

Figure 20. Portion of water distribution network in metropolitan Paris.

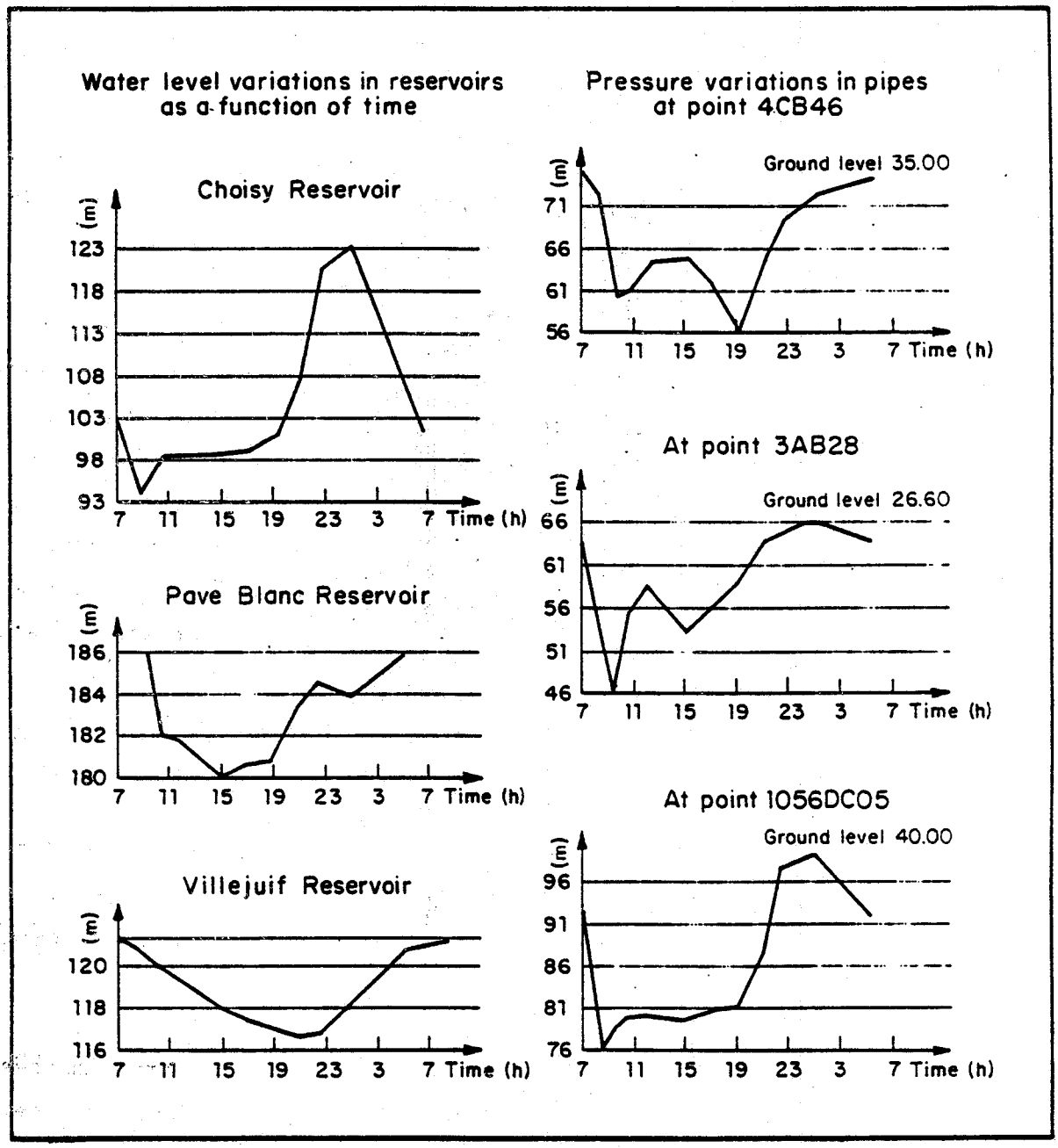

Figure 21. Computed water level and pressure variations at various points in the Parisien water distribution network.

SEDIMENTATION IN RESERVOIRS

Program Name: SEDRES

Purpose: Prediction of accumulation and distribution of sediment disposition in reservoirs

Origin: Developed by Karim, M.F., Croley, T.E., and Kennedy, J.F., at the Iowa Institute of Hydraulic Research (IIHR), University of Iowa, 1978-79

General Description: SEDRES is a mathematical model for the prediction of accumulation and distribution of deposited sediment in reservoirs over long time periods. SEDRES estimates the volume of sediment trapped in the reservoir during each time interval, and distributes it by elevation on the basis of either the standard type-curves developed by Borland (1960), or the distribution patterns obtained from post-operation sediment surveys. The inputs to the model are water and sediment inflows, initial elevation-area-capacity relationships for the reservoir, and sediment characteristics. Adjusted reservoir capacities and areas, and incremental and cumulative sediment volumes deposited in each elevation interval, are computed by SEDRES for each time period.

Particular Features: The compaction of deposited sediments with time is considered in the model. The compaction of each type of sediment (sand, silt, and clay) is computed separately as a function of its age and submergence condition for each time interval.

Restrictions: SEDRES is suitable for predicting long-term changes in elevation-area-capacity relations of reservoirs. The effects of density currents, tributary inflows to the reservoir, and sediment entrainment from the bed are ignored.

Published References:

Croley, T.E. and Karim, F., "Sedimentation in the Coralville Reservoir", Iowa Institute of Hydraulic Research, Limited Distribution Report No. 63, January 1979.

Karim, F. and Croley, T.E., "Sedimentation in the Red Rock Reservoir", Iowa Institute of Hydraulic Research, Limited Distribution Report No. 64, June 1979.

Karim, F. and Kennedy, J.F., "Sedimentation in the Saylorville Lake", Iowa Institute of Hydraulic Research, Limited Distribution Report No. 68, July 1979.

Additional Information Available: Descriptive report

Example of Application: SEDRES was applied to three Iowa reservoirs - Coralville on the Iowa River, and Red Rock and Saylorville on the Des Moines River - to predict accumulation and distribution of sediment deposition for 100 years of simulation. Reductions in conservation and flood control storages of the Red Rock Reservoir with time, as predicted by SEDRES, are shown in Figure 22. The effects of seven different operation plans on the rate of depletion of reservoir capacity are shown in this figure.

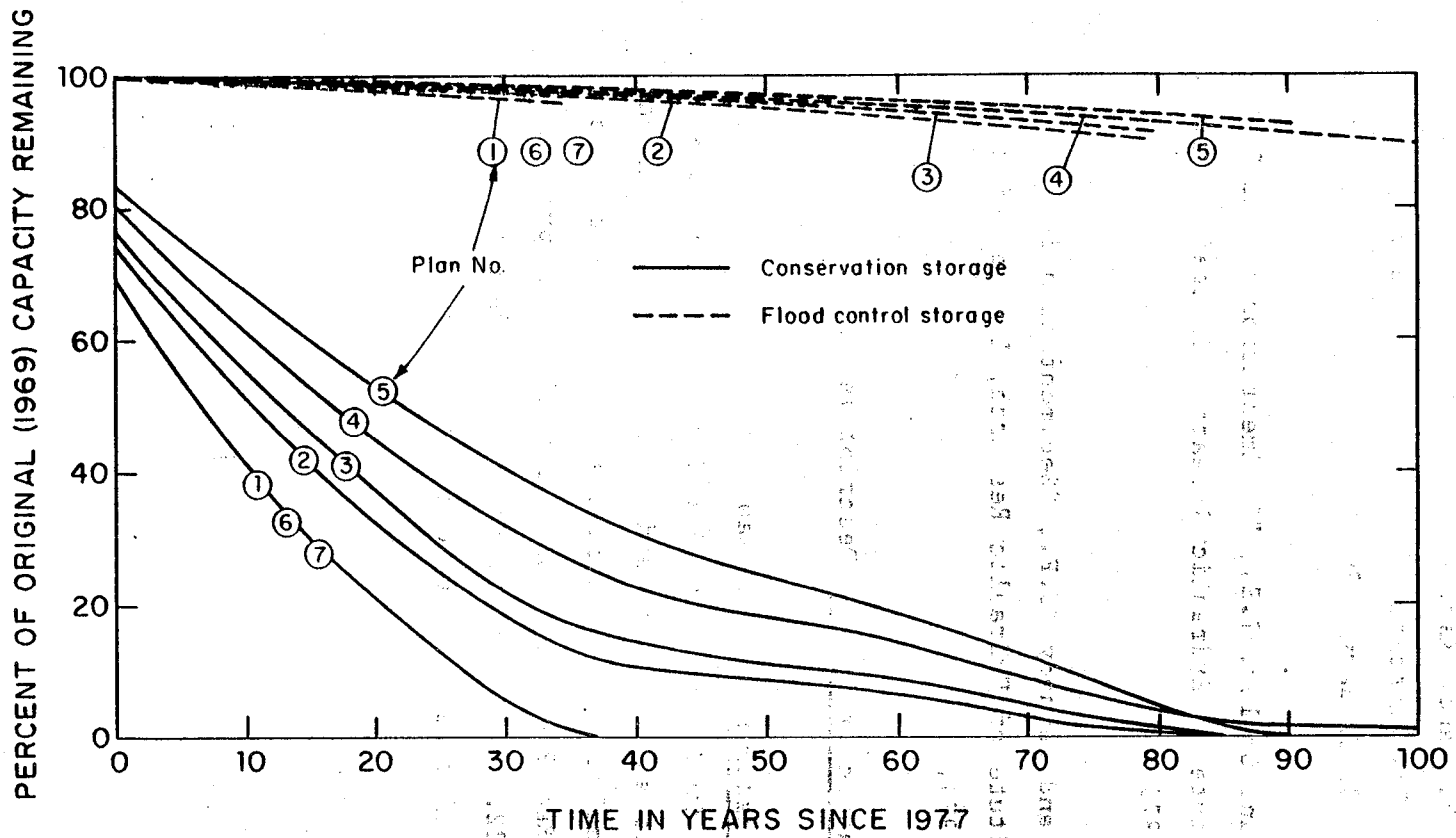

Figure 22. Computed storage loss in Red Rock Reservoir.

UNSTEADY CONTAMINANT DISPERSION IN RIVER AND CANAL NETWORKS

Program Name: CONDOR

Origin: Developed by P. Sauvaget, P. Bellody, and A. Preissmann at SOGREAH, 1981-83. Available by agreement with SOGREAH.

General Description: CONDOR, part of the CARIMA system, computes the one-dimensional mixing and decay of one or more contaminants in a branched or looped system of rivers and canals. Normally CONDOR accepts as input the unsteady discharges, velocities, and water levels previously computed by CARIMA. The user then defines the various contaminants of interest, their decay rates and/or interactions with each other, their initial distribution in the network, and their variation in time at all inflow boundaries. CONDOR then computes the fate of each contaminant subject to advection, diffusion, and decay/interaction, furnishing the time-variation of contaminant concentration at every computational point of the model. CONDOR is designed for use in engineering analyses of:

* salt-water intrusion in estuaries and delta systems of channels.
* fate of pollutants in river and canal systems.
* effects of river modifications on contaminant dispersion.
* treatment plant/outfall configurations required to meet water quality standards.

Particular Features: CONDOR uses a fractional-step method in which advection, diffusion, and decay/reaction are computed separately in each time step. Advection is computed by the Holly-Preissmann (1977) characteristics method, chosen for its simplicity of implementation coupled with exceptionally high accuracy. Diffusion is computed by an implicit Crank-Nicholson scheme. Decay and reaction are computed using implicit finite difference approximations of the relevant ordinary differential equations. These various methods have been

implemented in such a way as to be compatible with all the hydraulics works features of CARIMA (weirs, flood gates, etc.)

Restrictions: CONDOR assumes that the contaminants are fully mixed over the cross-section, treating advection and diffusion as one-dimensional processes. During high flows, the methodology used for computing mixing in flood plain cells may prove to be inadequate. Flow dynamics are assumed to be unaffected by dissolved contaminants.

Published References:

Holly, F.M. Jr. and Preissmann, A. (1977), "Accurate Calculation of Transport in Two Dimensions", JHYD, ASCE, Vol. 103, No. HY11, November, pp. 1259-1277.

Sauvaget, P. (1985), "Dispersion in Rivers and Coastal Waters 2. Numerical Computation of Dispersion", Developments in Hydraulic Engineering-3, P. Navak, Editor, Elsevier Applied Science Publishers, Barking, Essex, England.

Example of Application:

Figure 23 shows a schematic looped system of delta channels used for operational testing of CONDOR. Discharge hydrographs enter the model at points I003, J003, K004, L002 and G003; a tidal boundary condition is presumed to exist at points N001 and M001, where water levels undergo twice-daily sinusoidal variations with a tidal range of 3 meters. A constant salt concentration of 25 parts per thousand (ppt) was maintained at the tidal boundaries N001 and M001. Both diffusion and decay/reaction were suppressed for this demonstrative calculation.

Figure 23 also shows the time-variation of concentration computed by CONDOR at points C001, A006, and D002. Features such as the short-duration salinity decreases at C001 and A006, and the trapping of relatively fresh water at D002, reflect the complex dynamics of flow in looped delta systems.

The attainment of 25 ppt at C001 and A006, as well as the rapidity of the concentration rises and freedom from oscillations, reflect the accuracy of the Holly-Preissmann method for advection.

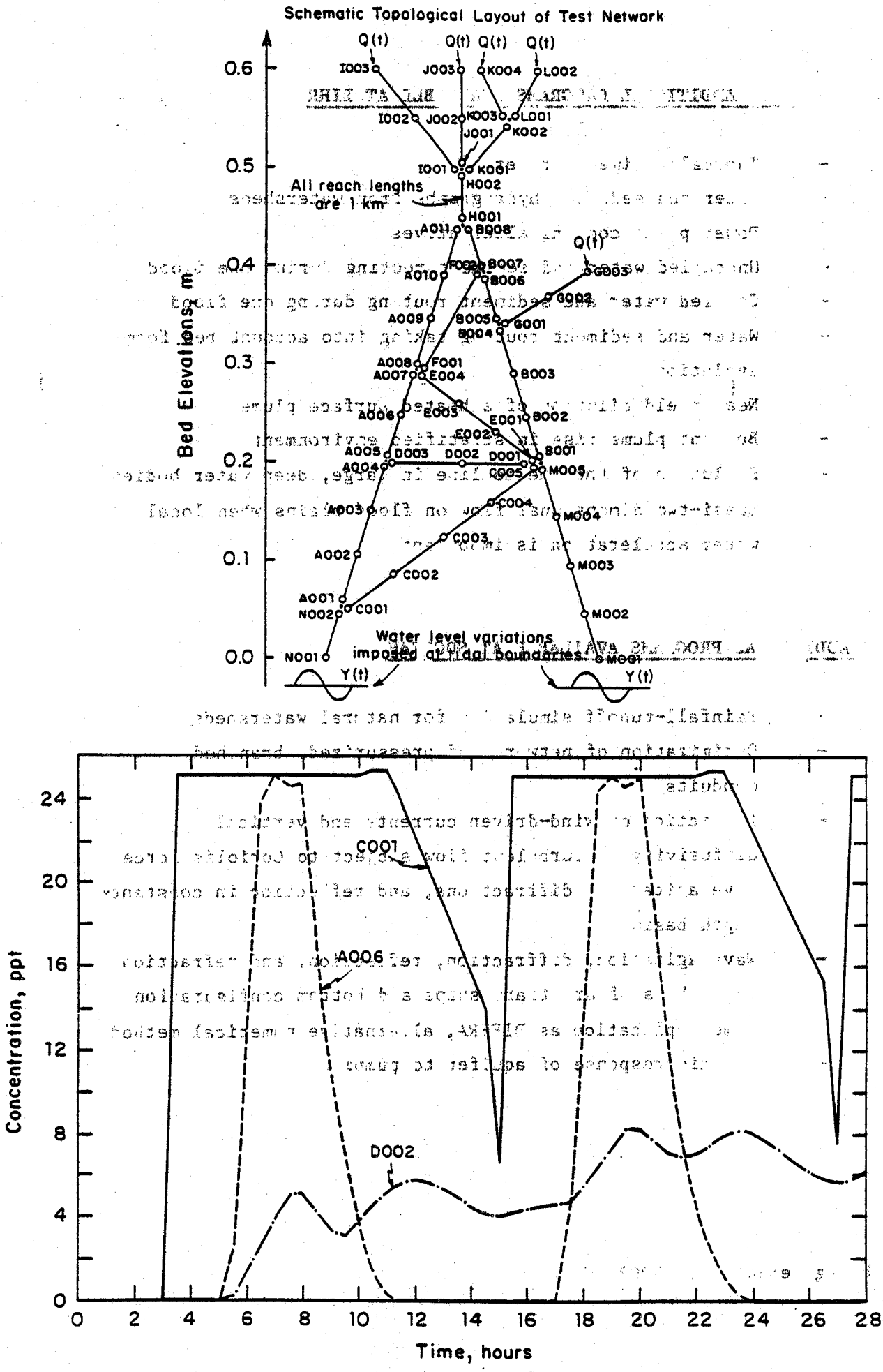

Figure 23. Example application of CONDOR.

IV. ADDITIONAL PROGRAMS AVAILABLE AT IIHR

ITRM	-	Thermal regime in rivers
DWM	-	Water and sediment hydrographs from watersheds
ICOOL	-	Power plant cooling alternatives
CHAR I*	-	Uncoupled water and sediment routing during one flood
CHAR III*	-	Coupled water and sediment routing during one flood
CHAR IV*	-	Water and sediment routing taking into account bed form evolution
JECHAU*	-	Near field dilution of a heated surface plume
PANACHE*	-	Buoyant plume rise in stratified environment
THERMO*	-	Evolution of the thermocline in large, deep water bodies
MEKOO2*	-	Quasi-two dimensional flow on flood plains when local water acceleration is important

V. SELECTED ADDITIONAL PROGRAMS AVAILABLE AT SOGREAH

BILIK	-	Rainfall-runoff simulation for natural watersheds
COSTAR	-	Optimization of networks of pressurized, branched conduits
CREOLE	-	Prediction of wind-driven currents and vertical diffusivity in turbulent flow subject to Coriolis force
DIFC	-	Wave agitation, diffractions, and reflection in constant-depth basins
DIFFRA	-	Wave agitation, diffraction, reflection, and refraction in harbors of arbitrary shape and bottom configuration
DIVINE	-	Same application as DIFFRA, alternative numerical method
ESTRA	-	Dynamic response of aquifer to pumping

*Available by agreement with SOGREAH

HISTOZ, HOULOGR, HOULSTAT	-	Statistical analysis of wave recordings
LAC	-	Evolution of water quality parameters in a stratified lake or impoundment
OPERET	-	Multipurpose reservoir optimization by dynamic programming
PASHA	-	Spectral analysis of random wave recordings
PLUTO	-	Rainfall-runoff transformation on urban catchments
PROPRETE	-	Optimization of looped pressure networks using dynamic programming
REFRA, REFRAN	-	Wave refraction and reflection in ports
REGULA	-	Stochastic analysis of flow regulation reservoir
STRATES	-	Simulation of unsteady estuarine flow with continuous vertical stratification

DYNAMICS OF ALLUVIAL-CHANNEL RESPONSE:

CASE STUDIES WITH THE COMPUTATIONAL MODEL **IALLUVIAL**

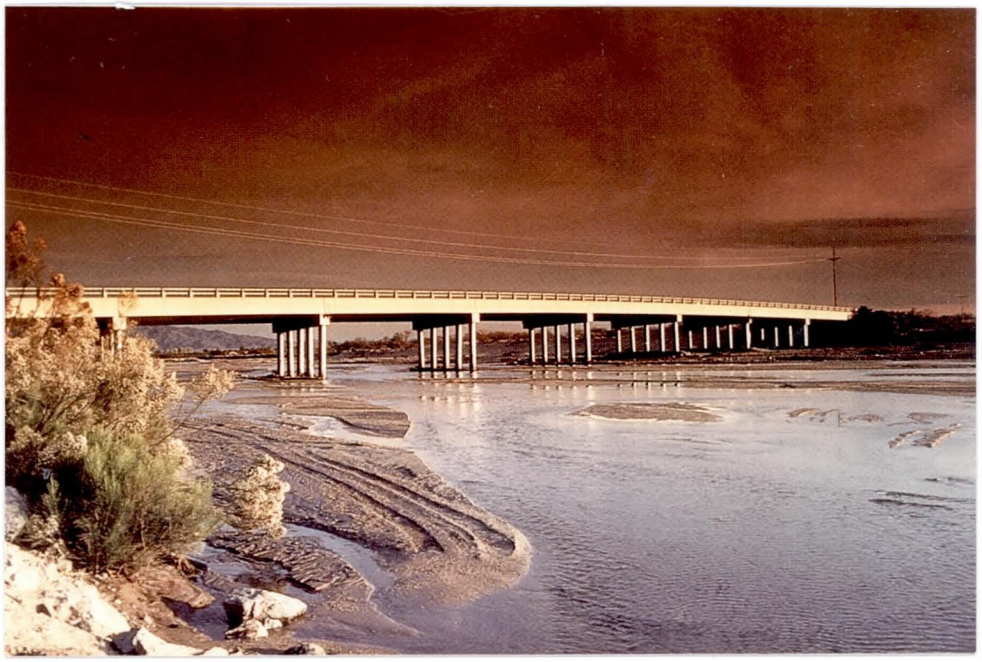

HYDRO LIBRARY

djd

80.0-00-1-09/86

PREFACE

The computer program IALLUVIAL, a state-of-the-art model for simulating water and sediment movements in alluvial channels, was developed by Dr. Fazle Karim under the overall guidance of Dr. John F. Kennedy, Professor and Director of the Institute of Hydraulic Research, University of Iowa. Some of the later developments of the model, including improvement in computational efficiency and streamlining of code, was contributed by Dr. Forrest M. Holly of the University of Iowa. Dooley-Jones & Associates (DJA) takes great pleasure in introducing IALLUVIAL for simulating dynamic response of the rivers in Arizona and the Southwestern region of the United States to man-made or natural changes in their water, sediment, or geometric characteristics.

In addition to IALLUVIAL, DJA maintains a competent staff of professionals capable of operating various other computer models, including HEC-1 (flood hydrograph), HEC-2 (water-surface profiles), HEC-5 (reservoir regulation), HEC-6 (water and sediment routing), FLUVIAL-11 (water and sediment routing), WQRRS (water quality), DAMBRK (dam break analysis), DWOPER (channel network), and Kentucky Pipe Network model. Several computer models have been developed in-house at DJA, e.g., SESCAL, HGRAPH, RRAP, PCHYD, HYDRO and COTHYD for hydrologic and hydraulic computations and plotting of results. DJA has performed numerous studies in the past by utilizing these models for the design and implementation of many water resources projects in the states of Arizona and California.

We are confident that the addition of IALLUVIAL to our growing list of computer models will enhance DJA's capability to analyze and simulate morphological characteristics of rivers and the impacts of various improvement works. We are proud of our past association, and look forward to working more closely with the various local, state, and federal agencies in Arizona and the Southwestern region of the United States in planning, design, and implementation of various water resources projects in the future.

Jerry R. Jones, P.E.
Executive Vice President

Roger E. Baele, P.E.
Vice President - Water Resources

DYNAMICS OF ALLUVIAL-CHANNEL RESPONSE: CASE STUDIES WITH THE COMPUTATIONAL MODEL IALLUVIAL

M. F. KARIM

DOOLEY-JONES & ASSOCIATES, INC.
35 E. TOOLE AVE., P.O. BOX 1830
TUCSON, ARIZONA 85702

SEPTEMBER, 1986
DJA JOB NO. 85-215

Rpt. A5

EXECUTIVE SUMMARY

Dynamics of alluvial-channel responses to natural or man-made changes in flow, sediment or geometric regimes are simulated by a computational model, IALLUVIAL, in three case studies. IALLUVIAL incorporates several state-of-the-art formulations of the underlying physical processes, e.g., ability to simulate flow resistances, without the need to specify Manning's "n" a priori; a sediment-transport relation verified for wide ranges of flow and sediment characteristics; consideration of subsurface sediment layers with different compositions; contributions of tributary sediment inflows and bank erosion; and bed armoring and sorting formulations based on the most recent understanding of the phenomena. The formulations incorporated in the model eliminate most of the deficiencies of existing erodible-bed models, which were pointed out in a comprehensive evaluation study by the National Research Council in 1983. Changes in bed and water-surface elevations and bed-sediment characteristics simulated by IALLUVIAL for the Salt and Missouri Rivers have been found to be in good agreement with the corresponding observed values. In particular, IALLUVIAL prediction of the Salt River bed evolution during 1977-83 was in much better agreement with the observed values than that of HEC-6. These applications validate the model as a reliable and useful tool for engineers in predicting dynamic responses (to natural or man-induced changes) of the sand-bed rivers, as well as of the gravel and cobble-bed, relatively steep-slope streams of the Southwestern region of the United States.

TABLE OF CONTENTS

		PAGE NO.
I.	INTRODUCTION	1
II.	THE COMPUTATIONAL MODEL: IALLUVIAL	4
III.	PREDICTION OF SEDIMENT TRANSPORT	7
IV.	PREDICTION OF FRICTION FACTOR	13
V.	CASE STUDY I: SALT RIVER 100-YEAR FLOOD	14
VI.	CASE STUDY II: SALT RIVER BED EVOLUTION, 1977-83	19
VII.	CASE STUDY III: MISSOURI RIVER DEGRADATION DOWNSTREAM OF GAVINS POINT DAM	26
VIII.	CONCLUSIONS	33
IX.	REFERENCES	34

I. INTRODUCTION

Dynamics of alluvial-channel response to natural phenomena or man's activities is complex and is only understood qualitatively. Satisfactory quantification of a river's self-adjustment process in response to man-induced perturbation of its sediment-transport equilibrium (e.g., sand and gravel mining, bridge and highway construction, channelization and realignment, river flow regulation by dams and reservoirs, etc.) or to natural variations in climatic, hydrologic, or sediment inputs during major floods or from year to year, remains a goal of river engineers throughout the world. Availability of fast computers during the last two decades has led to the development of mathematical models as additional tools to aid the engineers to evaluate and implement various river development projects, and to assess the impacts of such projects on the environment and the future evolution of rivers. In spite of their limitations, such models have proved to be invaluable tools in the hands of experienced engineers. This report describes salient features and applications of IALLUVIAL, a mathematical model developed at the Institute of Hydraulic Research, the University of Iowa, under the sponsorship of the U.S. Army Corps of Engineers (Omaha District), and the National Science Foundation. Computer code of IALLUVIAL has been updated by engineers at Dooley-Jones & Associates for application to the rivers of the semi-arid, southwestern region of the United States. The option to use geometric data in HEC-2 (or HEC-6) format has been added in this updated version.

Several erodible-bed numerical models, similar to IALLUVIAL, were evaluated by the National Research Council (1983) on behalf of the Federal Emergency Management Agency. In their recommendations, National Research

Council (1983) pointed out the following deficiencies of the models examined in their study (e.g., HEC2SR, KUWASER, UUSWR, HEC-6, FLUVIAL-11, and SEDIMENT-4H):

"a. Unreliable formulation of the sediment-discharge capacity of flows.

b. Inadequate formulation of the variable friction factor of erodible-bed flows, and, in particular, the dependency of friction factor on depth and velocity of flow, sediment concentration, and temperature.

c. Inadequate understanding and formulation of the mechanics of bed coarsening and armoring, and their effects on sediment-discharge capacity, friction factor, and degradation suppression of flows.

d. Inadequate understanding and formulation of the mechanics of bank erosion, and therefore, limited capability to incorporate this contribution into the sediment input to the flows from bank erosion and the effects of channel widening."

Development of IALLUVIAL was directed towards overcoming these dificiencies (specifically items a, b, and c) by incorporating state-of-the-art knowledge of the constituent physical processes. A brief overview and implementation of these features in the model are described in Sections II, III, and IV.

A numerical model is simply a quantification and solution of the mathematical formulas or relationships governing constituent physical processes; a model is as good as the accuracy of these relations in representing the actual physical processes. Two most important constituent processes in an erodible-bed model are simulations of sediment discharges and friction factors in alluvial-channel flows (as stated by items a and b of NRC's conclusions). In particular, computation of sediment discharges (which, in turn, strongly depend on friction factors), is the single-most important ingredient, because simulation of bed degradation/aggradation results essentially from a book-keeping process involving sediment-transport capacities at the two ends of a computational subreach. Accordingly, the capability of IALLUVIAL to simulate the sediment discharges and friction factors in alluvial channels is described in Sections III and IV. Three case studies are then presented in Sections V, VI, and VII, followed by conclusions in Section VIII.

II. THE COMPUTATIONAL MODEL: IALLUVIAL

Natural streams respond dynamically to natural or man-induced changes in hydrological, sediment and geometrical regimes. A river's self-adjustment process in response to such imposed or natural changes, in the process of restoring to a new quasi-equilibrium state, takes place in a variety of interrelated ways, e.g., changes in depth, velocity, width, slope, friction factor, sediment discharge, bed-sediment composition (coarsening or bed armoring), and channel-bed geometry. The program IALLUVIAL has been developed to simulate these river responses, both short-term and long-term.

IALLUVIAL is a quasi-steady, one-dimensional water-and sediment-routing model. It utilizes finite-difference numerical techniques to solve the governing equations of alluvial-channel flows, e.g., equations of water and sediment continuity (by size fraction), energy equation, and relations for sediment discharge and friction factor. The numerical technique used in the model for backwater (and sediment-discharge) computation includes two options: the standard-step method; and a more efficient and accurate Newton-Raphson scheme which solves simultaneously the equations of energy, water continuity, sediment discharge, and friction factor. A unique feature of IALLUVIAL is the employment of a coupled set of sediment-discharge and friction-factor relations, which incorporates the dependence of alluvial-bed friction factor on sediment discharge. The salient features of the model are summarized below:

* Incorporates a sediment-discharge relation developed from wide ranges of flume and field data; tested and verified for both sandy and gravel-bed streams.

* Dependence of friction factor on sediment discharge is incorporated through a coupled set of sediment-discharge and friction-factor relations. Specification of roughness coefficient, Manning's "n", is thus not needed in input data.

* Simulates sediment sorting and bed armoring. The model incorporates armoring procedures appropriate for both sand-bed and gravel-and cobble-bed streams.

* Effects of bed armoring on sediment discharge and friction factor are included.

* Computationally efficient for simulating long time periods.

* Option to use geometric data in HEC-6 format is included in updated version.

* Capable of utilizing contributions from tributaries and bank erosion.

* Vertical nonhomogeneity in size distribution of different sub-surface layers of bed sediments are accounted for in sediment-sorting procedure.

* Options for river-bed dredging/mining and externally imposed bed-width changes with time are included.

* Tested and verified for simulating observed degradation/aggradation/friction factor/armoring for rivers of Arizona.

Further study is underway at Dooley-Jones & Associates, Inc. to improve the model and incorporate additional features.

III. PREDICTION OF SEDIMENT TRANSPORT

The single most important ingredient in any numerical model for erodible-bed channels is satisfactory simulation of sediment-transport capacities at various channel sections representing a river reach. IALLUVIAL utilizes a coupled set of sediment-discharge and friction-factor relations, known as Total-Load Transport Model (TLTM). The formulation of TLTM takes into account the well-known fact that the friction factors of alluvial streams are heavily dependent on their sediment discharges, and avoids the need to specify a fixed hydraulic roughness, such as Manning's coefficient, a priori. In keeping with this concept, the friction-factor relation includes sediment discharge as one of the independent variables, and an iteration scheme is used to compute sediment discharge and friction factor from the following pair of equations:

Sediment-discharge predictor

$$\text{Log}\left(\frac{q_s}{\sqrt{g(s-1)D^3_{50}}}\right) = -2.278 + 2.972 \log V_1 + 1.006 \log V_1 \log V_3 + 0.299 \log V_2 \log V_3 \qquad (1)$$

Friction-factor predictor

$$\text{Log}\left(\frac{U}{\sqrt{g(s-1)D_{50}}}\right) = 0.102 + 0.269 \text{ Log } V_2 + 0.207 \text{ Log } V_4 - 0.178 \log V_3 + 0.173 \log V_5 \qquad (2)$$

where

$$V_1 = \frac{U}{\sqrt{g(s-1)D_{50}}} \; ; \; V_2 = \frac{d}{D_{50}}; \quad V_3 = \frac{u_* - u_{*c}}{\sqrt{g(s-1)D_{50}}} \; ;$$

$$V_4 = S \cdot 10^3; \quad V_5 = \frac{q_s}{\sqrt{g(s-1)D^3_{50}}} \; ;$$

q_s = volumetric bed-material discharge/unit width (includes both bed load and suspended load, but not wash load), U = mean flow velocity; d = mean flow depth; D_{50} = median bed-material size, S = energy slope; u_* = bed shear velocity; u_{*c} = critical shear velocity obtained from Shields' diagram; g = gravitational constant; and s = specific gravity of sediment particles.

Equations (1) and (2) were developed on the basis of physical and dimensional considerations, and the coefficients obtained from multiple-regression analysis of a large number (615 flows) of flume and river data. For given water discharge, energy slope, and sediment size, TLTM solves equations (1) and (2) simultaneously to obtain depth, velocity, friction factor, and sediment discharge. Application of TLTM to a large body (947 flows) of laboratory and field data yield satisfactory prediction of sediment discharges, as shown in Table 1. The ranges of relevant variables for the data base from which TLTM is developed are as follows:

	Minimum	**Maximum**
Depth (ft.)	0.10	17.35
Velocity (ft./sec.)	1.04	9.45
Slope	0.00015	0.024
D_{50} (mm)	0.13	28.65
Concentration (ppm)	20	49,300
Gradation Coeff.	1.00	1.96
Temperature (^oC)	0.6	38.0
Froude No.	0.09	2.08

TABLE 1
SUMMARY OF SEDIMENT-DISCHARGE AND
FRICTION-FACTOR RESULTS BY TLTM

Data Set	No. of Pts	Sediment Discharge Mean Ratio	Sediment Discharge Mean Norm.* Error (%)	Friction Factor Mean Ratio	Friction Factor Mean Norm.* Error (%)
Guy et al (.19mm)	29	1.45	69.3	1.00	40.6
Guy et al (.27mm)	17	1.51	52.4	0.80	41.1
Guy et al (.28mm)	32	1.36	52.1	0.97	35.9
Guy et al (.32mm)	29	1.97	102.9	0.74	33.0
Guy et al (.45mm)	27	0.95	37.0	1.18	48.0
Guy et al (.93mm)	23	1.07	24.5	0.80	25.1
Williams	24	2.12	112.5	0.85	18.4
Vanoni-Brooks	21	0.92	47.6	1.18	56.9
Missouri R.(Cat. A)	60	1.02	36.9	1.04	32.2
Missouri R.(Cat. B, C)	26	1.20	47.0	0.90	20.0
Missouri R. (RS)	17	1.07	48.9	1.28	33.7
Sato, et al (#1)	136	1.01	32.1	0.92	16.7
Meyer-Peter & Muller	41	0.90	39.7	0.96	15.9
Gilbert	43	0.70	35.0	0.81	35.4
Waterways Expt. Sta. (#1)	90	0.98	29.5	0.93	10.4
Willis-Kennedy	31	0.76	39.2	0.72	28.8
Missouri R. (Sioux City)	51	1.09	41.3	0.46	54.6
Middle Loup R.	45	0.80	31.9	0.80	35.4
Niobrara R.	25	1.72	72.6	0.56	43.7
ACOP Canals	34	0.63	44.6	0.84	29.2
Rio Grande	58	0.80	46.7	0.79	31.5
Elkhorn R.	23	0.35	67.2	0.92	25.4
Sato, et al (#2)	45	0.87	38.4	0.84	21.8
Waterways Expt. Sta. (#2)	20	1.18	45.9	0.93	13.6
All data	947		44.8		28.50

*Mean Normalized Error (%) = $\frac{100}{N} \sum_{i=1}^{N} \frac{|X_{mi} - X_{ci}|}{X_{mi}}$

Where: X_{mi} = measured value of ith flow

X_{ci} = computed value of ith flow

N = total number of flows

The validity of TLTM to predict sediment discharges of the ephemeral streams of Arizona was investigated. A difficulty in this task was the lack of availability of a complete set of sediment discharge and related hydraulic and geometric data for many rivers of Arizona. Even though a relatively large number of sedient-discharge measurements were made for some rivers, the associated data on sediment size distributions were not available, so that estimates of median bed-sediment size (D_{50}) or the portions of measured suspended discharges that are wash load cannot be made. After careful scrutiny, 21 data points from four rivers - San Pedro, Little Colorado, Virgin, and Gila - were found suitable for comparison of measured and computed sediment discharges. Graphical comparison of the measured and computed sediment discharges for these 21 flows are shown in Figure 1. Measured sediment discharges used in Figure 1 include measured suspended-sediment discharges (as reported by USGS), with adjustment made to exclude wash loads estimated from the measured size distributions of bed materials and suspended discharges. Bed load contribution, assumed as 10% of suspended loads, was added to obtain the "measured" total sediment discharges shown in Figure 1.

It is seen from Figure 1 that the computed sediment discharges agree reasonably well with the measured values. Considering the uncertainty and practical difficulties involved in field measurements and the assumptions that have to be made for estimating some quantities, prediction accuracy of TLTM for sediment-discharge capacities of these four rivers may be considered to be satisfactory. Notwithstanding the limited availability of data, this comparison demonstrates the validity of IALLUVIAL simulation of sediment

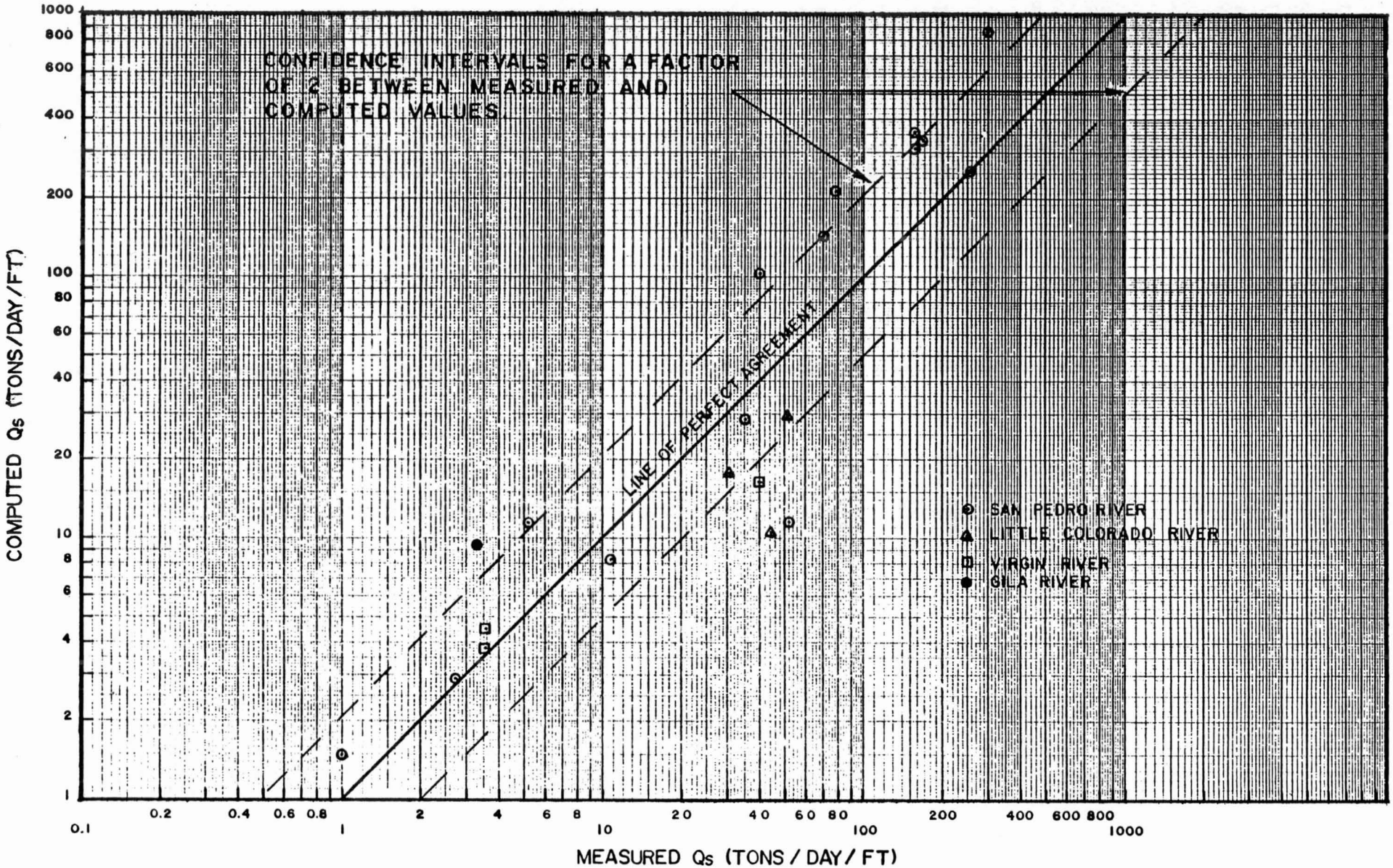

FIGURE I

COMPARISON OF MEASURED AND COMPUTED SEDIMENT DISCHARGES BY IALLUVIAL

CALC. BY F.K., DWN. BY R.H.F. (8-25-86)

discharges for Arizona rivers. It may be noted that, to the best of the author's knowledge, Figure 1 represents the first attempt to compare measured sediment discharges with the values computed by any sediment-transport model for these rivers.

In a recent study at the University of British Columbia, Vancouver, Canada, the sediment discharges predicted by TLTM for the Fraser River were found to be in better agreement with the measured values than those computed by other sediment discharge relations.

IV. PREDICTION OF FRICTION FACTOR

Accurate prediction of the variable friction factor in a movable-bed model is an important factor for valid simulation of sediment discharges and bed evolution over long periods. As discussed before, IALLUVIAL incorporates a friction-factor relation, eqn. (2), which accounts for the dependency of friction factor on sedment discharge. Thus, friction factor or roughness coefficient is continuously updated automatically in each time increment during entire simulation period, and the dynamic interdependence between flow and sediment characteristics, changing channel geometry, bed-form configuration, and roughness coefficient is properly accounted for. This is a significant improvement over the existing models, in which constant roughness coefficients, Manning's "n", are specified and treated as invariant with time.

The friction-factor relation included in IALLUVIAL was found to yield satisfactory prediction for a large number (947 flows) of flume and river data, as shown in Table 1. Relevant measured data are not available to check its validity for rivers in Arizona. However, an indirect validation of the friction-factor relation is presented in the next section in a case study for the Salt River, as demonstrated by the satisfactory prediction of the water-surface profile in Figure 4.

V. CASE STUDY I: SALT RIVER 100-YEAR FLOOD

The Salt River is located in Maricopa County, Arizona and is a tributary to the Gila River. The selected reach for this case study is the same as that used in the comparative analysis of six erodible-bed models by the National Research Council (1983). The study reach, shown in Figure 2, extends from just downstream of I-10 highway bridge to the Hohokam Expressway. Salt River experienced major floods in three years between 1978 and 1980. The 100-year design flood hydrograph, as shown in Figure 3, is used as the input hydrograph. This design hydrograph resembles closely the flood of February 1980, which had a peak flow of 185,000 cfs and a duration of 15 days. Bed-material sizes ranged from 0.22 mm to 185.0 mm, with the median size D_{50} approximately 60 mm. All input data utilized in this case study are the same as those used in NRC (1983) study.

Computed thalweg and water surface profiles simulated by IALLUVIAL are shown in Figure 4. Computed profiles by four other models (HEC2SR, HEC-6, FLUVIAL-11, and SEDIMENT-4H), also shown in Figure 4, are taken from NRC (1983) report. As observed data for this river reach are not available, Figure 4 compares the results simulated by IALLUVIAL with those obtained from four other models. It is seen from Figure 4 that water-surface profiles computed by all five models closely parallel each other, with the exception of HEC2SR which gives consistently lowest elevations. Computed thalweg profiles by different models, however, differ significantly from each other, with FLUVIAL-11 yielding considerably higher bed elevations than other models. Deviations at or near upstream boundary are likely due to somewhat different boundary conditions applied by different models.

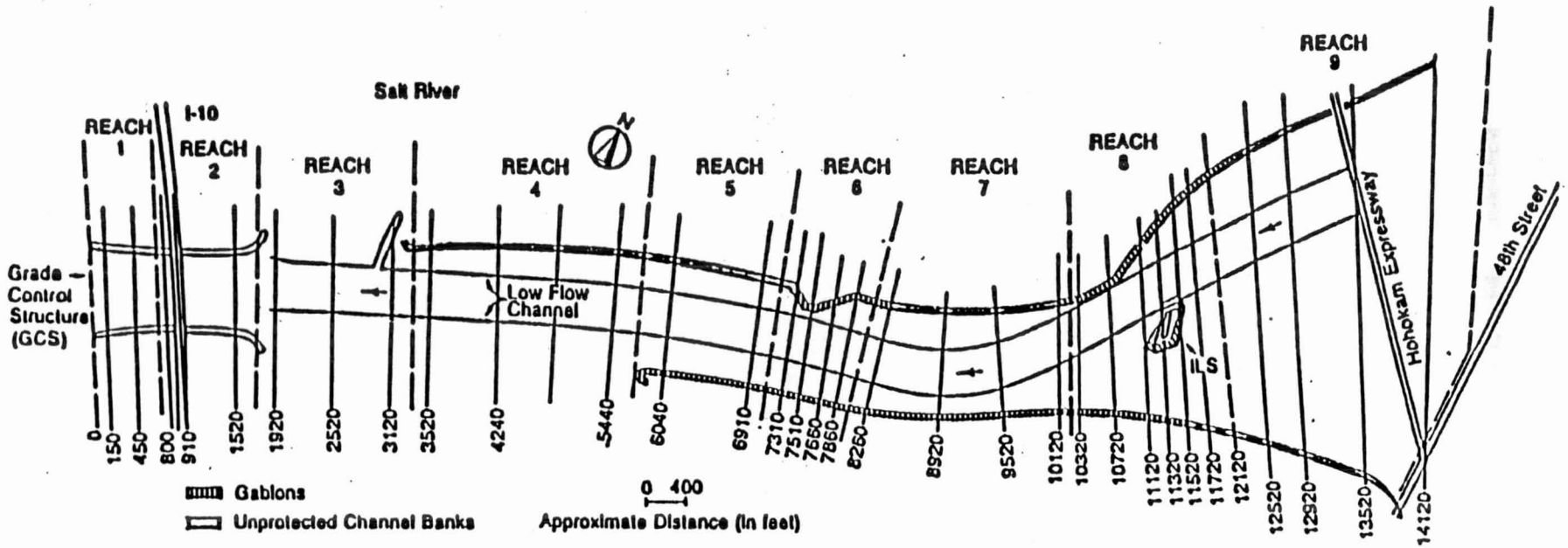

FIGURE 2 SALT RIVER REACH FOR CASE STUDY I (TAKEN FROM THE NATIONAL RESEARCH COUNCIL (1983)).

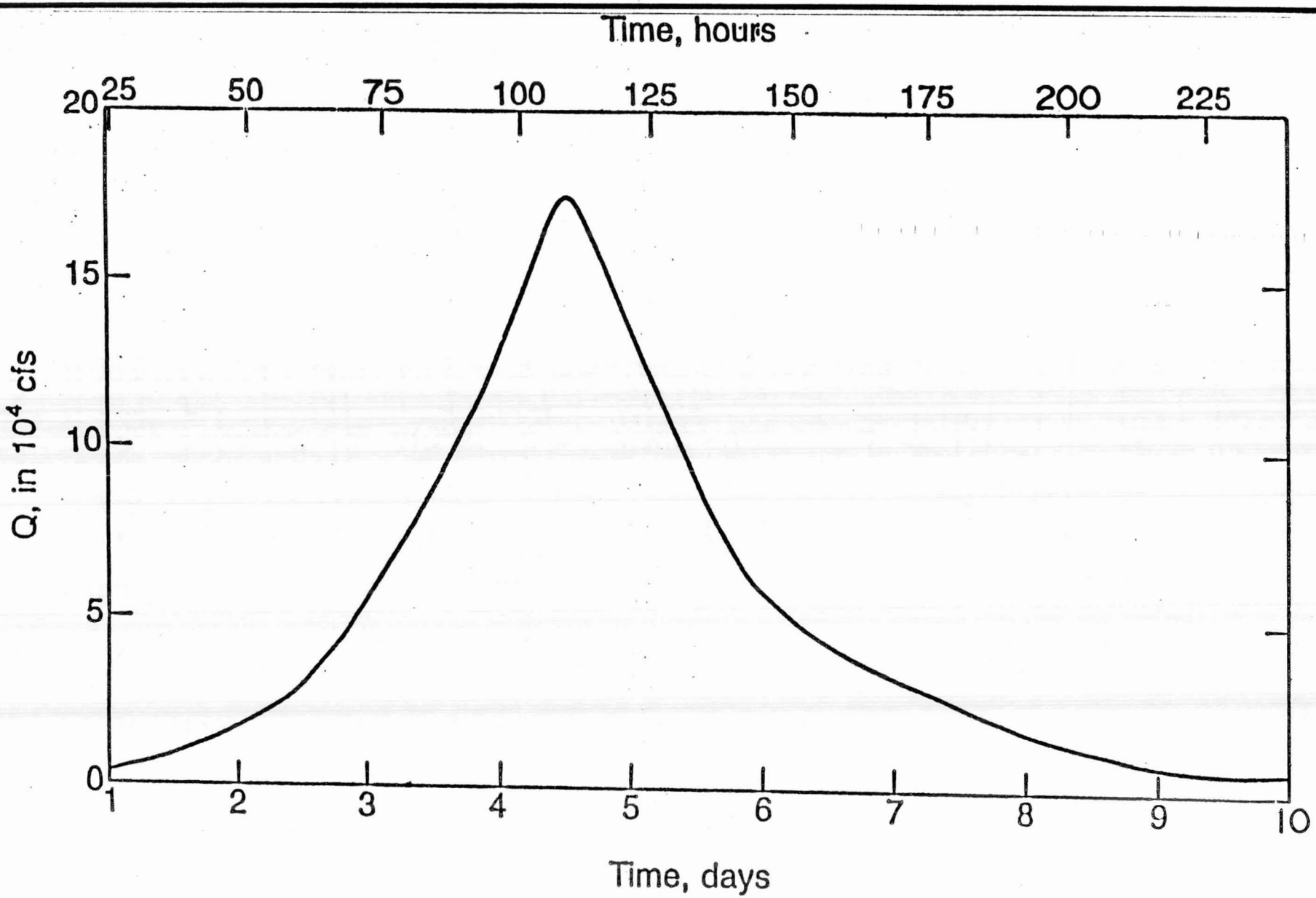

FIGURE 3
SALT RIVER 100-YEAR-FLOOD HYDROGRAPH

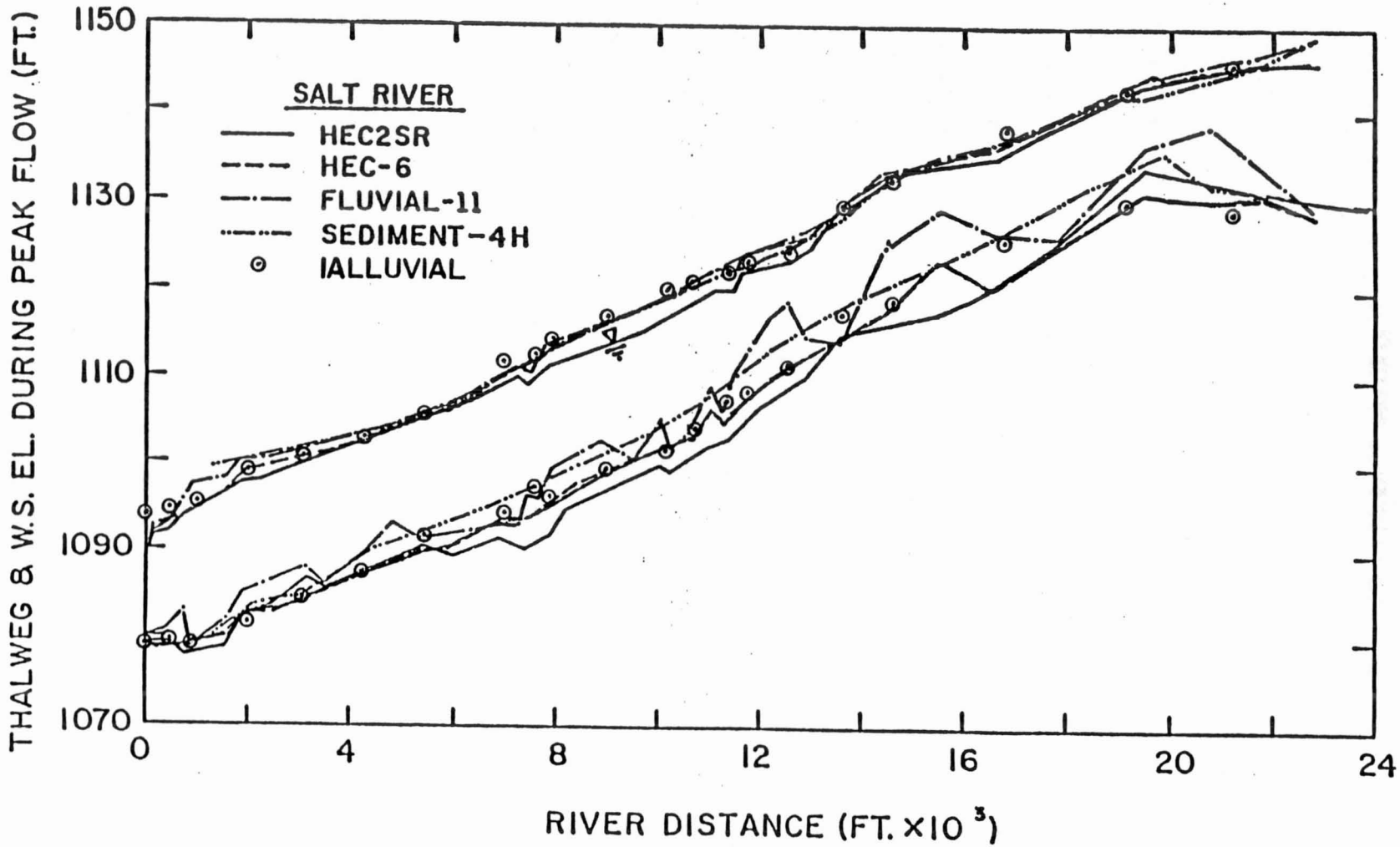

FIGURE 4 COMPARISON OF THALWEG AND WATER-SURFACE PROFILES AT PEAK FLOW COMPUTED USING IALLUVIAL AND FOUR OTHER MOVABLE-BED MODELS.

CALC. BY F.K., DWN. BY R.H.F (8-25-86)

The important point indicated by Figure 4 is that IALLUVIAL simulated water-surface elevations that are close to those computed by other models, even though pre-determined roughness coefficient (Manning's "n") as used by other models are not utilized (or necessary) in IALLUVIAL simulation. Two significant drawbacks of using fixed roughness (Manning's "n") are: (1) even though trial-and-error procedure of selecting Manning's "n" may reproduce closely measured water-surface elevations for a given flow condition, it is likely that the same "n" values are not applicable at other flow conditions during a long simulation period; and (2) computed depths, velocities, and energy slopes resulting from a backwater computation are fairly sensitive to Manning's "n" values while water-surface elevations are less sensitive to "n"; thus, "n" values calibrated on the basis of water-surface elevations may lead to significant errors in calculated depths, velocities, and energy slopes, and even larger errors in sediment discharges which strongly depend on these parameters. For example, "n" values calculated from friction factors given by IALLUVIAL simulation vary from approximately 0.02 to 0.04 at different sections, while a fixed value of 0.03 was used in HEC2SR simulation at all sections (Figure 4). It is likely that such differences in calculated depths and velocities, even though water-surface elevations are nearly the same, resulted in wide variations in computed sediment discharges and therefore in thalweg elevations, as shown in Figure 4 (of course, different sediment-discharge formulas utilized contributed partly to such variations). IALLUVIAL eliminates these shortcomings by incorporating dynamic dependence between flow resistence, hydraulic parameters, and changing bed elevations and sediment characteristics.

VI CASE STUDY II: SALT RIVER BED EVOLUTION, 1977-83

The Salt River reach for this case study, approximately 2 miles long, is located between 35th Avenue and 51st Avenue of the City of Phoenix, Arizona (Figure 5). This reach of the Salt River is the same as that analyzed by Dust, Bowers, and Ruff (1986) for application of HEC-6 model.

Portions of the study reach are braided as shown in Figure 6. The upper layer (1.5 to 2.0 ft.) of the river bed is composed primarily of sandy gravel and well-grounded cobbles (Figure 7), with localized pockets of fine to medium sand. Flow in the study reach of the Salt River is controlled by the Granite Reef Dam located approximately 20 miles upstream.

The simulation period covered in this case study is 1977-83. Geometric data, bed-sediment distribution and flow hydrograph are the same as utilized by Dust, Bowers, and Ruff (1986). Bed-material size distribution with D_{50} approximately 23 mm, measured from samples taken in the summers of 1983-84, was assumed to represent the initial (1977) conditions (since 1977 data were not available). As discussed in Sections IV and V, Manning's "n" values are not required as inputs to IALLUVIAL as a friction-factor predictor is included in its formulation. The 1977-83 study period of the Salt River reach had a total of approximately 180 days of flow, with four major flood events in February 1978, December 1978, January 1979, and February 1980. The input hydrograph representing the study period is shown in Figure 8.

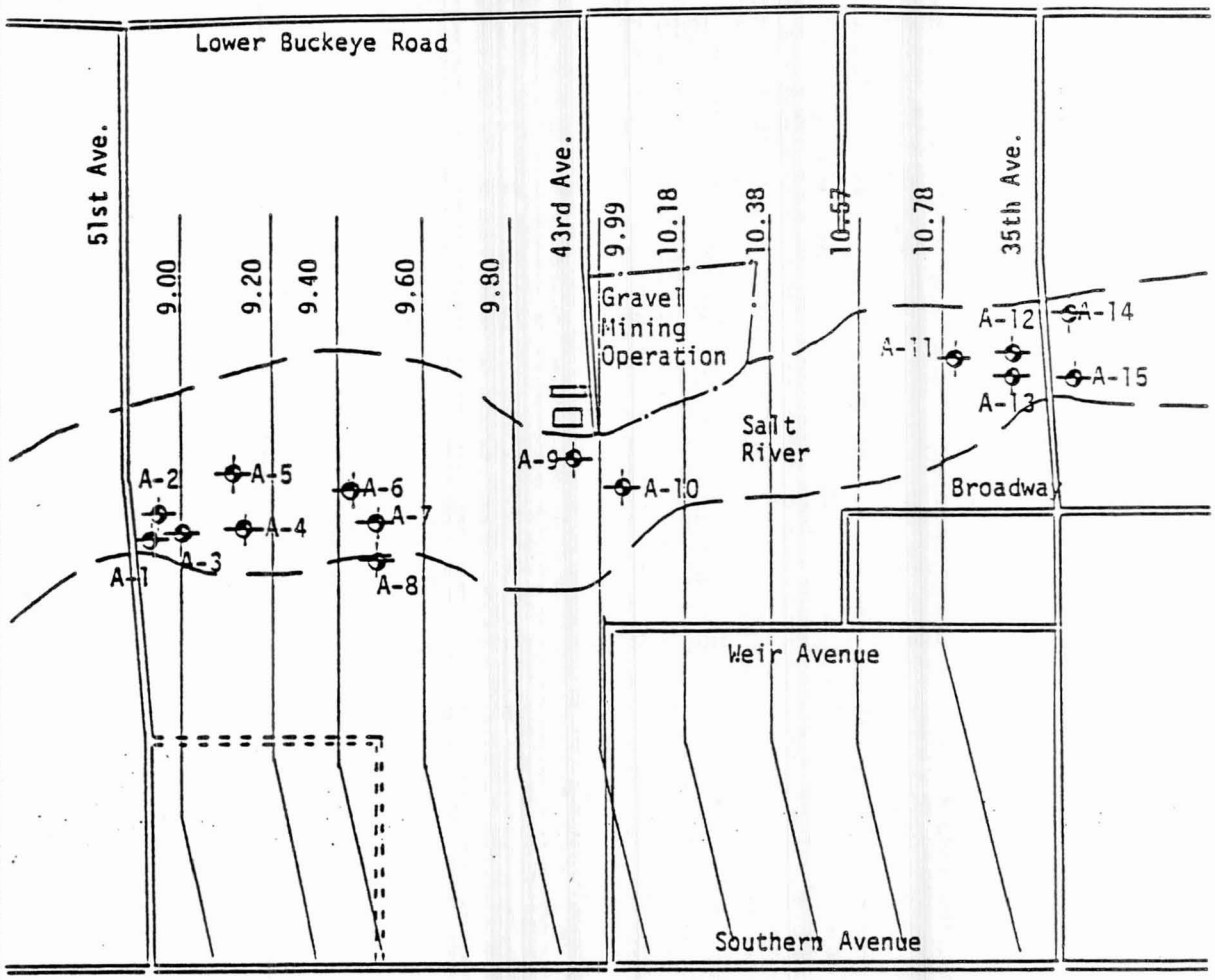

LEGEND:

10.57 Cross Section Number

Sediment Samples of Bed and Bank Material

Floodplain Boundaries (U.S.G.S.)

N

2000 4000

Scale in Feet

FIGURE 5 SALT RIVER STUDY REACH FOR CASE STUDY II (TAKEN FROM DUST, BOWERS, AND RUFF (1986)).

Figure 6. The Salt River at 35th Avenue; flow direction is from right to left (photograph by Larry Foppe, April 1983), (taken from Dust, Bowers, and Ruff (1986)).

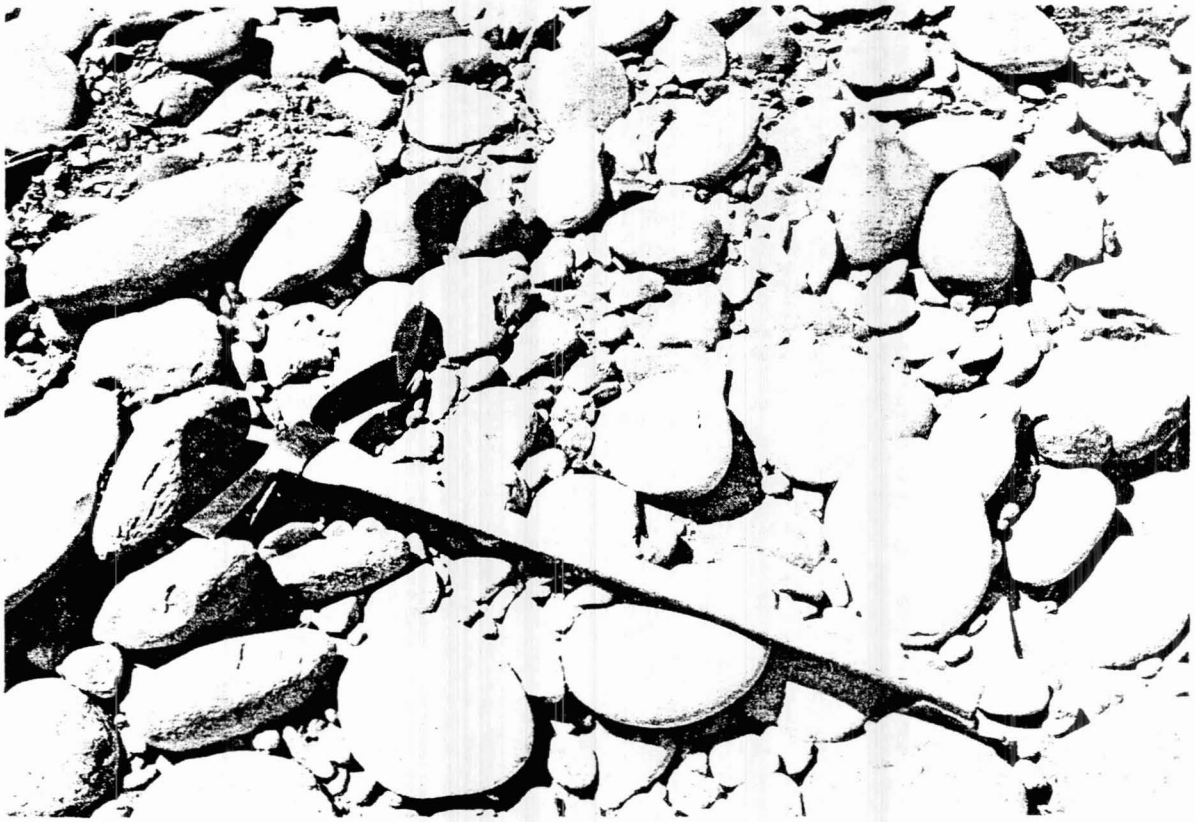

Figure 7. Close-up of Armored bed surface of the Salt River near cross section 9.20; flow direction is from left to right (photograph by David Dust, May 1984), (taken from Dust, Bowers, and Ruff (1986)).

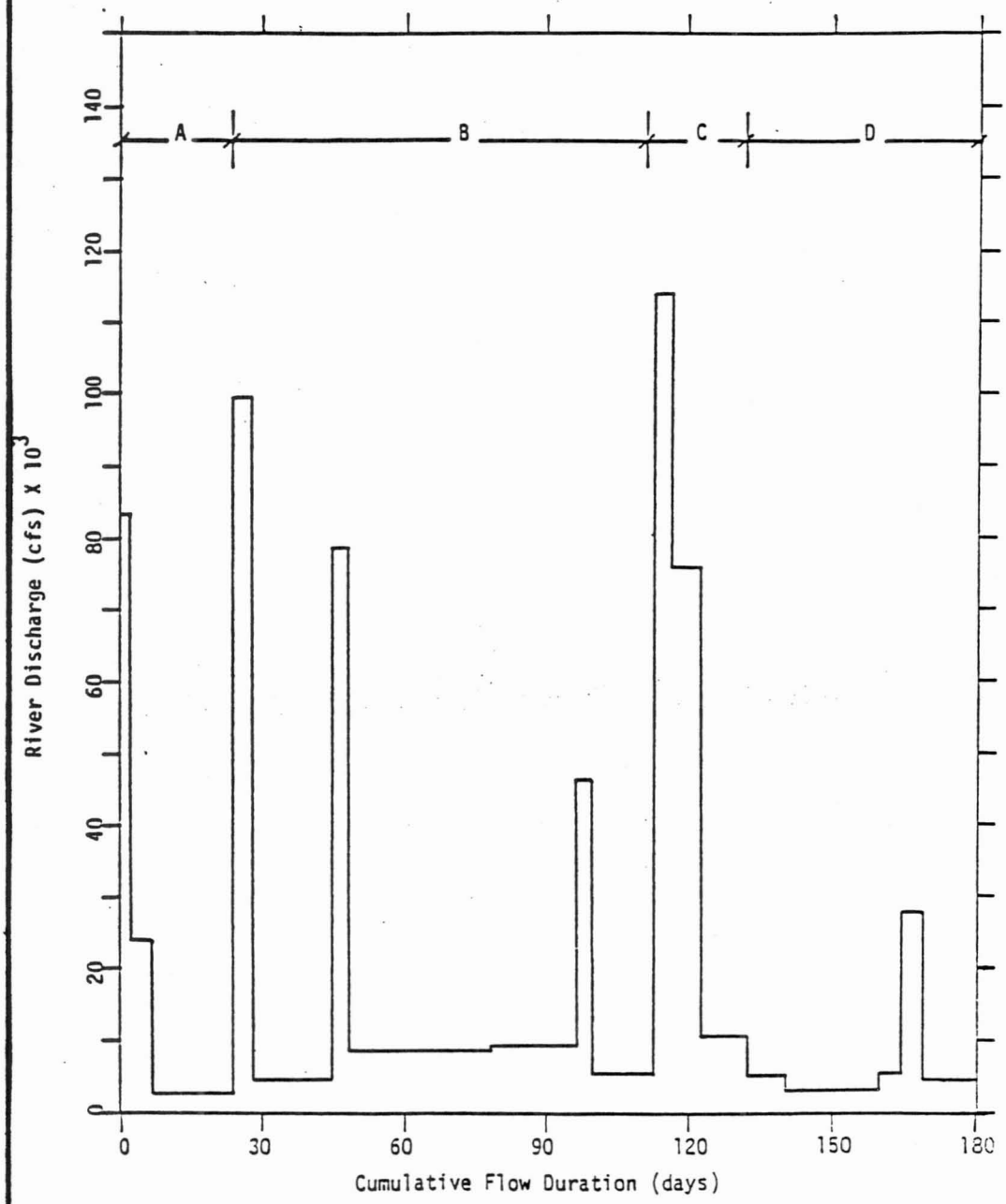

FIGURE 8: FLOW HYSTOGRAM FOR THE SALT RIVER INDICATING MAJOR FLOOD EVENTS, 1977-83 (TAKEN FROM DUST, BOWERS, AND RUFF (1986)).	A: Flood of Feb 28-Apr 11, 1978
	B: Flood of Dec 16, 1978-May 31, 1979
	C: Flood of Jan 29- June 3, 1980
	D: Flood of Dec 9, 1982-Feb 29,1983

The changes in bed elevation in the study reach of the Salt River computed by IALLUVIAL are shown in Figure 9. Also shown in this figure are the measured bed-elevation changes and those computed by HEC-6, which are taken from Dust, Bowers, and Ruff (1986). It is seen from Figure 9 that IALLUVIAL simulation is in good agreement with the measured bed-elevation changes, except at Sections 9.99 and 10.57. The discrepancy between measured and computed bed-elevation changes at these sections is likely due to the location of gravel mining operation in the vicinity and upstream of Section 9.99. In particular, a new main channel developed during the study period near Section 9.99 due to the diversion of flow through the gravel pit; this change of channel geometry is not included in input data set and, therefore, some discrepancy is expected at and in the vicinity of this section. In view of the uncertainties involved in the input data representing the study reach, the IALLUVIAL-simulated bed elevation changes of the Salt River reach, shown in Figure 9, appear to be in excellent agreement with the field measurements.

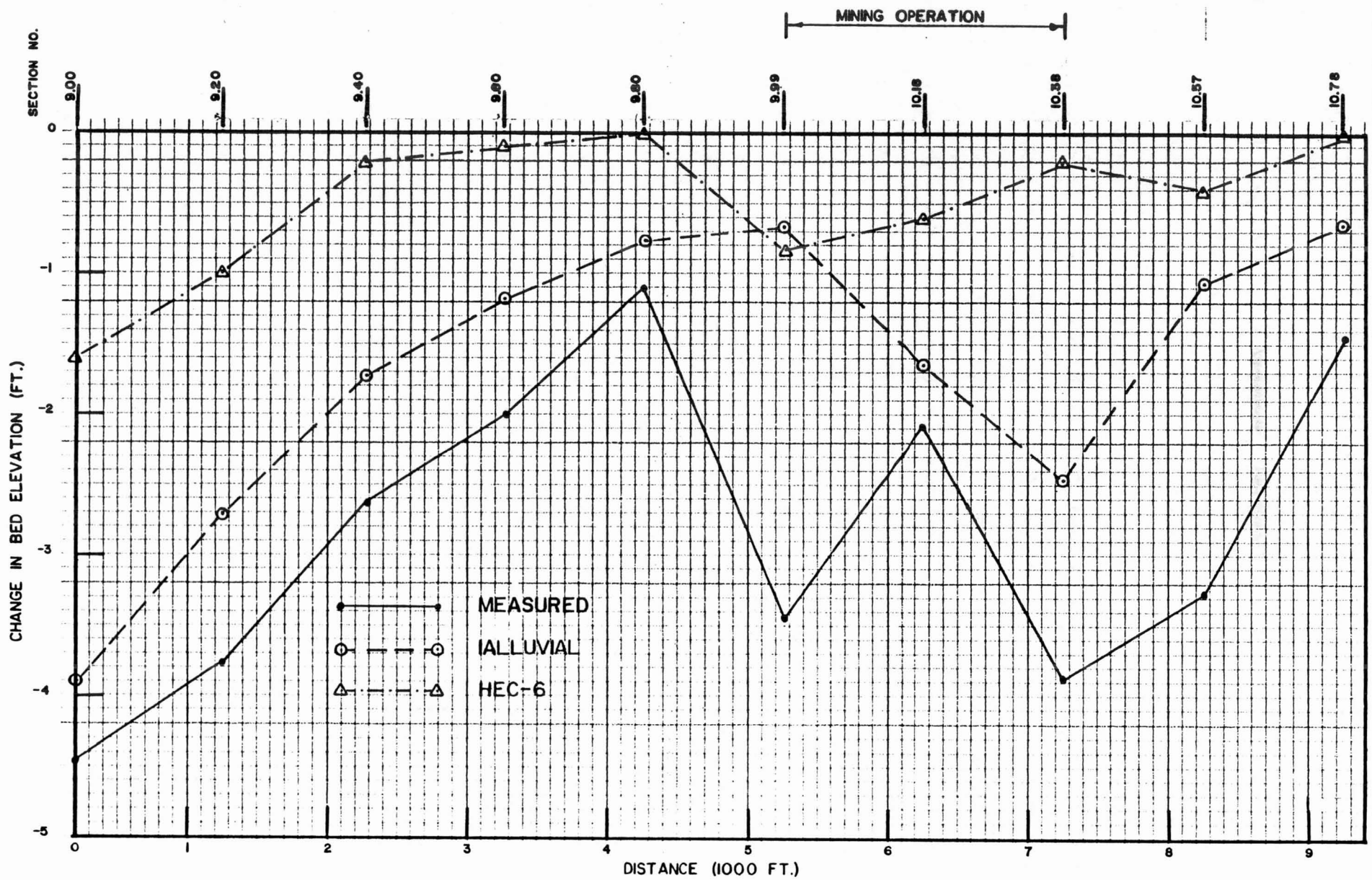

FIGURE 9 COMPARISON OF MEASURED AND COMPUTED BED-ELEVATION CHANGES OF THE SALT RIVER.

DSN. BY F. K., DWN. BY R. H. F. (8-25-86)

VII. CASE STUDY III: MISSOURI RIVER DEGRADATION DOWNSTREAM OF GAVINS POINT DAM

The Missouri River reach included in this case study is about 195 miles long, extending from Gavins Point Dam (RM 810.9) to Omaha (RM 615.9), Nebraska (Figure 10). Since the closure of the dam, in 1956, extensive channelization and bank-stabilization projects have been undertaken along this reach for the purpose of maintaining a navigation channel and other purposes. These activities have transformed a major part of this Missouri River reach from a wide sinuous channel containing numerous islands and bars (Figure 11), to a narrow, straightened channel of relatively uniform width, varying between 600 and 700 feet. The purpose of this case study is to simulate the impacts of the Gavins Point Dam and channelization works during the 20-year period (1956-76) since the closure of the dam in 1956.

Flow in the Missouri River reach is controlled by the Gavins Point Dam. Discharge is approximated by a two-step hydrograph: 36,000 cfs during the navigation season (April to November), and 15,000 cfs during the non-navigation season (December to March). Sediment inflows from eight tributaries joining this river reach and bank erosion from a 50-mile reach downstream of the dam are considered in simulation. The initial bed-material distribution utilized is the same throughout the reach, with D_{50} = 0.30 mm. Sediment concentration at the upstream boundary is zero, assuming complete entrapment of sediments by the dam.

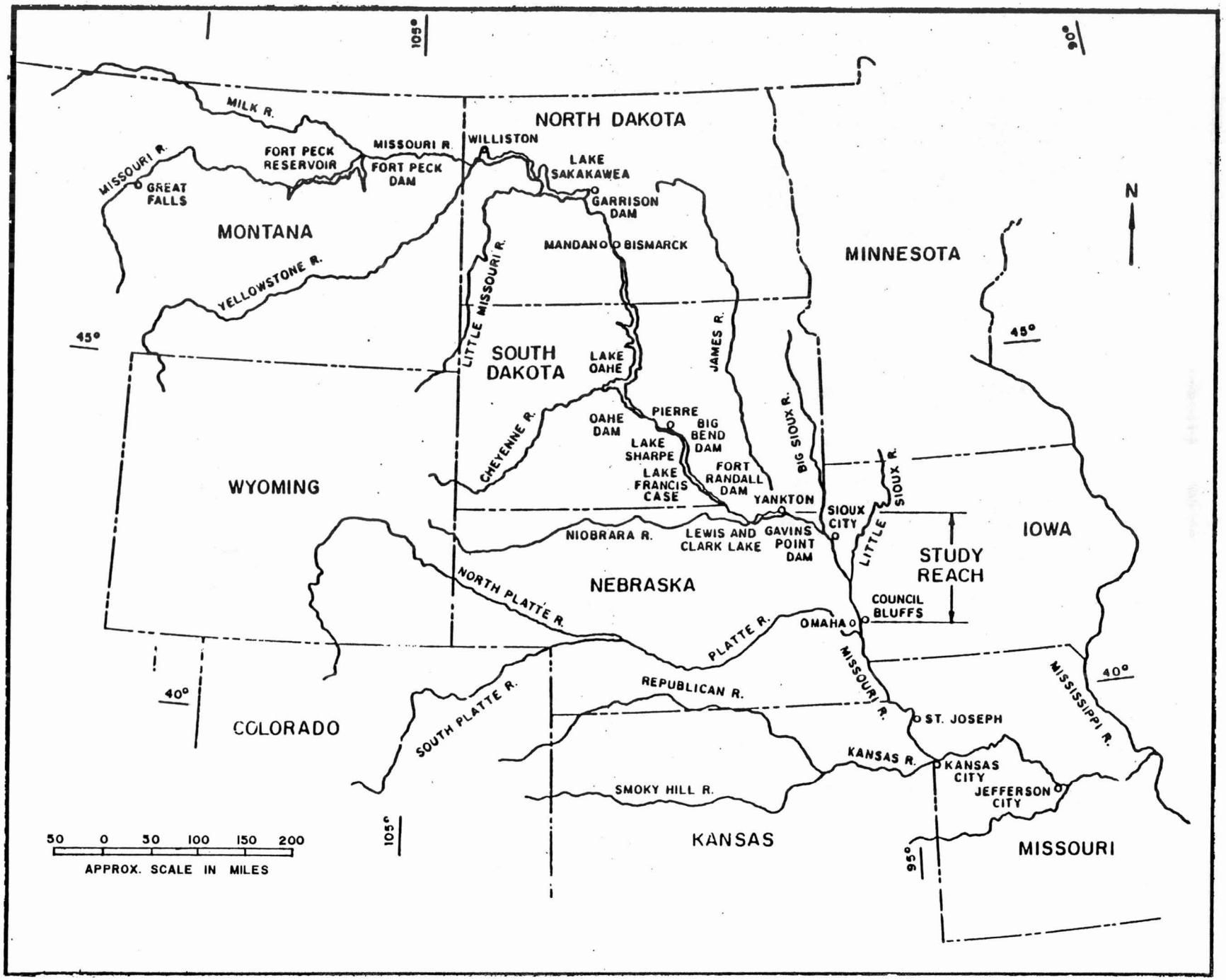

FIGURE 10 MISSOURI RIVER BASIN.

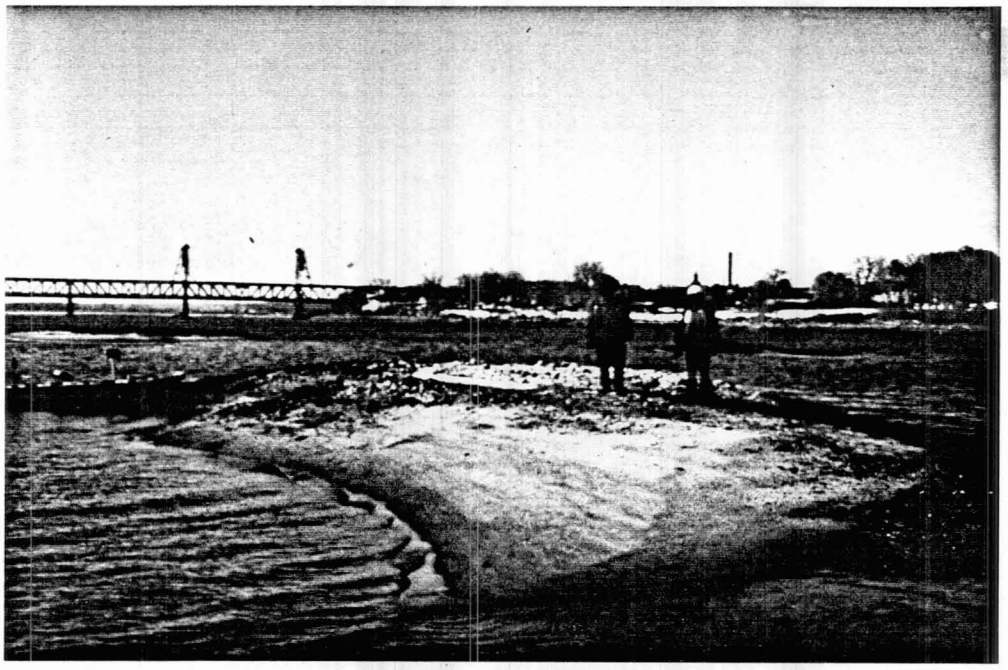

Figure 11. A view of the Missouri River about 4 miles downstream of the Gavins Point Dam, March 1980 (flow was nearly stopped by closing all gates of the dam).

Figure 12 shows excellent agreement between the measured and the computed changes in water-surface elevations after 20 years (1956-76) of simulation by IALLUVIAL (water-surface elevation changes were used in comparison, since data on bed-elevation changes were not available). Measured and computed median grain sizes (D_{50}) are plotted in Figure 13. Measured and computed D_{50}'s are in good agreement (Figure 13), except in a short reach near the dam; this discrepancy is believed to be due to field samples taken in this reach being mixtures of sediments from surface armor layers and the subsurface layers. Bed armoring of the Missouri River near the Gavins Point Dam, shown in Figure 14, was simulated satisfactorily by IALLUVIAL, as depicted in Figure 15.

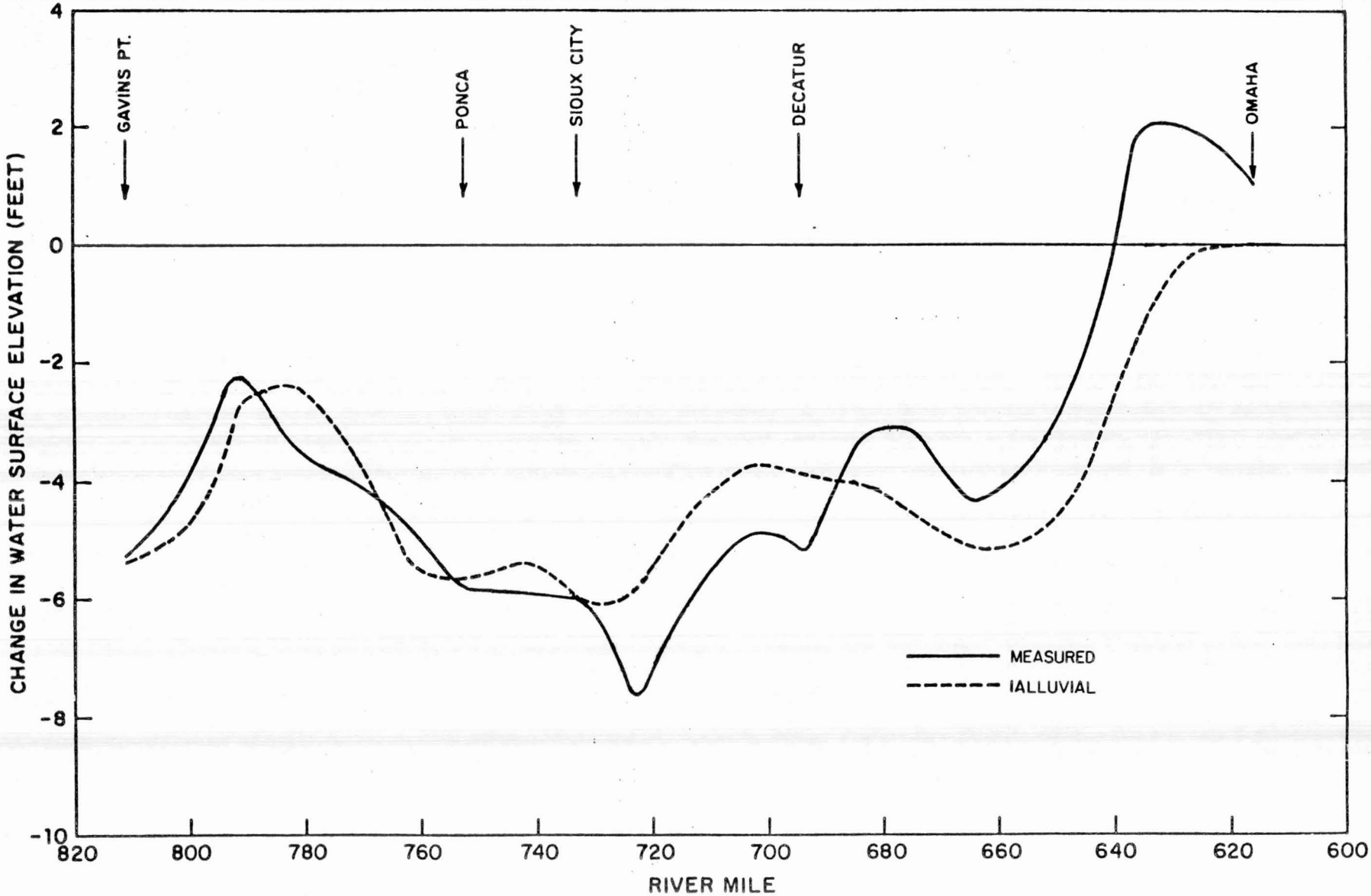

FIGURE 12 COMPARISON OF MEASURED AND COMPUTED CHANGES IN WATER-SURFACE ELEVATION AFTER 20 YEARS FOR THE MISSOURI RIVER.

CALC. BY F. K. , DWN. BY R. H. F. (8-25-86)

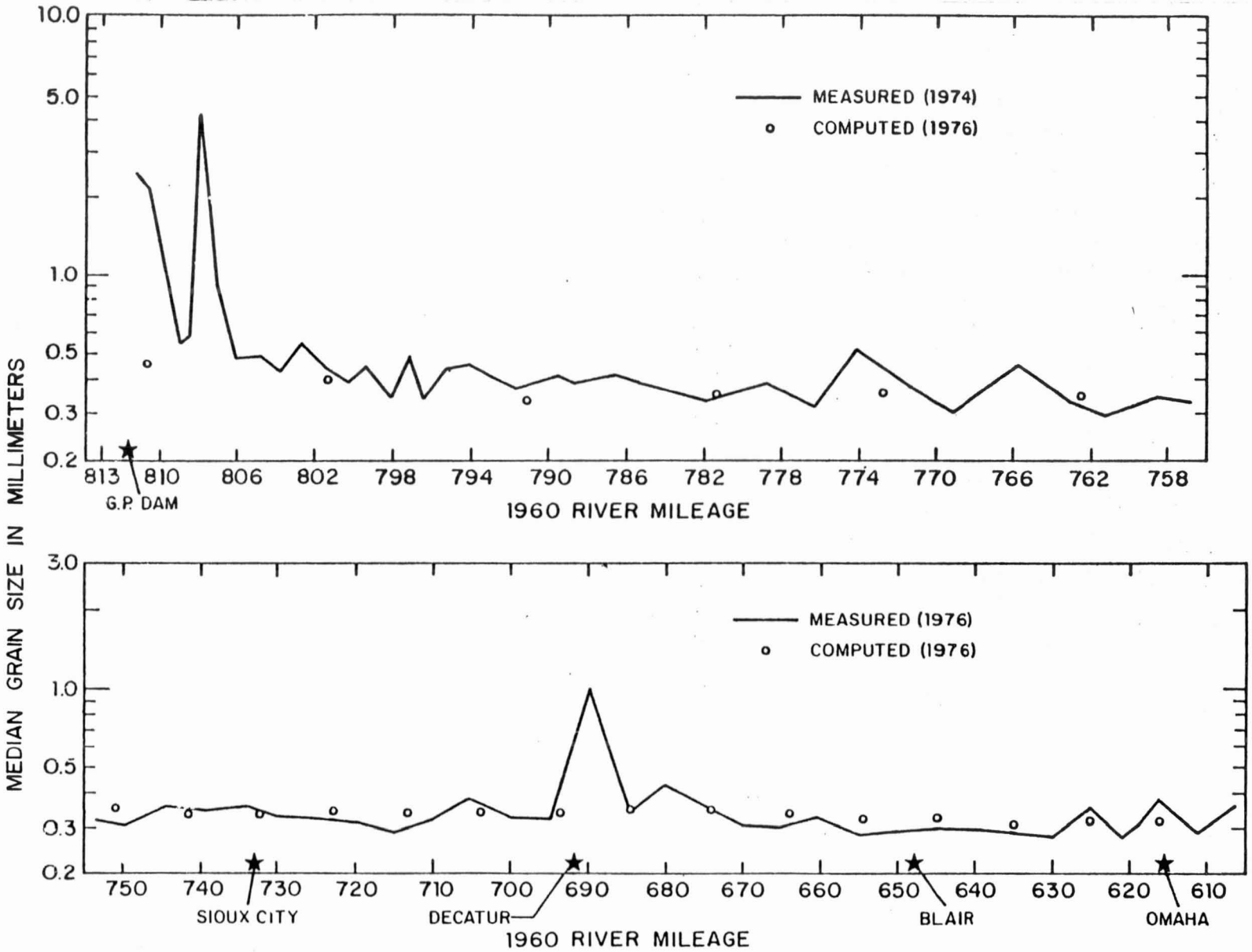

FIGURE 13 COMPARISON OF MEASURED AND COMPUTED MEAN BED-MATERIAL SIZES (D_{50}) OF THE MISSOURI R.

Figure 14. Photograph of the Missouri River bed armoring (March 1980).

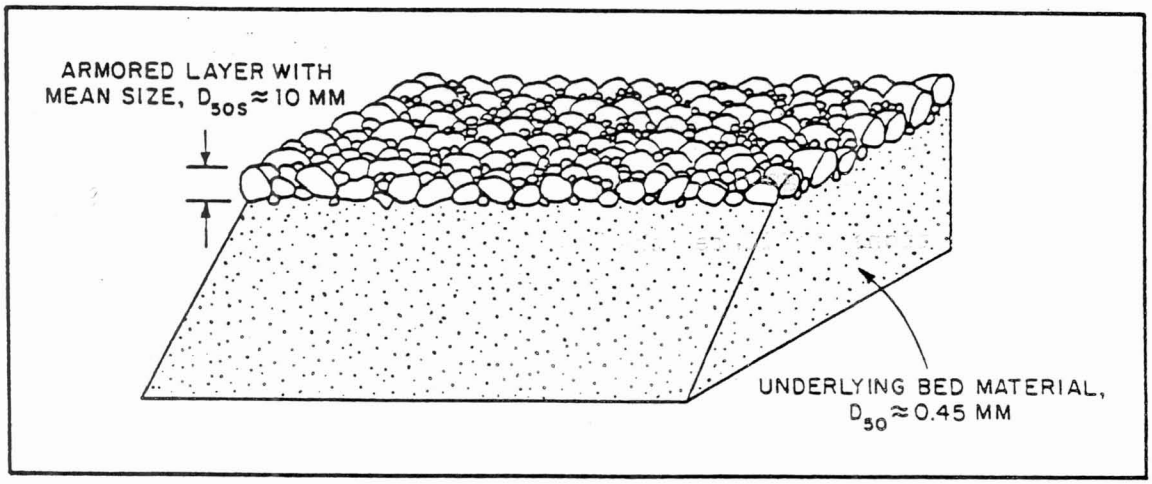

Figure 15. Schematic representation of armored bed near Gavins Point Dam, as simulated by IALLUVIAL.

VIII. CONCLUSIONS

Evolution of bed and water-surface elevations and bed-sediment characteristics in alluvial streams are simulated by IALLUVIAL in three case studies. IALLUVIAL incorporates several state-of-the-art features of alluvial-channel processes, e.g., ability to simulate flow resistance without the need to specify Manning's "n" a priori; a sediment-transport relation verified for a wide range of flow and sediment characteristics; nonhomogeneity of bed-sediment composition in the vertical direction (or subsurface layers with different compositions) are taken into consideration; contributions from tributary sediment inflows and bank erosion are included; formulation of bed armoring and sorting are based on knowledge gained from the most recent research investigations; and computationally efficient for both short and long-term simulations. These features are among the improvements which were recommended by the National Research Council (1983) for improving the existing erodible-bed models.

Changes in bed and water-surface elevations and bed-sediment characteristics simulated by IALLUVIAL for the Salt and Missouri Rivers have been found to be in good agreement with the corresponding observed values. These applications validate the model as a reliable and useful tool for engineers in predicting alluvial-channel responses to natural or man-made changes (e.g., sand and gravel mining, highway and bridge construction, channelization and realignment, river flow regulation by dams and reservoirs, etc.), for the sand-bed rivers, as well as for the gravel and cobble-bed, relatively steep-slope streams of the southwestern region of the United States.

IX. REFERENCES

Bowers, M.T., and Ruff, P.F., 1983, "An Evaluation of Computer Models to Predict the Erosion and Deposition of Sediment for Selected Streams in Arizona", Arizona State University, Tempe, Arizona, August 1983.

Dust, D. W., Bowers, M. T., and Ruff, P. F., 1986, "Application of HEC-6 to Ephemeral Rivers of Arizona", Arizona Department of Transportation, Phoenix, Arizona, January 1986.

Holly, F. M., and Karim, M. F., 1983, "Computer Simulation Prognosis for the Degradation of the Missouri River Between Gavins Point Dam and Iowa's Southern Border", Iowa Institute of Hydraulic Research, University of Iowa, Iowa City, Iowa, August 1983.

Karim, M. F., and Kennedy, J. F., 1982, "IALLUVIAL: A Computer-Based Flow- and Sediment-Routing Model for Alluvial Streams and Its Application to the Missouri River", Iowa Institute of Hydraulic Research, Report No. 250, University of Iowa, Iowa City, Iowa, August 1982.

Karim, M. F., and Kennedy, J. F., 1983, "Computer-Based Predictors for Sediment Discharges and Friction Factors of Alluvial Streams", U.S. Army Corps of Engineers, Missouri River Division, MRD Series No. 29, July 1983.

Karim, M. F., 1985, "IALLUVIAL: Analysis of Sediment Continuity and Application to the Missouri River", Iowa Institute of Hydraulic Research, Report No. 292, University of Iowa, Iowa City, Iowa, December 1985.

National Research Council, 1983, "An Evaluation of Flood-Level Prediction Using Alluvial-River Models", Committee on Hydrodynamic Computer Models for Flood Insurance Studies, National Academy Press, Washington, D.C.

United States Geological Survey, 1965, "Water Resources Data for Arizona", Part 2, Water Quality Records, U.S. Department of the Interior.

United States Geological Survey, 1966, "Water Resources Data for Arizona", Part 2, Water Quality Records, U.S. Department of the Interior.

United States Geological Survey, 1967, "Water Resources Data for Arizona", Part 2, Water Quality Records, U.S. Department of the Interior.

United States Geological Survey, 1969, "Water Resources Data for Arizona", Part 2, Water Quality Records, U.S. Department of the Interior.

United States Geological Survey, 1972, "Quality of Surface Waters of the United States, 1967", Parts 9-11, Water Supply Paper No. 2015.